Decision Making Strategies for Probabilistic Aerospace Systems Design

A Thesis
Presented to
The Academic Faculty

by

Nicholas Keith Borer

In Partial Fulfillment
of the Requirements for the Degree
Doctor of Philosophy

School of Aerospace Engineering
Georgia Institute of Technology
May 2006

Decision Making Strategies for Probabilistic Aerospace Systems Design

Approved by:

Dr. Dimitri Mavris
Professor, Faculty Advisor
Georgia Institute of Technology

Craig Nickol
Aerospace Engineer
NASA Langley Research Center

Dr. Daniel Schrage
Professor
Georgia Institute of Technology

Sharon Padula
Senior Research Scientist
NASA Langley Research Center

Dr. Alan Wilhite
Professor
Georgia Institute of Technology

Date Approved: 21 February 2006

It would be well if engineering were less thought of, and even defined, as the art of constructing. In a certain important sense it is rather the art of not constructing; or, to define it rudely but not inaptly, it is the art of doing that well with one dollar, which any bungler can do with two after a fashion.

- Arthur Mellen Wellington, *The Economic Theory of the Location of Railways*

To mom and dad, for their love,

patience, and unwavering support

ACKNOWLEDGEMENTS

I would like to extend thanks to the many individuals who have helped me through this endeavor. Dr. Dimitri Mavris, my advisor, has given years of support and encouragement throughout my tenure at Georgia Tech. I cannot say enough about the opportunities he has provided for me and am grateful to have had the chance to work with him all these years. Dr. Daniel Schrage and Dr. Alan Wilhite both bring their considerable experience in aerospace systems design to my reading committee and I feel privileged to be able to receive their comments. Craig Nickol of NASA Langley served as my advisor for the GSRP fellowship and has given me invaluable advice and support since he first came to NASA. His experiences with the Multi-mission Maritime Aircraft (MMA/P-8A) while at the Naval Air Systems Command provided much insight into the practical world of multi-mission systems design. Sharon Padula of NASA was kind enough to meet with me several times during my stay at Langley. She and Dr. Wu Li provided much-needed input regarding optimization and decomposition techniques during our many conversations. They also kept me honest when it came to some of the mathematical techniques I was experimenting with.

Many others at NASA Langley provided guidance, encouragement, and help both during and after my visits. I would like to extend thanks to my first GSRP technical advisor Bob McKinley, Branch Head Bill Kimmel, and everyone at the Aerospace Systems Analysis Branch for their support.

ASDL at Georgia Tech has provided me with a wealth of contacts, experiences, and most importantly, good friends. I would like to thank Dr. Michelle Kirby and Jeff Schutte for their assistance with the QuEST technology study and for providing the models used to develop the reduced-order surfaces seen in Chapter VII. Newly-minted Dr. Michael Buonanno, who was also a GSRP fellow with me, provided valuable help with a few Matlab models as well as a good sounding board for ideas. Dr. Bryce Roth, now an employee at GE Transportation in Cincinnati, provided sound advice. He also introduced me to the Commemorative Air Force

and vintage aircraft restoration. Rob McDonald spent many hours chewing over various ideas, algorithms, ponderings, LaTeX queries... and also made a good carpool partner down to the CAF. During the final weeks of writing, I accosted many ASDLer's and forced them to proofread a chapter. If there is a typo, misspelling, or grammatical error within this document, it is not for lack of trying to eliminate them all.

I will not attempt to list all of my friends at Georgia Tech who have made the past several years so much fun... to do so would take up far too much room. I would like to give a special thanks to The Golden Pheasant regulars for many challenging nights of three-man, the back-porch crew at Rocky who cannot be deterred even in sub-freezing temperatures, all of the current and former residents of Casa de Shalimar, and who can forget The Day of Chili? My time in Atlanta has been very enjoyable because of you, making my upcoming departure that much more bittersweet. I'll save a seat at Fenway for you.

My family and friends from around the globe have given their encouragement and love throughout my life no matter where I hang my hat. I've been a long way from home for a long time, and I could not have made it without your understanding and support. Mom, Randy, Dad, Laura, Scott, Mike, Jon... thanks.

Last but certainly not least, I would like to thank Mary Margaret Stoeckle for her years of patience and support, never mind filling out the lion's share of my bibliography database. I'm looking forward to finally being able to share the same area code with you.

Thank you all – without you, I could accomplish nothing.

TABLE OF CONTENTS

LIST OF TABLES

LIST OF FIGURES

LIST OF SYMBOLS OR ABBREVIATIONS

γ_j	interdependent correction to static relative importance of j^{th} metric
λ_j	entropy-based relative importance of j^{th} metric
μ	mean
θ_{ij}	angle between i^{th} and j^{th} polynomial coefficients
ρ	beam density
$\mathbf{\Sigma}$	matrix of singular values of $\mathbf{B}$
σ	standard deviation
σ_{ult}	beam ultimate strength
A	beam aspect ratio (width/depth)
AITEK	airfoil shape factor
ANOVA	analysis of variance
APPn	approach noise
ASM	available seat mile
$\mathbf{B}$	matrix of response surface equation coefficients (minus intercept term)
c	constraint
$\mathbf{C}^{\oplus}$	recomposition matrix from important characteristic tradeoffs
CDF	cumulative distribution function
CO_2	carbon dioxide
CP	compromise programming
DOCi	direct operating cost plus interest
DoE	design of experiments
E	Young's modulus for beam *or* total entropy of decision space
EPNL	effective perceived noise level
$e(\overline{y}_j)$	entropy of j^{th} metric
FAA	Federal Aviation Administration

FPR	fan pressure ratio
GW	gross weight (also TOGW)
HPCPR	high pressure compressor pressure ratio
k	number of design variables
L	beam length
LC1	loading condition 1 for beam design problem
LC2	loading condition 2 for beam design problem
LC3	loading condition 3 for beam design problem
LPCPR	low pressure compressor pressure ratio
LTO	landing-takeoff cycle
m	number of alternatives
MADM	multiple attribute decision making
MCDM	multiple criteria decision making
MCS	Monte Carlo simulation
MDO	multidisciplinary design optimization
MFE	model fit error
MODM	multiple objective decision making
MRE	model representation error
n	number of decision metrics
NASA	National Aeronautics and Space Administration
NO_x	oxides of nitrogen
OPR	overall pressure ratio
P_z	load for beam in loading condition z
PDF	probability density function
QuEST	Quiet, Efficient Subsonic Transport
r	number of important characteristics
R_1	Euler buckling factor of safety for beam design problem, LC1
R_2	ultimate compressive failure factor of safety, LC1
R_3	ultimate bending failure factor of safety, LC2

R_4	maximum compressive displacement, LC1
R_5	maximum bending displacement, LC2
R_6	beam mass, all loading conditions
R_7	ultimate bending failure factor of safety, LC3
R_8	maximum bending displacement, LC3
$\mathbf{R}_c^{\oplus}$	values of important characteristic tradeoffs
$\Delta(R_i)$	grade of interdependency of i^{th} metric
R_j	current value of j^{th} metric
R_j^*	best value of j^{th} metric
R_j^-	worst value of j^{th} metric
rO	rated output of all operating engines
RSE	response surface equation
RSM	response surface methodology
S	beam cross-sectional area
SAW	simple additive weighting
SLn	sideline noise
SOA	state of the art
SOO	single-objective optimization
SQP	sequential quadratic programming
SS_E	sum of squares of error
SS_R	sum of squares of regression
SVD	singular value decomposition
SWEEP	wing quarter chord sweep
S_{yy}	total sum of squares
t	threshold
TMCI	threshold-modified contrast intensity
TOFL	takeoff field length
TOGW	takeoff gross weight (also GW)
TOn	takeoff noise

TOPSIS	technique for order preference by similarity to ideal solution
TWR	thrust-to-weight ratio
$\mathbf{U}$	unitary matrix from decomposition of $\mathbf{B}$
v	number of terms in response surface (minus intercept term)
VAPP	approach speed
VISTA	Vehicle Integration, Strategy, and Technology Assessment
VSP	Vehicle Systems Program
$\mathbf{V}^{\mathrm{T}}$	coefficients of all characteristics for $\mathbf{B}$
$\mathbf{V}_1^{\mathrm{T}}$	coefficients for characteristics in column space of $\mathbf{B}$
w_j^d	dynamic relative importance of j^{th} metric
w_j^s	static relative importance of j^{th} metric
WSR	wing loading
$\vec{x}$	vector of design variables
$\vec{\tilde{x}}$	modified vector of design variables with higher-order terms
$\overline{y}_{ij}$	normalized value of j^{th} metric of i^{th} alternative

SUMMARY

Modern aerospace systems design problems are becoming increasingly focused on multi-mission capability and adaptation to new or emerging requirements. The design cycle times of these very complex systems are relatively long as are their times in service. Over this period, the initial requirements specified for the aircraft will likely change, as will the operational environment. These trends point towards a need for a strategy to design to multiple requirements that are uncertain in nature.

Current approaches for aircraft sizing and synthesis are based on optimization of a single objective. Other requirements enter this formulation as constraints which are not easily moved. Changes in these constraints may be necessary in order to deal with the inevitable changes seen during the design cycle. It may not even be possible to move these constraints because the configuration variables can become more or less locked in at later stages in the design process. Furthermore, the constraint approach does little to determine the impact a particular requirement has on the others and therefore does not facilitate compromise. This can be partially remedied by considering parametric requirements; however, it can become very difficult to size a vehicle to a wide range of metrics. This often necessitates that the bounds on the design variables and parametric requirements be limited such that sizing convergence is possible.

This document presents a new approach for sizing and synthesis dubbed *multipoint sizing*. This technique does not attempt to size the vehicle for one particular mission. Rather, it uses the requirements targets or directions of improvement as goals and attempts to modify the design variables to approach these desired points. This technique allows the use of Multiple Criteria Decision Making (MCDM) techniques for aerospace systems design. MCDM works by creating a composite objective function from an original set of objectives, in this case formed by the requirements normalized by their direction of improvement.

Using MCDM for systems design allows for the uncertainty in the requirements to be mapped over to uncertainty in the relative importance of these requirements or *decision metrics*. In this fashion, a user can define a distribution for the importance of a particular metric, and the solution that is most invariant with respect to changes in the relative importance will be robust with changes in the requirements.

Unfortunately, MCDM for aerospace systems design brings a host of new problems. Most of these systems can be described as *large-scale* problems, meaning that there are many decision metrics. It can be difficult to consistently assign relative importance (deterministic or probabilistic) from a large pool of metrics. Furthermore, most MCDM methods assume independent, monotonically increasing utility, which can lead to poor compromises and exploitation of interdependent metrics.

This research identifies a series of strategies that enables intelligent use of MCDM in large-scale systems design. The relative importance is broken into a two-part model with a static and dynamic contribution. The static contribution is a monotonic value that retains a control for user-based importance. This user contribution also allows for probabilistic studies by allowing the user to input a distribution instead of a fixed value. The static value is modified by a concept related to entropy, found by measuring the diversity of the decision space. Those metrics with little diversity from the best single-metric solution in the decision space are given less importance than those with great diversity, reflecting that more compromise is possible in the more diverse metrics. The dynamic contribution makes local changes in the relative importance based on a simple utility model with two inflection points. These points are the constraint, defined as a point below which performance is unacceptable, and the threshold, defined as a point of diminishing returns. If the metric falls below the constraint the relative importance jumps; if it climbs above the threshold it drops to zero; and in between it tapers from the static value to the threshold.

Sometimes it is desirable for a decision maker to use polynomial surrogate models to approximate the effect of the design variables on the decision space. These polynomials represent an approximate functional mapping between the design and decision space. As such, the coefficients of these polynomials provide very useful information. First, the vector

angles between these coefficients in polynomial space represent the degree of interdependence of the metrics: acute angles indicate positive dependence, near right angles indicate relative independence, and obtuse angles indicate an adverse relationship. Using these angles, an additional correction can be made to the static relative importance contribution based on the interdependence of the models, balancing what might be an otherwise unfairly penalized metric in the basic MCDM formulation.

The coefficients of these polynomials also enable the use of linear decomposition techniques. This helps identify the number of linearly dependent tradeoffs present in the decision space, which are generally unimportant to the actual variation of the metrics. The subset of linearly independent tradeoffs represent the *characteristic tradeoffs* of the decision space. These characteristics provide a means for compact visualization of multidimensional spaces that before had to be viewed in large-dimensional scatterplot matrices. This so-called *decomposition-based visualization* provides key information on the nature of the underlying tradeoffs within the decision space.

These techniques are developed alongside a conceptually simple example for illustrative purposes. They are then assembled into a generalized strategy that is applied to a technology selection study for a long-range civil transport. The results of the new strategy are compared with modern single- and multiple-objective formulations. The advanced decision-making techniques presented in this research identify a characteristically balanced solution to systems design with multiple requirements. The method also provides a significant reduction in solution variability due to uncertain requirements.

CHAPTER I

INTRODUCTION

This document begins with a statement by Arthur Mellen Wellington regarding the nature of engineering [Wellington, 1914]. To further this theme, this author would argue that engineering is the art, or perhaps better yet, the science of problem solving. As the science of engineering has evolved, the modern engineer has created a variety of tools to satisfy a diverse array of problems, including numerical optimization and solving routines, computer-aided design and manufacturing, probabilistic schemes, and more. Perhaps the "art" of engineering really lies in the discovery of a new scientific process to solve a previously unsolvable problem.

If engineering provides the tools for problem solving, then systems engineering provides the means to assemble these tools to solve larger problems. Like the basic techniques, it can be seen as both an art and a science. The art is user know-how, the experience necessary to assemble the right tools to solve the problem, whereas the science is the application of dedicated decomposition and decision making techniques to an appropriate class of problems. As the science begins to replace the art, the "art" of systems engineering changes once again, and will perhaps soon lie in the user's ability to judge the appropriateness of a solution method or the solution itself.

Design is a problem solving technique that may require a small suite of engineering tools, with systems design as the art / science of decision making from multiple (subsystem) design problems. In light of this, most engineering systems design problems have multiple and conflicting objectives. Furthermore, the satisfactory attainment level for each objective ("requirement") is likely uncertain early in the design process. Systems with long design cycle times will exhibit more of this uncertainty. This is further complicated if the system is expected to perform for a relatively long period of time, as now it will need to grow as new requirements are identified and new technologies are introduced. These points

identify a need for a systems design technique that enables decision making amongst multiple objectives in the presence of uncertainty.

Traditional design techniques deal with a single objective or a few objectives that are often aggregates of the overarching goals sought through the generation of a new system. Other requirements, although uncertain, are viewed as static constraints to this single- or multi-objective optimization problem. With this formulation, enabling tradeoffs amongst the requirements, objectives, or combinations thereof is a slow, serial process that becomes increasingly complex as more criteria are added.

Recent years have seen increased effort to automate disciplinary analyses and facilitate their integration. This is coupled with increases in computational power and speed, finally enabling systems engineers with the ability to monitor and integrate high-fidelity resources into design studies. This generation of engineers can now use advanced decision-making techniques to identify the best tradeoff solution from a pool of alternatives with greater accuracy than ever before.

Or can they? As attractive as many decision making and support tools are, they too are limited if one does not fully understand the underlying assumptions within the plethora of decision making routines available today. New integration routines enable an increase of the overall design scope, further exacerbating the problems posed by modern decision making approaches. This leaves the systems engineer with a few alternatives. It is relatively easy to learn and understand the limitations of state-of-the-art decision making techniques, so one could attempt to tailor the requirements of the problem and their associated analyses to a chosen technique. However, this can be time-consuming and perhaps impossible for many large-scale problems. Another option is to create an entirely new decision making technique uniquely suited to the problem. This has the potential to yield the greatest results but does so at great effort with little chance for generality. A final option is to augment existing decision making techniques in an attempt to make up for any shortfalls. This thesis takes the last approach in its attempt to explore large-scale systems design.

1.1 Organization

This document presents the case for a refined decision making method that is applicable to a wide range of large-scale systems design problems. The case for this research is presented in a logical progression beginning with the motivation, a brief background in many of the pertinent techniques culminating in a position on the state-of-the-art, development and implementation of several new techniques, application to a large-scale problem, and finally recommendations for future work. The development and implementation see some iteration between theoretical elucidation and illustration of concepts using a simple example problem.

Throughout this manuscript, the reader is directed to a variety of formalized statements to understand the contribution a particular section of text has to the overall research. An **Observation** is usually a summarized statement of insight into a particular phenomenon gained from literature, anecdotal evidence, or experience. As its name implies, a **Research Question** is a formal query that follows one or more **Observations**. A **Hypothesis** is a proposed solution to one or more **Research Questions** that can be tested with a variety of experiments. These experiments are given as broad **Research Tasks**, which often have many sub-components. The process may either confirm the hypotheses or lead to still further observations. Every effort was made to adhere to the basic principles of the scientific method while giving appropriate background into the many subjects this research is built upon. However, as is true in any scientific endeavor, discovery does not always take a textbook form. Hence, these formalized terms serve more as an organizational tool for the reader's understanding then they do for the author's actual investigation process.

1.2 Motivation

The motivation for this research began with the author's involvement in a first-year graduate design competition involving a multi-mission aircraft. This competition required the design team to determine the salient characteristics of a vehicle with multiple, conflicting mission requirements and subsequently to design an aircraft to these features. The identification of these features followed an analysis of the vehicle's "mission space" to determine which requirements would be the design drivers [Mavris and Borer, 2001].

This first attempt at multi-mission sizing represented a technique that is most typical of modern multi-mission vehicle design; that is, to design the aircraft to only the most stringent requirements. Though effective, it does little to accommodate tradeoffs and can quickly result in an infeasible design. If nothing else, this initial design project broached two subject areas critical to the development of the method outlined in this research proposal: the need for a multi-mission sizing method and for the ability to capture uncertainty in requirements specification and exploration. These focal points were microcosms of the larger problem of decision making for large-scale systems design.

1.2.1 Multi-Mission Sizing

The first 11 seconds of manned heavier-than-air flight began on 17 December 1903. Since those first flights off the dunes of Kill Devil Hills more than a century ago, aircraft have evolved into massive, complex, and versatile machines. The first practical use of aircraft for carrying passengers or cargo was realized within a decade, and its military applications for observation and attack soon after. By the fourth decade, aircraft were used for an increasing variety of missions: cargo and troop transport, precision bombing, aerial photography, escort, interception, and many others. By the end of the sixth decade of powered flight manufacturers were building aircraft for every conceivable mission.

However, as the number of missions for aircraft increased, manufacturers and operators found that production and operation costs increased and tactical redundancy suffered. This problem was compounded as advances in technology required an even wider array of missions, such as supersonic attack, airborne early warning, and electronic surveillance. Certain aircraft were tasked with synergistic missions in an effort to alleviate these problems.

The notion of the multi-role aircraft, though not new, has seen increased emphasis over the years. This trend, though difficult to explicitly document, can be exemplified in the composition of a typical U.S. aircraft carrier air wing. Figure 1 compares the number of different aircraft types aboard a carrier versus the number of distinct missions performed by these aircraft for different historical periods, compiled from several different resources [Department of the Navy, 2005; Federation of American Scientists, 2005; Toppan, 2003].

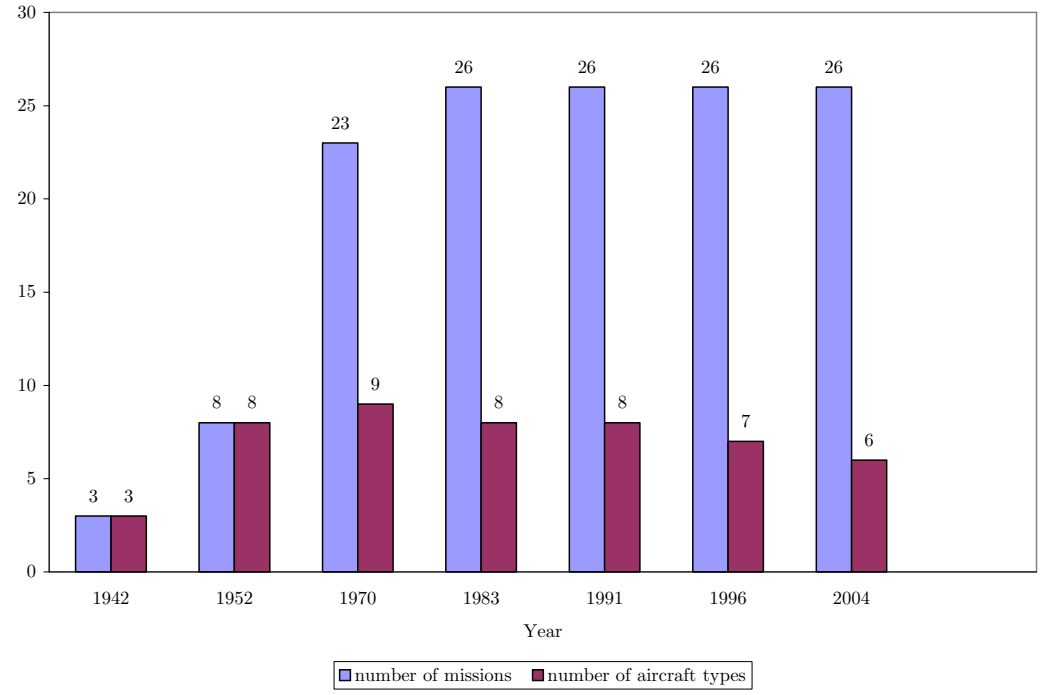

Figure 1: Carrier Air Wing Composition

This figure shows that the number of missions has climbed rapidly and levelled off with respect to aircraft carrier operations, yet the number of different aircraft types saw a short increase followed by a steady decrease. The carrier air wing of the future will deploy even fewer aircraft as new programs such as the multi-mission capable F/A-18E/F and F-35C aircraft enter service and replace aging airframes [Young et al., 1998; Sherman and Hardiman, 2003].

The increased emphasis on multi-role capability for aircraft can be traced to two principal reasons: affordability and redundancy. Employing a single aircraft type or variant of said type for several roles reduces the need for specialized equipment, personnel, training, and spare parts, among other resources. It also enables economies of scale through larger-scale mass-production of the same airframe. All of these attributes point to a reduction in overall life-cycle costs at tactical (and higher) levels. Redundancy is increased for many of the same reasons. As an example, consider two squadrons: one with 10 dedicated attack and 10 dedicated fighter aircraft, and one with 20 multi-role fighters. If five aircraft are lost on a fighter mission, the squadron with dedicated aircraft exhibits a 50% loss in fighter

capability, while the multi-role squadron can spread that loss out evenly over its attack and fighter capability as needed. This is important not only in military applications but also civil applications as many passenger air carriers begin to investigate the feasibility of intermodal (passenger by day, cargo by night) transports [Nelson et al., 2001].

The move towards multi-mission capability in aircraft is but one trend in aircraft design towards multiple requirements. However, the problem towards designing for multiple missions is indicative of a larger trend in aircraft design problems, which can be further characterized as large-scale systems design. Ultimately, every large-scale problem is multi-criteria in nature. This can be formally written as:

Observation 1: Aerospace systems design problems involve an increasing number of decision criteria.

Unfortunately, multi-mission capability comes at a price. One maxim in aerospace design is that *every additional requirement imposed on a system will compromise the design in some way.* This concept of "no free lunch" will manifest itself as a decrease in effectiveness in another requirement, such as a performance or vehicle-level cost measure. The only exception to this rule is in the trivial case of a completely dominated or redundant requirement, in which case the true multi-role capability of the system is not expanded.

1.2.2 Requirements Uncertainty

Successful design of any system begins with specification of requirements. These requirements are composed of one or more objectives and zero to many constraints. As aerospace vehicle design has progressed, the requirements imposed on vehicles have become more numerous and stringent. Requirements are influenced by advances in technology, the environment, politics, and many other factors.

Most engineering problem solving techniques begin with a static set of requirements. Any change to these requirements can change what was once the best solution to a different solution. As design cycle times increase, there is a larger chance that the various factors shaping the requirements will change as well, thus resulting in changes to the original requirements. This can have a substantial effect on modern aerospace vehicle design.

To compare design cycle times, consider that the Lockheed P-80 Shooting Star, the first operational jet fighter made in the United States, went from drawing board to first flight in 143 days [Rich and Janos, 1994]. Compare this to a modern jet fighter, the F-22 Raptor. The Raptor itself was conceived in 1983, first flew in 1997, and the first squadron just recently became operational in 2005. This example, though radical, exemplifies the increase in design cycle time: 143 days to 14 years! Even in this vein, one must consider that the original requirements for the F-22 date back to the Advanced Tactical Fighter concept first proposed in 1971 [Piccirillo, 1998]. Over that time numerous changes have been seen in the technological environment (stealth), political environment (the fall of the USSR), and the fiscal environment (budget deficits), to name a few.

Further complicating requirements specification is the concept of growth potential. Aerospace vehicles, at their extraordinary expense and complexity, are expected to perform for a relatively long period of time. Over this time the operational environment and associated requirements will change. Commercial operators will be faced with a different market, more stringent environmental regulations, and safety regulations. Military operators will face new enemies and weapons systems. A successful aircraft will need to have the ability to grow and change throughout its life cycle. Compare the service of the B-52 subsonic strategic bomber to that of the B-58 supersonic bomber: both were contemporaries; the earliest operational B-52 first flew in 1955 and the B-58 in 1960. The latest models of both aircraft were produced in 1962. However, the B-52 is so effective, affordable, and adaptable for strategic bombing that it is planned to remain in service until 2040, 85 years after the first model and 78 years after the last of the current models entered service! The B-58 only lasted until 1970, 10 years after entering service simply because it was not nearly as versatile or adaptable in its future environment [Baugher, 2005; Federation of American Scientists, 2005].

These and other empirical relations point to another maxim related to aerospace vehicle design: *The requirements specified for the system today will be different than those faced at the beginning of its operational life, which will further change throughout the system's entire life cycle.* This can be formalized as two observations relating to uncertainty in aerospace

systems design. These are:

Observation 2: Many of the requirements and goals in aerospace systems design problems are uncertain, though they often have an associated direction of improvement.

Observation 3: Long cycle design times and long system service lives exacerbate uncertainty in the original requirement targets.

The ever-increasing cost of aerospace systems indicates that more time will be spent on development of a given concept. This high development cost will necessitate that the system will be expected to perform for longer and in more unexpected roles. This uncertainty will have an effect on aircraft sizing and systems design methods.

CHAPTER II

REQUIREMENTS AND AIRCRAFT SIZING

The fundamentals of aerospace vehicle design deal with the broader spectrum of systems design methods and requirements specification, as well as specific vehicle-level modeling and simulation. The phenomena mentioned in the previous chapter indicate a shift in the operational needs of these systems. These needs must be accounted for in modern design and systems engineering methods. To gain an appreciation of the issues associated with multi-mission sizing, one must first understand the idiosyncracies associated with the engineering design process, requirements specification, and vehicle sizing. Each of these areas has evolved to take advantage of larger bodies of knowledge and better resources to tackle these various problems. The observations of the previous chapter lead to two primary research questions regarding the nature of designing to multiple requirements in the presence of uncertainty. These are:

Question 1: How do aerospace sizing and synthesis methods address multiple requirements? (Observation 1)

Question 2: Can modern systems design methods adequately deal with changing requirements? (Observations 2 and 3)

These questions guide the literature search and enable further observations. What follows is a brief overview of the origins and growth experienced in these fields.

2.1 The Engineering Design Process

Several models exist for the engineering design process related to aerospace vehicles. Raymer suggests a serial, three-tiered process of conceptual design, preliminary design, and detail design, with requirements feeding into the conceptual design process and fabrication following detail design [Raymer, 1999]. This text, meant as a single source for undergraduate

engineering students, presents a deliberately simplified process. More rigorous techniques involve more stages, such as detailed requirements generation studies and considerations of the entire life cycle of the vehicle. Asimow enumerates an eight-phase design process to embody all of these concepts, from feasibility studies to planning for retirement [Asimow, 1962]. Dieter revives and modernizes these concepts in his text on systems design [Dieter, 2000]. Of particular interest are the initial phases of what Dieter refers to as conceptual design and embodiment design. This refined design process is illustrated in Figure 2.

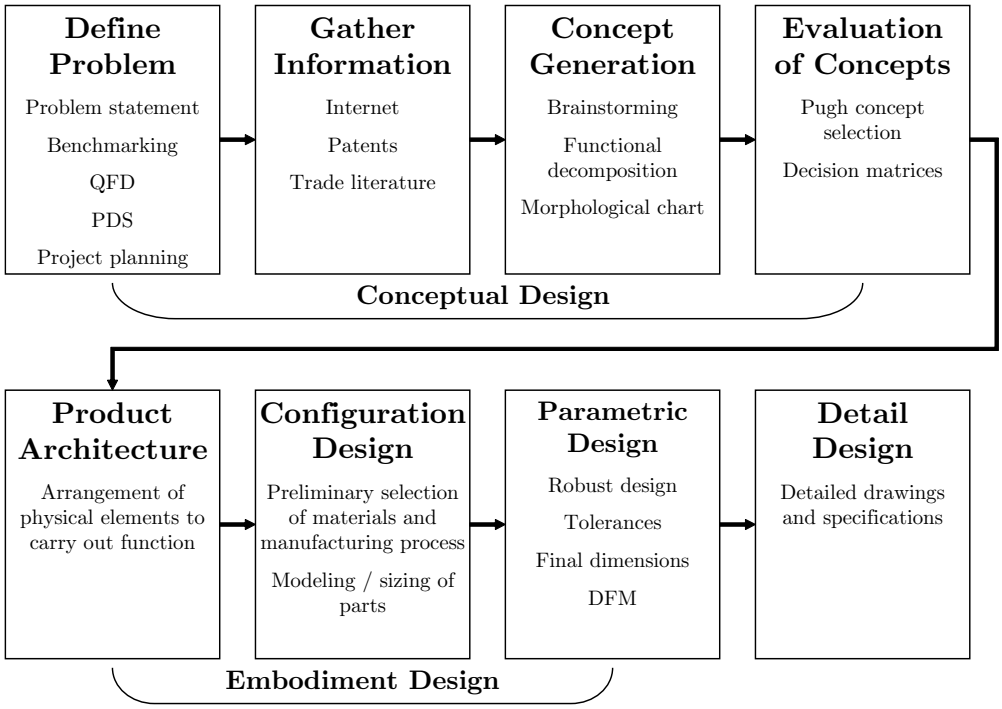

Figure 2: The Engineering Design Process [Dieter, 2000]

The life-cycle approach to engineering design is imbedded into the concept of systems engineering. The Defense Systems Management College [Leonard, 1999] defines systems engineering as:

> ...an interdisciplinary engineering management process to evolve and verify an integrated, life cycle balanced set of system solutions that satisfy customer needs.

The text further discusses four phases in the development of a design. The process first starts with concept studies, resulting in a *functional baseline*. This baseline is used in the system definition phase until an *allocated baseline* is defined, which carries over to the preliminary design stage. Here, the process continues until the definition of a *product baseline*, used in the final detail design phases. In general, these phases follow the same overall approach as those referenced by Raymer and Dieter above (requirements, conceptual design / system definition, preliminary / embodiment design, detailed design). However, the Department of Defense greatly elaborates on methods for identifying requirements for systems engineering. The core process involves requirements analysis, functional analysis, system synthesis, and system analysis and control. This process is illustrated in Figure 3.

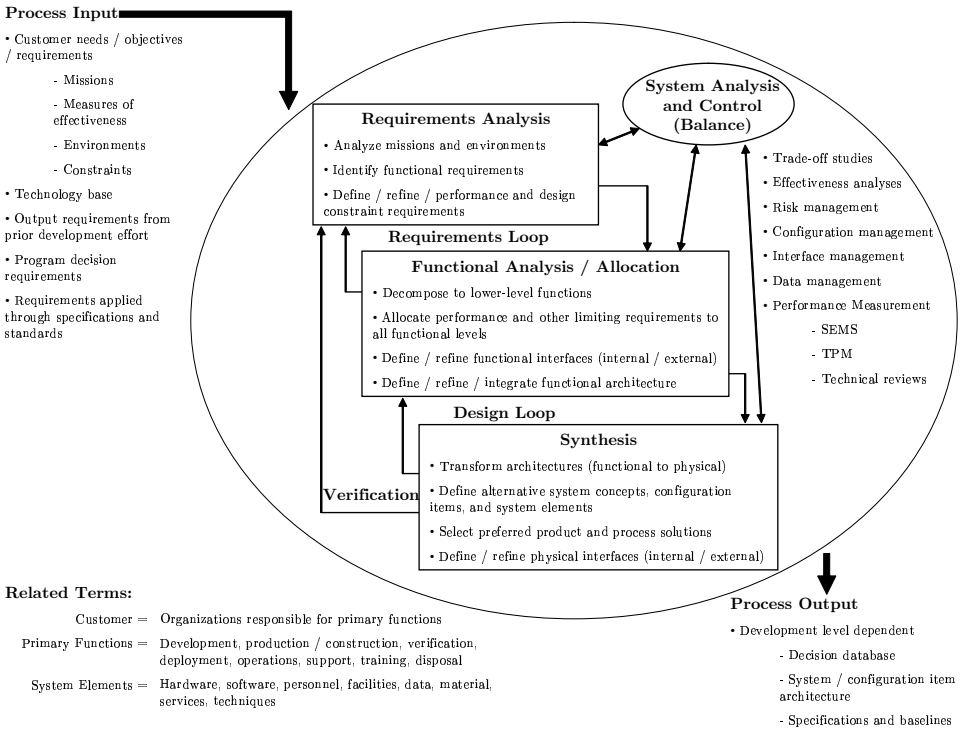

Figure 3: The Systems Engineering Process [Leonard, 1999]

The systems engineering approach is among the first to identify the need to include tradeoffs of functional requirements. However, as discussed later, the overall system requirements ("measures of effectiveness" in Figure 3) remain largely static after the initial requirements specification stage.

2.1.1 Requirements Specification

The objective of engineering design is to produce a product (mechanical or otherwise) capable of satisfying a need. This can be a new need brought about by scarcity, an improvement to an existing need brought about by technology, and any other number of cases. Alone, these needs are generally vague and do not necessarily imply a solution. The engineer then has a variety of tools available to translate these needs, "the voice of the customer," into technical requirements, "the voice of the engineer." Often in order to do this a few solution configurations are necessary, though the specific parameters of said configurations need not be determined. For example, there is a need to transport people across the Atlantic Ocean. There are a huge number of solutions available, however impractical: by sea, by air, by a giant bridge, by space, and more. With the configurations narrowed down, one may begin to create technical requirements. If the solution is an aircraft, what range should it be capable of traveling? How many passengers should it carry? What safety features should be incorporated? These and other questions form the basis of the generation of top-level requirements.

For small systems, requirements specification is relatively straightforward. Often there are a few constraints and one objective. These requirements (constraints and objective function) follow from a relatively simple set of rules - do not exceed the maximum stress, do not buckle under load, minimize cost of manufacture, etc. However, more complex systems involve multiple requirements that may be difficult to characterize. Thus, numerous methods have been developed within systems engineering to handle the translation of "needs" into "requirements." The needs may be characterized through items such as market surveys and customer questionnaires. This "voice of the customer" can be mapped to the "voice of the engineer" through Quality Function Deployment (QFD). This technique uses a series of "House of Quality" worksheets to determine relevant engineering requirements [Dieter, 2000]. These represent but a few of the options available when determining overall engineering requirements. Several other techniques used in systems engineering are outlined by Brassard [Brassard and Ritter, 1994].

Requirements specification techniques have evolved in step with design methods. Aircraft sizing, to be covered in greater detail in the subsections that follow, has advanced substantially as statistical databases and computer power have grown. As such, those setting the requirements are able to see the physical effects of "pushing the envelope" when specifying what it is a vehicle can do [Czysz et al., 1973; Parker, 1986; Gerhards et al., 2000]. Advanced systems engineering techniques have evolved such that requirements specification and systems design have become codependent [Schrage, 1999].

The design of aircraft often begins with the specification of several requirements. These take many forms, but can generally be classified into four groups [Borer and Mavris, 2003]:

Point-performance requirements are applied at a specific flight and loading condition. Examples include combat turn rate, maximum Mach number, and takeoff distance. These may be associated with a specific mission, but can also include non-mission specific critical conditions such as engine-out climb gradient.

Operational requirements refer to specific needs brought about by the operating environment, such as maximum ramp weight or resistance to corrosive conditions.

Mission requirements generally refer to specification of a mission profile. Examples include range, payload, and loiter time on station. These requirements may also specify flight at a certain condition, such as cruise at a specified Mach number or altitude, or may specify flight at an optimum condition.

Economic requirements relate to the costs associated with the aircraft. Examples of economic requirements are direct operating cost, acquisition cost, and development cost.

Most basic requirements are related to the missions the aircraft is expected to perform. These missions are in fact nominal abstractions of reality; a "slice" of the vehicle's overall mission capability. Some methods to design or "size" an aircraft to these requirements are expanded upon below.

2.2 Traditional Single-Objective Approaches

The earliest approaches to systematic aircraft sizing revolved around the minimization of a single objective. This objective had to be some sort of aggregate measure of development, production, and operating cost. It could then be minimized subject to critical performance parameters borne of the mission the vehicle would be expected to accomplish. This could in turn help the engineer determine the most "affordable" vehicle, where "affordability" is best thought of as ratio of performance to life-cycle cost, a sort of performance-to-dollar efficiency. The wealth of data and relatively homogenous vehicle designs post-World War II provided engineers with the data to provide such a single objective, and it was found that Takeoff Gross Weight (TOGW or GW) seemed to vary linearly or logarithmically with most cost metrics. The era of single-objective sizing was born.

One problem with single-objective optimization at the time was the lack of reliable numerical methods (or the machines to work them) for optimization. Thus, most techniques were graphical. The first sizing methods were therefore graphical as well. These first systems engineering techniques sought to bring together the multiple disciplines related to aircraft sizing into a few parametric "scaling laws" related to TOGW. Hiller Helicopters published their R_f method in the mid-1950s as a graphical technique for minimum gross-weight estimation [Joy and Simonds, 1956; Simonds, 1956]. In this work, R_f referred to the various scaling laws for the fraction of fuel weight to gross weight. These were mostly statistical regressions with respect to dimensional parameters, environmental parameters, other constants, and, of course, gross weight. In this work, the idea was to graph the curves of fuel required and fuel available. The point where they met would therefore be the right "size" to best meet the requirements, hence the moniker "sizing." The R_f method would further be used for minimization of gross weight by plotting several fuel required and fuel available curves for different settings of critical sizing variables such as thrust-to-weight ratio and wing loading (or disk loading for rotorcraft).

As the availability of numerical methods (and machines to handle these computations) increased, the purely graphical methods began to give way to numerical schemes combined

with graphical aids. Most notably, the fuel-balance technique evolved. This was a numerical scheme used to automatically evaluate vehicle scaling laws and find the gross weight where fuel required and fuel available met, hence, "fuel balance." A basic flowchart of the numerical fuel balance method is presented in Figure 4. This age also saw the increased emphasis on *synthesis*, the act of bringing together multiple disciplinary analyses into a single, integrated scheme. This enabled the initial scaling laws to expand to include more sophisticated terms for aerodynamics, propulsion, weight, structures, cost, and others. This in turn made more design variables available to the systems engineer while optimizing the vehicle to its requirements. Now the design engineer could make decisions from carpet plots of weight versus performance metrics. Some basic fuel-balance parametric sizing and synthesis techniques are illustrated by Pugliese [Pugliese, 1971].

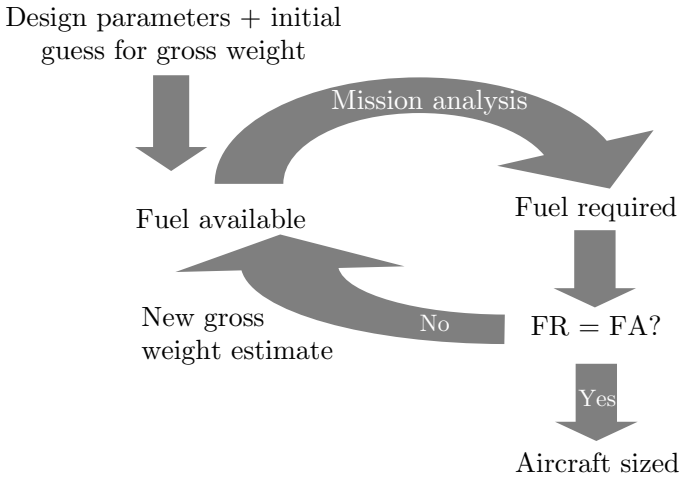

Figure 4: Numerical Fuel Balance Routine

In the years since, the statistical database for aircraft has increased substantially, allowing for more accurate and detailed scaling laws. Engineers sought to create better fits through more detailed, computer-assisted statistical techniques as well as by classifying various scaling laws for different classes of vehicles [Greenway and Koob, 1978]. Now "basic" techniques taught to today's undergraduate aerospace engineers include the tools provided by Roskam [Roskam, 1989], Mattingly [Mattingly et al., 2002], and Torenbeek [Torenbeek, 1982], to name a few. These techniques continue to work well for sizing single-mission

aircraft, especially those that fall within the realm of vehicle classes described thus far. However, these methods are becoming increasingly limited as engineers seek revolutionary concepts and configurations that are outside of the statistical database.

2.3 Modern Sizing Methods

The further increases in computational power over the years prompted the development of several stand-alone aircraft sizing codes. These monolithic codes are often semi-empirical, relying on statistical data and physics models that range from crude to highly sophisticated. Some examples of highly developed sizing and synthesis codes include NASA's FLight Optimization System (FLOPS) [McCullers, 1984] and AirCraft SYNThesis (ACSYNT) [Myklebust and Gelhausen, 1994] programs. Furthermore, these monolithic codes allow an engineer to track more than just gross weight; rather, they can have almost instant computation of other cost and performance metrics for more informed decision making and tradeoff analysis [Eckels, 1983; Simos and Jenkinson, 1986].

As advanced as they are, monolithic codes still suffer a lack of flexibility. Often, the codes contain assumptions that limit the diversity of configurations that can be investigated. Other times, in the name of generality or computational efficiency, these codes contain deliberately simplified analyses. In either case, they may not be appropriate on their own for the investigation of radical concepts or for higher-fidelity design exploration. However, they often have "handles" built in to allow for higher-fidelity results to be directly input into the system. This has allowed for the next evolution in systems synthesis and design: the integrated environment.

An integrated environment is a collection of disciplinary analyses capable of direct communication with one another. However, analysis codes use a variety of input and output formats, so it can be difficult to get the various codes to communicate effectively with any flexibility. Recent years have seen the development of environments capable of "wrapping" each code in such a way that inputs and outputs can be readily swapped amongst the codes. These codes (and wrappers) are available on a common server available to multiple workstations so that several engineers can access and change the data and run the sizing

programs as needed. Some environments used include Phoenix Integration's *ModelCenter* [Phoenix Integration, 2005] and Engineous Software's *iSIGHT* [Engineous Software, 2005]. An example of a *ModelCenter* environment is illustrated in Figure 5. These environments provide wrappers for a variety of programs, allow users to create custom wrappers, and give the user control over inputs and output parsing. They have been used to great effect as illustrated in a case study by Lockheed Martin [Carty, 2002]. Current developments in integrated environments cite the use of specialized formats that can be used without a central server, instead relying on distributed networks or the internet via XML protocols [Lin and Afjeh, 2002; Kam and Gage, 2003].

2.3.1 Multidisciplinary Design Optimization and Statistical Techniques

The availability of a suitable integrated environment gives the engineer enormous flexibility in the range of concepts that may be investigated. Further, once this environment is available, dozens of systems engineering, decision making, and optimization techniques become available. Perhaps the most fundamental is the Design Structure Matrix or n^2 diagram [AIAA Technical Activities Committee, 1991]. This tool allows for all of the disciplinary routines, dubbed Contributing Analyses (CAs), to be arranged in such a way as to show all of the interactions present in the entire system-level analysis. These interactions include inputs to some CAs that are composed of outputs of others. Depending on the arrangement within the DSM, these interactions can feedforward or feedback. Feedback causes error and further computational cost due to convergence, so the DSM can be arranged in such a way to eliminate or concentrate as many feeback loops as possible to reduce the overall system execution time. Feedforwards represent serial execution, so sometimes the DSM can be rearranged to parallelize CAs to further reduce total analysis time. The arrangement of the CAs can be determined automatically depending on these and other considerations [Rogers, 1997]. An example of DSM restructuring is presented in Figure 6. The DSM formulation opens up many different techniques such as Collaborative Optimization [Braun et al., 1996; Sobieszczanski-Sobieski et al., 1998], Optimizer Based Decomposition [Ledsinger and Olds, 1998], and Systems Sensitivity Analysis [Sobieszczanski-Sobieski, 1990; Olds, 1994].

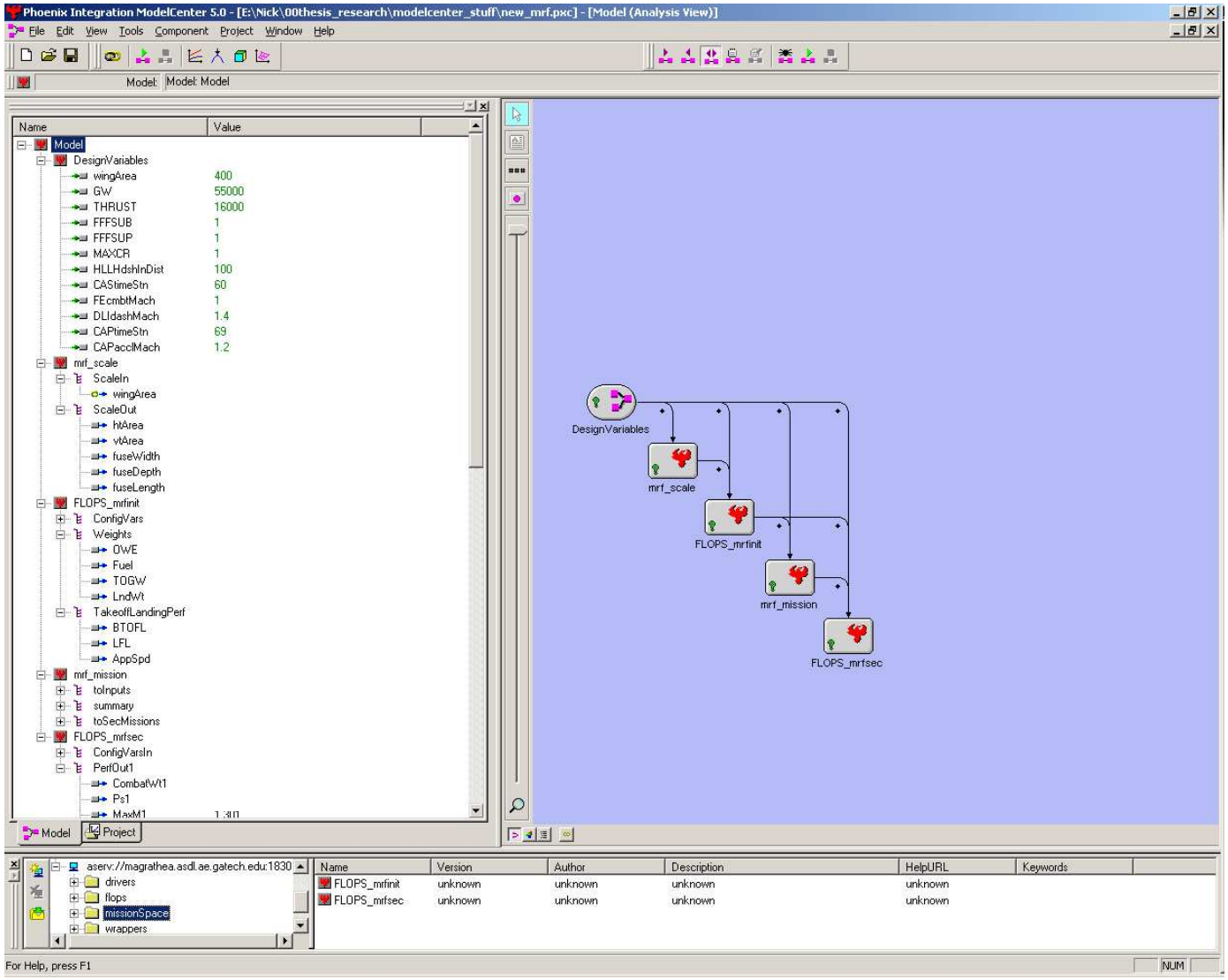

Figure 5: Example *ModelCenter* Integrated Environment

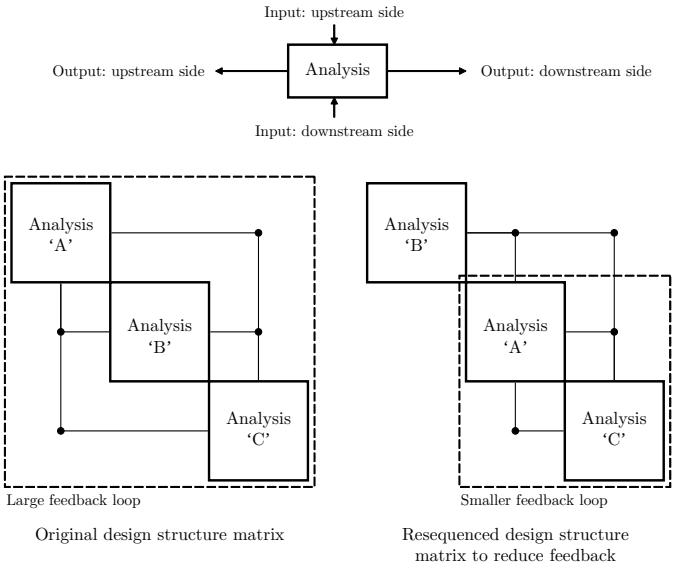

Figure 6: Sample Design Structure Matrix Before and After Restructuring

One drawback of working directly with the integrated environment is that the overall system evaluation time may be relatively long due to the execution times of the individual analyses, in series or parallel. Furthermore, feedbacks can exacerbate error or lead to computational instability. Even modern MDO methods may not enable an engineer to rapidly identify the best concept within the design space available to a given concept. Therefore, high-fidelity approximations and statistical techniques can be used to rapidly explore the large number of concepts available within the design space. Three principle methods are capable of this: Monte Carlo Simulation (MCS) of the design space combined with the original integrated environment, MCS of the design space combined with a surrogate model (approximation) of the original environment, or Fast Probability Integration (FPI) of the design space combined with the original environment [Fox, 1994; Mavris and Bandte, 1997]. The first is the highest fidelity solution but takes the most time; the latter two provide time savings at reductions in fidelity. All of these techniques rely on the generation of Cumulative Distribution Functions (CDFs) to determine the portion of the design space that can satisfy the specified requirements. These CDFs can be viewed individually to determine the probability of success for a given metric. However, this does not determine the probability of meeting more than just one particular metric. Bandte's Joint Probabilistic

Decision Making (JPDM) technique combines the multiple Probability Density Functions (PDFs) generated during probabilistic design to determine the portion of the design space that can meet more than one requirement [Bandte, 2000]. An illustration of a single CDF and a joint distribution function is given in Figure 7.

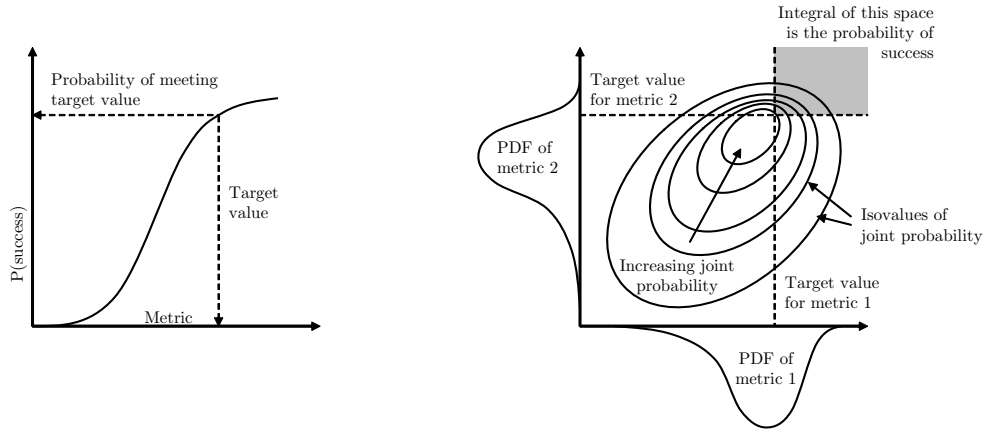

(a) Cumulative Distribution Function (b) Joint Probability Density Function

Figure 7: Probabilistic Decision Making

Several studies have been made using MCS with polynomial approximations [Mavris and Bandte, 1995; DeLaurentis et al., 1996], as well as MCS with FPI [Mavris et al., 1997]. A popular method for approximation of relatively well-behaved systems is Response Surface Methodology (RSM) [Neter et al., 1996] because it is capable of capturing linear, nonlinear, and interaction effects amongst the design variables. This technique is ultimately of great importance to this research and is discussed in greater detail in Appendix A.

The use of CDFs or JPDM also allows for probabilistic design of uncertain systems. There is usually some degree of uncertainty associated with various constants used within an analysis, especially those related to economic or environmental factors. These "noise" variables can be assigned ranges and probabilistically explored, much like a design space exploration. In this case, the CDF or JPDM environment does not give the portion of the design space capable of meeting a design goal; instead, it enables the designer to choose values for design variables that minimize the risk associated with uncertainty in the noise variables.

Design space exploration is only one of the uses of an integrated environment and approximation methods with statistical techniques. Technology forecasting is becoming increasingly popular as new requirements and operating environments push towards more radical solutions. Often, the state-of-the-art technologies embodied within the design space exploration exercises outlined above cannot meet these radical targets without some sort of technology infusion. Therefore, a method such as Technology Integration, Evaluation, and Selection (TIES) is used to identify promising technologies in conjunction with design space exploration [Mavris and Kirby, 1999]. TIES can be used probabilistically to determine the effect of uncertainty in each technology and thus pick the most robust suite available, ultimately reducing the risk of the design program [Kirby and Mavris, 1999]. Technology forecasting can also work in the other direction. That is, if an agency has a goal, such as reducing emissions or noise by a specified amount, Technology Impact Forecasting (TIF) can be implemented to identify the improvement required in individual technical metrics to meet this goal [Kirby and Mavris, 2002].

An area of recent interest within design space exploration methods is that of the role of requirements in systems design. Often, the methods outlined above refer to static requirements. The same statistical techniques can be applied to systems with varying requirements, and have been demonstrated with some success in conjunction with technology integration [Mavris and DeLaurentis, 2000; Baker and Mavris, 2001; Baker, 2002]. The research conducted within this document extends the work in the field.

2.3.2 Evolving Techniques

Of final interest in modern sizing methods is the recent introduction of volume-based techniques. Originally, the vehicle scaling laws were simply based on gross weight. Now, an increased emphasis is being placed on how the system scales volumetrically. Some preliminary "volume-balance" methods have been proposed by Raymer [Raymer, 2001]. Volume-based methods will continue to evolve as more radical, low fuel density concepts, such as hydrogen-powered low-emission vehicles, are considered [Guynn and Olson, 2002].

2.4 Multi-Mission Approaches

From its inception, sizing an aircraft required an enumeration of mission requirements. This "design mission" thus formed the basis of the fuel-required curve in the range (or endurance) related vehicle scaling laws. The design mission is met when the fuel required to propel the vehicle along the specified mission profile matches the fuel available within the vehicle. Over time, the design mission began to resemble less of a mission the vehicle would actually fly, but rather became a series of limiting conditions for what the vehicle could be expected to accomplish over a series of similar missions. The design mission approach represents a simplification of the actual operating conditions for a proposed vehicle so that it may fit into the current practice for sizing a vehicle. In a broader sense, this can be given as:

Observation 4: "Requirements" and their associated targets are often used to narrow the scope of aircraft sizing such that it can become a constrained single- or few-objective optimization problem.

As identified in the previous chapter, aircraft are increasingly being tasked with a wider variety of missions. This can make specification of a design mission difficult. One can envision several ways of incorporating disparate mission profiles into a single sizing mission, but each will likely fall under one of two main headings: size to the most critical mission, or size to a composite mission.

Sizing to the most critical mission is perhaps the simplest of these techniques and most similar to current practices. In this method, the designer first defines multiple mission profiles and associated mission-specific performance, payload, and cost constraints. The vehicle is sized to each of these missions subject to the various point-performance constraints associated to that particular mission, as well as the general non-mission specific constraints. Ultimately, the mission resulting in the largest gross weight vehicle becomes the only mission capable of meeting all of the other mission (fuel) requirements, and therefore becomes the de facto design mission. In this way, the vehicle is "overdesigned" with respect to some mission performance (range and endurance) metrics, though often others will suffer, such as off-design performance on the secondary missions and program cost.

One way to eliminate the potential for overdesign is to build a composite mission profile capable of parametrically modeling each of the specified missions. This composite mission would contain variable-length segments where necessary. These variables form a "mission space" that can be evaluated separately or together with the design space of the vehicle [Baker and Mavris, 2001]. Variation of both design and mission space values gives the designer a tool to further envision tradeoffs amongst the design variables and requirements. Ultimately, this can be quite helpful in choosing the final design mission when sizing the vehicle, and is the first step in eliminating the concept of a design mission entirely. Each point within the mission space represents a unique design mission to which the vehicle is sized. Secondary performance variables can be tracked and traded off in such a way that a solution may not meet the most stringent mission requirements, but may be able to more affordably meet most of them.

2.4.1 Shortfalls

By its vary nature, multi-mission systems design fits naturally into the realm of Multiple Criteria Decision Making (MCDM) techniques, including such aspects as the relative importance of each mission. This frame of mind is largely ignored in the sizing-based techniques listed above as they always boil down to specification of a single design mission meant to encompass all of the vehicle requirements. As system concepts become more radical and the specific missions required of the vehicle become more diverse, the chance of meeting all mission requirements (as in the first multi-mission sizing method) becomes improbable. Furthermore, "sizing" generally implies a fuel balance, which requires iteration and convergence to solve correctly. In a composite mission approach, large diversity in individual missions may entail composite mission parameter ranges that lead to numerical instability, especially during fuel balance convergence.

A final point worth mentioning is that neither of these techniques is fully adaptable to design with uncertain requirements. Certainly, the mission space model can capture uncertainty in mission-related elements, but other constraints, such as point-performance and

cost, may pose problems. The constraint lines can be moved, but constrained optimization techniques are generally not the well suited for probabilistic constraint evaluation. An unconstrained approach that allows for tradeoffs along the directions of improvement for the system-level metrics may provide a more robust solution with respect to changes in the requirements.

2.4.2 Multipoint Sizing for Multi-Mission Vehicles

One problem with any form of multi-mission "sizing" is that a fuel balance is always implied. In order for a fuel balance to have any meaning, a unique design mission must be specified that may or may not accurately represent the overall mission expectations of the aircraft. As mentioned above, the fuel balance was originally created as a method to estimate gross weight for mostly single-mission aircraft based on statistical scaling laws. It is possible to run this process in reverse; that is, specify gross weight and other pertinent design parameters and attempt to find which mission profiles the vehicle can fly. Such a procedure would be especially well-suited for multi-mission vehicle design because it becomes a simple matter to track pertinent individual mission performance parameters (such as segment range, endurance, and point performance). Instead of a fuel balance, the gross weight and other design parameters could be parametrically varied and mission performance tracked in each case. The best multi-mission aircraft would then be the vehicle with the design parameters and gross weight that best "fit" the individual mission requirements.

This approach is attractive because it enables MCDM to become an integral part of the design process. Multipoint sizing can use MCDM to directly tradeoff metrics for all of the individual missions as well as other, non-mission specific metrics. It is especially well-suited for automation as most aircraft analysis codes work much better and faster without the iteration and convergence required for a fuel balance.

However, such an sizing method requires selection of an MCDM method appropriate to aerospace systems design in the presence of uncertainty. This is a very diverse field that must be able to logically reduce the concepts into a small group of distinct solutions or objectives that can be handled rigorously and repeatedly. Therefore, the literature search

must expand to include discussion of a variety of decision making techniques. As this search is performed, the reader must keep in mind the following question, which is formalized as the third research question of this document:

Question 3: Is there a decision making formulation that is well-suited to systems design with uncertain requirements? (Observation 4)

CHAPTER III

DESIGN AND DECISION MAKING

Almost every aspect of life involves some form of decision making, whether it is large choice such as what job to pursue or a small choice such as what shirt to wear. Large or small, each decision has consequences that require us to forecast the effect of various alternatives. Once the choice is made, it is a matter of time to find whether the forecast was correct or erroneous due to some unexpected event or unanticipated factor.

Engineering design also involves decision making and forecasting, though the methods used appear to be far more concrete, at least on the surface. However, most of these analyses require a number of assumptions that may render the decision inaccurate. Thus, engineering design will have some degree of uncertainty.

Many design decisions involve the use of mathematical or numerical optimization to reach an "ideal" setting of variables with respect to a single criterion. Unfortunately, optimization is not a substitute for decision making. Zeleny challenges his readers with the statement [Zeleny, 1982]:

> No decision making occurs unless at least *two* criteria are present. If only one criterion exists, mere measurement and search suffice for making a choice.

This implies that single-objective optimization is not decision making at all. An analogy for the existence of multiple criteria in decision making can be made in the choice of shirt to wear. One may consider comfort, appearance, protection from the elements, and many other criteria. If only comfort were important than one would simply have to search through their closet and find the most comfortable shirt. Thus, optimization is more about developing and executing the right search algorithm for a single-objective problem whereas decision making is concerned with making a choice from multiple objectives.

Another necessary condition for decision-making is the availability of at least two distinct

alternatives. Choosing which shirt to wear is a moot point if an individual only owns one shirt or 100 identical shirts. If the option exists to not wear a shirt at all, then a decision can be made amongst differentiated alternatives.

Unfortunately, humans are poor at making rational, repeatable decisions despite the fact that they experience decision making on a daily basis. This is especially true when there are many more than two criteria to consider. The subjective nature of decision making, along with inherent biases and lack of proper processing of information, can lead to poor judgement. Shepard notes [Shepard, 1964]:

> At the level of the perceptual analysis of raw sensory inputs, man evinces a remarkable ability to integrate the responses of a vast number of receptive elements according to exceedingly complex nonlinear rules. Yet once the profusion and welter of this raw input has been thus reduced to a set of usefully invariant conceptual objects, properties, and attributes, there is little evidence that they can in turn be juggled and recombined with anything like this facility.

Shepard continues in this work by referring to a two-dimensional experiment with linearly correlated attributes. The subjects surveyed would make a plethora of choices related to individual biases for either of the dimensions. He concludes that while humans are capable of making subjective decisions, one should have some sort of computational aid to the process if at all possible.

Certainly, one needs some sort of analytical means to help evaluate and select concepts with multiple attributes. What follows is a description of some important components and a few selected techniques in the realm of Multiple Criteria Decision Making (MCDM).

3.1 Pareto Optimality

An attractive concept in MCDM is the reduction in number of alternatives one evaluates. One such reduction concept is to only choose from concepts that are Pareto optimal. A Pareto-optimal solution, also known as an efficient solution, is an alternative that is not dominated in at least one criterion. That is, there is no other feasible alternative with

the same or better performance considering all criteria [Zeleny, 1982]. The locus of these solutions is known as a Pareto frontier (also efficient frontier, efficient surface, and other permutations). This moniker refers to the work on economic theory by the Italian economist Vilfredo Pareto with regards to economic efficiency [Pareto, 1971]. A schematic of a two-dimensional "larger-is-better" Pareto frontier is given in Figure 8.

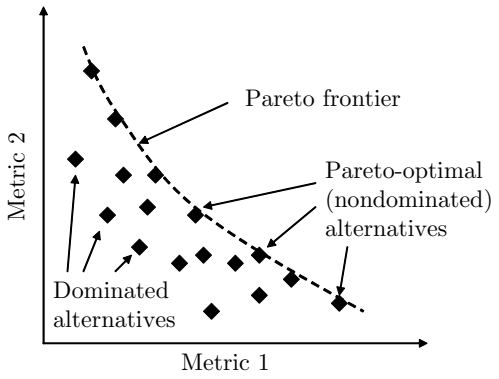

Figure 8: Two-Dimensional Pareto Frontier

In the strictest sense, one *always* wants to choose a solution from the Pareto frontier. Choosing another feasible solution not on the frontier implies that the decision maker is giving up some "free" performance in at least one of the decision metrics. In practice, however, this may not necessarily be the case. In order for Pareto optimality to hold, one must ensure that *all* of the decision metrics of interest are present, no matter what the nature of the data: cardinal, ordinal, and otherwise. Often, a decision maker may choose an alternative not on the Pareto frontier simply because another decision metric may be hard to quantify mathematically or may not be present in the data set. The remedy for this is to attempt to capture all of the decision criteria no matter what the nature of the data. In cases where subjective criteria emerge one can at least attempt to quantify the ranking relationship of the alternatives.

However, problems with Pareto optimal solutions do not end even if the decision maker has correctly quantified all of the metrics. The resolution of the Pareto frontier becomes increasingly difficult as the number of objectives increases. This has been documented for multiobjective problems where evolutionary algorithms are used to glean information on the

Pareto frontier [Deb, 2001]. Here, an initial population is necessary and an estimate can be made as to what fraction of this population will be nondominated. Guidance for population size selection for up to 10 objectives can be found in Figure 9. This figure shows that the proportion of nondominated solutions increases dramatically as the number of decision metrics increase. In effect, every alternative approaches Pareto-optimal performance as more metrics are added. Convergence depends greatly on the nature of the problem, but is a documented occurrence for large problems.

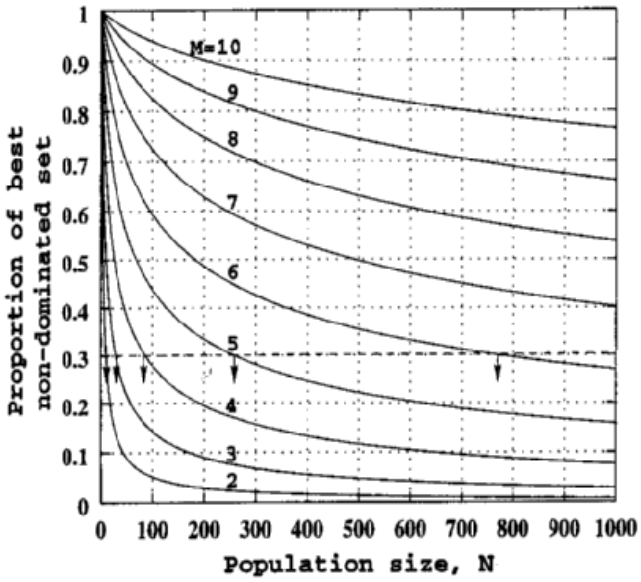

Figure 9: Nondominated Population Fraction for Increasing Number of Objectives [Deb, 2001]

Furthermore, the computational effort required to identify nondominated solutions increases nonlinearly as the population size increases. Some experimental observations show that computational effort increases approximately with the square of population size [Borer and Mavris, 2004]. As can be inferred from Figure 9, large populations contain mostly nondominated solutions. This seems to imply that pre-screening dominated solutions is not worth the computational savings realized from a reduction in number of decision alternatives for problems with many objectives. An appropriate analogy is to note that, with enough metrics, every concept becomes the best at something.

The fraction of nondominated population size can be carried over to continuous decision

spaces. Here, the Pareto optimal solutions would also be a continuous subset of the decision space. As the number of decision metrics (objectives) increases, the portion of the decision space that is completely dominated decreases until it is insignificant. Formally, this becomes the next observation:

Observation 5: As the number of decision metrics grows larger, the percentage of nondominated solutions increases until soon almost all portions of the decision space are nondominated.

This observation implies that resolution of the Pareto frontier is unnecessary for large decision-making problems. However, the concept of Pareto optimality is still attractive, so it is still desirable to use an MCDM technique that will always choose a nondominated solution in the event that dominated solutions exist within the decision space.

3.2 Axiomatic Design

While not explicitly under the heading of MCDM, Axiomatic Design is a process that seeks to resolve some of the issues with designing to multiple requirements. Notably, it attempts to remove conflict by maintaining independence amongst requirements. Suh defines two design axioms [Suh, 1990] as:

The Independence Axiom: Maintain the independence of the Functional Requirements.

The Information Axiom: Minimize the information content of the design.

The independence axiom ultimately establishes that the Functional Requirements (FR) must be independent such that only *one* is modified for any perturbation of a Design Parameter (DP). The information axiom states that the best design is the one which minimizes the number of FRs and DPs required to define the design.

An oft-used axiomatic design example is the choice of water faucet for household use as seen in Figure 10. In this case, the FRs are to control water temperature and water flow rate. A typical, "bad" design for a faucet has two handles and one spigot; one handle controls

the flow of hot water and one of cold water. Here, one cannot independently control either temperature or flow rate; rather, the user must modify inputs to both handles to change one of the outputs. The Axiomatic Design approach would select a more modern faucet with a two-degree of freedom handle. In the latter case, the vertical rotation of the handle controls the flow rate and the horizontal rotation controls the temperature. Here, the independence of the FRs is maintained with respect to the DPs.

(a) Standard Design (b) Axiomatic Design

Figure 10: Axiomatic Faucet Design [MIT Axiomatic Design Group, 2005]

In theory, Axiomatic Design seems to be a good approach for design. In practice it may be much harder to enforce, especially in systems engineering situations where the design parameters are high-level abstractions of individual subsystems and the functional requirements are industry or government standards. Often it becomes impossible or improbable to discern individual inputs for the design parameters. An aggregate set of requirements may be possible but difficult to relate. If a decomposition-based approach were used, it may become possible to create a set of independent functional requirements with transparency to the original requirements, though it would be much harder to enforce independence of design parameters. The attractive feature of independent requirements lies in the decision-making itself: if the requirements are truly independent there should be no bias from one solution to the next.

3.3 Multiple Criteria Decision Making Techniques

Multiple Criteria Decision Making is a necessarily broad subject area. There are many classes and subgroups of methods depending on the nature of the criteria considered, the

involvement of the decision maker, and the nature of the objective sought. Though the opinions of many authors differ on the subject, in this document MCDM will be used to refer to two different classes of methods: Multiple Attribute Decision Making (MADM) and Multiple Objective Decision Making (MODM) [Yoon and Hwang, 1995]. Some consider Multiple Attribute Utility Theory (MAUT) to be under this heading as well, but this subject will not be covered in detail here.

The principle difference between MADM and MODM techniques is the pertinent application. MADM techniques are focused on ranking and selection of a few options from a discrete pool of alternatives, usually not subject to constraints [Hwang and Yoon, 1981]. On the surface, MADM is more appropriate when a decision maker must choose from a pool of predefined concepts, such as the government's choice of five competing fighter configurations from different companies or one's choice of a stock portfolio. MODM techniques are more appropriate for design applications, as they focus on multiple objectives within a continuous space and are subject to active constraints [Hwang and Masud, 1979]. Both techniques capitalize on various weighting techniques to determine ranking or preference relationships between the various criteria.

A variety of techniques are available for both MADM and MODM depending on the nature of the information available to the decision maker or algorithm. Figures 11 and 12 are reproduced from the work of Hwang and his colleagues [Hwang and Yoon, 1981; Hwang and Masud, 1979] and display a taxonomy of MADM and MODM techniques, respectively. Note that MADM techniques vary by the type of information available whereas MODM techniques are categorized by both the type of information and the stage at which this information is needed.

The decisions made within aerospace systems design usually refer to cardinal data; that is, data associated with a quantity but not necessarily a preferential order (note that a ranking relationship may be derived from cardinal data if a goal or direction of improvement is noted). The data retrieved from engineering analyses are, with few exceptions, cardinal. Examples include gross weight, cost, sustained turn rate, and takeoff field length, to name a few. Some more subjective criteria may be ordinal in nature, that is, simply ranked with

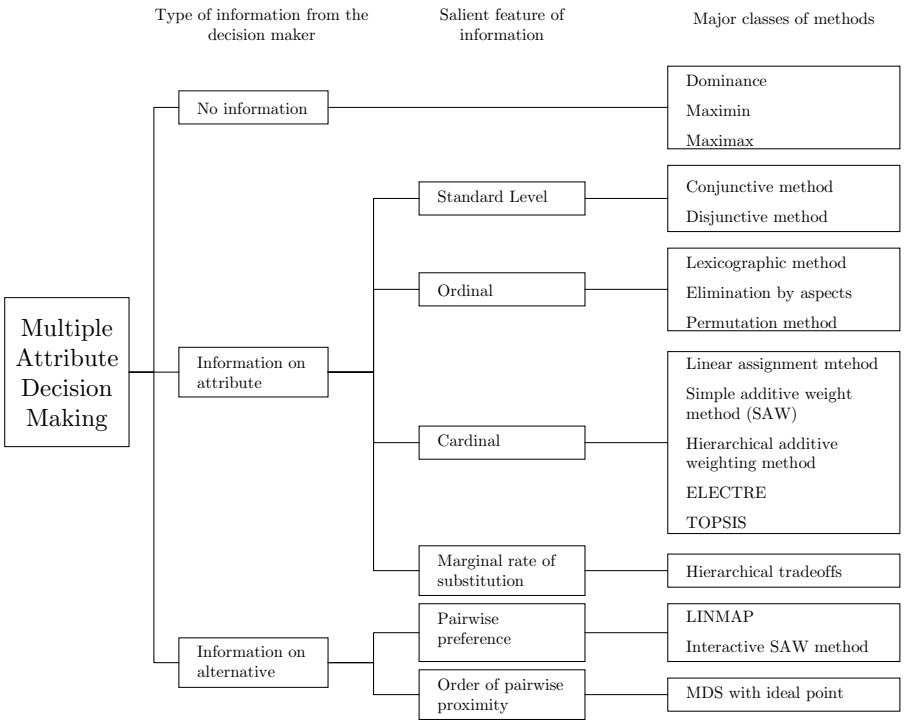

Figure 11: A Taxonomy of Methods for Multiple Attribute Decision Making [Hwang and Yoon, 1981]

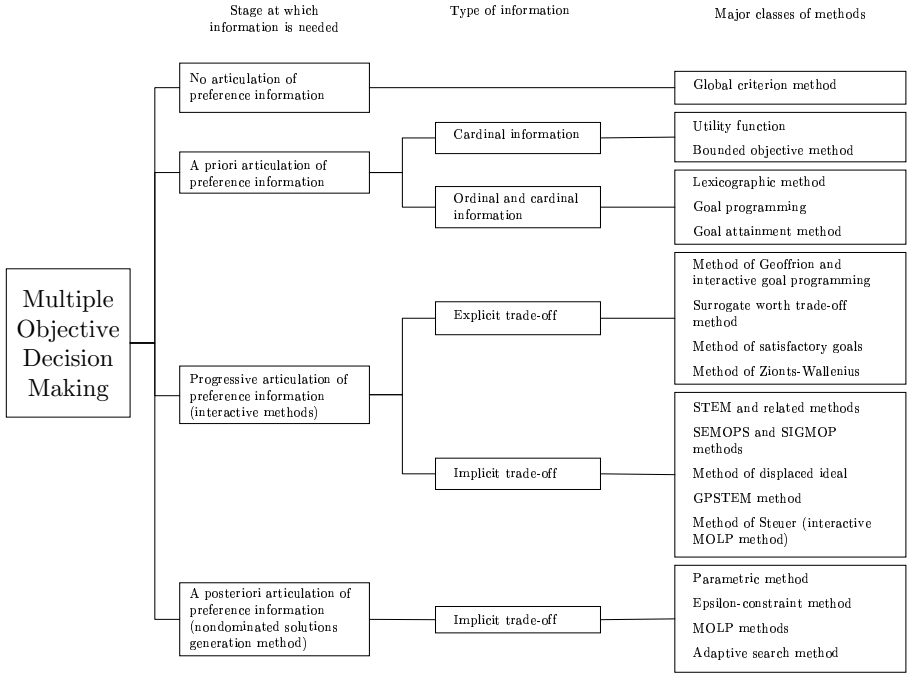

Figure 12: A Taxonomy of Methods for Multiple Objective Decision Making [Hwang and Masud, 1979]

respect to the other alternatives. An example may be a qualitative measure of reliability as low, medium, or high. This is far less common in engineering analysis. Therefore, only some of the cardinal methods shown in Figures 11 and 12 or their associated outgrowths will be elaborated upon further. For a more complete description of these techniques the reader is directed to more comprehensive references [Hwang and Masud, 1979; Hwang and Yoon, 1981; Zeleny, 1982; Triantaphyllou, 2000].

Most MCDM techniques assume monotonically increasing utility. If the decision maker is asked for any form of preference information, it is in the form of a static relative importance value which simply scales the contribution of the given metric to the composite objective function. This relative importance value simply scales the utility of the metric, which because of the monotonic assumption is simply bound to the functional form of the metric within the decision space. These techniques also assume that the decision metrics are independent of each other. As will be seen later, these assumptions can lead to poor results and will require some modification to be compatible with a wider range of design problems.

3.3.1 The Ideal Solution

A powerful concept in cardinal MCDM techniques is that of the *ideal solution*. This is the solution that embodies the best answer within the design domain for each of the attributes. Mathematically, the ideal solution can be stated as

$$Y^* = (y_1^*,\ y_2^*,\ \ldots,\ y_n^*) \tag{1}$$

where Y^* is the ideal solution and y_n^* is the best value of the n^{th} attribute. This solution is often made up of attributes from multiple alternatives (if such a solution was available with one alternative, it becomes the obvious choice). Sometimes the concept of the negative ideal solution becomes necessary for certain MADM techniques. As its name implies, the negative ideal solution has the opposite definition as the positive ideal. This represents an aggregate of the worst attributes from the available alternatives. The negative ideal solution is sometimes referred to in the literature as the "anti-ideal." Figure 13 shows a simple schematic of the positive and negative ideal solutions for a finite set of alternatives in two "larger is better" dimensions.

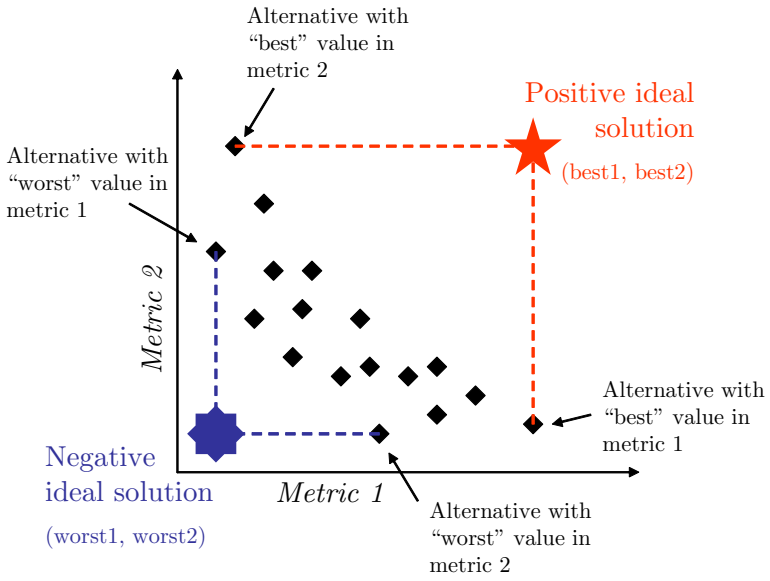

Figure 13: Positive and Negative Ideal Solutions from Several Alternatives

3.3.2 Simple Additive Weighting

Perhaps the most elementary, and most popular, cardinal MADM technique is the Simple Additive Weighting (SAW) method, also known in various forms as the Weighted Sum (WS) or Overall Evaluation Criterion (OEC) method. In these techniques, the attributes of each alternative are normalized, usually with respect to the best attribute value amongst the pool of alternatives (i.e. the respective value in the positive ideal solution). Sometimes the values are normalized by a vector sum of the characteristics of each attribute. Next, a series of numerical “weights” (relative importance values) are prescribed by the decision maker. These can be based on subjective observations by experts or on more advanced relative importance generation methods, to be covered later. These weights are usually normalized such that their sum is equal to one. Each alternative is evaluated by multiplying the weights by the normalized score in each respective attribute, then summing up the total. The alternative with the highest score is considered most preferable. Mathematically, SAW (when normalized by the best attribute) figures as

$$A^* = A_i \,|\, \max \frac{\sum_{j=1}^{n} (w_j \, \overline{y}_{ij})}{\sum_{j=1}^{n} (w_j)} \tag{2}$$

where A^* is the best alternative, A_i is the i^{th} alternative, n is the number of attributes, w_j

is the relative importance of the j^{th} attribute, and $\overline{y}_{ij}$ is the j^{th} normalized attribute of the i^{th} alternative. If "larger is better" for all y_j, then the normalization follows as

$$\overline{y}_{ij} = \frac{y_{ij}}{y_j^*} \tag{3}$$

where y_{ij} is the "raw" value of the j^{th} attribute of the i^{th} alternative. For a "smaller is better" case, the reciprocal of (3) is used.

Though simple and easy to understand, SAW and related methods are not well suited for rigorous decision making. Most notably, these methods will never pick a non-convex point on a Pareto frontier and will instead only choose the extremes [Mullur et al., 2003]. This is best visualized by projection of a non-convex frontier onto a series of SAW indifference curves. An indifference curve is a line along which a method will receive the same score. Figure 14 shows this for a two-dimensional "larger is better" series of alternatives with a non-convex Pareto frontier. Here, SAW will always rank alternatives A and B higher than alternative C, even though the latter alternative may be the best available mix of performance available.

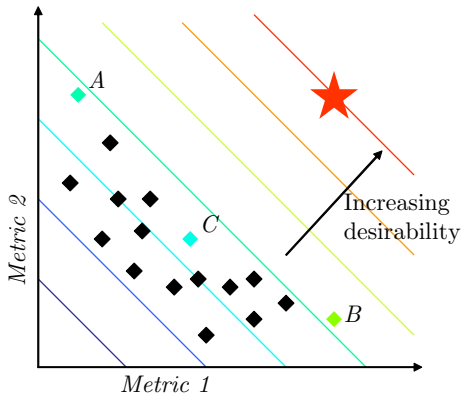

Figure 14: SAW Indifference Curves Projected Onto Non-Convex Pareto Frontier

3.3.3 TOPSIS

One MADM technique that attempts nonlinear decision-making is the Technique for Order Preference by Similarity to Ideal Solution (TOPSIS) [Yoon and Hwang, 1995]. The basic idea of TOPSIS is to rank the solutions based on the combination of Euclidean distance

from the positive *and* negative ideal solutions. The concept of Euclidean distance fits well into the spatially-oriented minds of most decision makers.

Conceptually, TOPSIS does not begin much differently than the SAW-related methods. Of primary importance is the normalization of the individual attributes, though TOPSIS accomplishes this through the 2-norm via

$$\overline{y}_{ij} = \frac{y_{ij}}{\sqrt{\sum_{i=1}^{m} y_{ij}^2}} \tag{4}$$

where m refers to the number of alternatives and all other notation is as in (3). Once normalized, the separation from the positive and negative ideal solutions is measured for each alternative through

$$S_i^* = \sqrt{\sum_{j=1}^{n} \left(w_j(\overline{y}_{ij} - y_j^*)\right)^2} \tag{5}$$

$$S_i^- = \sqrt{\sum_{j=1}^{n} \left(w_j(\overline{y}_{ij} - y_j^-)\right)^2} \tag{6}$$

where S_i refers to the separation measure, the subscript '$*$' refers to the positive ideal solution, and '$-$' refers to the negative ideal solution. All other notation is as before.

These separation measures are combined into a single measure dubbed the *closeness to the ideal solution* for each alternative. This is figured from

$$C_i^* = \frac{S_i^-}{S_i^* + S_i^-} \tag{7}$$

where C_i^* is the closeness measure for the i^{th} alternative. The solutions are then ranked in descending order; i.e. the alternative with the highest value for C_i^* is considered the "best," with the next-highest value as the "second-best," and so on.

The 2-norm would seem to indicate that this method is capable of capturing some non-convex Pareto optimal solutions. However, the use of both the positive and negative ideal solution measures flattens the indifference curves halfway between the positive and negative ideals. Therefore, this still leads to poor resolution and ranking of solutions on non-convex Pareto frontiers. Figure 15 shows two cases of TOPSIS, both for "larger is better" cases in two dimensions.

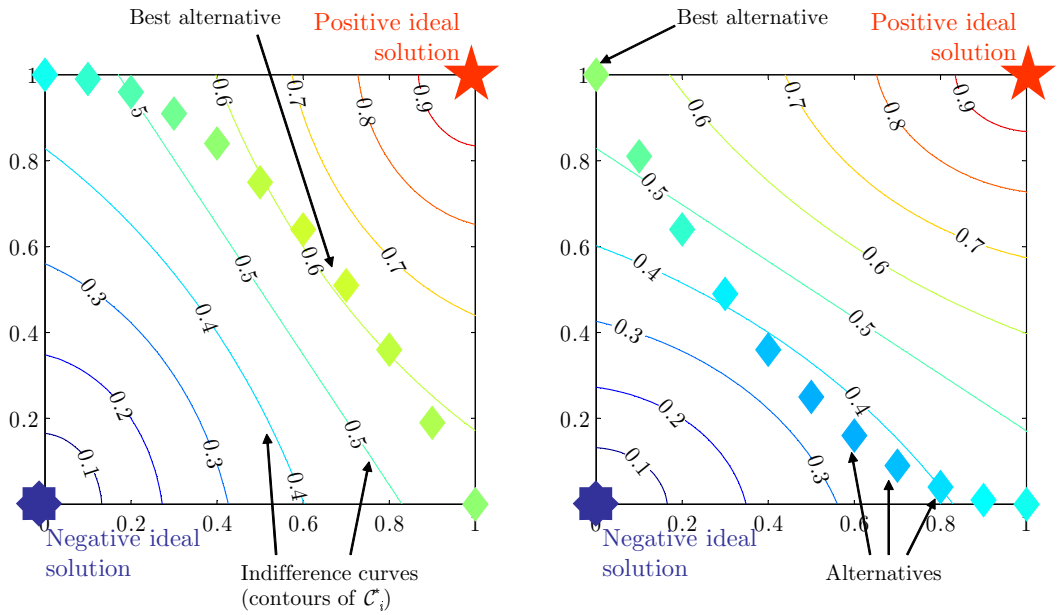

(a) Convex Pareto Frontier

(b) Non-Convex Pareto Frontier

Figure 15: TOPSIS Solutions for Two Non-Convex Pareto Frontiers

Figure 15 shows that the TOPSIS indifference curves given by this simple exercise are different than SAW. However, this method is still not capable of ranking non-convex alternatives and instead will rank an extreme alternative in this situation. This behavior of TOPSIS is cited by Yoon as being rational. He states [Yoon and Hwang, 1995]:

> When a [decision maker] recognize's ones solution is closer to the negative-ideal than to the positive-ideal, the [decision maker] is inclined to pick an alternative that consists of the best and worst attributes rather than one with two worse attributes. For example, one might want to get one A grade and one F grade rather than two D grades.

Hence, Yoon believes that a decision maker would never wish to choose a non-convex compromise solution over an extreme "thoroughbred" solution that has the best performance in one measure and the worst in another. However, there may be some cases where the decision maker may wish to enable shallow non-convex compromise or even all forms of compromise. TOPSIS does not allow such tailoring.

3.3.4 Compromise Programming

Compromise Programming (CP) is a quasi-MODM technique that is a combination of Multi-objective Linear Programming and Goal Programming [Zeleny, 1982]. The former approach is an extension of the popular linear programming techniques, such as the Simplex method [Chvátal, 1983] for problems with multiple objectives, hence its MODM identification. Goal programming is usually a linear programming technique as well, except with modified objective functions to reflect a specific goal. This is more of a "nominal the best" style of optimization where the goals frequently lie within the design domain but may not necessarily be a maximum or minimum of the alternatives within the concept space (hence the quasi-MODM identification). Compromise programming is very flexible and can be used for nonlinear problems. It too uses the concept of the positive ideal solution and in some cases the negative ideal solution.

A popular method for CP uses the positive and negative ideal solutions (or, in a continuous space, the "best" and "worst" values) and has an objective function of the form [Zeleny, 1982; Vanderplaats, 1999]

$$F(\vec{x}) = \left\{ \sum_{j=1}^{n} \left[\frac{w_j (F_j(\vec{x}) - F_j^*)}{F_j^- - F_j^*} \right]^p \right\}^{\frac{1}{p}} \tag{8}$$

where $F(\vec{x})$ is the overall objective function to be minimized, $\vec{x}$ is a vector of the design variables, $F_j(\vec{x})$ is the j^{th} objective (attribute) function, F_j^* is the "best" value of $F_j(\vec{x})$ (analogous to y_j^* in (3)), F_j^- is the "worst" value of $F_j(\vec{x})$, and p is a parameter dependent on the type of norm to be used in the optimization. The most common values for p are 1, 2, and ∞. When $p = 1$ the CP algorithm is essentially a weighted sum technique. For $p = 2$ CP finds the solution the minimum Euclidean distance away from the positive ideal, and for $p = \infty$ CP will find a solution that minimizes the maximum deviation from the ideal. The change in solution for different values of p is demonstrated for a two-dimensional "larger is better" convex and non-convex case in Figure 16.

Compromise programming seems well-suited for design problems because it is essentially a MODM (hence continuous) technique but allows the user to specify goals. It also allows the decision-maker to tailor preferences towards non-convex compromise solutions via p.

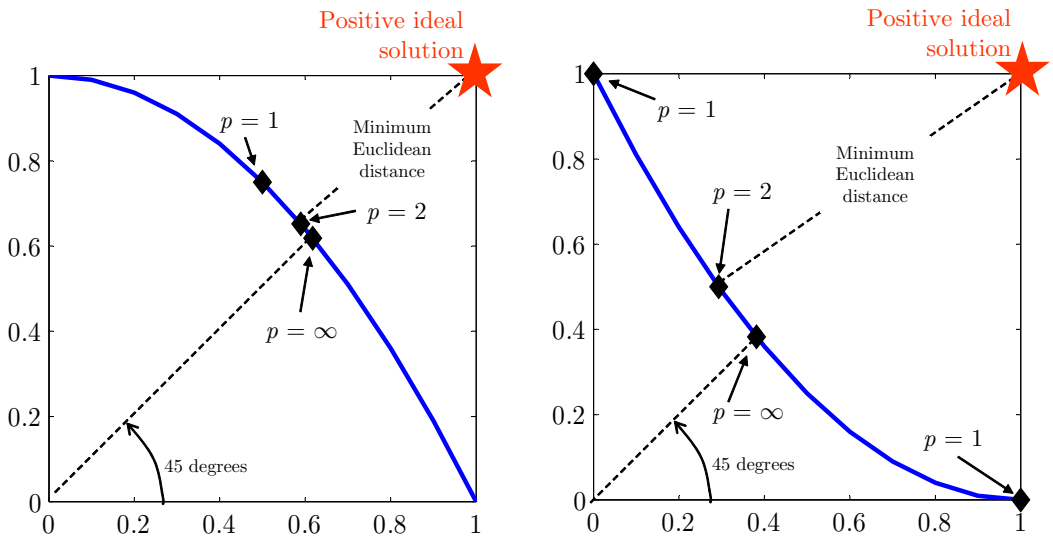

(a) Convex Pareto Frontier

(b) Non-Convex Pareto Frontier

Figure 16: Compromise Programming Solutions for Different Values of p

Furthermore, it is adaptable to a variety of normalization methods in addition to the ideal solution method given in equation (8).

3.3.5 MCDM for Systems Design

The choice of decision-making technique for systems design removes some of the burden of executing tradeoffs manually for the design engineer. However, the engineer must instead determine new criteria for the decision-making technique to be effectively used. It now becomes important to specify the relative importance of each metric to enable tradeoffs as opposed to actually specifying satisfactory levels of performance (though those too may still be important and can enter the problem as constraints). Further, as indicated from the small survey above, the individual MCDM techniques assign preference differently to various compromise situations, especially for non-convex solutions.

Systems design is not necessarily well-suited to a traditional design and decision making environment. Most detail design environments require fixed requirements and constraints, one or very few objectives, and a continuous or mixed continuous-discrete design space. The solution is often based on closed-form analysis. In contrast, most decision making environments are set up to handle a discrete solution space, have several attributes to consider for

each alternative, and are reliant on highly subjective methods. The former is well-suited to detail design optimization and the latter is better for making decisions from a pool of predefined concepts and "what-if" scenarios such as risk assessment. Effective systems design is often a combination of both environments. Some design and MDO frameworks were mentioned in Chapter II; these, combined with the MCDM techniques outlined in this chapter, form the building blocks for effective multiple criteria systems design.

CHAPTER IV

DECISION MAKING FOR LARGE-SCALE PROBLEMS

Decision making is an inherently multi-criteria problem that cannot be replaced by simple constrained optimization. Optimization is still a powerful tool, and can be used on a composite objective function based on the values of multiple decision metrics. This automated form of decision making comes with a host of additional caveats to consider: the typical assumptions and drawbacks of the chosen optimization method, and the assumptions and simplifications within the composite objective function (stemming from the decision-making algorithm). This is in addition to the limitations of the actual integrated analysis routine used in the optimization function calls. All of these issues, and more, demand the attention from the systems designer attempting to find the most desirable systems architecture. Fortunately, there is an abundance of literature to guide the systems engineer for selection of an appropriate optimization routine and integrated analyses. However, the effect of the assumptions and limitations of a specific decision-making routine on systems design has not been discussed in much detail. That is the aim of this research. This is not to say that multiple criteria systems design problems have not been discussed by the literature; indeed, there are many documents that enumerate strategies for resolution of the Pareto frontier, but these give little guidance as to actual concept selection from the nondominated concepts. Furthermore, as described in Section 3.1, the resolution and usefulness of the Pareto frontier diminishes considerably as the number of decision metrics increases. This can be stated as the final research question:

Question 4: Is there a benefit to finding nondominated solutions in large-scale systems design? (Observation 5)

The aim of this chapter is to attempt to create a generalized MCDM formulation for systems design and to study its results when applied to a design environment. For this

document, the moniker "large-scale problem" is used to describe design problems with a large number of decision metrics, generally with as many or more metrics than design variables.

The four research questions must be answered appropriately to enable large-scale systems design. As is often true with research, these questions and their answers will not be sufficient and will be revisited in later chapters as the generalized MCDM formulation evolves. However, these questions guide the research path and are important to keep in mind throughout the entire document.

4.1 Generalized Probabilistic MCDM Formulation

Fundamental to the description of a large-scale MCDM environment is the creation of a generalized probabilistic MCDM formulation. This environment should be able to capture uncertainty in the requirements themselves or in the decision maker's preference regarding one metric over another. Such a formulation must exhibit three salient qualities:

- Probabilistic
- Lack of internal constraints;
- Implicit tradeoffs.

Large-scale problems require a decision making environment that is probabilistic to handle uncertainty in the target values for the decision metrics, i.e. the requirements. Since this is an MCDM formulation, uncertainty in the requirements can be mapped over to uncertainty in the relative importance of each requirement. In this way, the actual attainment value of the requirement is not considered as much as its underlying utility. MCDM formulations use simplifying assumptions for monotonically increasing utility, so the best tradeoff attainment levels for each metric are tied to the functional form of the requirement itself along with a relative importance ("weighting") factor to scale this utility. Hence, an MCDM formulation can be made probabilistic by placing distributions about the relative importance of each metric.

Lack of internal constraints is very important in such a formulation because these constraints can bias an integrated environment or cause bad fits to data if surrogate models are used. This is often necessary for probabilistic analyses (refer to Chapter II for more details). These internal constraints may require iteration and convergence that are not transparent to the designer and therefore can cause problems when specifying other requirements. Furthermore, many constraints may actually be requirements or decision metrics and therefore it is important to allow the decision maker external access to these values.

Finally, any non-trivial decision making formulation requires tradeoffs. For large problems, the sheer number of tradeoffs is a combinatorial of the number of metrics, i.e. four requirements involves up to $3 + 2 + 1 = 6$ tradeoffs, ten requirements can involve $9 + 8 + 7 + 6 + 5 + 4 + 3 + 2 + 1 = 45$ tradeoffs, and so on. Therefore, it quickly becomes difficult to handle explicit tradeoffs. These can be made implicit with many MCDM formulations simply through definition of a positive and negative ideal solutions along with relative weights. Compromise programming is an attractive option because it can normalize the data to the positive and negative ideal solutions, is a continuous formulation, and allows the decision maker flexibility regarding the type of tradeoff to be made via the 1-, 2-, or ∞-norm. Compromise programming will also *always* capture a nondominated solution [Ismail-Yahaya and Messac, 2002].

These statements can be combined to form four hypotheses that serve as the backbone of this research. These are:

Hypothesis 1: Effective multiple criteria decision making for large-scale systems design requires an open, internally unconstrained integrated environment capable of evaluating all of the system-level requirements. (Question 1)

Hypothesis 2: Uncertainty in the target value of an individual requirement can be captured by:

(a) allowing the decision-making environment to tradeoff amongst multiple requirements, and

(b) mapping the uncertainty in each metric to a probability distribution about each

metric's relative importance, whose nature and bounds are determined by expert opinion. (Question 2)

Hypothesis 3: A decision making formulation must be chosen that always ranks nondominated solutions and is capable of non-convex tradeoffs. The solution that is most robust to change in the requirements is the MCDM solution whose rank is the most consistent for a range of individual relative importance measures. (Question 3)

Hypothesis 4: The subset of non-dominated solutions within a decision space can be adequately represented by the entire decision space for problems with many decision metrics. (Question 4)

These statements need to be tested to determine their validity. If they appear to be valid, further tests are necessary to determine what, if any, limits must be observed. Some research has been performed on related hypotheses in the past. This is summarized in the following section to provide some insight for the construction of research tasks.

4.2 Case Study: Notional Multi-Role Fighter

A case study was performed on the requirements selection and design of a notional multi-role fighter in an attempt to gain more information on the pertinent issues associated with large-scale systems design problems. This fighter was based on the growth of the McDonnell-Douglas F/A-18C Hornet configuration to the F/A-18E/F Super Hornet series of aircraft proposed by Boeing. The Super Hornet is supposed to supplement and eventually replace the missions currently performed by three aircraft in the U.S. Navy's inventory [Young et al., 1998]: the F/A-18C Hornet, A-6F Intruder, and F-14D Tomcat. The general idea of this study was to attempt to "grow" an existing aircraft configuration to attempt to meet or exceed the mission capabilities of the legacy aircraft. The study was conducted in such a way as to keep the growth configuration flexible to eventually investigate if the F/A-18C was the most effective configuration to work from. The study that follows is a summary from some recently published literature on the subject [Borer and Mavris, 2003, 2004]. The reader is referred to these documents for a more comprehensive review.

4.2.1 Problem Formulation

The main formulation of this study involved six steps: Requirements Classification, Baseline Concept Definition, Creation of Integrated Environment, Decision Space Population, Exploration of Requirements Tradeoffs, and finally, Decision Making. The first step was universal for all configurations, while steps two through five could be repeated for different concepts if necessary. The final decision could be based on the results from several concepts. This study only considered the F/A-18C configuration but the overall formulation was generic enough that any (or several) baselines could be used.

The requirements classification followed from examination of the missions of the legacy aircraft the Super Hornet was meant to replace. However, some of the latest data on the legacy aircraft was not available, so data was used from earlier models of the same aircraft. The mission requirements and profiles were collated from the Standard Aircraft Characteristics (SAC) charts of the F/A-18C [Naval Air Systems Command, 1996], A-6E [Naval Air Systems Command, 1984], and F-14A [Naval Air Systems Command, 1976]. In total, these aircraft performed 21 missions, though there was some redundant capability amongst the legacy aircraft so these only accounted for nine distinct mission profiles (albeit with different individual capabilities). For the most part, the most critical (in terms of payload-range) mission parameters were chosen when multiple airframes participated in the same mission profile. These missions are depicted in Table 1 with the "dominant" configuration in bold.

Table 1: Notional Multi-Role Fighter Missions

Mission	**Aircraft**
Hi-Hi-Hi	F/A-18C, F-14A, **A-6E**
Lo-Lo-Lo	F/A-18C, **F-14A**, A-6E
Hi-Lo-Hi	F/A-18C, **A-6E**
Hi-Lo-Lo-Hi / Interdiction	F/A-18C, **F-14A**, A-6E
Lo-Lo-Hi	**F-14A**
Close Support	F/A-18C, **F-14A**, A-6E
Fighter Escort	F/A-18C, **F-14A**
Deck-Launched Intercept	**F/A-18C**, F-14A
Combat Air Patrol	**F/A-18C**, F-14A

The analysis environment utilized the requirements fitting formulation for multi-mission design outlined in Section 2.4.2. This served as a test for the requirements fitting technique and ensured that the analysis codes would run smoothly for all nine missions. A total of 44 decision metrics were tracked: four mission performance metrics for each of the nine missions, five individual mission performance metrics, and three non-mission specific metrics. These are listed in Table 2. Most of these metrics were outputs from the integrated environment, though a few were inputs. Also, no explicit cost metric was available so gross weight was used as a measure of life-cycle cost.

Table 2: Notional Multi-Role Fighter Decision Metrics

Description	**Units**	**Total #**
Maximum Mach number	-	9
Maximum sustained load factor	g's	9
Specific excess power	ft/sec	9
Total range	nmi	9
Combat Air Patrol acceleration Mach number	-	1
Combat Air Patrol time on station	min	1
Close Air Support time on station	min	1
Deck-Launched Intercept dash Mach number	-	1
Hi-Lo-Lo-Hi / Interdiction dash distance	nmi	1
Approach speed	kts	1
Approach single engine rate of climb	ft/sec	1
Takeoff gross weight	lbs	1

The core of the analysis was NASA Langley's FLOPS [McCullers, 1984, 1998]. This code is capable of fuel-balance sizing or direct mission analysis of a configuration for specified gross weight, so it was used in the latter mode in keeping with the ideas of multipoint sizing. A baseline input file for the F/A-18C configuration was calibrated to actual performance and aerodynamic data [Naval Air Systems Command, 1996; McDonnell-Douglas Corporation, 1996]. A series of spreadsheets were used to scale the input FLOPS file for the various system-level inputs and to figure changes in store drags for the various missions. These files were wrapped in a ModelCenter [Phoenix Integration, 2005] environment for ease of execution and parsing data.

This integrated environment was executed multiple times for various settings within a

Design of Experiments (DoE) table for creation of quadratic Response Surface Equations (RSEs). The Design of Experiments and subsequent creation of the RSEs was handled with JMP [SAS Institute, 2005], a statistical analysis software package. Once created, the RSEs were validated through a series of statistical tests within JMP and finally through a comparison of several random input cases. All tests indicated that the RSEs were good approximations to the data provided by the original analysis environment.

The RSEs served as a rapid way to evaluate the various responses in a probabilistic MCDM environment. The overall scheme involved creation of a random population of 100,000 data points. The RSEs were used to rapidly create a 44-element vector of attributes for each of these 100,000 alternatives. Note that no screening was performed on these alternatives to determine which, if any, were not Pareto optimal. TOPSIS was used to rank each of the alternatives subject to a complex scheme for determination of the relative importance of each metric. Ultimately, each of the 44 metrics had its own relative importance value. The uncertainty in the actual requirements was simulated via uncertainty in the relative importance. A total of 5,000 random weighting scenarios were developed in a Monte Carlo Simulation for TOPSIS evaluation; hence, each of the 100,000, 44-metric alternatives were ranked 5,000 times via TOPSIS. In this fashion, the idea was not to pick the design that was ranked first in any individual TOPSIS execution, but rather the design that most often appeared in the top few percent of every TOPSIS trial. This design would be the most robust with respect to unexpected changes (uncertainty) in the requirements. Figure 17 illustrates the prominent features of this analysis.

4.2.2 Results and Implications

The top one percent of the TOPSIS-ranked population were recorded for each of the 5,000 MCS trials. Of these 5,000 trials, one particular alternative appeared in the top one percent of the population 2,365 times, and 26 alternatives appeared over 2,000 times. If the top designs all have similar inputs and outputs, then any one of these designs represents one that will be invariant with small changes in preference.

Unfortunately, this was not the case. The resulting input and output histograms for the

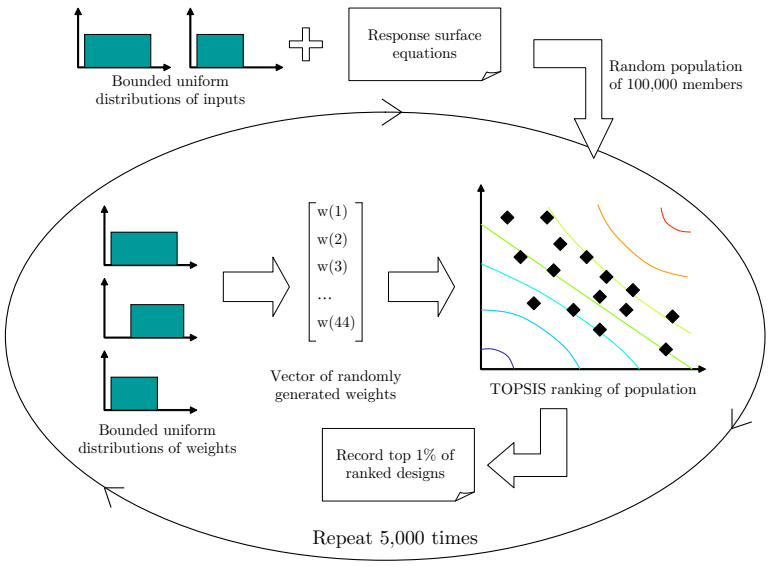

Figure 17: Notional Multi-Role Fighter Problem Formulation and Execution

top recurring designs showed considerable spread, including gross weight. Furthermore, the recurrence was much smaller than hoped. At best, the top recurring design was in the top one percent 2,365 out of 5,000 trials, slightly more than 47% of the time. This level of risk is unacceptable for most programs. Recurrence could be increased with a smaller range and refined distributions within the MCS trials, but seemed to be indicative of bigger problems.

One such problem with this formulation was the large number of requirements. Unfortunately many of the requirements were highly dependent on the same parameters as others, potentially creating "double-weighting" (and more) situations within the TOPSIS trial. That is, if two requirements were essentially the same metric, then including them in any MCDM approach will act as if that one metric were twice as important.

Another potential problem with available MCDM formulations is a lack of threshold values. Often, there is a threshold beyond which a decision maker becomes indifferent to the value of a particular metric. TOPSIS and other MCDM formulations will essentially try to exploit the responses with the greatest slope in finding a solution (this slope may be partially mitigated with the weighting factors). However, this may not be desirable once a metric reaches or approaches a certain value, and instead the optimization effort should be spent in other dimensions even if they have a lower slope.

4.3 MCDM Example Application

The notional multi-role fighter case study causes some suspicion to be cast towards the validity of the generalized probabilistic decision making formulation. Certainly it shows that some of the initial statements regarding probabilistic decision making need further testing. While this application is an excellent example of multi-mission design, it is very complicated and therefore can be difficult to focus on potential problems in the overall problem formulation. A simpler systems design problem with closed-form analyses and intuitive requirements will be much better suited to the development of algorithms and experiments to test the hypotheses given earlier in this chapter.

4.3.1 Multiple Criteria Beam Design

Structural design is not usually associated with multiple criteria decision making. It is typically a minimum-mass optimization problem subject to a number of constraints and boundary conditions representative of the most critical conditions the member is expected to face. In this case, minimizing mass represents a quasi-cost function. Structural design can be made into a multiple criteria problem by using the same techniques discussed for multipoint aircraft sizing. All of the requirements become objectives, including former objectives and constraints. The requirements for this example follow from a series of different loading conditions ("missions") and are calculated from simple structural analysis principles.

The design problem is a three-dimensional vertical beam with a fixed end condition. The beam has two design variables, both relating to cross-section. These are cross-sectional area (S) and aspect ratio (A), the latter of which is defined as the ratio of width to depth. The beam length and material properties are constants. Figure 18 gives the pertinent information for this example problem.

The beam requirements are given in three different loading conditions: one end-loaded compressive case and two cantilever cases. Each of these loading conditions has specific requirements for displacement and factor of safety for ultimate failure (maximum stress). The compressive case has an Euler buckling factor of safety requirement. Finally, the beam is to be designed to minimize weight. Figure 19 illustrates these loading conditions.

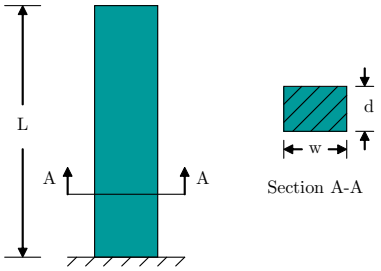

Length (L) = 100 cm

Design Variables:

Area (S = wd) = 10 to 50 cm^2

Aspect Ratio (A = w/d) = 1 to 2

Material: 2014-T6 aluminum

Density (ρ) = 2,790 kg/m^3

Young's Modulus (E) = 7.31×10^{10} Pa

Ultimate Strength (σ_{ult}) = 4.69×10^{8} Pa

Figure 18: Pertinent Dimensions and Material Properties of Beam Design Problem

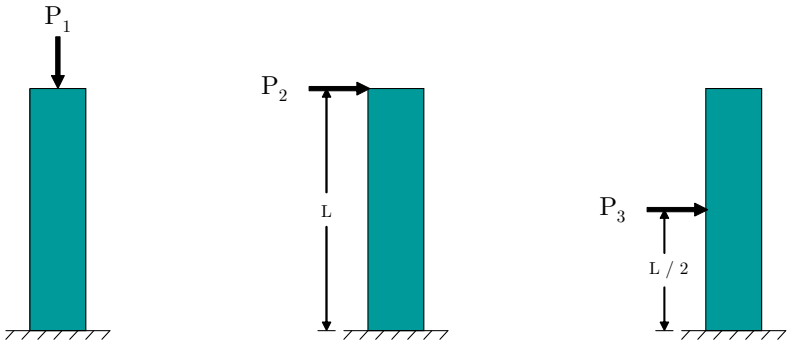

Loading Condition 1 (LC1)

P_1 = 30,000 N

Loading Condition 2 (LC2)

P_2 = 5,000 N

Loading Condition 3 (LC3)

P_3 = 10,000 N

Figure 19: Loading Conditions for Beam Design Problem

Inspection of Figure 19 shows that loading conditions two and three are redundant. The maximum stress factors of safety for these two cases will be identical and the maximum displacement of loading condition three will be dominated by loading condition two. This is deliberate; the idea is to duplicate the issues associated with redundant requirements. To further simplify notation, these eight requirements are labeled as follows (with LC referring to the appropriate loading condition):

- R_1: Euler buckling factor of safety (LC1)
- R_2: ultimate compressive failure factor of safety (LC1)
- R_3: ultimate bending failure factor of safety (LC2)
- R_4: maximum compressive displacement (LC1)
- R_5: maximum bending displacement (LC2)
- R_6: beam mass (all loading conditions)
- R_7: ultimate bending failure factor of safety (LC3)
- R_8: maximum bending displacement (LC3)

The functional form of the eight requirements are found from classical structural analysis techniques [Young and Budynas, 2001; Hibbeler, 1997]. Before discussing the functional form of the equations, there are some preliminaries to consider:

$$w = \sqrt{SA} \tag{9}$$

$$d = \sqrt{\frac{S}{A}} \tag{10}$$

$$I_w = \frac{1}{12}\frac{S^2}{A} \tag{11}$$

$$I_d = \frac{1}{12}S^2A \tag{12}$$

where w is the width of the beam as indicated in Figure 18, d is the depth, I_w is the second moment of area about the width axis, and I_d is the second moment of area about the depth axis. With these in mind, the functional form of the eight requirements can be stated both

with respect to the notation of equations (9) through (12) and with respect to the design variables S and A:

$$R_1 = \frac{\pi^2 E I_w}{4 P_1 L^2} \qquad f\left(\frac{S^2}{A}\right) \tag{13}$$

$$R_2 = \frac{\sigma_{ult}}{\frac{P_1}{S}} \qquad f(S) \tag{14}$$

$$R_3 = \frac{\sigma_{ult}}{\frac{P_2(\frac{w}{2})}{I_d}} \qquad f\left(\frac{S^{\frac{3}{2}}}{A^{\frac{1}{2}}}\right) \tag{15}$$

$$R_4 = \left(\frac{P_1}{S}\right) LE \qquad f\left(\frac{1}{S}\right) \tag{16}$$

$$R_5 = \frac{P_2 L^3}{3 E I_d} \qquad f\left(\frac{1}{S^2 A}\right) \tag{17}$$

$$R_6 = \rho S L \qquad f(S) \tag{18}$$

$$R_7 = \frac{\sigma_{ult}}{\frac{P_3(\frac{L}{2})(\frac{w}{2})}{I_d}} \qquad f\left(\frac{S^{\frac{3}{2}}}{A^{\frac{1}{2}}}\right) \tag{19}$$

$$R_8 = \frac{\left(\frac{5}{8}\right) P_3 L^3}{6 E I_d} \qquad f\left(\frac{1}{S^2 A}\right) \tag{20}$$

where E refers to the Young's modulus of elasticity, P_1 through P_3 is the load associated with loading conditions one through three, respectively, L refers to the beam length, and ρ refers to the material density.

Inspection of the functional forms given in equations (13) through (20) indicates that only five of these requirements are linearly independent. As expected, all of the LC3 requirements are the exact same functional form as the LC2 requirements; R_7 will be perfectly correlated with R_3, and R_5 will be perfectly correlated with R_8. Furthermore, two seemingly independent requirements, R_2 and R_6, are perfectly correlated. However, they are exactly opposite in terms of direction of improvement, but they will effectively cancel each other out if the assumption of monotonically increasing utility is made. Also, the presence of two functionally opposing objectives indicates that every solution within the design space is Pareto optimal since at least one of these two requirements will always be nondominated.

Basic engineering intuition leads to some assertions regarding this problem. First, the requirements of loading condition three should be completely dominated by loading condition two and therefore should not be a factor in the design problem (as long as the

constraints, if any, for LC3 are the same or lower than those for LC2). Further, some of the requirements will be dominated by other trades. Compressive failure factor of safety and compressive deflection should be minimal, and therefore inconsequential to the final design when compared to Euler buckling and cantilever bending.

The beam analysis is carried out through a series of files and functions created in Matlab [The Mathworks, Inc., 2005], with the formulae for the requirements taken exactly from equations (13) through (20). The design space domain for this problem varied S from 10 to 50 cm^2 and A from 1.0 to 2.0. The plots of each of the eight requirements within the design space are given in Figure 20. These plots represent a mapping of the design domain to the decision domain, also known as the decision space.

4.3.2 Polynomial Surrogate Modeling

One attractive feature of the beam design problem as a test case is the fast execution time of its integrated analysis routine in Matlab. However, most large-scale systems design problems involve analysis routines that have much longer execution times and can become computationally prohibitive to run in a Monte Carlo simulation as is necessary for probabilistic decision making. As mentioned earlier, Response Surface Methodology (RSM) is a powerful concept for speeding up execution time. This technique is also central to some of the decomposition and visualization techniques to be discussed in later chapters. As a whole, successful approximation of an integrated environment enables a wide variety of analysis and visualization techniques.

In keeping with the philosophy of probabilistic design via RSM, a series of response surfaces were developed for the beam design problem (despite its already fast execution time). These response surfaces were created via the methods outlined in Appendix A. Typical Response Surface Equations (RSEs) for aerospace systems design problems are quadratic polynomials with two-factor interactions. However, the large design domain and non-linearity of the decision metrics required that cubic polynomials with three-factor interactions be created as surrogate models for the beam metrics. These difficulties are traditionally handled with independent or dependent variable transformation; however, there are some advantages

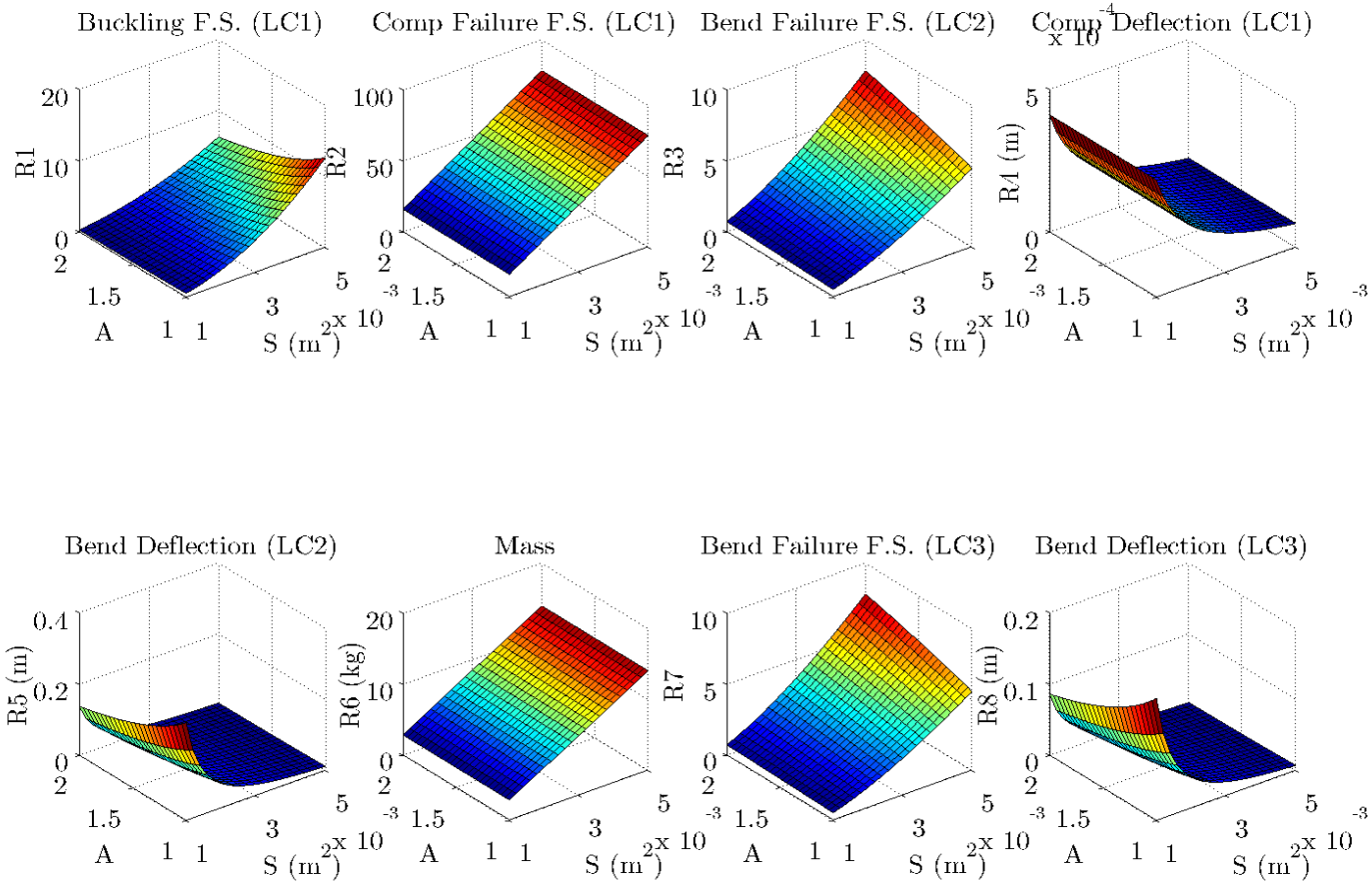

Figure 20: Beam Requirements throughout Design Space

to be realized when using non-transformed models that will be discussed later.

A five-level Design of Experiments was used to create these response surfaces to give sufficient error terms to the regression model. There are a host of validation techniques to determine if the response surfaces adequately represent the dataset, a few of which are given in Appendix A. Most of these were performed, but the most telling validation is the comparison of a randomly generated field of points compared through the original analysis routine and the surrogate models. This comparison for the actual versus predicted results for the beam response surfaces is shown in Figure 21.

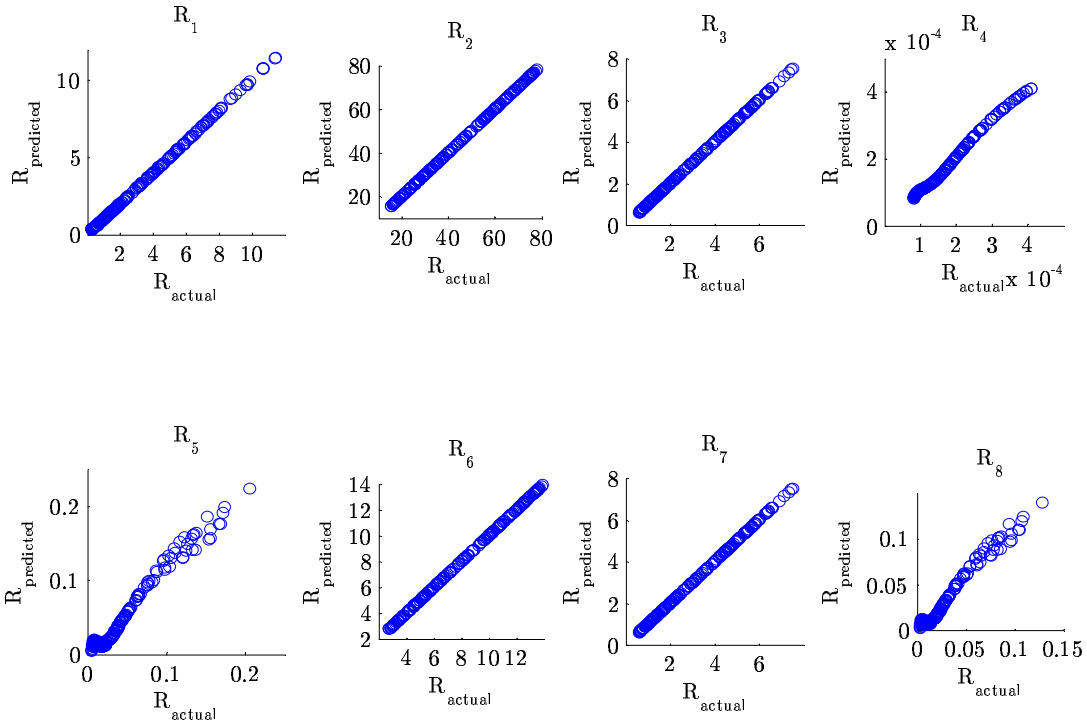

Figure 21: Actual versus Predicted Results for Surrogate Models

The plots in Figure 21 show that the response surfaces adequately represent the decision space. There are some regions of error; however, these are mostly at the extremes of the decision space and should not have much bearing on the results of the environment.

4.4 Initial Experiments for Beam Design Problem

A number of experiments are necessary to test the hypotheses outlined in Section 4.1. These are carried out in order of relevance, and are summarized as follows:

Task 1: Attempt to resolve the Pareto frontier for the beam design example and determine the portion of the space that is nondominated. (Hypothesis 4)

Task 2: Compare the results of deterministic Compromise Programming (CP) for the beam design example for six and eight requirements. Compute a single objective constrained solution as a control experiment for both variations. Compute the same results using the polynomial surrogate models for comparison to the results with the actual analyses. (Hypotheses 1 and 3)

Task 3: Compare the results of probabilistic Compromise Programming for the beam design example for six and eight requirements over a moderate range of relative importance. (Hypotheses 2 and 3)

These initial experiments should be able to provide enough data to determine whether the hypotheses are reasonable. If not, they may require modification due to subsequent observations. The six-requirement beam design problem uses metrics defined from loading conditions one and two, as well as beam mass, given by equations (13) through (18). The eight-requirement problem adds in loading condition three, equations (19) and (20). These are already known to be redundant, so the comparisons are to see if the addition of these requirements biases the solution.

Most of the experiments require optimization. To this end, a Sequential Quadratic Programming (SQP) constrained optimization routine is used that is part of Matlab's Optimization Toolbox. Specifically, the routine is Matlab's `fmincon` function with default settings [The Mathworks, Inc., 2005]. SQP is a gradient-based optimizer, hence it may only find local minima. As such, most results are based on multiple starting points. For a more detailed discussion of gradient-based optimization and SQP, the reader is referred to the comprehensive work by Vanderplaats [Vanderplaats, 1999], among others.

4.4.1 Resolution of Nondominated Solutions

Section 3.1 discusses the concept of Pareto optimality and the attractiveness of using MCDM on nondominated concepts. However, this section also observed the tendency of problems with many decision metrics to have little or no dominated portions within the decision space. As such, one of the hypotheses of this research is that resolution of nondominated solutions is unnecessary for large-scale systems design as these problems are defined by a large number of metrics. This hypothesis can be tested for the beam design problem by taking a discrete sample of the decision space and attempting to resolve the number of nondominated concepts within this space.

Advanced methods for generating efficient, well-distributed Pareto frontiers are found in the literature [Mattson et al., 2002; Ismail-Yahaya and Messac, 2002; Messac and Ismail-Yahaya, 2001]. However, the beam design problem is small enough that it can use a simple Pareto dominance scheme, however inefficient, to find all of the nondominated solutions from a random sample of the decision space. This simple algorithm uses pairwise comparison of each data point to each data point "downstream." If the algorithm finds any downstream point that completely dominates the current point, it discards the current point and resumes the process at the next point. If the point is nondominated for all downstream points, it is added to the registry of nondominated points, which eventually becomes the Pareto frontier. Mathematically, this process starts with a dataset

$$\mathbf{D} = \left[\begin{array}{cccc} \vec{d_1} & \vec{d_2} & \dots & \vec{d_n} \end{array} \right] \tag{21}$$

where $\mathbf{D}$ is the sample data from the decision space composed of n data vectors $\vec{d}$ for each metric. The length of $\vec{d}$ depends on the number of random samples taken, denoted by m. Hence, $\mathbf{D}$ is an $m \times n$ matrix. The data comes from a uniformly random sample of the design space (S and A) mapped to the decision data (R_1 through R_8) via the analysis routines.

From here, each row of $\mathbf{D}$ is compared with all subsequent rows of $\mathbf{D}$. A row is said to be *dominated* when

$$d_{i,j} < d_{i+s,j}, \qquad s = i+1 \dots n, \qquad \forall j. \tag{22}$$

If a row never satisfies equation 22, it is considered *nondominated* and is kept as a data point for the Pareto frontier. Otherwise, the point is discarded.

This procedure was performed for the six-requirement beam design problem with 1,000 randomly selected data points. Evaluating the eight-requirement problem was unnecessary since it was known that the last two requirements were mathematically redundant. Of these 1,000 data points, *all* were found to be nondominated, illustrating the validity of Hypothesis 4. Further tests with more data points did not reveal *any* dominated alternatives.

If the beam design problem has a completely nondominated decision space for the six-requirement problem, perhaps it has some dominated solutions for smaller two-dimensional spaces. This analysis would further enable visualization via a scatterplot. If *any* of the resulting 15 two-dimensional comparisons (since the 30 comparisons would be symmetric) contained completely nondominated points, then this would indicate that the entire six-requirement problem should be nondominated as well. This analysis was completed, and the resulting scatterplot is shown in Figure 22. Here, the nondominated points are shown in red and the dominated points in blue. For this analysis, only 200 random data points were used for clarity.

Figure 22 suggest that two of the two-dimensional Pareto frontiers consist of the entire decision space. These are the frontiers between R_2-R_6 (compressive failure and beam mass) and between R_4-R_6 (compressive deflection and beam mass). This is to be expected; equations (14) and (18) are both direct functions of S with opposing desirability, and equation (16) improves with $\frac{1}{S}$. This figure also shows that the bulk of the nondominated tradeoffs occur between all other metrics and R_6; again, not surprising, as the beam mass is a quasi-cost function. However, even with R_2 and R_4 removed from the dataset, all 1,000 of the random data points still remain nondominated in four-dimensional space.

It is important to note that the use of the Pareto frontier moniker for this simple algorithm may not be perfectly appropriate. Pareto dominance is generally considered to be a global quantity while nondominance may simply refer to a local set. This algorithm is designed to search a randomly-generated population and use a simple dominance algorithm to find a "locally Pareto" frontier. True resolution of the global Pareto frontier of the decision

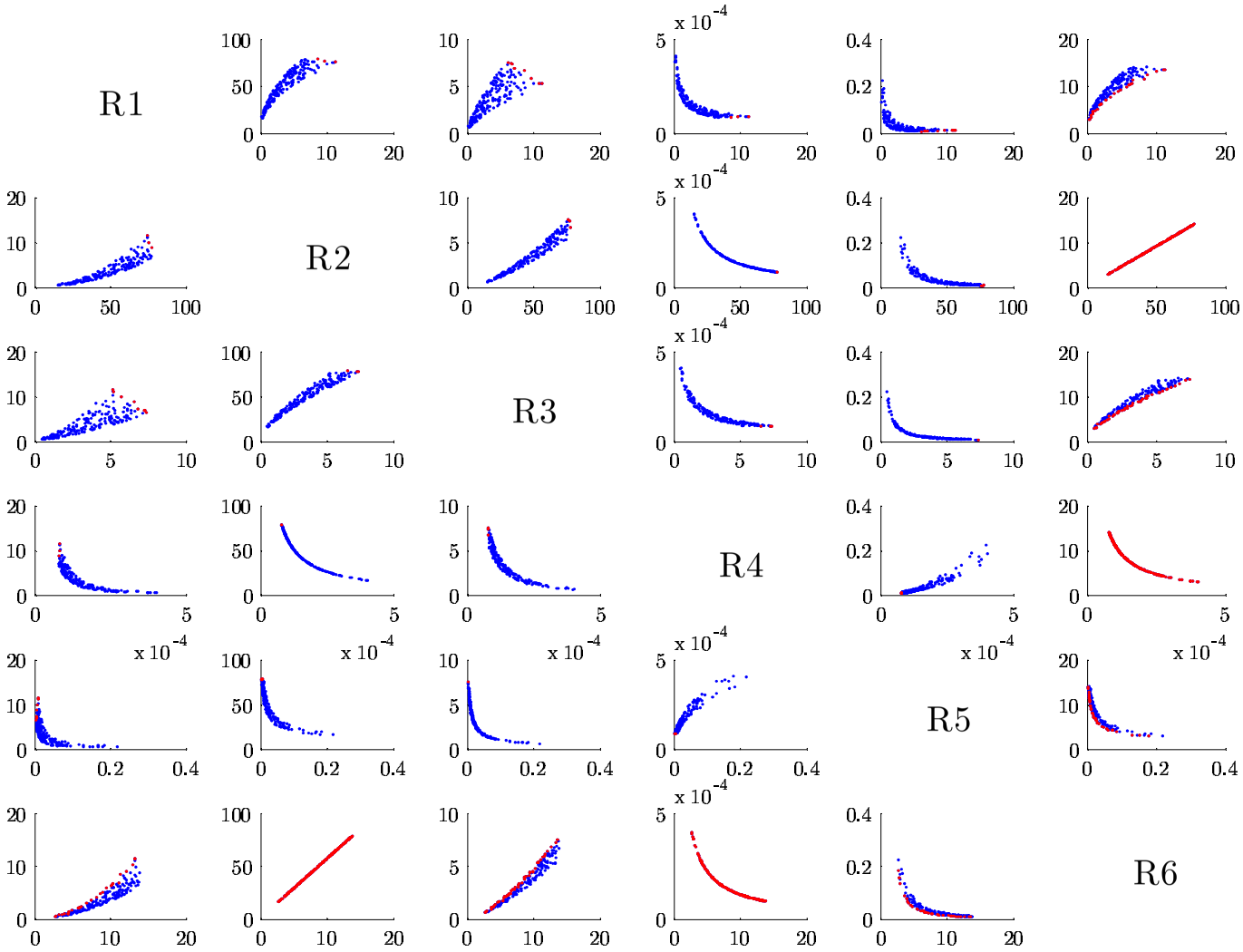

Figure 22: Two-Dimensional Nondominated Alternatives for Six-Requirement Beam Design Problem

space or representative set thereof requires optimization. Methods abound in the literature for resolution of globally Pareto optimal sets [Ismail-Yahaya and Messac, 2002; Mattson et al., 2002]. This experiment is a verifiably simple exercise to show the nondominance of all of a random population of the decision space (local Pareto optimality).

4.4.2 Deterministic Decision Making

The deterministic portion of the decision making environment needs to be tested before completion of the probabilistic environment. These tests included a control group consisting of a constrained Single Objective Optimization (SOO) problem and several CP optimization runs for a variety of cases.

The control case requires an objective function and several constraints. The optimization statement for the control case follows.

Minimize:

$$F(\vec{x}) = R_6(\vec{x}) \tag{23}$$

Subject to:

$$g_1(\vec{x}) = 1.5 - R_1(\vec{x}) \leq 0 \tag{24}$$

$$g_2(\vec{x}) = 1.5 - R_2(\vec{x}) \leq 0 \tag{25}$$

$$g_3(\vec{x}) = 1.5 - R_3(\vec{x}) \leq 0 \tag{26}$$

$$g_4(\vec{x}) = R_4(\vec{x}) - 0.1 \leq 0 \tag{27}$$

$$g_5(\vec{x}) = R_5(\vec{x}) - 0.1 \leq 0 \tag{28}$$

$$g_6(\vec{x}) = 1.5 - R_7(\vec{x}) \leq 0 \tag{29}$$

$$g_7(\vec{x}) = R_8(\vec{x}) - 0.1 \leq 0 \tag{30}$$

$$\vec{x}^{\,l} \leq \vec{x} \leq \vec{x}^{\,u} \tag{31}$$

where $F(\vec{x})$ is the objective function, $g(\vec{x})$ are inequality constraints, $\vec{x}^{\,l}$ is the lower bound of the design variables, and $\vec{x}^{\,u}$ is the corresponding upper bound. For this problem, the design variable vector is $\vec{x} = (S, A)$, and $R_1(\vec{x})$ through $R_1(\vec{x})$ are as defined previously in

equations (13) through (20). The values of the constraints were set arbitrarily as 1.5 for the factors of safety and 0.1 meters for the deflections (the analyses required inputs in meters).

A total of four control experiments were run for the deterministic portion. Two experiments were run for a six-requirement case (eliminating R_7 and R_8, hence equations (29) and (30) from the optimization statement) and two for the full eight-requirement case. Of these pairs of experiments, one was run for the actual analyses and the other using the polynomial surrogate models.

The deterministic compromise programming cases have no inequality constraints other than the side constraints on the bounds of the design space. The optimization statement for the CP cases follows.

Minimize:

$$F(\vec{x}) = \left\{ \sum_{j=1}^{n} \left[\frac{w_j(R_j - R_j^*)}{R_j^- - R_j^*} \right]^p \right\}^{\frac{1}{p}} \tag{32}$$

Subject to:

$$\vec{x}^{\,l} \leq \vec{x} \leq \vec{x}^{\,u} \tag{33}$$

where R_j^* is the best and R_j^- is the worst value of the j^{th} metric in the decision space. These best and worse values were found via single-objective optimization within the design space. Enumeration of these values ensures that the compromise objective function comes from normalized decision metrics. For these initial experiments, the relative importance of each metric was set to be equal to all others and summed to one, $w_j = \frac{1}{n}$.

Like the control cases, the CP cases required a total of four experiments: two with six requirements and two with eight requirements. As before, each pair of cases was evaluated with the actual and approximate analyses. The six-requirement cases again neglected the contributions of R_7 and R_8. The results of the control and CP experiments are shown in Table 3 for the original analyses and again in Table 4 for the polynomial surrogate models. Note that these (and all results that follow) are given in their native format, though all of the values were normalized during execution to ensure efficient optimizer operation.

Several interesting observations result from these tables. The multi-objective solutions are far larger, heavier, and overdesigned than the single-objective constrained solution. This

Table 3: Deterministic Results Comparison for Beam Design Problem (Actual Analyses)

Value	SOO: 6 Req.	SOO: 8 Req.	CP: 6 Req.	CP: 8 Req.
S, m^2	0.001941	0.001941	0.004418	0.004788
A	1.259	1.259	1.000	1.288
R_1	1.500	1.500	9.778	8.919
R_2	30.35	30.35	69.06	74.85
R_3	1.500	1.500	4.590	5.877
R_4, m	2.11E-04	2.11E-04	9.29E-05	8.57E-05
R_5, m	0.05769	0.05769	0.01402	0.009269
R_6, kg	5.416	5.416	12.33	13.36
R_7	-	1.500	-	5.877
R_8, m	-	0.03606	-	0.005793

Table 4: Deterministic Results Comparison for Beam Design Problem (Surrogate Models)

Value	SOO: 6 Req.	SOO: 8 Req.	CP: 6 Req.	CP: 8 Req.
S, m^2	0.001950	0.001950	0.004429	0.004794
A	1.239	1.239	1.000	1.294
R_1	1.500	1.500	9.808	8.966
R_2	30.49	30.49	69.25	74.94
R_3	1.500	1.500	4.614	5.901
R_4, m	2.17E-04	2.17E-04	1.00E-04	8.97E-05
R_5, m	0.06875	0.06875	0.01757	0.01396
R_6, kg	5.441	5.441	12.36	13.37
R_7	-	1.500	-	5.901
R_8, m	-	0.04297	-	0.008722

is largely because all of the objectives are opposed in direction of importance in some way to the beam mass objective. Since all of these objectives use even relative importance for the metrics, the assumption of monotonically increasing utility now makes minimizing beam mass much less important than the other metrics since they tend to "gang up" against it.

The results for the original analyses and the surrogate models compare very well. All of the control and compromise programming solutions are very close, though the bending deflection models (R_5 and R_8) are off by approximately 50% for the compromise programming cases. However, this was expected because the surrogate models did not test well at the extremes, as seen before from Figure 21. These results are closer (within 20%) for the control cases, but these again are near an extreme in the decision space. Furthermore, the absolute error in either case is less than half a centimeter, which is quite small even if it is a large relative error. If the bending deflection seemed to be a design driver this could be problematic; however, this is not the case for this analysis. In all, the surrogate modeling appears to yield satisfactory results.

The most notable observation is that the two compromise programming solutions are different for the six- and eight-requirement cases. This contradicts engineering intuition, which implies that both beams should be identical because of the redundancy of R_7 and R_8. Note that the control single-objective cases are identical regardless of the presence of the last two requirements. Of course, the only driving constraints for the single-objective cases are the compromise between bending and buckling resistance, as both R_1 and R_3 (and R_7 for the eight-requirement case) are exactly on the constraint. This indicates a philosophical issue in the CP formulation. To compare, the objective functions for the six- and eight-requirement CP cases are shown in Figure 23.

The difference in these objective functions is a result of the "double-weighting" of the bending requirements. Though the intuitive solution for both is the same, the compromise programming solutions are different. Note that the six-requirement problem is more favorable towards an increase in Euler buckling factor of safety, whereas the eight-requirement problem is more biased towards bending. This is principally caused by the addition of two

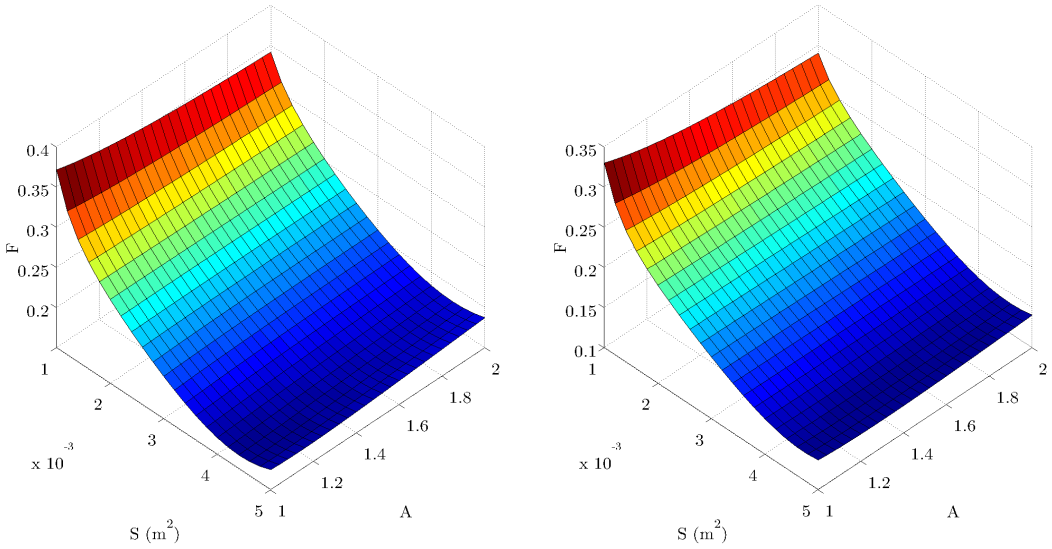

(a) Six Requirements

(b) Eight Requirements

Figure 23: Objective Function for Beam Design Problem Using Evenly Weighted Compromise Programming

redundant bending metrics. The current formulation does not support the choice of "requirements groups" or other "characteristic directions" amongst dependent requirements and is thus prone to such errors. The creation of such characteristic requirements could follow from decomposition of the original requirements. These characteristic requirements would be a subset of the originals and would enable tradeoffs amongst key metrics.

Both objective functions also show a highly undesirable region near the minimum mass solution (minimum S) and a preference for higher-mass solutions (larger S). Certainly, the minimum-weight solution may not be the best compromise alternative, but the assumption of monotonically increasing utility may not hold beyond a "threshold" value of the other requirements. The current formulation does not handle threshold or constraint values in the weighting scheme, instead simply using static values for relative importance.

4.4.3 Design to Probabilistic Requirements

The probabilistic experiment utilized the same basic approach as the deterministic problem, though this time no control single-objective scenario was attempted. This was because the analogy for uncertainty of the relative importance of a single objective has no meaning. Also,

only the results of the experiments using the actual analyses (as opposed to the surrogate models) are presented for clarity. Two experiments were run, one for the six-requirement beam design problem and the other for the eight-requirement problem. To be consistent with Hypothesis 2, the relative importance of each metric was considered uncertain. As in the deterministic experiments, the base relative importance value was set at $\frac{1}{n}$. Each of these values was allowed to vary uniformly by ±50%, but then re-normalized such that the sum of all w_j would equal one. A total of 1,000 uniformly random cases were executed using the CP problem statement as given by equations (32) and (33). The results of each case were tracked, and the means and standard deviations of the results are given below in Table 5.

Table 5: Probabilistic Results Comparison for Beam Design Problem

	6 Requirements			**8 Requirements**		
Value	μ	σ	σ **%**	μ	σ	σ **%**
S, m^2	0.004358	5.26E-04	12.1%	0.0045847	4.39E-04	9.6%
A	1.248	0.3733	29.9%	1.468	0.3873	26.4%
R_1	8.344	2.662	31.9%	7.867	2.591	32.9%
R_2	68.12	8.219	12.1%	71.68	6.869	9.6%
R_3	4.973	0.9571	19.3%	5.803	0.8453	14.6%
R_4, m	9.57E-05	1.29E-05	13.5%	9.04E-05	9.60E-06	10.6%
R_5, m	0.01282	0.0044131	34.4%	0.009600	0.0027334	28.5%
R_6, kg	12.16	1.467	12.1%	12.79	1.226	9.6%
R_7	-	-	-	5.803	0.8453	14.6%
R_8, m	-	-	-	0.006000	0.001708	28.5%

The results in Table 5 are dubious at best. They indicate a relatively large relative standard deviation, showing that there appears to be no single solution that is particularly invariant with respect to changes in the importance of an individual requirement. Furthermore, there are nontrivial differences between the six- and eight-requirement solutions. Table 6 expands upon these differences by examining the mean shift, $\mu_6 - \mu_8$, with a Student's t-test [Hayter, 1996]. The p-value listed reflects the chance that the means are equal (the null hypothesis in this case).

The shifts in the mean indicate that on average the eight-requirement solutions are more resilient to bending at the expense of the axial loading cases. This further lends credence

Table 6: Mean Shift from Six- to Eight-Requirement Probabilistic Solutions

Value	$\mu_6 - \mu_8$	σ	***t*-Statistic**	***p*-Value**
S, m^2	-2.27E-04	6.51E-04	11.04	8.19E-27
A	-0.2192	0.5302	13.07	3.71E-36
R_1	0.4772	3.644	4.141	3.75E-05
R_2	-3.552	10.18	11.04	8.23E-27
R_3	-0.8305	1.198	21.93	2.47E-87
R_4, m	5.29E-06	1.54E-05	10.90	3.29E-26
R_5, m	0.003224	0.004923	20.71	1.58E-79
R_6, kg	-0.6340	1.816	11.04	8.20E-27

to the argument that MCDM can bias a problem if redundant requirements are introduced. The p-values from the t-test indicate that there are statistically significant differences in the means of the populations.

The scatterplots of the resulting design variables for the 1,000 sample designs are even more telling. These are presented for the six- and eight requirement cases in Figure 24. The scatterplot of the decision space for the six-requirement case is illustrated in Figure 25. The requirements scatterplot for the eight-requirement case is not shown due to difficulty with resolution of such a large number of requirements in scatterplot form.

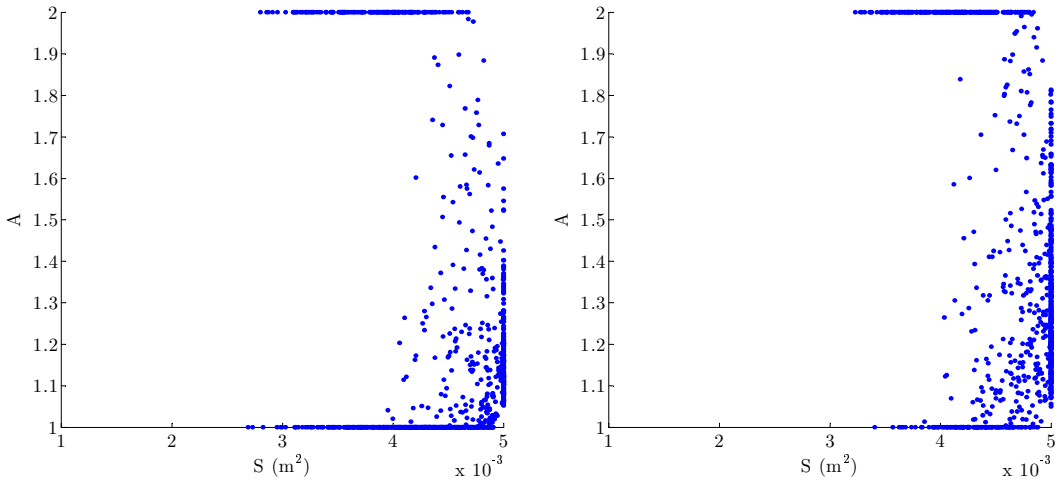

(a) Six Requirements (b) Eight Requirements

Figure 24: Design Variable Scatterplots for Beam Design with Probabilistic Requirements

These figures add some insight to the results in Tables 5 and 6. The design variable scatterplots in Figure 24 show that the algorithm is still designing very heavy beams, given

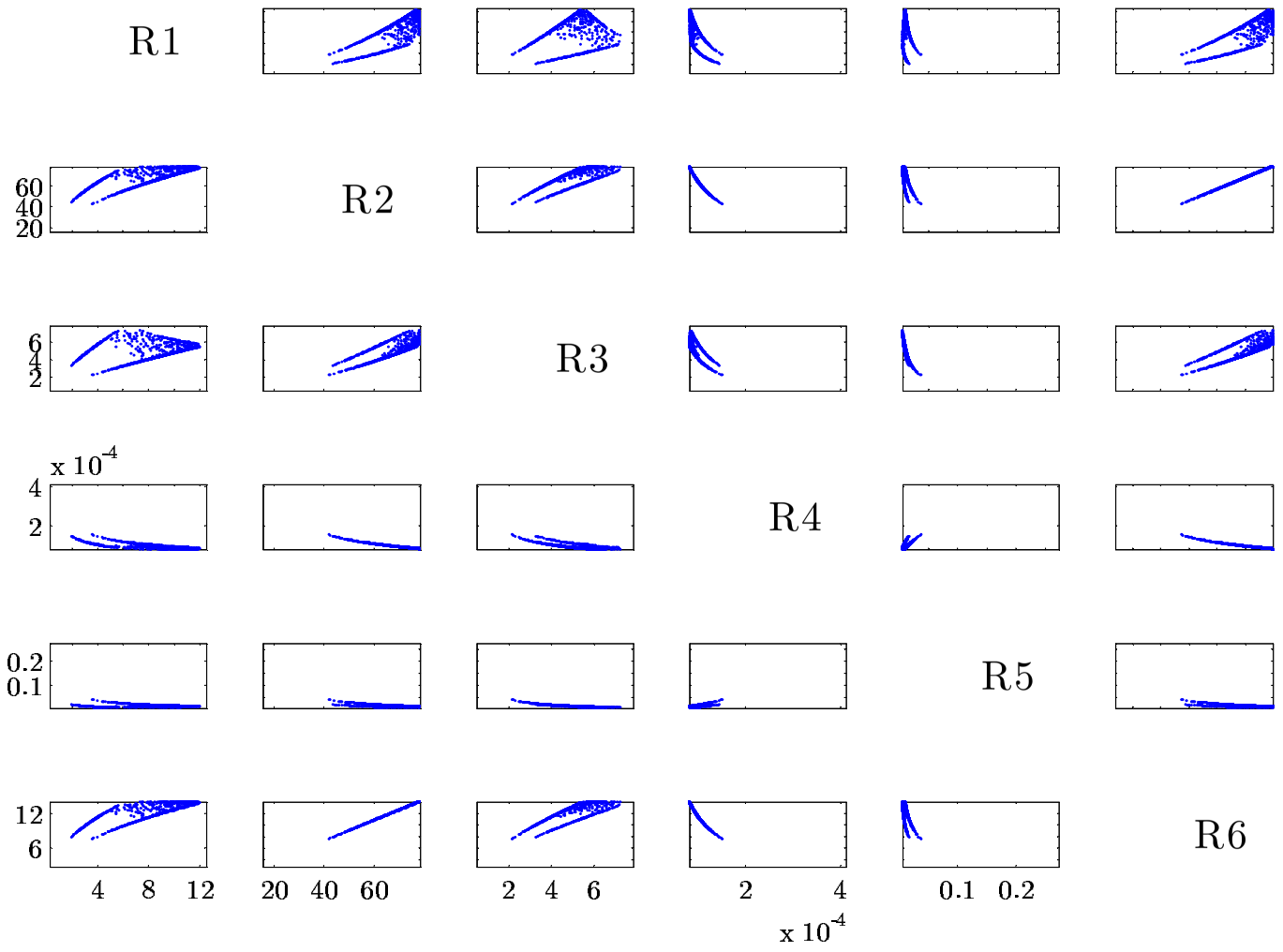

Figure 25: Response Scatterplots for Beam Design with Six Probabilistic Requirements

the relatively large cross-sectional areas S, but the choice of beam aspect ratio A varies between the extremes of the space, with a few transitional cases in between. However, there is a noticeable shift towards higher aspect ratio designs for the eight requirement case. Furthermore, the spread exhibited by the uncertainty is quite large. Certainly, a difference of fifty percent in the relative importance of a given metric is large, but causes a huge swing in the solutions. It would be difficult to choose the mean design in this situation, since it appears that the problem is either trying to design a beam that is more resistant to either bending or axial loads, as opposed to finding a compromise solution.

Figure 25, though difficult to view, helps better interpret these design variable choices for the six requirement design problem. The results of the experiment for the resolution of nondominated solutions, especially those of Figure 22, imply that all of the requirements are in opposition to R_6 (beam mass) in some way. However, the results between R_1 and R_3 seen in Figure 25 best indicate the bending-versus-axial trades happening in the probabilistic study. The long, sweeping lines made up of many data points in these plots are at the the extremes of A, either at $A = 1.0$ or 2.0, with the fewer other (truly compromise) datapoints lying in between. The two-dimensional Pareto surface is visible in the upper-right corner of this subplot.

4.4.4 Implications

Ultimately, these results show that even moderate uncertainty in the relative importance of the decision metrics results in extreme variations in the final design choice. Certainly it is possible to narrow the ranges of the distributions on the relative importance, but even small differences seem to cause large changes in the CP design choice.

This radical effect of moderate changes in relative uncertainty calls the validity of the utility models of MCDM into question. These experiments considered the "base" relative importance of each metric to be identical; however, this is often not the case and the decision maker may wish to assign different values to the metrics (as in the notional multi-role fighter example). The same decision maker is prone to human error; certainly, moderate changes can occur based on the decision maker's recent experiences or other, more irrational factors.

Furthermore, a committee of many people may have widely differing opinions on the value of a given metric. The sheer number of metrics may overwhelm any decision maker's ability to come up with rational, repeatable relative importance values. These moderate differences in relative importance can have a critical impact on the outcome, as seen in the probabilistic experiments for the beam design problem. These points can be summarized as follow-up observations:

Observation 7: Moderate changes in the relative importance of a decision metric can have a substantial impact on the final, compromise outcome of a classic MCDM algorithm.

Observation 8: It becomes increasingly difficult for human experts to consistently choose relative importance values as the complexity of an MCDM problem increases.

Another interesting result from the deterministic and probabilistic analyses was the identification of dependent decision criteria. The relative importance values are assigned as if the criteria are independent; however, this assumption seems poor. The deterministic analyses showed that this caused various "supportive" metrics to "gang up" on those they oppose that have no or fewer supporting metrics. The probabilistic analyses showed what appeared to be the existence of relatively independent components within the decision space, in this case the components of bending resistance, axial resistance, and mass. This is summarized as:

Observation 9: Complex MCDM problems likely have interdependent metrics, but may have an underlying subset of independent characteristics that can describe the necessary system-level tradeoffs.

This chapter began with the statement of four hypotheses regarding the nature of the problems to be solved for large-scale systems design. It seems appropriate that it should end with a statement of follow-up research questions that result from the initial hypotheses and experiments. These research questions are in response to the follow-up observations listed above, and are:

Question 5: Is there a simple utility approximation that can be easily implemented within classic MCDM techniques? (Observations 7 and 8)

Question 6: Is it beneficial to identify an independent subset of characteristic tradeoffs from the original requirements? (Observation 9)

The first of these follow-up research questions seeks to continue to use MCDM and adapt its simple utility model as opposed to burdening the decision maker with finding detailed utility functions. The second seeks to simplify decision making and its associated visualization through decomposition of the original requirements.

CHAPTER V

IMPORTANCE AND INTERDEPENDENCE

The deterministic and probabilistic results for the beam design problem point out significant issues with using a standard MCDM formulation for large-scale design. Instead of discarding this approach, however, it may be possible to augment the existing methods in light of the discoveries of the previous chapter. Two areas in particular seem to need attention: the utility model used in MCDM and interdependence of tradeoffs.

In the absence of any other guide, and desiring to not spiral into full-blown utility analysis, a number of intelligent assumptions can be made to create a simplified, yet accurate, utility model. This model should be able to help the decision maker determine the relative importance of any number of decision metrics, no matter how many, by examining the diversity of solutions within the decision space. It should also include a few simple inflection points that can be easily defined for a variety of metrics. This becomes:

Hypothesis 5: The relative importance of a given metric must be able to account for (Question 5):

(a) the diversity of solutions within the decision space,

(b) any true constraints that exist within the decision space, and

(c) diminishing utility along the metric's associated direction of improvement.

The interdependence of the decision metrics indicates a complexity that belies the more basic tradeoffs at the heart of the decision space. Hence, it may be possible to use the functional mapping from the design to the decision space to find these underlying characteristic dimensions and exploit them. This becomes the final hypothesis of this research:

Hypothesis 6: A linearly independent subset of approximate tradeoffs can be created from the original requirements to enable better visualization and execution of the underlying compromise within the decision space. (Question 6)

These hypotheses must be tested with the same or better scrutiny as the initial statements. Using the approaches of the first three research tasks, the method will be further developed and tested as follows:

Task 4: Create a relative importance model capable of creating consistent values with respect to solution space diversity and any inflection points in the expected utility. Test the development of this model by the procedures used in Tasks 2 and 3. (Hypothesis 5)

Task 5: Investigate methods for linear decomposition of the original requirements for visualization and interdependent decision making. Test the development of this model by the procedures used in Tasks 2 and 3. (Hypothesis 6)

5.1 Characterizing Relative Importance

One of the central, and most overlooked, tenets of MCDM lies in the determination of the relative importance of one metric over another. It is a very difficult task as the metrics are often very different in scope and scale throughout the decision space. This difficulty is exacerbated as the number of metrics grows. As seen in the previous chapter, even moderate changes in the relative importance of one metric over another can result in drastically different outcomes. Hence, this area shall receive intense scrutiny in the pages that follow.

Relative importance is the means for MCDM to describe changes in utility of one metric over another. Current MCDM formulations limit the relative importance of a metric to a single, static value. In effect, the utility of the metric is directly linked to its functional form in the decision space, scaled by an associated relative importance value. Actual changes in utility can be due to a variety of different factors, and may change throughout the decision space. For this research, a two-part model is proposed, given as

$$w_j = w_j^s + w_j^d(\vec{y}) \tag{34}$$

where w_j is the relative importance (sometimes referred to as "weight") of the j^{th} metric, w_j^s is the *static* importance of the metric, and $w_j^d(\vec{y})$ is the *dynamic* importance. The static value is useful as before, used to denote a general sense of how important one metric is over another. It can also continue to be used as the source of uncertainty in the decision space.

The dynamic contribution is used to modify the utility locally across the decision space to account for any inflection points or diminishing utility throughout the space. Hence, it is listed as a function of the vector $\vec{y}$ used to describe the current point in the decision space. Recall that there is a functional mapping between the design and decision spaces, hence $\vec{y} = f(\vec{x})$, so the dynamic contribution can just as easily be written as $w_j^d(\vec{x})$.

5.1.1 Entropy and Static Relative Importance

The choice of static relative importance for individual metrics can follow from basic systems engineering concepts, such as those given in Chapter II. These values are usually chosen by a qualified individual or panel of experts that debate the importance of one particular metric to another. However, as noted before, it becomes increasingly difficult to assign importance to individual requirements as their number and diversity increases. Therefore, a decision maker needs some sort of aid when choosing these values. This method should be repeatable and backed by a scientific process.

One constant in any decision making problem is the presence of two or more differentiated alternatives, as described in Chapter III. The decision space becomes richer in the diversity of available concepts as this differentiation increases. It is highly desirable to be able to measure this diversity and apply it to the enumeration of static importance. Such a method would penalize those metrics with a low diversity (assign a low static relative value) and reward other metrics with greater contrast from the best value in the decision space (assign higher relative importance). Hence, if one were picking players for a basketball team, it may seem intuitive that height is very important. However, if all of the subjects in the decision pool were the same height, or very close in height, then height would no longer be considered an important metric. Hence, the *contrast intensity* of a given metric from its best value within the decision space is related to how far it is out of *equilibrium*, and with what frequency.

Classical thermodynamics shows that a closed system at equilibrium will be at maximum entropy. Thermodynamic equilibrium implies that all "observable states" are macroscopically unchanging throughout the entire system [Moran and Shapiro, 1995]. This principle

is related to gas dynamics via the famous Boltzmann equation, in one of many published forms as

$$S = k \ln W \tag{35}$$

where S is the entropy of the system, k is a constant, and W is the number of microstates in a given macrostate. This quantity is maximized at the *most probable macrostate*, which is the macrostate with the maximum number of microstates, hence, $S_{max} = k \ln W_{max}$. This important relation serves as the link between statistical mechanics and classical thermodynamics [Anderson, Jr., 1989; Vincenti and Kruger, Jr., 1965].

Philosophically, this principal can be applied to finding the relative importance of a metric by using an entropy-like measure. The "entropy" can be used to measure how far a particular decision space is from equilibrium, with maximum entropy occurring at equilibrium. In this analogy, "equilibrium" in a metric is reached when all of the alternatives have identical values (therefore all have the best available value) in that particular metric.

With this in mind, *contrast intensity* can be thought of as the inverse of entropy. That is, the contrast intensity of a metric will increase as its individual elements move further from the best value. Figure 26 illustrates this concept of contrast intensity.

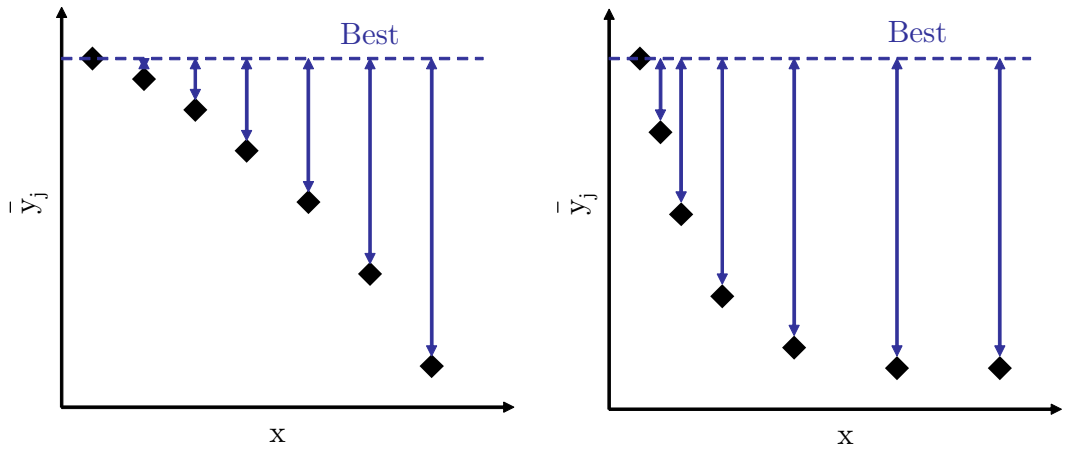

(a) Lower Contrast (b) Higher Contrast

Figure 26: Contrast Intensity

This concept is not original, and has been used for a variety of operations research problems to characterize relative importance [Soofi and Retzer, 1992; Soofi, 1990]. Zeleny

gives a formulation for entropy-based relative importance from a discrete pool of alternatives [Zeleny, 1982]. The procedure is as follows, using the notation introduced in Chapter III.

Recall that a vector $\overline{y}_j = (\overline{y}_{1j}, \overline{y}_{2j}, \ldots, \overline{y}_{ij} \ldots \overline{y}_{mj})$ characterizes the set $\overline{Y}$ in terms of the j^{th} normalized attribute for m alternatives. Note that the method of normalization will have a direct effect on the outcome of the problem. For this research, the 2-norm is used to keep the Euclidean notion of distance (much like TOPSIS). Any preferred method may be used, though it is desirable to normalize these quantities such that zero represents the lowest possible value and one is the largest possible (due to the natural log function). Hence, this document normalizes the metrics via

$$\overline{y}_{ij} = 1 - \left(\frac{y_{ij} - y_j^*}{y_j^- - y_j^*} \right)^2 \tag{36}$$

recalling that y_j^* and y_j^- denoted the best and worst values of the j^{th} metric, found via single-objective optimization of each metric. Then define

$$\overline{Y}_j = \sum_{i=1}^{m} \overline{y}_{ij} \qquad j = 1, 2, \ldots, n \tag{37}$$

recalling that there are m total alternatives and n total metrics. The *entropy* of the j^{th} metric is measured as

$$e(\overline{y}_j) = -K \sum_{i=1}^{m} \frac{\overline{y}_{ij}}{\overline{Y}_j} \ln \frac{\overline{y}_{ij}}{\overline{Y}_j} \tag{38}$$

where $K > 0$, $0 \leq \overline{y}_{ij} \leq 1$, and $e(\overline{y}_j) \geq 0$. If all $\overline{y}_{ij}$ become identical for a given j, then $\frac{\overline{y}_{ij}}{\overline{Y}_j} = \frac{1}{m}$, and $e(\overline{y}_j)$ assumes its maximum value, $e_{max} = \ln m$. Thus, setting $K = \frac{1}{e_{max}}$ will ensure that all of the $e(\overline{y}_j)$ values will sum to one. This normalization helps for comparative purposes. Notice the similarity of equation (38) to the classical Boltmann equation for thermodynamics, given in equation (35).

The *total entropy* of $\overline{Y}_j$ is defined as

$$E = \sum_{j=1}^{n} e(\overline{y}_j) \tag{39}$$

The relative importance of a metric is inversely proportional to its entropy (or, as defined before, proportional to the contrast intensity). The entropy-based importances are then

defined as

$$\lambda_j = \frac{1}{n-E}[1 - e(\overline{y}_j)] \tag{40}$$

where λ_j is the entropy-based importance of the j^{th} metric. Equation (40) is normalized such that each individual value is between zero and one and the sum of all of the importance values equals one.

If necessary, the decision maker may still modify the entropy-based relative importance with a preference. This defines the final static contribution to the relative importance as

$$w_j^s = \frac{w_j^{pref}\lambda_j}{\sum_{j=1}^{n} w_j^{pref}\lambda_j} \tag{41}$$

where w_j^{pref} is the value of the relative importance chosen by the decision maker. Note that in the absence of other strong preference information, this value is usually one.

This discrete formulation can be used for a continuous decision space with some error. As before, a random sample of the design space can be mapped over to create a representative random sample of the decision space to form the basis for the contrast intensity calculations. This process is akin to Monte Carlo integration of a multidimensional function [Press et al., 1997], though not explicitly so.

This formulation was tested on the six- and eight-requirement formulation for the beam design problem. A total of 5,000 uniformly random samples were taken from the design space and were subsequently mapped to the decision space using the original analysis routines (the surrogate models were not used for clarity, though they are equally applicable). Typical results for the entropy-based relative importance are shown in Table 7. The results of the entropy analysis depend on the quality of the random sample, though the error was found to be approximately one percent during a few trials with this case.

This initial entropy analysis is telling. First, both the six- and eight-requirement problems both seem to have the same relative spacing, and the redundant requirements (R_7 and R_8) are exactly correlated with the values for R_3 and R_5 for the eight-requirement form. Note also that R_2 and R_6, which are of the exact same functional form, have virtually identical values. However, the actual order is flipped for the six- versus the eight-requirement

Table 7: Entropy-Based Static Relative Importance

Value	6 Req.	8 Req.
λ_1	0.3469	0.2779
λ_2	0.1804	0.1447
λ_3	0.2337	0.1885
λ_4	0.05315	0.04162
λ_5	0.007737	0.006467
λ_6	0.1781	0.1459
λ_7	-	0.1885
λ_8	-	0.006467

case. The difference in relative importance in either case is less than 0.3%, so this is likely a result of the slight error in the random sampling technique.

The ranking of the metrics indicates that R_1 is by far the most important of the requirements, followed by R_3 (and R_7 for eight requirements). Next on the list is a virtual dead heat between R_2 and R_6, with R_4 of much lesser importance and R_5 (and R_8) virtually unimportant. This indicates that the most important metrics, in descending order, appear to be buckling, bending strength, compressive strength, mass, and finally compressive and bending deflection. Since these are based on the contrast of each metric within the decision space, one can logically conclude that the level of average contrast in the metrics descends in this order, with buckling being the higher contrast metric and compressive deflection the closest to "equilibrium." This is easily viewed for this simple problem via the requirements surfaces, as seen from the previous chapter in Figure 20. This figure identifies what should intuitively be low- versus high-contrast metrics.

While an entropy-based approach seems to simplify selection of static relative importance, it has a few drawbacks. Most notably, it considers contrast from all parts of the decision space to be important. It is very possible that the best value of the decision space is in a region far beyond a point where continued improvement matters to a decision maker. This point, hereon referred to as the *threshold* of the metric in this document, is very important to the development of the dynamic relative importance model described in the next subsection. However, the threshold will also be important to the development of *threshold-modified static relative importance*.

To better understand the concept of a threshold, first consider the maximum and minimum ranges within the decision space. Simple, single-objective optimization can find the maximum and minimum possible values for each decision metric within the design space domain. The ranges of the beam problems's decision metrics are given in Table 8 for the design space domain as listed before in Section 4.3.1.

Table 8: Ranges for Decision Metrics in Beam Design Problem

Metric	**Worst** (y_j^-)	**Best** (y_j^*)
R_1	0.2505	12.53
R_2	15.63	78.17
R_3	0.4944	7.817
R_4, m	4.10E-04	8.21E-05
R_5, m	0.2736	0.01094
R_6, kg	13.95	2.790
R_7	0.4944	7.817
R_8, m	0.1710	0.003420

This table shows that some metrics are well above any maximal desirable value throughout a significant portion of the decision space. For example, compressive failure factor of safety, R_2, ranges from a low of 15.63 to a high of 78.17. Certainly this is well above a threshold, for the decision maker will not want the MCDM algorithm to attempt to improve this value at the expense of another. Other metrics, such as Euler buckling factor of safety, R_1, show a high relative change, in this case from 0.2505 to 12.53. Certainly, a factor of safety below 1.0 is unacceptable, but most likely 12.53 is excessive, so the threshold may lie somewhere in between.

The presence of a threshold should modify the entropy concept by considering all items at or above the threshold in equilibrium. In this way, any contrast above the threshold will not be counted towards the contrast intensity; indeed, it will penalize it by increasing the entropy of that particular decision metric. This is depicted for a notional metric in Figure 27. In this definition, "above" when relating to the threshold is relative to the direction of improvement of the metric. Hence, for the deflection metrics (lower is better), the threshold will be a lower limit, as would be any threshold for the mass metric.

This definition can be checked once again on the static relative importance of the beam

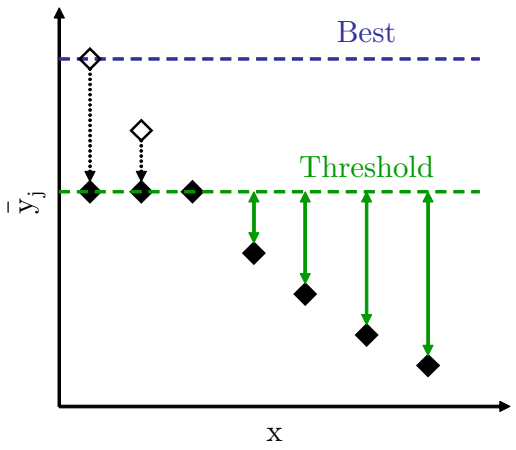

Figure 27: Threshold-Modified Contrast Intensity

metrics. For this simple exercise, consider all factors of safety to have a threshold of 3.0 and all deflection criteria a threshold of 0.05 meters. That is to say that all values of factor of safety beyond 3.0 will be considered in equilibrium and therefore further contrast beyond this value will only increase the entropy of the metric, hence decreasing its contrast intensity and subsequent relative importance. Conversely, any deflection value below 0.05 meters will be treated in the same way. Since beam mass is the only "cost" function, it will have no threshold, indicating that if everything else is at or above the threshold, then seek the minimum cost (mass) solution.

Recall that in the previous chapter, Figure 20 displayed the variation in beam requirements throughout the design space. Figure 28 now displays the same requirements with the addition of the thresholds. It is easy to see how the addition of thresholds will change the contrast intensity of the decision space for this problem. The sampling method described earlier can be used to find the threshold-modified contrast intensity, and the typical results are given in Table 9.

These results are far more promising. Most noticeable is the drop in λ_2 and λ_4 to near-zero. These values should be zero as their entire ranges for the associated beam requirements are beyond their thresholds. They are instead at near zero because of the machine limitations used in their computation. Now beam mass heads the list as the most important contributor, as all of the other metrics are impacted due to the presence of the

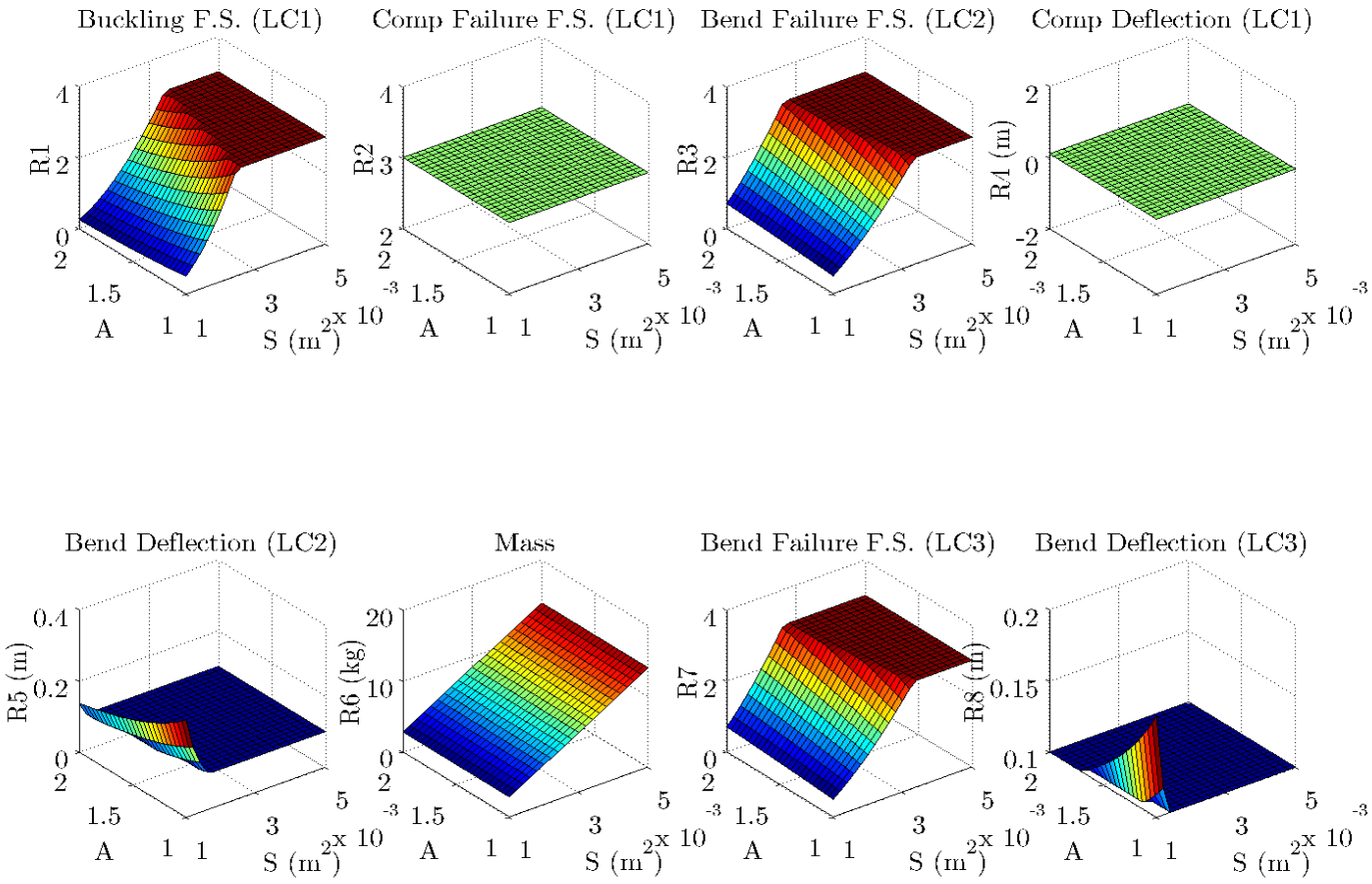

Figure 28: Threshold-Modified Beam Requirements throughout Design Space

Table 9: Threshold-Modified Entropy-Based Static Relative Importance

Value	6 Req.	8 Req.
λ_1	0.3082	0.2465
λ_2	1.84E-12	1.48E-12
λ_3	0.2287	0.1864
λ_4	1.84E-12	1.48E-12
λ_5	0.01048	0.009471
λ_6	0.4527	0.3649
λ_7	-	0.1864
λ_8	-	0.006371

threshold throughout their full ranges. Some of the relative importance values seem to have increased; this is an artifact of the process as it requires the static relative importance values to sum to one.

Though this adds the burden of selecting a threshold value when determining static relative importance, these values are relatively intuitive to select. They simply represent the best possible performance the decision maker desires; the point beyond which further improvement is inconsequential. This concept, along with others, is very important for the calculation of dynamic relative importance.

5.1.2 Constraints, Thresholds, and Dynamic Relative Importance

The second portion of the two-part relative importance model is the dynamic contribution. This is used to represent the effect of local changes in utility due to the current value of the decision metric. The goal is to keep this function simple to specify by identifying a general model with a few intuitive inflection points. The threshold, described above, can serve as one of these inflection points. At the opposite end of the spectrum is the constraint, which can serve as another inflection point.

The lack of internal constraints in the generalized MCDM formulation allows the engineer direct control over these values. Furthermore, it embodies the basic approach in probabilistic MCDM: elimination of as many constraints as possible to enable tradeoffs. Many requirements that are considered "constraints" are actually arbitrary performance levels set forth by a committee well before system definition and synthesis are performed.

These performance levels may be set to dominate performance of an existing concept, as a minimum goal for performance, or sometimes simply to help define the problem better for typical single-objective optimization or fuel-balance sizing. Elimination of these constraints is crucial to MCDM as it allows for implicit tradeoffs to be made on high-payoff objectives at the expense of less important objectives. For example, a military fighter may have a constraint on maximum sustained turn rate. Constraining the space to meet this turn rate may eliminate otherwise favorable compromise solutions, such as marginally lower turn rate for a large increase in speed or decrease in cost. However, some actual constraints do exist, usually for safety, certification, or resource reasons. Several examples of true constraints can be seen in meeting the Code of Federal Regulations for civil transport design [Federal Aviation Administration, 2005]. For this research, the term *constraint* refers to the minimum acceptable value of a given metric. In this way, it is essentially the opposite of the threshold term defined in the previous section.

The concept of threshold values continues as introduced in the previous section on static relative importance. Thresholds are even more important for the dynamic contribution to the relative performance if the threshold lies somewhere within the decision space. Beyond the threshold, improvement in the metric becomes inconsequential. Modeling this behavior is crucial if a metric has an associated threshold.

In a basic sense, the ideal dynamic contribution to importance will rise sharply if its associated constraint is violated. This makes it the most important objective in the space until the constraint is satisfied. At this point, the dynamic contribution quickly drops to zero and the MCDM algorithm proceeds using only the static value. If the metric improves much beyond its constraint and has a threshold value the dynamic importance will become slightly negative, becoming more negative until it reaches the threshold, upon which it is equal to exactly the opposite of the static value. Therefore, the sum of the static and dynamic contributions equals exactly zero at or beyond the threshold, effectively negating any influence of that particular metric on the MCDM algorithm.

Specifically, this dynamic function cannot have too sharp of a change in value. If it were too sharp it could increase the difficulty associated with gradient-based optimizers.

Therefore, continuous, smooth functions should be used whenever possible. Further, these dynamically modified importance values should *not* be re-normalized to sum to one, else any change in one value would change all others. This could also have an adverse effect on gradient-based optimizers.

The constraint portion of the dynamic importance model should approximate a step function. One attractive option is to find a smooth approximation of the Heaviside Step Function, also known as the Unit Step Function [Weisstein, 2005]. An approximation to this is defined as

$$w_j^{dc}(\vec{x}) = -1\left[-\frac{1}{2} + \frac{1}{\pi}\tan^{-1}\left[\alpha(\overline{y}_j(\vec{x}) - \overline{c})\right]\right] \tag{42}$$

where w_j^{dc} refers to the constraint contribution to the j^{th} dynamic importance, $\overline{y}_j(\vec{x})$ refers to the current value of the j^{th} metric, $\overline{c}$ refers to the normalized constraint value, and α is a scale factor for controlling smoothness of the step function. Larger values of α will make the step function more abrupt. If α is too abrupt there may be problems with gradient-based optimizers, whereas if it is too small it will not jump fast enough near the constraint. Early experiments indicate that a good value of α is approximately 200, though this is best tailored to the individual problems and optimization algorithms used.

The threshold should not be approximated with another step function because this concept is related to a gradual decay in utility as the threshold is approached. This decay can be modeled as an inverse power relationship. It should be zero at the constraint (or the edge of the design space, if no constraint is present) and should be opposite of the static relative importance at the threshold value. A model for this is

$$w_j^{dt}(\vec{x}) = -w_j^s\left(1 - \frac{\overline{t} - \overline{y}_j(\vec{x})}{\overline{t} - \overline{c}}\right)^{\frac{1}{4}} \tag{43}$$

where w_j^{dt} is the threshold contribution to the j^{th} dynamic importance and $\overline{t}$ is the normalized threshold value. Note that both $\overline{c}$ and $\overline{t}$ should be normalized by the same procedure as most response surface equations; that is, by the mean and variance of their respective responses. If $\overline{c}$ is less than -1.0 then the entire decision space is beyond the constraint; likewise for $\overline{t}$. If either value is greater than 1.0 it implies that the entire space is smaller than the constraint or threshold value.

Equations (42) and (43) can be combined into a single dynamic function that is valid across the entire space no matter what its nature. This is represented by

$$w_j^d(\vec{x}) = \begin{cases} \left[\frac{1}{2} - \frac{1}{\pi}\tan^{-1}\left[\alpha(\overline{y}_j(\vec{x}) - \overline{c})\right]\right] - w_j^s\left(1 - \frac{\overline{t} - \overline{y}_j(\vec{x})}{\overline{t} - \overline{c}}\right)^{\frac{1}{4}} & ; \quad \overline{y}_j(\vec{x}) \leq \overline{t} \\ -w_j^s & ; \quad \overline{y}_j(\vec{x}) > \overline{t} \end{cases} \tag{44}$$

with the notation as noted before. A plot of an example dynamic function for all $y_j(\vec{x})$ is given in Figure 29. Note that this is one model that is used throughout the examples that follow but it is very easy for it to take other forms as appropriate for specific applications.

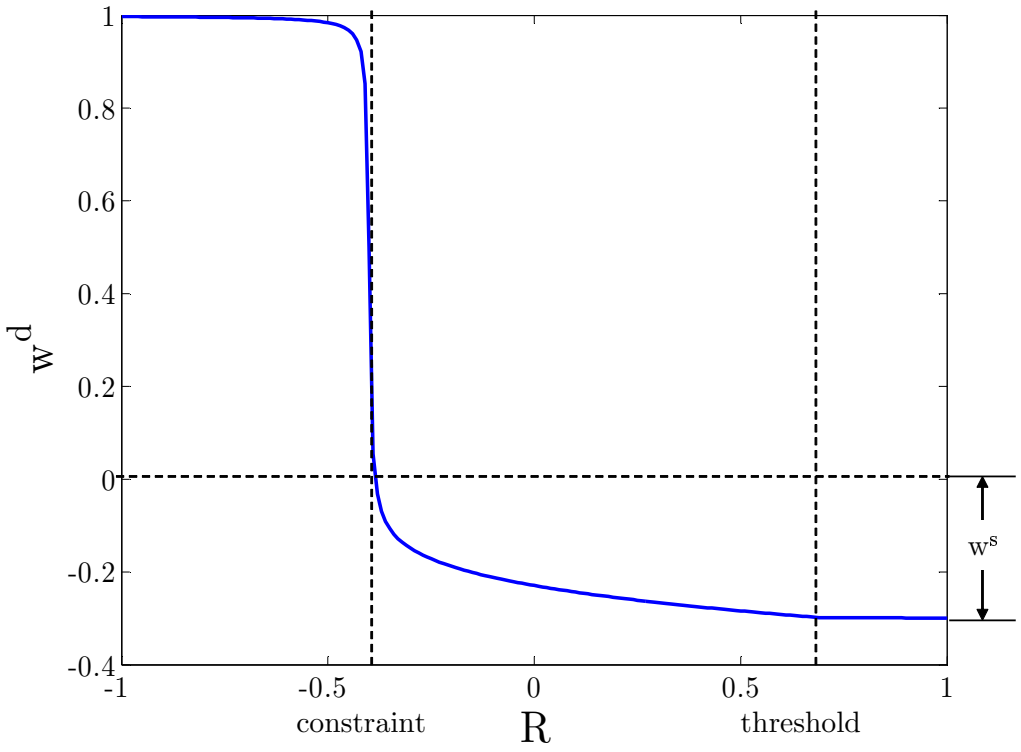

Figure 29: Example Dynamic Weight Variation

This model allows for specification of relative importance with local changes in the utility by using two intuitive inflection points. Most systems design engineers are familiar with the concept of a constraint; this vastly improved relative importance model only requires a design engineer to specify one additional point for each metric, the threshold. This makes it possible to avoid enumeration of utility functions for each metric but instead allows dynamic relative importance to be the map from the decision space to an implied utility.

5.1.3 Experiments with Modified Relative Importance Models

The beam design problem helped discover some of the problems with basic MCDM methods for large-scale problems; hence, it is implemented again to see if the two-part relative importance model improved the results. First, the results were computed considering only the static portions for the relative importance, but with the entropy-based importance values. The results for the six- and eight-requirement problem are compared in Table 10, both with and without the threshold-modified entropy relations. The relative importance values used were representative of those given in Tables 7 and 9. Note that these experiments were conducted using the original beam analysis routines and not the surrogate models for clarity of presentation.

Table 10: Deterministic Entropy-Based Results for Beam Design Problem

	6 Requirements		**8 Requirements**	
Value	**Entropy**	**Entropy (TM)**	**Entropy**	**Entropy (TM)**
S, m^2	0.004826	0.002668	0.005000	0.003247
A	1.000	1.000	1.119	1.000
R_1	11.67	3.567	11.19	5.281
R_2	75.45	41.71	78.17	50.75
R_3	5.241	2.155	5.487	2.892
R_4, m	8.50E-05	1.54E-04	8.21E-05	1.26E-04
R_5, m	0.01175	0.03843	0.009780	0.02596
R_6, kg	13.46	7.445	13.95	9.058
R_7	-	-	5.847	2.892
R_8, m	-	-	0.006112	0.01622

This table shows that the CP solutions using the entropy-based relative importance appear to be as bad, if not worse, than the solutions with the original assumption of even importance given in Table 4 in the previous chapter. There is a dramatic difference between these solutions using the standard entropy formulation and the threshold-modified solutions. The latter solutions appear to be far more reasonable, especially the six-requirement model, given the reduction in beam mass but otherwise acceptable performance in the other metrics with respect to thresholds. Note that the threshold-modified cases still have several requirements that register above the threshold values, but they do so by much less than the standard entropy-based solutions.

These formulations can be further contrasted by viewing the differences between the objective functions. These are compared in Figure 30 for the six-requirement case and Figure 31 for eight requirements. The scales of the function values differ on the vertical axes in these figures to better illustrate the objective function surface. The reader is referred to Figure 23 from the previous chapter for viewing the original CP objective functions.

The pairwise comparison within the figures is quite telling. While the original entropy formulation does little to change the general shape of the objective function, the threshold-modified values change the shape significantly. The threshold modification gives the beam mass contribution to the overall objective function enough influence that it causes a highly undesirable region towards the higher-mass solutions (large values of S). However, there still appears to be bias in the six- versus eight-requirement solutions as they are significantly different.

The addition of the dynamic relative importance model to the beam design problem causes more changes in the CP solution. The dynamic portion of the model as given in equation (44) is used with the threshold-modified static relative importance model to create the total importance of each metric. The thresholds and the constraints used for the beam design problem are given in Table 11. The thresholds are the same as before, and the constraints are the same as used in the single-objective control experiments. Once again, there was no threshold or constraint for beam mass, indicating that in the absence of all other influences, R_6 should be minimized. The variation of total relative importance with these constraints and thresholds is shown in Figure 32.

Table 11: Constraints and Thresholds for Beam Design Problem

Metric	**Constraint**	**Threshold**
R_1	≥ 1.5	≥ 3.0
R_2	≥ 1.5	≥ 3.0
R_3	≥ 1.5	≥ 3.0
R_4, m	≤ 0.1	≤ 0.05
R_5, m	≤ 0.1	≤ 0.05
R_6, kg	-	-
R_7	≥ 1.5	≥ 3.0
R_8, m	≤ 0.1	≤ 0.05

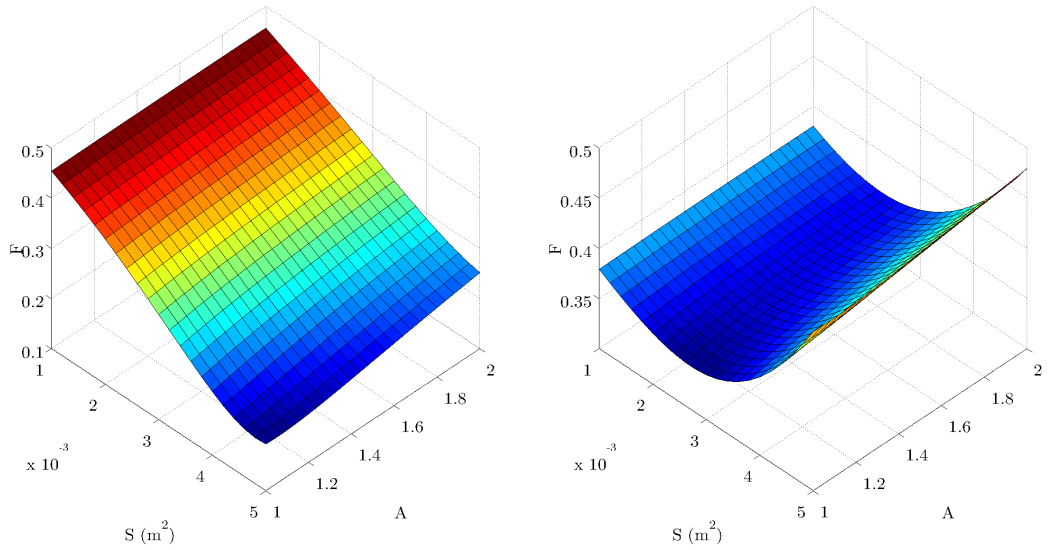

(a) Basic Entropy Formulation (b) Threshold-Modified Formulation

Figure 30: Objective Functions for Six Requirements with Entropy-Based Relative Importance

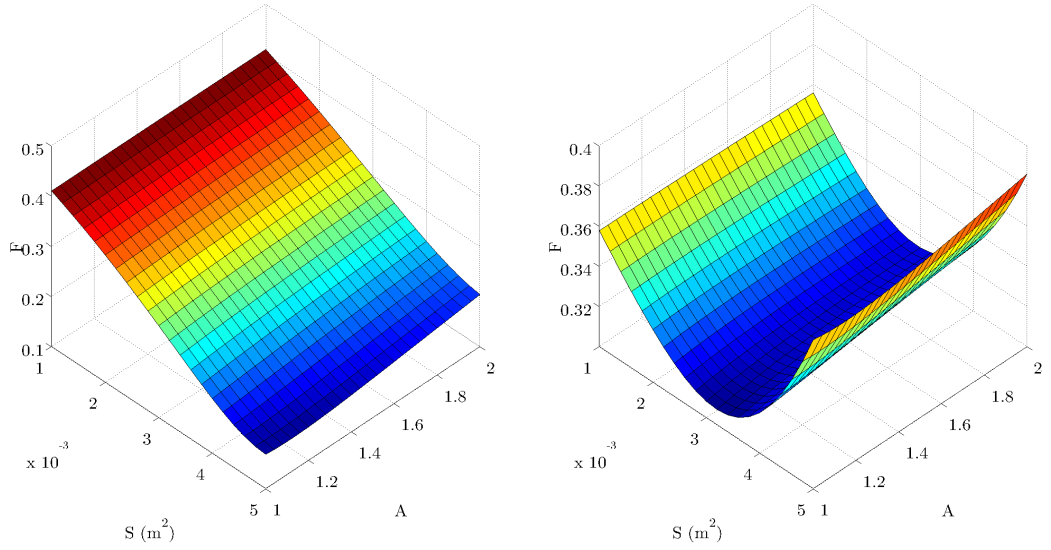

(a) Basic Entropy Formulation (b) Threshold-Modified Formulation

Figure 31: Objective Functions for Eight Requirements with Entropy-Based Relative Importance

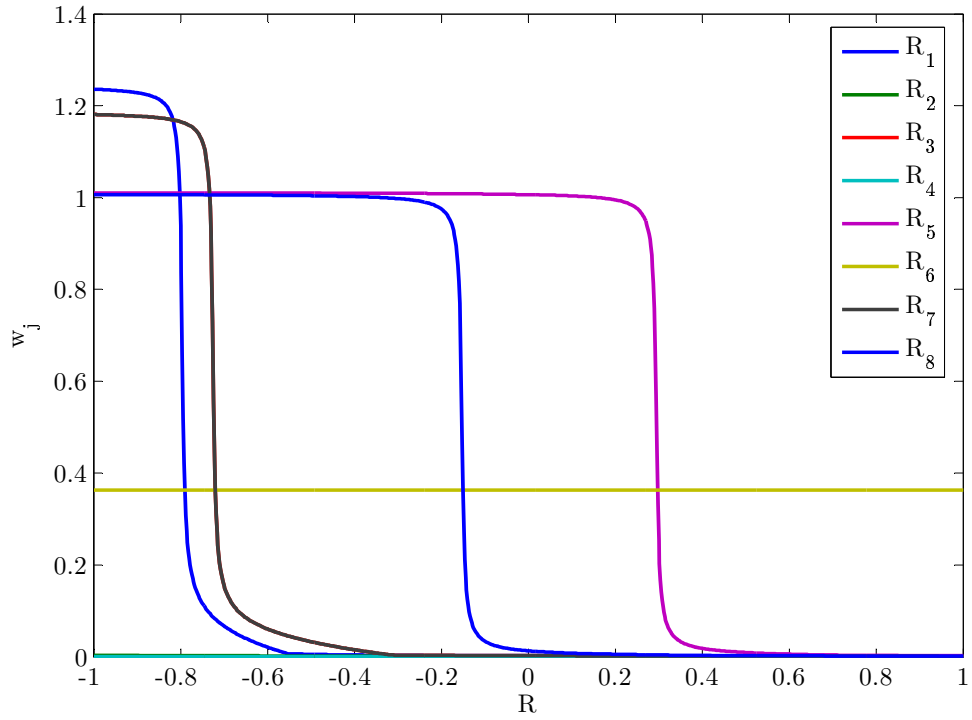

Figure 32: Variation of Relative Importance for Beam Design Problem versus Normalized Response Value

This figure is given for the eight-requirement model; the six-requirement model is similar though the actual importance values are scaled slightly. The responses are all normalized such that "larger is better" and to a scale of -1 to 1. Note that the native direction of improvement for the deflections (as well as beam mass) is "smaller is better," but this is accounted for in the normalization process. The familiar shape of the dynamic importance contribution, first shown in Figure 29, is apparent in this latest figure. Requirements violating a constraint have a relative importance that is greater than one, and requirements at or past their threshold values are at zero (or approximately zero, as there is some machine error). Some of the requirements are always beyond their thresholds; these are R_2 and R_4, hence they always appear to be at zero in this chart. R_7 exactly overlaps R_3 because these two requirements are identical mathematically. At the extremes of the requirements space, only R_6 contributes to the relative importance, indicating that it will be the only active requirement in this space.

Compromise programming for the full two-part relative importance model gives even

more promising results. These are compared in Tables 12 and 13 for six and eight requirements, respectively. The results of the control single-objective experiment and the various CP problems are repeated in these tables to show the improvement in the solution method. The effect of the dynamic importance model on the objective functions is shown for both cases in Figure 33.

Table 12: Deterministic Results for Six-Requirement Beam Design Problem

Value	SOO Control	Even	Entropy	Entropy (TM)	Dynamic
S, m^2	0.001950	0.004429	0.004826	0.002668	0.002330
A	1.239	1.000	1.000	1.000	1.1500
R_1	1.500	9.808	11.67	3.567	2.364
R_2	30.49	69.25	75.45	41.71	36.43
R_3	1.500	4.614	5.241	2.155	1.886
R_4, m	2.17E-04	1.00E-04	8.50E-05	1.54E-04	1.76E-04
R_5, m	0.06875	0.01757	0.01175	0.03843	0.04380
R_6, kg	5.441	12.36	13.46	7.445	6.501

Table 13: Deterministic Results for Eight-Requirement Beam Design

Value	SOO Control	Even	Entropy	Entropy (TM)	Dynamic
S, m^2	0.001950	0.004794	0.005000	0.003247	0.002419
A	1.239	1.294	1.119	1.000	1.248
R_1	1.500	8.966	11.19	5.281	2.349
R_2	30.49	74.94	78.17	50.75	37.82
R_3	1.500	5.901	5.487	2.892	2.079
R_4, m	2.17E-04	8.97E-05	8.21E-05	1.26E-04	1.70E-04
R_5, m	0.06875	0.01396	0.009780	0.02596	0.03744
R_6, kg	5.441	13.37	13.95	9.058	6.750
R_7	1.500	5.901	5.847	2.892	2.079
R_8, m	0.04297	0.008722	0.006112	0.01622	0.02340

Next, it is necessary to test the sensitivity of the deterministic solution to the constraints and thresholds. Therefore, the constraints and thresholds were varied for a "wide" case (lower constraints, higher thresholds) and "narrow" case (same constraints, lower thresholds). The levels for the constraints and thresholds are depicted in Table 14. These tests were only conducted with the six-requirement form of the beam design problem.

As the gap between the thresholds and constraints widen, one would expect the solution to approach the non-dynamic entropy-based model. Narrowing of the constraint-threshold

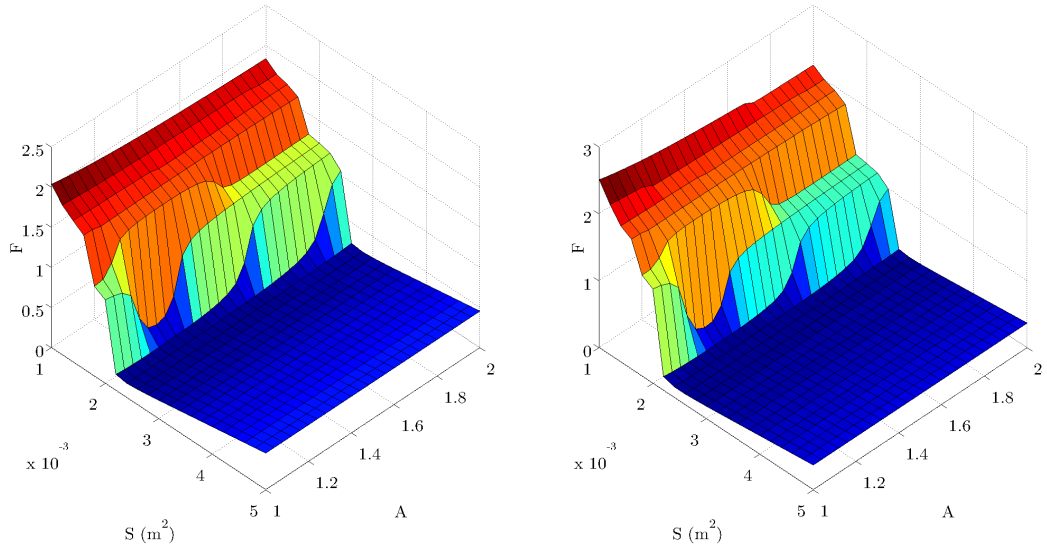

(a) Six Requirements

(b) Eight Requirements

Figure 33: Objective Functions for Beam Design with Dynamic Relative Importance

Table 14: Constraint and Threshold Levels for Sensitivity Analysis Scenarios

	Wide Scenario		**Narrow Scenario**	
Metric	**Constraint**	**Threshold**	**Constraint**	**Threshold**
R_1	≥ 1.0	≥ 6.0	≥ 1.5	≥ 2.0
R_2	≥ 1.0	≥ 6.0	≥ 1.5	≥ 2.0
R_3	≥ 1.0	≥ 6.0	≥ 1.5	≥ 2.0
R_4, m	≤ 0.2	≤ 0.025	≤ 0.1	≤ 0.075
R_5, m	≤ 0.2	≤ 0.025	≤ 0.1	≤ 0.075
R_6, kg	-	-	-	-

gap should cause the solution to approach the single-objective constrained optimization results. The results trend towards these extremes, as seen in Table 15. The percent difference expressed here is from the six-requirement dynamic solution from Table 12.

Table 15: Deterministic Results for Six-Requirement Constraint and Threshold Sensitivity Study

	Wide Scenario		**Narrow Scenario**	
Value	**Result**	**% Diff**	**Result**	**% Diff**
S, m^2	0.002659	14.1%	0.002155	-7.5%
A	1.000	-13.0%	1.209	5.1%
R_1	3.544	49.9%	1.925	-18.6%
R_2	41.58	14.1%	33.69	-7.5%
R_3	2.144	13.7%	1.720	-8.8%
R_4, m	1.54E-04	-12.4%	1.90E-04	8.1%
R_5, m	0.03868	-11.7%	0.04873	11.3%
R_6, kg	7.420	14.1%	6.013	-7.5%

The net result appears that moderate changes in the thresholds and constraints do have a sizeable effect on the solution; however, it is generally not as large as the magnitude of the change itself (i.e. doubling the threshold does not double the response). The results are less pronounced than those seen for moderate changes on the relative importance values themselves. The changes in the objective functions are readily seen in Figure 34, which helps to explain some of the differences from the baseline dynamic model results.

The final step is to apply the full two-part relative importance model to the probabilistic design problem. This time, the uncertainty in the relative importance enters in the w_j^{pref} term in the static component of importance as seen from equation (41). These values, previously taken as $\frac{1}{n}$ for the deterministic studies (evenly distributed user preference) was varied by 50% on either side as in the probabilistic study in Chapter IV. The values of the mean and standard deviations of the design and response variables are given in Table 16.

These results seem to indicate that the probabilistic solutions are more tightly clustered. One interesting observation is the contrast between the standard deviation about beam aspect ratio, A. This design variable setting determines tradeoff between buckling and bending strength. In the six-requirement case, the standard deviation is 6.2%, whereas the eight-requirement case is at 5.6%. This indicates that the eight-requirement model may

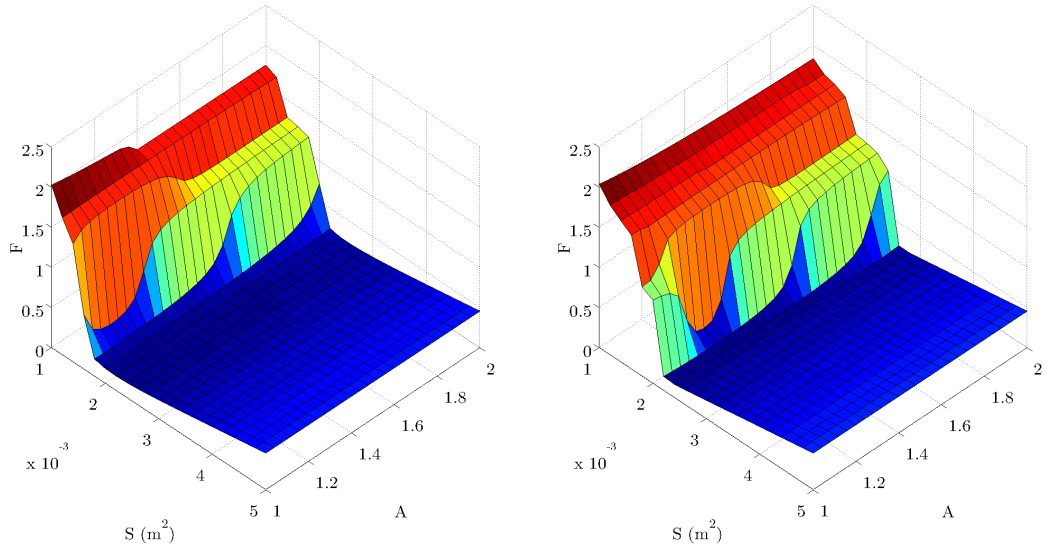

(a) Wide Scenario

(b) Narrow Scenario

Figure 34: Objective Functions for Beam Constraint and Threshold Sensitivity Study

Table 16: Probabilistic Results Comparison for Beam Design Problem with Dynamic Relative Importance Model

	6 Requirements			**8 Requirements**		
Value	μ	σ	σ %	μ	σ	σ %
S, m^2	0.002342	1.06E-04	4.5%	0.002441	1.15E-04	4.7%
A	1.169	0.07193	6.2%	1.274	0.07159	5.6%
R_1	2.362	0.2307	9.8%	2.353	0.2236	9.5%
R_2	36.61	1.654	4.5%	38.16	1.793	4.7%
R_3	1.917	0.1555	8.1%	2.130	0.1776	8.3%
R_4, m	1.76E-04	7.75E-06	4.4%	1.68E-04	7.80E-06	4.6%
R_5, m	0.04314	0.004901	11.4%	0.03645	0.004326	11.9%
R_6, kg	6.534	0.2952	4.5%	6.811	0.3200	4.7%
R_7	-	-	-	2.130	0.1776	8.3%
R_8, m	-	-	-	0.02278	0.002704	11.9%

still be biased in favor of bending resistance due to the addition of the redundant bending requirements. This statement can be expanded upon by analyzing the mean shift from the six- to the eight-requirement case, including a Student's t-test as before. The results of this comparison are given in Table 17.

Table 17: Dynamic Model Mean Shift from Six- to Eight-Requirement Probabilistic Solutions

Value	$\mu_6 - \mu_8$	σ	***t*-Statistic**	***p*-Value**
S, m^2	-9.92E-05	1.53E-04	20.44	7.05E-78
A	-0.1047	0.09886	33.50	1.50E-165
R_1	0.008535	0.3160	0.8540	0.3932
R_2	-1.551	2.398	20.44	6.96E-78
R_3	-0.2130	0.2316	29.09	2.79E-135
R_4, m	7.10E-06	10.8E-05	20.81	3.61E-80
R_5, m	0.006688	0.006388	33.11	7.64E-163
R_6, kg	-0.2767	0.4280	20.44	7.06E-78

As with the first probabilistic case, the shifts in the means appear to be nontrivial as given by the p-values. One notable exception is the shift exhibited by the buckling requirement, R_1. This has a high enough p-value that considered alone it would not be advisable to discard the null hypothesis. Hence, it appears that the addition of the bending requirements does not change the beam's response to buckling, but rather makes it stronger in bending while maintaining its buckling strength.

Viewing the scatterplots of the design variables and requirements of the probabilistic analysis further shows the improvements in decision making with the two-part relative importance model. The resulting plots for the design variables are shown in Figure 35 for both the six- and eight-requirement cases. Only the six-requirements scatterplot for the responses is shown in Figure 36 due to difficulties with viewing the eight-requirement case on a single page.

The scatterplots of the design variables indicate that the cases are much more tightly clustered than those of the previous probabilistic analysis. Certainly, the notion of taking the mean and standard deviation of these datasets is more than an academic exercise as was the case with the results shown in Figure 24 in Chapter IV. One of the most striking features

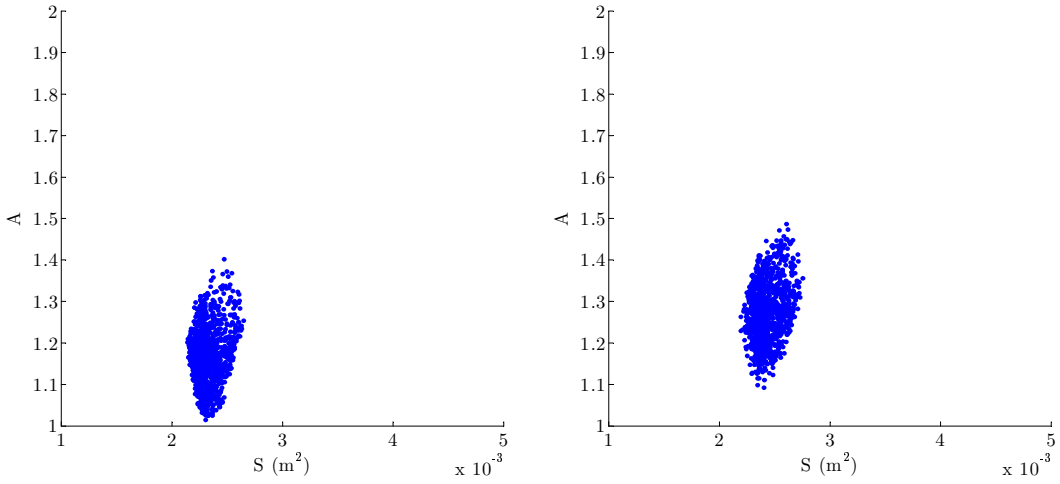

(a) Six Requirements (b) Eight Requirements

Figure 35: Design Variable Scatterplots for Beam Design with Probabilistic Requirements

is the difference in the spread along the S and A axes. The values for cross-sectional area exhibit much less spread than beam aspect ratio. This is likely because the tradeoffs that exist between buckling and bending resistance. Further, the eight-requirement results are all scattered about a higher aspect ratio, further indication that the eight-requirement solution is biased towards bending. The response scatterplot for the six-requirement problem, while still difficult to resolve, indicates that the actual variation in the requirements is much more tightly clustered within the decision space than seen from the results with the original MCDM formulation (Figure 25 in the previous chapter).

It appears that the two-part relative importance model with its modified entropy formulation is working by reducing variation in the decision space, even with moderately large changes in the relative importance. Certainly the results are much better than the initial studies from the previous chapter. However, the solution is still biased by the nature of the requirements themselves, and viewing the results for many requirements (greater than six) can be very difficult. Solution of these problems requires further exploration into the nature of the decision space.

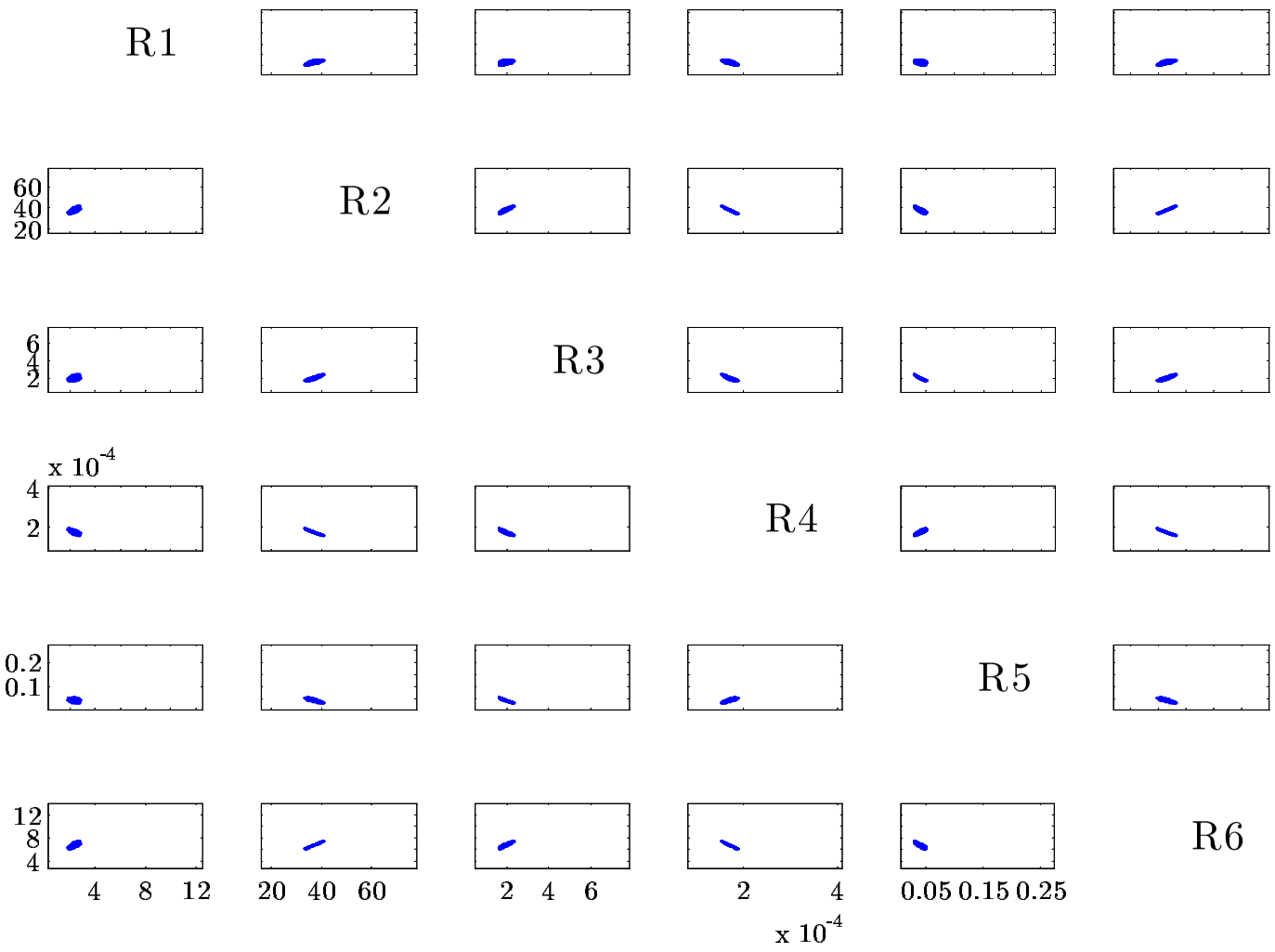

Figure 36: Response Scatterplots for Beam Design with Six Probabilistic Requirements

5.2 Requirements Decomposition

To further address the needs of decision-making methods for large-scale systems design, the next logical step is to address requirements decomposition methods. In this case, decomposition would be used to identify a subset of characteristic tradeoffs in a decision space. This subset may be small enough to allow for multidimensional visualization as well as ease tradeoff analysis. Linearly independent tradeoffs could allow for bias-free compromise, one of the issues outlined in the results up to this point.

The idea of requirements decomposition (or compression) is not new. The principles of Axiomatic Design [Suh, 1990], detailed in Chapter III, discuss the need for a minimal set of independent functional requirements. In perfect Axiomatic Design, these independent functional requirements are controlled by only one design parameter. In this vein, there are no "tradeoffs" to consider, only optimal values for each metric; a de facto ideal solution.

Unfortunately, independence of the functional requirements is *very* hard to enforce and becomes all but impossible for large-scale systems. Zeleny gives an example with dependent requirements and notes some of the issues associated with creation of composite attributes [Zeleny, 1982]:

> The problem is that [as] the number of attributes increases... such composite attributes are often difficult to quantify and even to conceptualize.

Tradeoffs are inevitably the result of interactions between the functional forms of the requirements. These interactions, carefully presented, are often the crux of design, decision making, and compromise. All but the simplest systems will be compromised; else, the ideal solution would always be possible. However, this is not to say that a *linearly* independent set of requirements is not desirable for MCDM. If one believes the set of existing requirements helps to "paint a picture" of the decision space, then these requirements should be able to be decomposed into their cardinal directions for a linearly independent, though interacting, set of *characteristic requirements*.

One unrealized advantage of polynomial surrogate models is that the approximate functional form of the requirements to the design parameters is known. Furthermore, this form

is common to each of the individual responses, creating a system of linear equations. If this system of equations is linearly dependent or nearly so then it is possible to find a linearly independent subset of equations to describe the same phenomena.

5.2.1 Decomposition Techniques for Linear Systems

One of the most fundamental decomposition techniques for matrices is diagonalization via eigenvalues and eigenvectors [Strang, 1988; Nakos and Joyner, 1998]. A square matrix can be represented as the product of three orthogonal matrices via

$$\mathbf{A} = \mathbf{S}\mathbf{\Lambda}\mathbf{S}^{-1} \tag{45}$$

where $\mathbf{A}$ is a diagonalizable square matrix, $\mathbf{S}$ is a matrix of eigenvectors of $\mathbf{A}$, and $\mathbf{\Lambda}$ is a diagonal matrix of the associated eigenvalues. The rows of $\mathbf{S}^{-1}$ form an orthogonal basis for the row space of $\mathbf{A}$; that is, these rows represent a linearly independent set of vectors. If $\mathbf{A}$ is singular, some of the eigenvalues in $\mathbf{\Lambda}$ will be zero and therefore the associated eigenvectors will be unimportant to the recomposition of $\mathbf{A}$. Similarly, if $\mathbf{A}$ is nearly singular, there will be some eigenvalues that will be nearly zero. The associated eigenvectors will be of little importance to the recomposition and may be neglected with little error. This procedure is used in vibrational analysis to determine the important natural modes of a structure [James et al., 1994].

It is very rare that the number of requirements equals the number of design variables, so a square matrix is quite uncommon. One technique that is comparable to eigenanalysis is Singular Value Decomposition (SVD). This is a factorization method that retains some of the qualities of eigenanalysis yet is applicable to non-square matrices. In its basic form, SVD is written as

$$\underbrace{\mathbf{A}}_{a\times b} = \underbrace{\mathbf{U}}_{a\times a}\underbrace{\mathbf{\Sigma}}_{a\times b}\underbrace{\mathbf{V}^{\mathrm{T}}}_{b\times b} \tag{46}$$

where $\mathbf{A}$ is a rectangular $a \times b$ matrix of rank c, $\mathbf{U}$ and $\mathbf{V}^{\mathrm{T}}$ are orthonormal matrices and $\mathbf{\Sigma}$ is a diagonal matrix of *singular values*. SVD orders the columns of $\mathbf{U}$ and $\mathbf{V}^{\mathrm{T}}$ such that each column of the former and row of the latter correspond to the singular values on the diagonal of $\mathbf{\Sigma}$ in descending order. Thus, the most important columns of $\mathbf{U}$ and rows of $\mathbf{V}^{\mathrm{T}}$

appear first. Further, the first c columns of $\mathbf{U}$ form an orthonormal basis for the column space of $\mathbf{A}$. Likewise, the first c rows of $\mathbf{V}^{\mathrm{T}}$ form an orthonormal basis for the row space of $\mathbf{A}$. SVD is very stable and, as its name implies, works well with singular or near-singular matrices. In the case of near-singular matrices, the singular values along the diagonal of $\mathbf{\Sigma}$ will have some near-zero or zero values. The columns of $\mathbf{U}$ and rows of $\mathbf{V}^{\mathrm{T}}$ that correspond to these small singular values are therefore unimportant to the recomposition of $\mathbf{A}$ and can be neglected with little loss in accuracy. For more information on SVD, the reader is referred to [Strang, 1988], part of which is reproduced in Appendix B.

5.2.2 Singular Value Decomposition for Response Surface Equations

Response surface equations are already of great use to the systems engineer because of their speed, versatility, and high-fidelity capability. For the decomposition methods outlined below to work correctly, the RSEs *must* be normalized such that magnitudes of each response are comparable to all others. This includes normalizing the inputs used to create the RSEs followed by normalization of the equations.

As outlined in Appendix A, the general form of a quadratic RSE is

$$R = b_0 + \sum_{i=1}^{q} b_i x_i + \sum_{i=1}^{q} b_{ii} x_i^2 + \sum_{i=1}^{q-1} \sum_{j=i+1}^{q} b_{ij} x_i x_j \tag{47}$$

where b_0 is an intercept invariant with respect to the design variables, b_i are the coefficients for main (linear) effects, b_{ii} are coefficients for the quadratic effects, b_{ij} are coefficients for interaction terms, and x_i or x_j refers to one of q design variables. One can assemble all of the coefficients via

$$\vec{b} = (b_1, b_2, \ldots, b_q, b_{11}, b_{12}, \ldots, b_{1q}, b_{22}, b_{23}, \ldots, b_{qq})^{\mathrm{T}} \tag{48}$$

such that all coefficients can be represented by a single vector (intentionally omitting the intercept term). Likewise, $\vec{x}$, the vector of design variables, can be arranged as a new vector

$$\vec{\tilde{x}} = (x_1, x_2, \ldots, x_q, x_1x_1, x_1x_2, \ldots, x_1x_q, x_2x_2, x_2x_3, \ldots, x_qx_q)^{\mathrm{T}} \tag{49}$$

such that $R = b_0 + \vec{b}\vec{\tilde{x}}$. Then, for multiple response surface equations, the responses can be arranged such that

$$\vec{R} = \vec{b}_0 + \mathbf{B}\vec{\tilde{x}} \tag{50}$$

where $\vec{R} = (R_1, R_2, \ldots, R_n)^{\mathrm{T}}$ is a vector of n responses, $\vec{b}_0$ is a vector of the intercept terms b_0 from each response, and $\mathbf{B} = (\vec{b}_1, \vec{b}_2, \ldots, \vec{b}_n)^{\mathrm{T}}$ is a matrix of RSE coefficients for the n responses.

Now, each row of $\mathbf{B}$ represents the coefficients for a separate response surface equation. If $\mathbf{B}$ is singular or is close to being singular, then some of the response surface equations, and hence the responses themselves, are linearly dependent. This can be seen from singular value decomposition of the $\mathbf{B}$ matrix:

$$\mathbf{B} = \mathbf{U}\mathbf{\Sigma}\mathbf{V}^{\mathrm{T}} \tag{51}$$

In this case, $\mathbf{B}$ is an $n \times v$ rectangular matrix, where v is the length of $\vec{\tilde{x}}$ (from equation (49)) and represents the number of terms in the response surface. The rank of $\mathbf{B}$ depends on its shape; usually, $n < v$ so the matrix will be at most of rank n. Note that if $n > v$ then there will *always* be linear dependence amongst the responses, and the matrix will be at most of rank v. For now, the reader can assume that the rank of the matrix will be n, in cases where it is not a simple substitution will be required in subsequent equations.

Assuming $n < v$, $\mathbf{B}$ is at most of rank n. Therefore, $\mathbf{U}$ is an $n \times n$ orthonormal matrix, $\mathbf{\Sigma}$ is an $n \times v$ diagonal matrix, and $\mathbf{V}^{\mathrm{T}}$ is a $v \times v$ orthonormal matrix. Furthermore, the first n rows of $\mathbf{V}^{\mathrm{T}}$, denoted $\mathbf{V}_1^{\mathrm{T}}$, form an orthonormal basis for the row space of $\mathbf{B}$. Therefore, a *linearly independent* set of RSEs can be created to describe the same decision space given by the original RSEs. These are found from

$$\vec{R}_c = \mathbf{V}_1^{\mathrm{T}} \vec{\tilde{x}} \tag{52}$$

where $\vec{R}_c$ represents the equations for the *characteristic requirements* of the system. These requirements have no associated direction of improvement on their own but instead form a series of independent equations used to model the decision space. The n singular values along the diagonal of the $\mathbf{\Sigma}$ matrix correspond to the first n rows of the $\mathbf{V}^{\mathrm{T}}$ matrix, which in effect ranks the importance of the characteristic requirements to the recomposition of the original decision space. Thus, a near-zero singular value indicates that the particular characteristic requirement associated to that singular value does not describe much of

the variation seen in the decision space (made up of all of the original requirements) and therefore can be removed from consideration without much impact on the decision making process. This is key in determining both the important characteristic requirements and reducing the size of the decision space.

Normalization of the inputs *prior* to fitting the response surfaces and further normalizing the response surface coefficients by the outputs is of utmost importance. Otherwise, responses with a high absolute (native) magnitude will dominate the others and create singular values with false meanings. The same is true of the inputs as those with high absolute magnitudes may dominate those terms in the model with very low magnitudes. The singular value is analogous to the inverse of the condition number of a matrix. Hence, a poorly scaled system of equations (in this case, a non-normalized $\mathbf{B}$ matrix) may produce very high condition numbers (low singular values) simply due to scaling and not due to true linear dependence.

Recomposition of the original requirements follows from the basics of SVD outlined in equation (51). A matrix of constants can be defined such that the characteristic requirements can be quickly converted to the originals. First, one must define the cutoff point of "important" requirements via the singular values. This cutoff location is denoted with r, such that $r \leq n$. This carries over to the coefficient matrix for the characteristic requirements, with the "important" characteristics denoted by $\mathbf{V}_1^{\oplus \mathrm{T}}$, or simply $\mathbf{V}^{\oplus \mathrm{T}}$ for brevity. It follows that

$$\underbrace{\vec{R}_c^{\oplus}}_{r\times 1} = \underbrace{\mathbf{V}^{\oplus \mathrm{T}}}_{r\times v}\underbrace{\vec{\tilde{x}}}_{v\times 1} \tag{53}$$

where the $\oplus$ superscript denotes the first r values. The recomposition matrix is defined as

$$\underbrace{\mathbf{C}^{\oplus}}_{n\times r} = \underbrace{\mathbf{U}}_{n\times n}\underbrace{\mathbf{\Sigma}^{\oplus}}_{n\times r} \tag{54}$$

with $\mathbf{C}^{\oplus}$ as the matrix of constants to recompose the requirements using

$$\vec{\hat{R}} = \vec{b}_0 + \mathbf{C}^{\oplus}\vec{R}_c^{\oplus} \tag{55}$$

where $\vec{\hat{R}}$ are the recomposed approximation of the n original requirements. The accuracy

of these values will depend on how many marginally important characteristic requirements are neglected in $\vec{R}_c^{\oplus}$, but the differences between $\vec{\hat{R}}$ and $\vec{R}$ are usually quite small.

This process can be visualized with a simple linear example. Consider a decision space with three requirements L_1, L_2, and L_3 composed of linear combinations of three design variables x_1, x_2, and x_3. There are three degrees of freedom in this linear model, hence it is very possible that the three requirements are independent. However, this example considers one of the requirements to be dependent on another to illustrate the benefits of SVD. The three requirements are characterized by

$$\begin{bmatrix} L_1 \\ L_2 \\ L_3 \end{bmatrix} = \begin{bmatrix} -2 & -4 & 2 \\ 1 & 2 & -1 \\ 2 & -1 & -3 \end{bmatrix} \begin{bmatrix} x_1 \\ x_2 \\ x_3 \end{bmatrix} \tag{56}$$

or, in more compact form, as $\vec{L} = \mathbf{A}\vec{x}$. It is easily seen that L_1 and L_2 are linear combinations; in this example $L_1 = -2L_2$. All requirements are considered larger-is-better, and the inputs x_1 through x_3 vary between -1.0 and 1.0. The positive ideal solution is $\vec{L}^* = (8, 4, 6)^{\mathrm{T}}$ and the negative ideal is $\vec{L}^- = (-8, -4, -6)^{\mathrm{T}}$. The coefficient matrix is normalized such that $\vec{\bar{L}}^* = (1, 1, 1)^{\mathrm{T}}$ and $\vec{\bar{L}}^- = (-1, -1, -1)^{\mathrm{T}}$, where the bar denotes the normalized value. The normalized coefficient matrix is decomposed via equation (51). This results in

$$\mathbf{U} = \begin{bmatrix} -0.6547 & 0.2671 & 0.7071 \\ 0.6547 & -0.2671 & 0.7071 \\ 0.3778 & 0.9259 & 0.000 \end{bmatrix}, \mathbf{\Sigma} = \begin{bmatrix} 0.9067 & 0 & 0 \\ 0 & 0.5628 & 0 \\ 0 & 0 & 0.000 \end{bmatrix},$$

$$\text{and } \mathbf{V}^{\mathrm{T}} = \begin{bmatrix} 0.4999 & 0.6526 & -0.5694 \\ 0.3110 & -0.7488 & -0.5852 \\ 0.8083 & -0.1155 & 0.5774 \end{bmatrix}.$$

These results include one zero singular value on the diagonal, correctly indicating the existence of only two linearly independent characteristic requirements. The coefficients for these characteristics are the first two rows of $\mathbf{V}^{\mathrm{T}}$.

Figure 37 shows a plot of the original decision space domain in three dimensions. The three lines in this plot represent the directions of the three characteristics, given by the

"hanger" matrix **U**. Note that $\vec{U}_3$ points out of the plane of the decision domain, indicating that this characteristic is not important to the decision maker. Vectors $\vec{U}_1$ and $\vec{U}_2$ show the directions of the characteristic requirements R_{c1} and R_{c2}. The third vector, pointing out of the plane, shows the direction of the nullspace of the requirements.

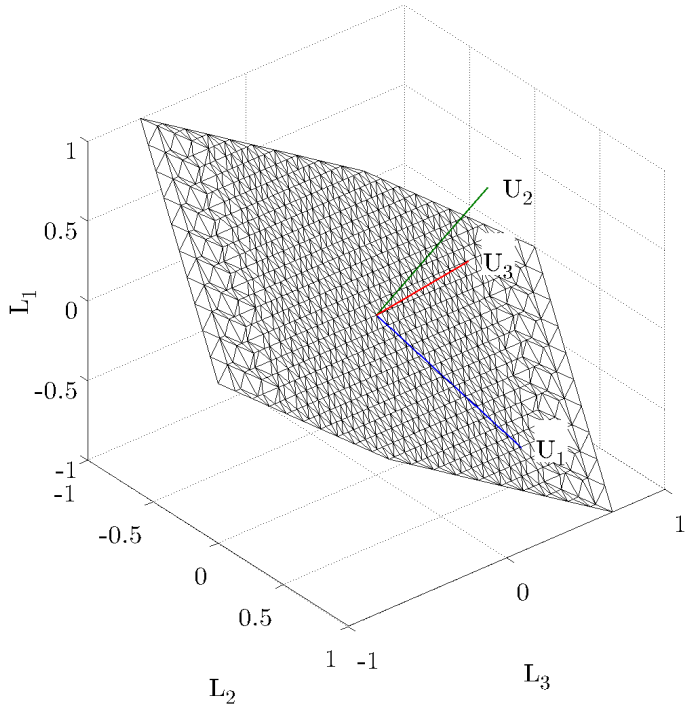

Figure 37: Decision Space Domain in Native Dimensions for Linear Example

Figure 38 shows the decision domain mapped to the two-dimensional characteristic space. Here, three lines indicate the relative directions of improvement for the three requirements L_1 through L_3. These directions come directly from the recomposition matrix $\mathbf{C}^{\oplus}$ as defined in equation 54.

Decomposition of the beam design problem proceeds in a similar way. The responses are normalized such that

$$\bar{R}_j = \frac{R_j - \mu_j}{2\left(R^* - R^-\right)} \tag{57}$$

where R_j is the j^{th} response, μ_j is the mean of the response, and R^* and R^- are the best and worst values of this response in the decision space, as before. This ensures that the responses are normalized from -1 to 1. The response surfaces are created as outlined in Section 4.3.2

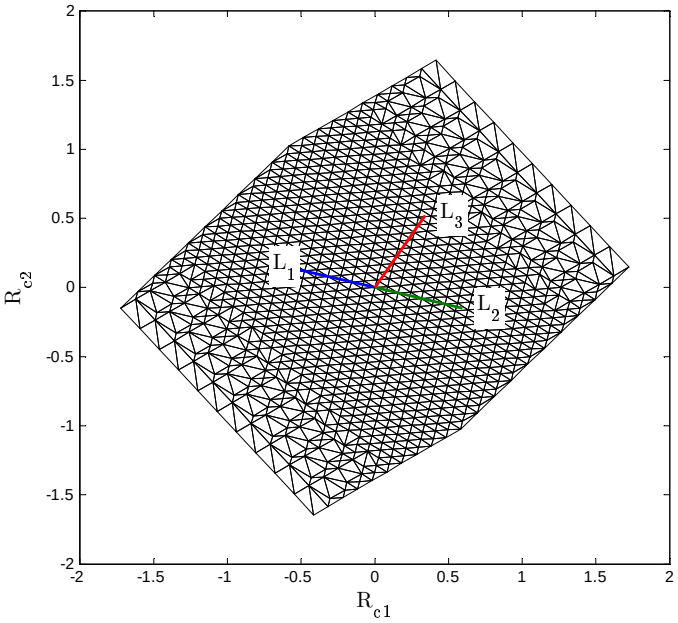

Figure 38: Decision Space Domain in Characteristic Dimensions for Linear Example

with normalized inputs, also ranging from -1 to 1. The resulting RSE coefficients are given in Table 18. These are only shown to three decimal places to illustrate the contrast between terms, though the analysis used more precision.

Table 18: Third-Order Normalized Response Surface Coefficients for Beam Problem

	b_0	b_1	b_2	b_{11}	b_{12}	b_{22}	b_{111}	b_{112}	b_{122}	b_{222}
R	-	S	A	S^2	SA	A^2	S^3	S^2A	SA^2	S^3
R_1	-0.548	0.652	-0.159	0.231	-0.241	0.076	0.000	-0.080	0.083	-0.026
R_2	0.000	1.000	0.000	0.000	0.000	0.000	0.000	0.000	0.000	0.000
R_3	-0.276	0.860	0.143	0.147	0.143	-0.013	-0.018	0.025	-0.012	0.002
R_4	-0.702	-0.500	0.000	0.702	0.000	0.000	-0.500	0.000	0.000	0.000
R_5	-0.996	-0.099	-0.023	0.674	0.223	0.053	-0.595	-0.234	-0.077	-0.018
R_6	0.000	1.000	0.000	0.000	0.000	0.000	0.000	0.000	0.000	0.000
R_7	-0.276	0.860	0.143	0.147	0.143	-0.013	-0.018	0.025	-0.012	0.002
R_8	-0.996	-0.099	-0.023	0.674	0.223	0.053	-0.595	-0.234	-0.077	-0.018

These coefficients show, correctly, that R_2 and R_6 are basically linear mappings from the normalized value of S to the decision space. This corresponds to the native functional forms of each of these requirements. The coefficients from Table 18 are collated into a matrix, minus the intercept terms, as in equations (48) and (50). The coefficient matrix is

decomposed using SVD as in equation (51). The resulting matrices are:

$$\mathbf{U} = \begin{bmatrix} -0.300 & 0.157 & 0.839 & -0.074 & 0.419 & 0.000 & 0.000 & 0.000 \\ -0.479 & 0.099 & 0.048 & -0.115 & -0.495 & 0.669 & -0.230 & 0.012 \\ -0.406 & 0.174 & -0.310 & 0.324 & 0.322 & 0.011 & -0.004 & -0.707 \\ 0.304 & 0.467 & 0.254 & 0.713 & -0.341 & 0.000 & 0.000 & 0.000 \\ 0.121 & 0.582 & -0.131 & -0.354 & 0.068 & -0.230 & -0.669 & 0.000 \\ -0.479 & 0.099 & 0.048 & -0.115 & -0.495 & -0.669 & 0.230 & -0.012 \\ -0.406 & 0.174 & -0.310 & 0.324 & 0.322 & -0.011 & 0.004 & 0.707 \\ 0.121 & 0.582 & -0.131 & -0.354 & 0.068 & 0.230 & 0.669 & 0.000 \end{bmatrix},$$

$$\mathbf{\Sigma} = \begin{bmatrix} 2.058 & 0 & 0 & 0 & 0 & 0 & 0 & 0 & 0 \\ 0 & 1.592 & 0 & 0 & 0 & 0 & 0 & 0 & 0 \\ 0 & 0 & 0.441 & 0 & 0 & 0 & 0 & 0 & 0 \\ 0 & 0 & 0 & 0.264 & 0 & 0 & 0 & 0 & 0 \\ 0 & 0 & 0 & 0 & 0.113 & 0 & 0 & 0 & 0 \\ 0 & 0 & 0 & 0 & 0 & 1.21 \times 10^{-15} & 0 & 0 & 0 \\ 0 & 0 & 0 & 0 & 0 & 0 & 4.92 \times 10^{-16} & 0 & 0 \\ 0 & 0 & 0 & 0 & 0 & 0 & 0 & 1.16 \times 10^{-17} & 0 \end{bmatrix},$$

and

$$\mathbf{V}^{\mathrm{T}} = \begin{bmatrix} -0.985 & -0.036 & 0.091 & 0.005 & 0.001 & -0.137 & -0.026 & -0.016 & 0.001 \\ 0.158 & -0.001 & 0.754 & 0.171 & 0.043 & -0.586 & -0.173 & -0.051 & -0.015 \\ 0.021 & -0.489 & 0.239 & -0.791 & 0.132 & 0.090 & -0.049 & 0.220 & -0.041 \\ -0.030 & 0.455 & 0.389 & -0.181 & -0.197 & 0.199 & 0.709 & 0.152 & 0.061 \\ -0.056 & 0.199 & 0.394 & 0.190 & 0.268 & 0.686 & -0.438 & 0.144 & -0.104 \\ 0.000 & -0.649 & 0.224 & 0.368 & -0.394 & 0.315 & 0.202 & -0.163 & 0.266 \\ 0.000 & -0.029 & 0.014 & 0.007 & 0.716 & 0.019 & 0.228 & -0.332 & 0.569 \\ 0.000 & -0.192 & -0.096 & 0.338 & 0.266 & -0.134 & 0.186 & 0.843 & 0.075 \\ 0.000 & 0.231 & -0.029 & -0.166 & -0.362 & -0.040 & -0.381 & 0.239 & 0.764 \end{bmatrix}.$$

These results are consistent with what is expected. Most notable is the appearance of three near-zero singular values in $\mathbf{\Sigma}$. The functional form of the original requirements was such that there were only five linearly independent responses, indicated in the previous chapter in equations (13) through (20). Singular value decomposition has correctly indicated the dependence of three requirements. Furthermore, there appear to be only two characteristics that are very important, with singular values of 2.058 and 1.592. The next most important characteristic has a singular value of 0.441, making it about one-fourth as important as the next higher value. The singular values further descend in importance from there. This seems to indicate that the requirements space could be adequately captured with linear combinations of $r = 3$ characteristic requirements $R_c^{\oplus}$, perhaps even $r = 2$, as opposed to the eight original requirements. The equations for these characteristics are composed of the first r rows of $\mathbf{V}^{\mathrm{T}}$. Finally, it is important to note that the last row of $\mathbf{V}^{\mathrm{T}}$ has to be part of the nullspace of the decision space. Indeed, one can speculate that the last four rows of $\mathbf{V}^{\mathrm{T}}$ form a basis for the nullspace due to the near-zero entries of the last three singular values.

5.2.3 Multidimensional Visualization with Characteristic Requirements

The extraction of linearly independent characteristic requirements seems to allow for improved MCDM by finally ensuring independent decision metrics. This technique is similar to principal components analysis, where eigenanalysis identifies the most influential factors that are linear combinations of the original factors [Dunteman, 1989]. However, the requirements decomposition process is not to identify influential factors; rather, it serves to find an underlying set of independent decision metrics.

A complicating factor for this type of requirements decomposition occurs because it also removes critical decision information. A characteristic requirement no longer has an associated direction of improvement. One can easily imagine a situation with two linearly dependent metrics that collapse into one characteristic requirement but improve in opposite directions. One does not wish to maximize or minimize the characteristic, but rather wishes to find a nominal point on it. Even in the simple example before, $L_1 = -2L_2$. Hence,

these characteristic requirements are more of a "ridge" in the decision space along which important tradeoffs occur. In this sense they are perhaps better dubbed *characteristic tradeoffs*. While they may not have a direction of improvement, they do convey important decision information regarding the tradeoffs of one original requirement versus another.

The notion of characteristic tradeoffs has other uses. Recall that the high dimensionality of large-scale decision spaces makes visualization of the space difficult, if not impossible. The decision space for the probabilistic results of the six-requirement beam design problem is difficult to view within the confines of these pages, and the eight-requirement results are not plotted at all in this document for this reason. However, it may be possible to view a scatterplot of the most important characteristic dimensions.

This approach would require giving some meaning to the characteristic directions. Recall that $\mathbf{C}^{\oplus}$ provides the linear map from the characteristic requirements to the original values as given in equation (54). This matrix is the key towards providing decision information to the characteristic. Consider the recomposition matrix values for the eight-requirement beam design problem, given in Table 19. These values come from the product of the $\mathbf{U}$ and $\mathbf{\Sigma}$ matrices resulting from the exercises in the previous subsection.

Table 19: Recomposition Matrix for $r = 3$ Characteristic Requirements

$\vec{c}_1$	$\vec{c}_2$	$\vec{c}_3$	**Contribution**
-0.6164	0.2497	0.3704	R_1
-0.9852	0.1577	0.0211	R_2
-0.8360	0.2769	-0.1367	R_3
0.6253	0.7434	0.1122	R_4
0.2499	0.9259	-0.0577	R_5
-0.9852	0.1577	0.0211	R_6
-0.8360	0.2769	-0.1367	R_7
0.2499	0.9259	-0.0577	R_8

The "contribution" portion of this table indicates the contribution the characteristic requirement makes to the original requirements. Hence, the first characteristic requirement maps -0.6164 of its variation to R_1, -0.9852 to R_2, and so on. Note that the original directions of improvement are retained here, so improving R_2 happens by increasing it and

improving R_6 happens while decreasing. Therefore, raising the value of the first characteristic has the effect of improving R_6 and degrading R_2. All of this information can be viewed graphically on a bar chart. The bars can be color-coded to denote whether a metric is improved upon or degraded with an increase in the characteristic requirement. Degree-of-conflict charts are shown in Figure 39 for the first two characteristic tradeoffs of the beam design problem.

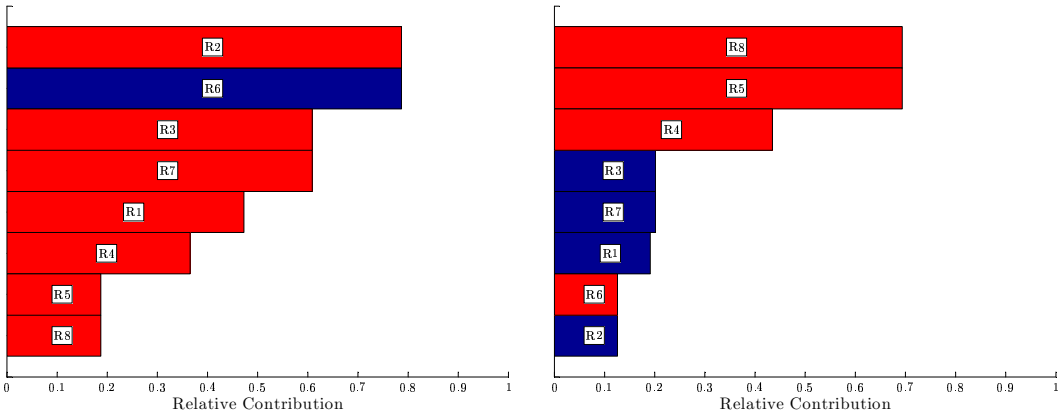

(a) First Characteristic

(b) Second Characteristic

Figure 39: Degree of Conflict Plots for Beam Characteristic Requirements

These charts show that R_6, beam mass, is directly in conflict with all other metrics along the first characteristic. Also, this characteristic contributes the most to R_6 and R_2. The mass and all deflection requirements are in opposition with the strength requirements along the second characteristic. These plots help give meaning to the results of the requirements decomposition.

The culmination of decomposition-based visualization is a multidimensional scatterplot of the characteristic space with a the degree of conflict charts along the diagonal. These charts allow the user to give some sort of intuitive meaning to each of the scatterplot dimensions. An example of such a plot is given in Figure 40. Though this plot complicated, it allows a decision-maker to better understand the tradeoffs within the decision space. This dataset is the output of the eight-requirement probabilistic study performed in Chapter IV, now able to be viewed on a single page.

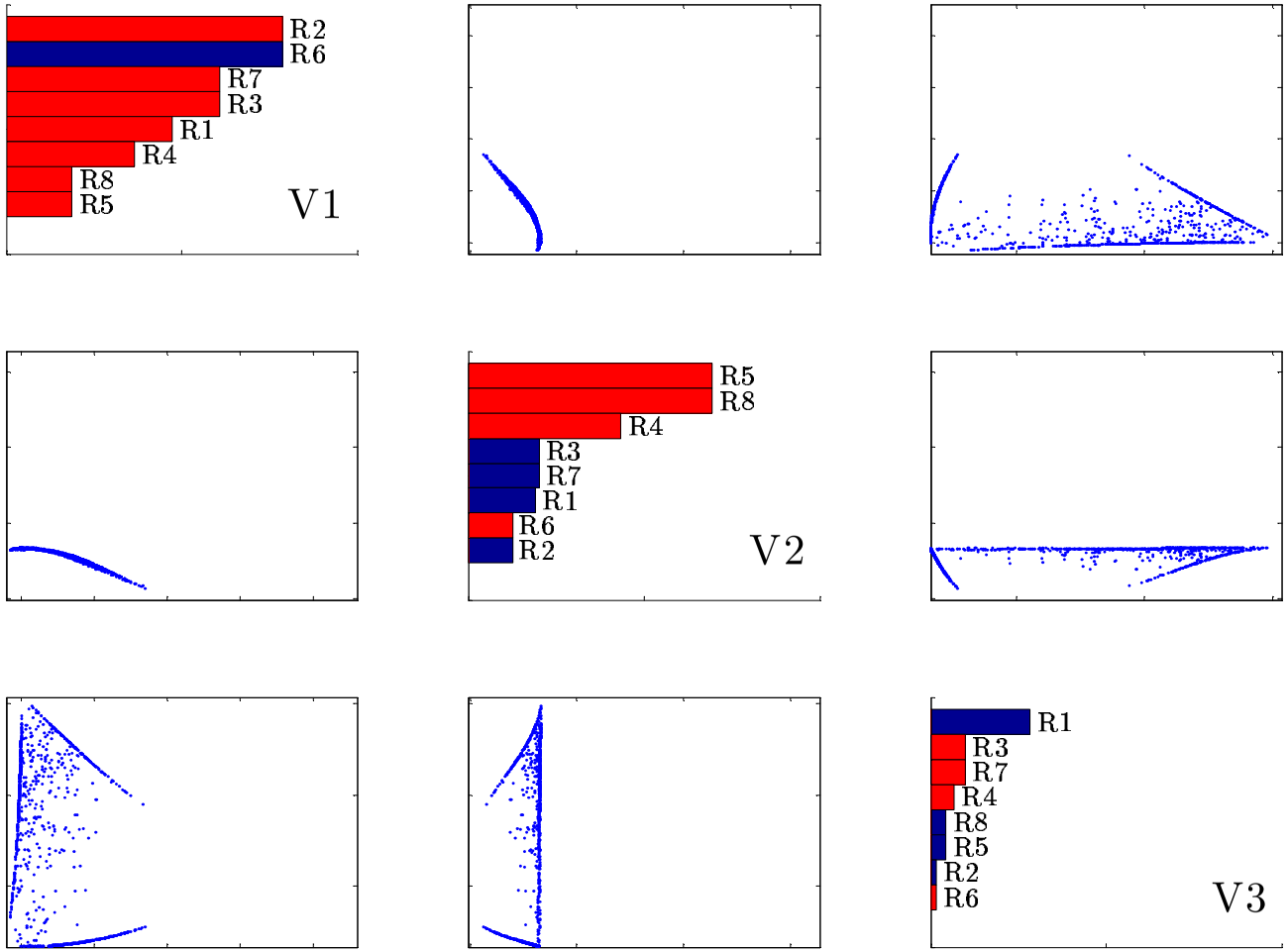

Figure 40: Decomposition-Based Visualization of Beam Design Problem with Three Characteristic Tradeoffs

5.2.4 Interdependent Relative Importance Modeling

As seen from the six- versus eight-requirement beam design problem results, all of the techniques illustrated thus far have yet to remedy the problems for decision making with interdependent criteria. It was initially hoped that requirements decomposition would provide the key by allowing decision making amongst the characteristic tradeoffs; however, the key issue becomes in quantifying target values along the characteristics. A cursory search of the literature reveals little in the subject of interdependence in decision making, though it is beginning to appear as a subject in Fuzzy Logic problems as they relate to operations research and management issues [Carlsson et al., 2004]. These developments may provide some guidance for modifying relative importance to account for interdependence.

The scant literature on interdependence for decision making does indicate a procedure that can be modified for the current systems design formulation. The work by Carlsson and Fullér uses the idea of *supporting* and *conflicting* requirements while creating a composite objective. They define the following for two objectives $f_i(x)$ and $f_j(x)$, $x \in \mathbb{R}^n$ [Carlsson and Fullér, 1996, 1995]:

- f_i supports f_j on X (denoted by $f_i \uparrow f_j$) if $f_i(x') \geq f_i(x)$ entails $f_j(x') \geq f_j(x)$, for all x', $x \in X$;
- f_i is in conflict with f_j on X (denoted by $f_i \downarrow f_j$) if $f_i(x') \geq f_i(x)$ entails $f_j(x') \leq f_j(x)$, for all x', $x \in X$;
- f_i and f_j are independent on X, otherwise.

The *grade of interdependency* is then given by

$$\Delta(f_i) = \sum_{f_i \uparrow f_j, i \neq j} 1 - \sum_{f_i \downarrow f_j, i \neq j} 1, \quad i = 1, \ldots, n \tag{58}$$

where $\Delta(f_i)$ is the grade of interdependency of the objective f_i. If $\Delta(f_i)$ is positive and large then f_1 supports a majority of the objectives, if it is positive and small it supports more objectives than it hinders, and the opposite is true if $\Delta(f_i)$ is negative (large and small, respectively). Finally, if $\Delta(f_i) = 0$ then f_i is independent from all others or supports the same number of objectives as it hinders.

Carlsson and Fullér continue in these works to define a number of linear membership functions that depend on the nature of the individual objectives and their corresponding grade of interdependency. Though initially appealing, some problems are apparent. Most notably, to what degree does a function support or conflict with another? Should an f_i that is only partially supported by one f_j have the same contribution to $\Delta(f_i)$ as another f_j' that strongly supports f_i? Such a distinction is not made in equation (58).

Fortunately, the use of polynomial surrogate models allows for this distinction using a slightly modified process. The **B** matrix, assembled via the vectors of the response surface equation coefficients as in equation (48), represents a *functional mapping* from the design to the decision space. These coefficients can also serve as vectors in a polynomial space. Therefore, the cosine of the angles between the coefficient vectors in polynomial space represent the degree of support or conflict from one response to the others.

The angle between two vectors is given as [Strang, 1988]

$$\theta_{ij} = \cos^{-1}\left(\frac{\vec{b}_i \cdot \vec{b}_j}{\|\vec{b}_i\|\|\vec{b}_j\|}\right) \tag{59}$$

where θ_{ij} is the angle from the coefficients of response i to j in polynomial space. This leads to a modified definition of grade of interdependency for this research, defined as

$$\Delta(R_i) = -1 + \sum_{j=1}^{n} \cos(\theta_{ij}) \tag{60}$$

where $\Delta(R_i)$ is the grade of interdependency for the i^{th} requirement. The -1 term in the equation is because $\theta_{ii} = 0$ and $\cos(0) = 1$, so this quantity is removed from the interdependency measure. As such, a positive value of $\Delta(R_i)$ indicates that a particular response is linearly supportive and a negative value indicates that it is in conflict. This is inherently a pessimistic measure and only captures the linear interdependence exhibited by the requirements on each other. For example, two metrics given by $R_1 = x$ and $R_2 = x^2$ will appear independent in this formulation. However, it should still capture some of the dependence amongst the decision metrics.

The degree of conflict information is then used to modify the relative importance measures, once again through the static contribution in the two-part model. This modification

depends on if $\Delta(R_i)$ is supportive or conflicting. It can be given as

$$\gamma_j = \begin{cases} \frac{1}{\Delta(R_i)+1} & \text{if } \Delta(R_i) > 0 \\ |\Delta(R_i)| + 1 & \text{if } \Delta(R_i) < 0 \\ 1 & \text{if } \Delta(R_i) = 0 \end{cases} \tag{61}$$

The *adjusted static relative importance* is finally defined as

$$w_j^{s*} = \frac{w_j^s \gamma_j}{\sum_{j=1}^{n} w_j^s \gamma_j} \tag{62}$$

with w_j^{s*} representing the adjusted static relative importance of the j^{th} requirement. When this formulation is used, w_j^{s*} replaces w_j^s for calculation of the dynamic importance, as in equation (44).

While powerful, this method is currently limited in application. It is sometimes desirable to create a surrogate model via transformation of independent or dependent variables, and also to add additional terms to the polynomial if necessary. This can have an adverse effect on the interdependent corrections. The correction technique relies on the polynomials for each requirement remaining in the exact same functional form; it is this form that serves as a mapping from the design to the decision space. Independent variable transformation could have an adverse effect by changing the correlation from a particular design variable to the polynomial space, leading to different definitions for the characteristic tradeoffs. Further, the addition of one or two terms to a specific model changes the degrees of freedom in the polynomial space, which may cause changes in the interdependence model. If such terms are important, they should be included in *all* polynomial models during regression. This allows all of the models to have an additional degree of freedom.

This process can be tested on the deterministic results for the beam design problem. The vector angles for all eight requirements are summarized in Table 20, found by applying equation (59) to the coefficients from Table 18. These angles are used to find the $\Delta(R_i)$ values given in equation (60) and subsequent adjusted static relative importance values. As equation (61) requires a static relative importance value, this is determined in the same fashion as the threshold-modified values in Subsection 5.1.1. However, the values from that section were created using the actual analyses, so new values were created using the

polynomial surrogate models. While not perfect, they are close to these earlier values. The $\Delta(R_i)$, threshold-modified entropy-based relative importance (created using the surrogate models), and adjusted relative static importance values are shown in Table 21 for the six- and eight-requirement beam design problem.

Table 20: Vector Angles of Requirements for Beam Design Problem

θ_{ij}°	R_1	R_2	R_3	R_4	R_5	R_6	R_7	R_8
R_1	0.0	31.2	38.7	77.6	94.5	148.8	38.7	94.5
R_2	31.2	0.0	16.4	59.9	84.1	180.0	16.4	84.1
R_3	38.7	16.4	0.0	69.2	93.2	163.6	0.0	93.2
R_4	77.6	59.9	69.2	0.0	31.5	120.1	69.2	31.5
R_5	94.5	84.1	93.2	31.5	0.0	95.9	93.2	0.0
R_6	148.8	180.0	163.6	120.1	95.9	0.0	163.6	95.9
R_7	38.7	16.4	0.0	69.2	93.2	163.6	0.0	93.2
R_8	94.5	84.1	93.2	31.5	0.0	95.9	93.2	0.0

Table 21: Adjusted Static Importance for Beam Design Problem

	6 Requirements			**8 Requirements**		
Value	$\Delta(R_j)$	w_j^s	w_j^{s*}	$\Delta(R_j)$	w_j^s	w_j^{s*}
R_1	0.9176	0.2757	0.06250	1.620	0.2131	0.03496
R_2	1.419	1.87E-12	3.35E-13	2.481	1.51E-12	1.86E-13
R_3	1.081	0.2430	0.05076	2.026	0.1854	0.02634
R_4	1.423	1.87E-12	3.35E-13	2.631	1.51E-12	1.78E-13
R_5	0.7187	0.02257	0.005708	1.664	0.01804	0.002911
R_6	-3.419	0.4587	0.8810	-4.481	0.3851	0.9074
R_7	-	-	-	2.026	0.1854	0.02634
R_8	-	-	-	1.664	0.01297	0.002093

The adjustments to the static importance are large for the grouped problem. This is because all of the requirements are in opposition to R_6 (beam mass) to some degree. This agrees with what is seen in the first characteristic tradeoff as given in Figure 39(a). This large opposition causes the static importance of R_6 to rise dramatically to adjust for the interdependence of all the other metrics.

These adjustments propagate to the deterministic CP results. Table 22 gives the results of the CP problem with interdependency corrections to the static importance (dubbed "grouped" in this table). These results are computed for both the six- and eight-requirement

problem and are compared with the results from the two-part model from Tables 12 and 13. The deterministic results of the surrogate models without grouping are compared as well to illustrate again that the surrogate models represent the original solution well.

Table 22: Deterministic Results Comparison for Beam Design: Dynamic Models

	6 Requirements			8 Requirements		
Value	**Original**	**Surrogate**	**Grouped**	**Original**	**Surrogate**	**Grouped**
S, m^2	0.002330	0.002320	0.002064	0.002419	0.002429	0.002068
A	1.150	1.163	1.210	1.248	1.258	1.232
R_1	2.364	2.299	1.730	2.349	2.311	1.702
R_2	36.43	36.28	32.27	37.82	37.97	32.33
R_3	1.886	1.883	1.614	2.079	2.099	1.633
R_4, m	1.76E-04	1.74E-04	2.02E-04	1.70E-04	1.65E-04	2.01E-04
R_5, m	0.04380	0.04364	0.06022	0.03744	0.03184	0.05830
R_6, kg	6.501	6.474	5.760	6.750	6.777	5.770
R_7	-	-	-	2.079	2.099	1.633
R_8, m	-	-	-	0.02340	0.01990	0.03644

The grouped results are the most promising thus far. The differences between the six- and eight-requirement solutions are very small. Also, this table shows that the surrogate models are accurate representations by virtue of the similarities between the ungrouped dynamic solutions for both the original and response surface analyses. Inspection of the objectives side-by-side as in Figure 41 illustrates the similarity of the grouped functions. There are slight differences in scaling, but both have almost exactly the same optimum.

These promising results allow for the final probabilistic analysis of the beam design problem using the interdependence tools developed above. Once again, a total of 1,000 uniformly random cases were selected as before, with the user-specified relative importance varying on either side by 50%. The results were again tracked for the six- and eight-requirement design problem and are summarized in Table 23.

The probabilistic analysis of the full dynamic, threshold-modified entropy-based interdependent beam design indicates a very tightly distributed solution even for this relatively wide range of user-specified relative importance. The responses themselves are all above their corresponding constraints but do not unfairly sacrifice any one metric for a marginal

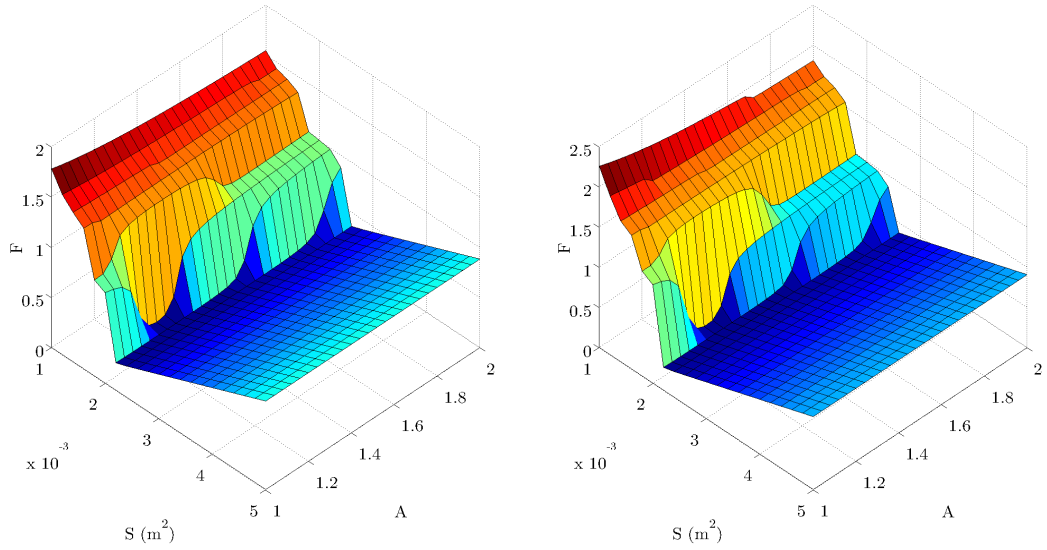

(a) Six Requirements

(b) Eight Requirements

Figure 41: Objective Functions for Beam Design with Interdependent Dynamic Relative Importance

Table 23: Probabilistic Results Comparison for Beam Design with Interdependent Dynamic Relative Importance

	6 Requirements			**8 Requirements**		
Value	μ	σ	σ %	μ	σ	σ %
S, m^2	0.002067	1.20E-05	0.58%	0.002070	8.32E-06	0.40%
A	1.210	0.009113	0.75%	1.232	0.004279	0.35%
R_1	1.737	0.03151	1.81%	1.707	0.01728	1.01%
R_2	32.31	0.1871	0.58%	32.37	0.1300	0.40%
R_3	1.616	0.01189	0.74%	1.635	0.009372	0.57%
R_4, m	2.01E-04	1.45E-06	0.72%	2.01E-04	1.00E-06	0.50%
R_5, m	0.06007	9.02E-04	1.50%	0.05812	6.94E-04	1.19%
R_6, kg	5.767	0.03339	0.58%	5.776	0.02320	0.40%
R_7	-	-	-	1.635	0.009372	0.57%
R_8, m	-	-	-	0.03633	4.34E-04	1.19%

improvement in another. The addition of the two redundant requirements, as in the eight-requirement solution, appears to have little effect on the optimum. However, a formal analysis of the mean shift is necessary, and appears in Table 24.

Table 24: Mean Shift Analysis for Probabilistic Results with Interdependent Dynamic Relative Importance

Value	$\mu_6 - \mu_8$	σ	***t*-Statistic**	***p*-Value**
S, m^2	-3.29E-06	0.00001462	7.107	2.25E-12
A	-0.02214	0.01029	68.04	0
R_1	0.02990	0.03632	26.04	1.78E-114
R_2	-0.05137	0.2286	7.107	2.24914E-12
R_3	-0.01894	0.01517	39.48	3.57E-206
R_4, m	4.03E-07	1.77E-06	7.217	1.05E-12
R_5, m	0.001944	0.001142	53.82	1.74E-297
R_6, kg	-0.009168	0.04079	7.107	2.25E-12

This mean shift analysis indicates that the two population means are even more likely to be different than previous results, as represented by the extremely low p-values. However, this is likely an artifact of the large sample size ($n = 1,000$) and the small standard deviation of the mean shift, caused by very small deviations in the results themselves. So, while the means are still different with statistical significance, they appear *much* closer in a relative sense than in any of the other importance schemes attempted thus far. Furthermore, these differences may now be due to the noise in the entropy formulation (random discrete representation of a continuous function) or the surrogate models (modeling and regression error) as this error is similar in magnitude to the absolute mean shift. The eight-requirement solution may simply be propagating more error via the addition of two requirements.

The full effect of the two-part relative importance model combined with the interdependence corrections does substantially reduce the variation seen in the MCDM solution with respect to moderate changes in user-specified relative importance. The probabilistic design variable scatterplots are compared in Figure 42 for the original formulation, the two-part model with threshold-modified entropy, and finally the interdependence corrected model, for both the six- and eight-requirement experiments. The final model still shows some bias

due to to redundant requirements as the interdependence formulation can only correct linear dependence amongst the terms the model, but the overall change is clearly the smallest amongst the three methods.

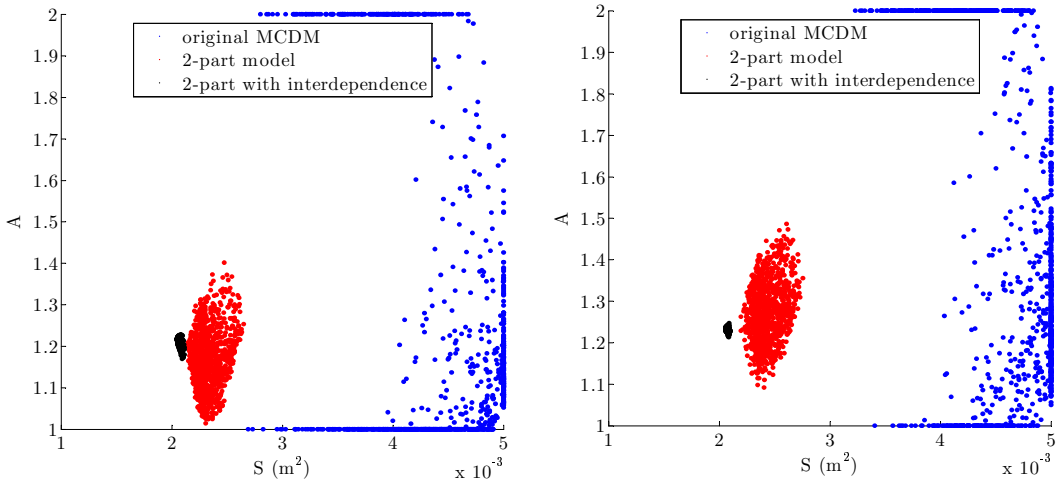

(a) Six Requirements (b) Eight Requirements

Figure 42: Comparison of Probabilistic Design Variable Scatterplots

The results of the six- and eight-requirement scatterplots can now be visualized via the decomposition technique described in the previous subsection. This enables more compact visualization of both of these solutions. The solution variations of the three methods (basic monotonic MCDM, MCDM with the two-part model, and the two-part model with interdependence corrections) are seen in Figures 43 and 44 for the six- and eight-requirement studies, respectively. While similar, the change in the number of requirements changes the mathematical form of the characteristics, hence they may be similar for the six- versus eight-requirement models but not the same. However, the characteristics will always be linearly independent.

These figures are interesting because of the vast amount of information they contain. Visualization of both scenarios shows that the first characteristic improves beam mass while degrading all other performance. The second characteristic improves strength at the expense of deflection and mass. The third characteristic is not very important, but has the greatest effect on buckling strength. The reduction in solution variation from the full two-part

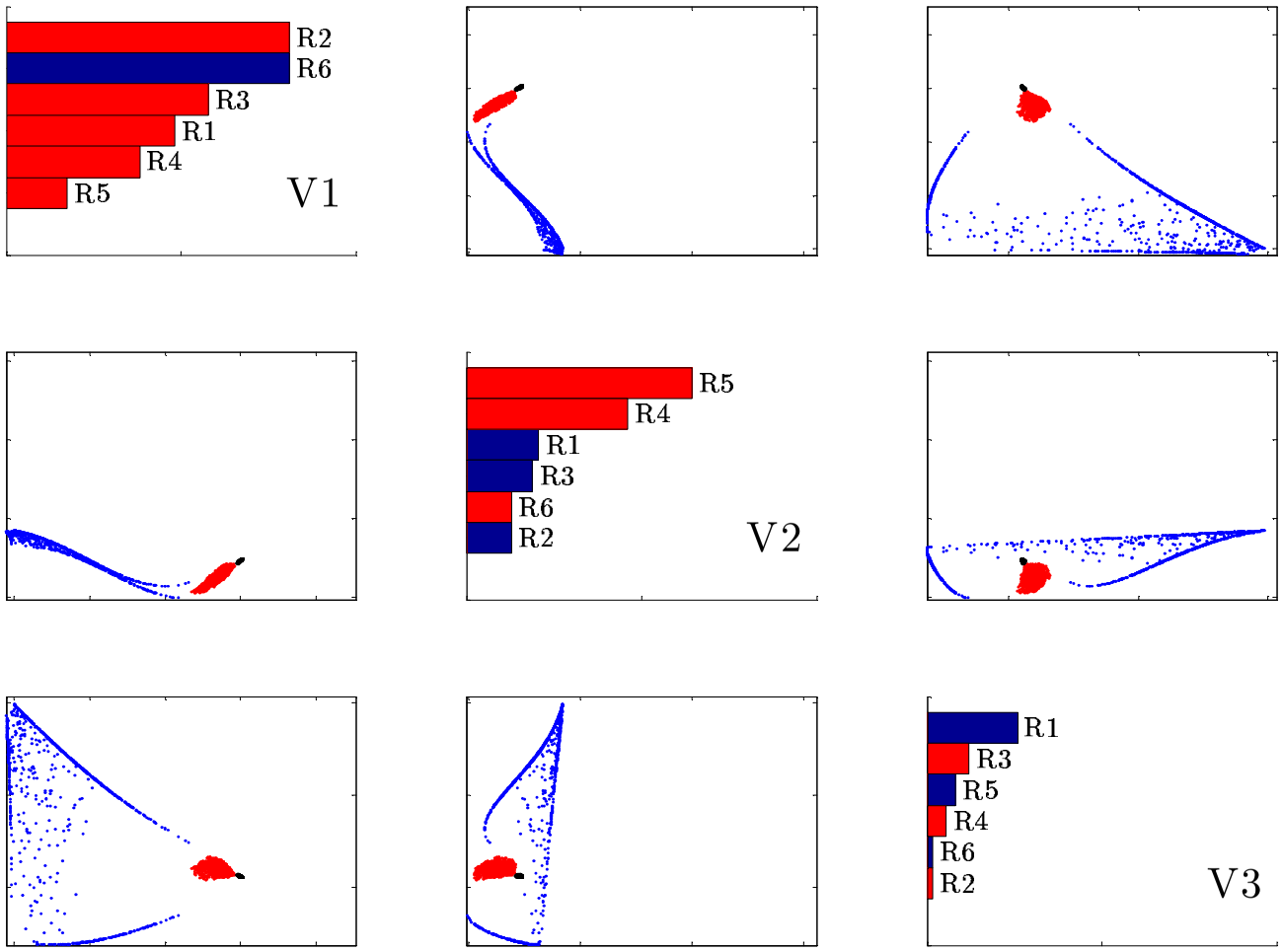

Figure 43: Comparison of Decomposition Scatterplots for Six-Requirement Probabilistic Solutions - Original Results in Blue, 2-Part Model Results in Red, Interdependent Corrected Results in Black

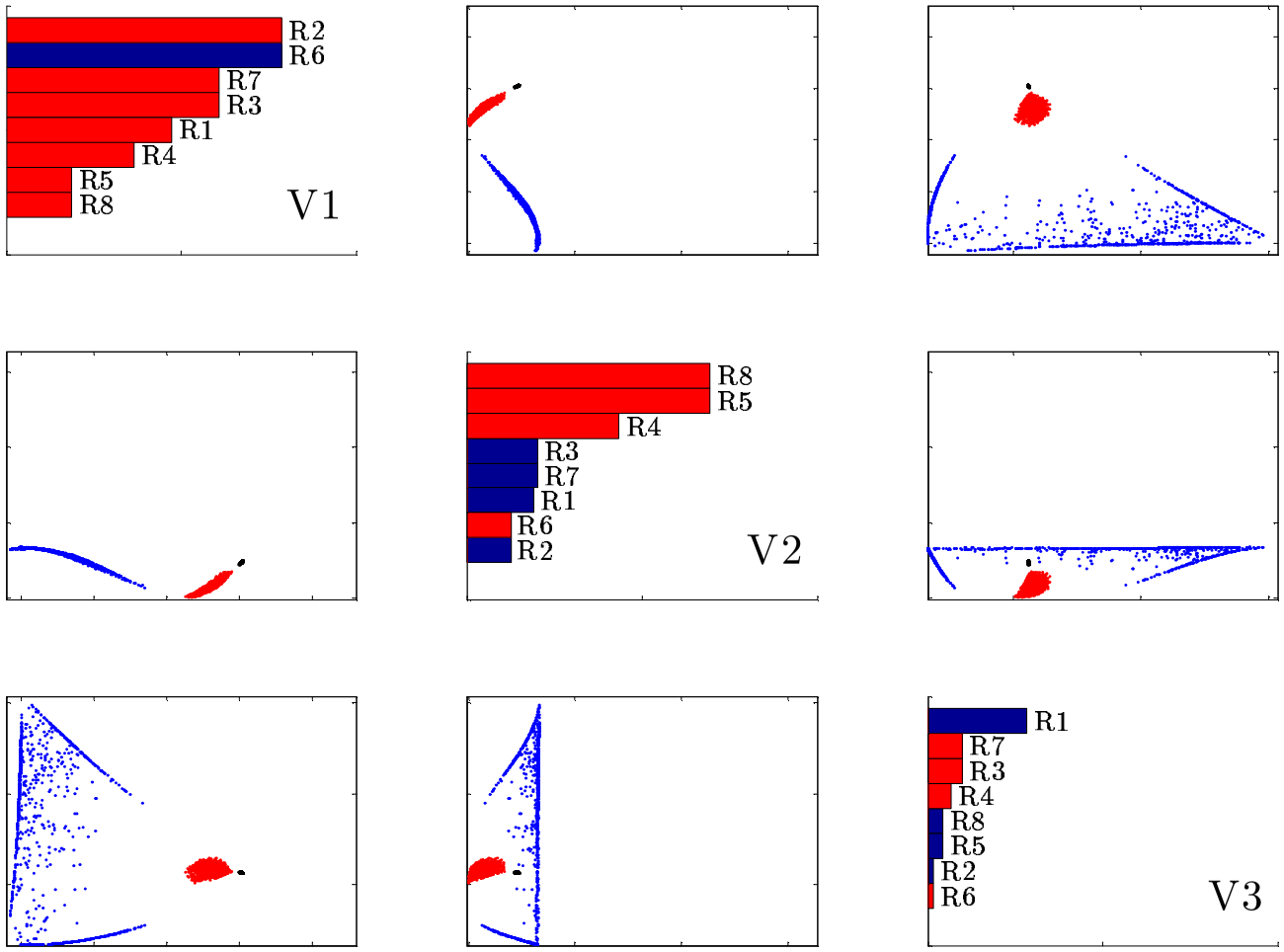

Figure 44: Comparison of Decomposition Scatterplots for Eight-Requirement Probabilistic Solutions - Original Results in Blue, 2-Part Model Results in Red, Interdependent Corrected Results in Black

MCDM model with interdependence corrections is readily apparent from these plots.

These plots also depict how each of the methods deal with tradeoffs. The interdependence-balanced solutions favor higher values for the first characteristic, indicating lower mass solutions. Note how this differs greatly from the original MCDM formulation. All of the methods seem to pick the approximately the same balance for the strength-versus-deflection dimension, favoring lower values here (in $V2$) likely due to the detrimental effect it has on the deflection values for only marginal gain in strength. The third characteristic seems indicative of the buckling strength trade, and the interdependence-balanced solution prefers a slightly lower value here. Note how the original MCDM solution varied significantly in this third characteristic. In all, it appears that these decomposition plots are a very efficient means to illustrate the important tradeoffs in any decision making problem, and also serve as a way to illustrate how the decision making algorithm deals with these tradeoffs.

CHAPTER VI

METHODS FOR PROBABILISTIC LARGE-SCALE DECISION MAKING

Every systems design problem is different in some way. Were it not different, there would already be an existing solution in place to meet the perceived needs. However, this does not mean that one cannot follow a generalized strategy to help solve these problems. A generalized solution strategy is the "science," and the tuning of a strategy or series thereof for a particular problem is the "art" of systems engineering.

This document has developed methods for the science of systems engineering as it applies to large-scale design problems. The sections that follow present the details of a strategy for probabilistic large-scale decision making. As with any other, this strategy will require "tuning." It was borne of a necessity for aerospace vehicle design, but should be general enough to apply to any large systems design problem. A flowchart of the basic method is given in Figure 45, and the sections below elaborate on these methods.

6.1 Requirements Definition

Systems engineering literature is ripe with methods for identifying the core problem, establishing needs, and eventually enumerating design requirements. These methods vary in scope from customer surveys, market analysis, translation of requirements (vague customer needs to engineering targets), and many, many more. A few methods for requirements generation were referenced earlier in Chapter II. These techniques serve as the launching point for any large-scale systems design problem.

In terms of the basic design strategy for solving probabilistic, large-scale problems, the Department of Defense requirements analysis procedures serve as a good model for top-level requirements specification. This is part of the "Requirements Analysis" seen in the process in Figure 3 from Chapter II. This process asks seven basic questions [Leonard, 1999]:

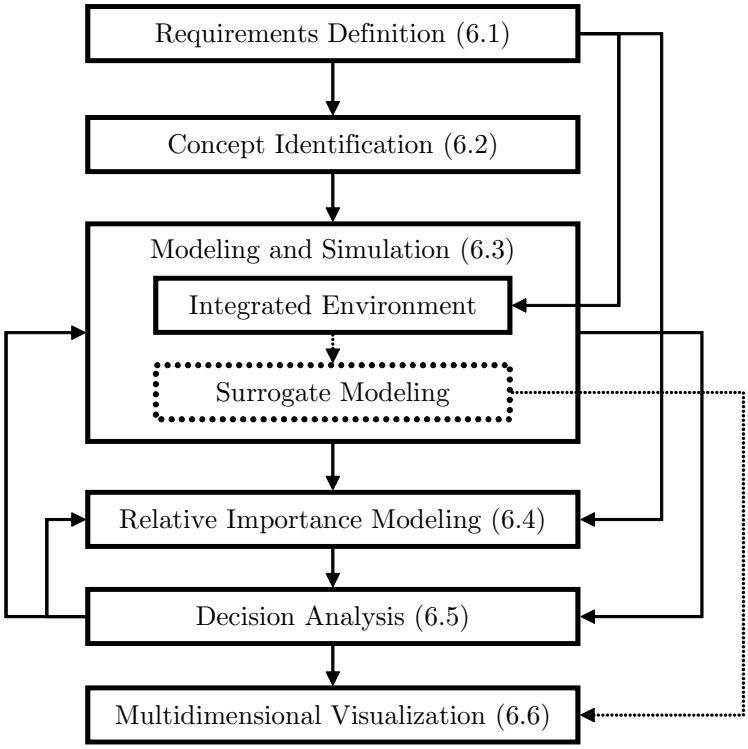

Figure 45: A Basic Strategy for Probabilistic Large-Scale Decision Making

Operational distribution or deployment: Where will the system be used?

Mission profile or scenario: How will the system accomplish its mission objective?

Performance and related parameters: What are the critical system parameters to accomplish the mission?

Utilization environments: How are the various system components to be used?

Effectiveness requirements: How effective or efficient must the system be in performing its mission?

Operational life cycle: How long will the system be in use by the user?

Environment: What environments will the system be expected to operate in an effective manner?

Recall that these requirements are essentially used for multipoint sizing as outlined in Subsection 2.4.2. As such, they provide a "snapshot" of the vehicle capability at certain

boundary conditions. This eliminates the need for a single design point or design mission and allows for the specification of many different metrics.

In addition, the Department of Defense process enumerates several attributes of a "good" requirement that are generally applicable across systems. However, these apply to specific targets for requirements, with no allowance for constraint or threshold values. For the following probabilistic decision making method to work properly, the user *must* consider three values in addition to the requirement itself:

- Direction of improvement or nominal-the-best value (*maximize* range, *minimize* cost, *nominal* fuel-air ratio of 14.1).
- True constraint values, such as standardized regulations (FAR, MILSPEC, etc.) or minimum acceptable performance (no worse than the state of the art).
- Threshold values, defined as a point where further improvement in the metric no longer increases the perceived utility of the solution. These values will likely be more vague and harder to specify than the constraints. An example may be for a range threshold of 12,500 statute miles for a transport - any range over this will be greater than one-half the maximum circumference of the earth, therefore, no two points on the planet will be inaccessible at this range.

There may be a few requirements that do not have a constraint or threshold. If at all possible, at least one metric should be free of a threshold to enable continued optimization in regions where all other metrics are beyond their thresholds. It is also possible that the decision maker will find that the metrics, their constraints, or thresholds, do not adequately influence the solution or have too much influence. As such, requirements specification may become an iterative process as the decision maker reevaluates the needs of the system.

6.2 Concept Identification

Identifying a baseline concept is perhaps one of the most challenging aspects of systems design. Once selected, this concept has a great effect on the composition of the decision space for future exploration. As the level of information and the requirements evolve, what

was once the best concept may soon be limited by the extremes of its performance, where another concept may be more attractive. Unfortunately, the huge number of alternatives at this stage makes full investigation of the concept space difficult, if not impossible.

Many systems engineering methods have been created to ease concept selection. These are mostly subjective techniques used by a committee to evaluate a handful of alternatives. Generation of suitable alternatives for comparison is also a challenging task. One popular concept is the creation of a *morphological chart* to ease the generation of new concepts [Dieter, 2000]. This chart follows from a functional decomposition of a few basic alternatives to create sub-concepts for further evaluation. Table 25 gives an example morphological chart for a High Speed Civil Transport[Mavris et al., 1998].

Table 25: Morphological Chart for a High Speed Civil Transport [Mavris et al., 1998]

Characteristics	**Alternatives**			
Layout	wing & tail	wing & canard	wing, tail & canard	wing
Fuselage	cylindrical	area ruled	oval	
Pilot visibility	synthetic vision	conven-tional	nose droop	
Engine	mixed-flow turbofan	turbine bypass	mid tandem fan	FLADE
Fan	none	one stage	two stage	three stage
Combustor	conventional	RQL	LPP	
Nozzle	conventional	acoustic liner	mixed ejector	mixed ejector & acoustic liner
Low speed	flaps	flaps & slots	circulation control	
High speed	conventional	LFC	NLFC	HLFC
Materials	aluminum	titanium	high temp. composite	
Process	chordwise stiffened	spanwise stiffened	monocoque	hybrid

One drawback of a morphological chart is the incredible number of alternatives possible. In the simple example from Table 25 there are 995,328 possible combinations (discounting incompatibilities). For large-scale systems design the functional decomposition and enumeration of options can result in exceptionally large combinations. Not all combinations are

desirable or even feasible, but often a large enough subset exists that it cannot be simply evaluated with basic systems engineering concept selection methods.

A promising method is evolving that combines concept selection with top-level modeling and simulation to be able to quickly evaluate a large pool of alternatives [Buonanno, 2005]. This method uses a suite of interactive evolutionary algorithms to downselect the large number of concepts available from a morphological chart. It is capable of decision making amongst multiple criteria, though the interdependence of metrics or changes in utility are not explicitly addressed. Such a technique is very powerful and could be used to select a few concepts for further evaluation as in this strategy, but would have the greatest impact if combined with some of the relative importance and interdependent corrections made to MCDM in this research.

At the other side of the spectrum, the user may already have a concept baseline in mind. This can be based on heuristics, evolution of a previous concept, or expert opinion. No matter the source, the end result of this phase of the strategy should be a baseline concept that can be described with a series of top-level parametric variables. Equally important is the ranges of interest for these variables; i.e. the upper and lower bounds for the design space. As before, this may be an iterative process. If the decision-maker consistently finds that the best solution is at the extremes of the design space they may wish to expand or relocate its bounds.

6.3 Modeling and Simulation

Determination of the requirements (decision space dimensions), baseline concept, and design space boundaries are crucial to the development of an appropriate modeling and simulation environment. Here, the design variables are varied and the requirements are output as needed. However, as noted in Chapter II, it is rare that a single, monolithic analysis routine is capable of adequately handling the necessary inputs and outputs. Even if it does handle all of the appropriate data, it is doubtful that it can do so with reasonable fidelity for complex systems design problems. Hence, it is often necessary to create an integrated environment.

Establishing an integrated environment is a challenging exercise. The user, knowing what responses must be calculated (decision space) and with what variables (design space), evaluates the tools at their disposal. It is important to know the assumptions of each tool, its fidelity, and any secondary inputs and outputs that are necessary for the creation of the system-level responses. If the analyses available are not sufficient, they must be modified if possible; else new routines must be created to provide the system with the needed information. Once gathered, the analyses must be assembled into a compatible architecture. This assembly is typically setup to minimize execution time, relative error, or a combination thereof. Chapter II highlighted some of these methods, such as the creation of a design structure matrix. This thesis is by no means a treatise on creation of such an environment; the reader is directed to the plethora of resources and literature on the subject [Kam and Gage, 2003; Lin and Afjeh, 2002; Zweber et al., 2002]. This can include rearranging of routines within the design structure matrix for more effective analysis [Rogers, 1997]. Ultimately, at the conclusion of this phase, the user must ensure that the integrated analysis package can understand the inputs from the design space and adequately output the metrics in the decision space.

Once created, the integrated environment should be used to find the vector of best and worst solutions, $\vec{R}^*$ and $\vec{R}^-$, respectively. These are found through single-objective optimization of each of the decision metrics using only the limits of the design space as constraints (in this case as side constraints). The direction of improvement for each of the metrics will determine whether the "best" values are at a maximum or minimum of the metric. The same holds true for determination of the "worst" values, with the exception that these are found through optimization of the metrics with a change in sign. Single-objective optimization is not necessary if the best and worst value of a metric are at a known nominal location.

6.3.1 Surrogate Models

Some of the decision making techniques given in this research, such as decomposition-based visualization and interdependence analysis, require the use of polynomial surrogate models.

If possible, the integrated environment should be approximated by normalized polynomial response surfaces. The basic tenets of creating polynomial surrogate models via response surface methodology are covered in Appendix A. There are a number of methods emerging that create surrogate models using more advanced techniques, such as space-filling designs [Barros et al., 2004]. Any method used to create these response surfaces is acceptable as long as they adequately represent the original integrated analysis routine. This *requires* verification via statistical methods and random testing. Else, the results will be no better than the poor quality of the surrogate models.

Many other methods exist for creation of surrogate models. While they do not currently enable decomposition-based visualization or interdependence corrections, other surrogate models have a host of other benefits, usually related to reduced system execution time. This can be of great importance, especially for the sampling method used to find the entropy-based relative importance of the metrics in the decision space. This can also be quite helpful in reducing the computational effort required for the probabilistic studies. The reader is referred a survey on the topic [Li and Padula, 2005] to aid in their choice of surrogate models, understanding that anything other than untransformed polynomial response surfaces does not enable the decomposition or interdependence analysis outlined in this document.

6.4 Relative Importance Model

Much of the research in this document has been devoted to the development of a multi-tiered approach to relative importance centered on a two-part model. This model has a static contribution, representing the monotonic portion of relative importance, and a dynamic contribution, reflecting local changes in the utility based on the current value of the decision metric. Figure 46 presents the flow of information required for the two-part relative importance model suggested by this research.

Most decision metrics encountered in systems design are cardinal in nature or can be mapped to cardinal data. As such, the static (monotonic) contribution to the relative importance is normalized such that the sum of the individual values is one. The final static

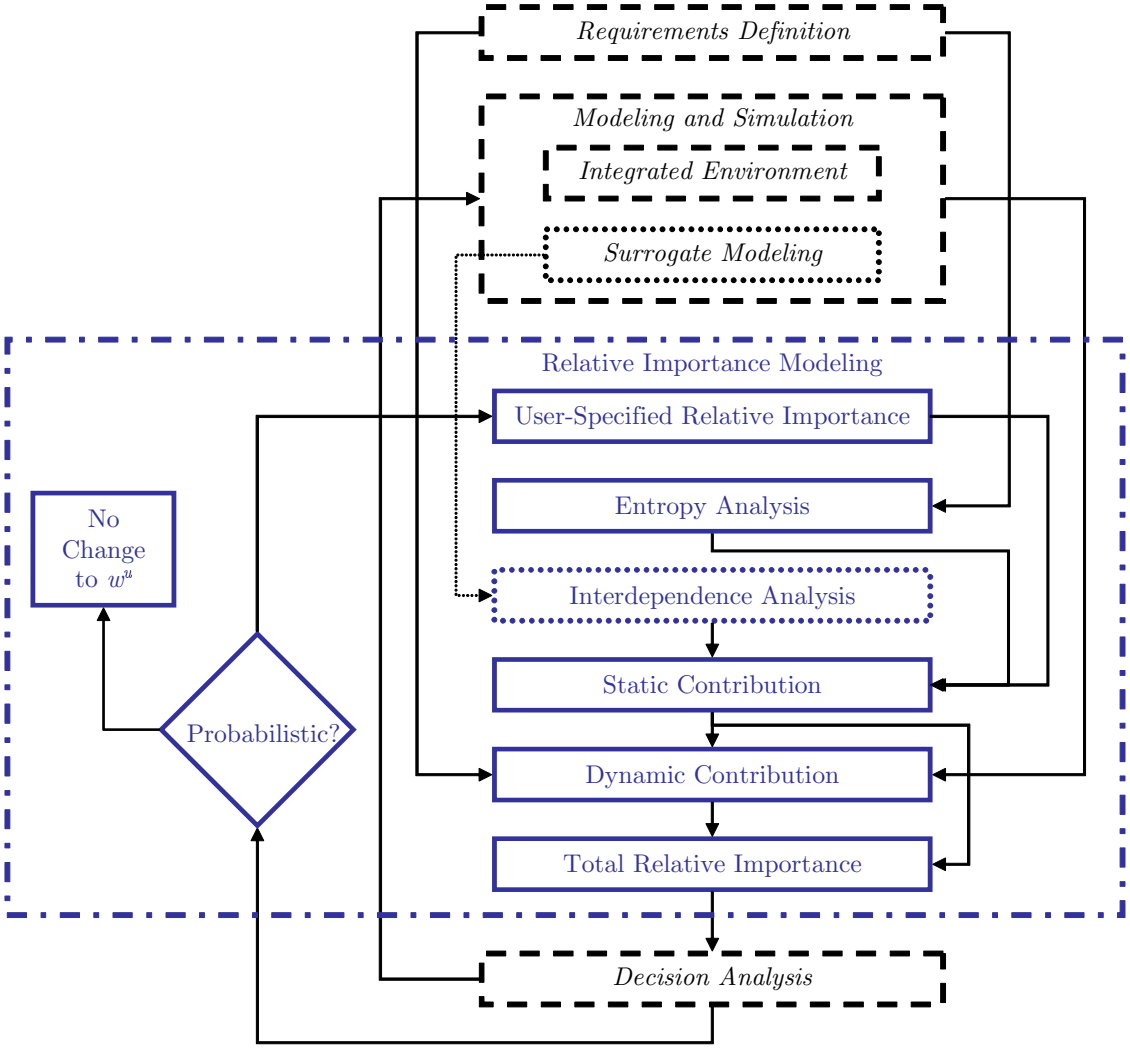

Figure 46: Information Flow for Two-Part Relative Importance Model

relative importance is found as

$$w_j^s = \frac{w_j^u \lambda_j \gamma_j}{\sum_{j=1}^{n} w_j^u \lambda_j \gamma_j} \tag{63}$$

where w_j^u is the user-specified relative importance, λ_j is the threshold-modified entropy-based relative importance, and γ_j is the interdependence correction. Procedures for finding each of these contributions follow this section. Note that the total relative importance is not renormalized after addition of the dynamic contribution. This is to keep all of the other values from changing when there is a local change in one of the metrics due to proximity to a constraint or threshold, ensuring greater smoothness in the composite objective function for optimization.

6.4.1 Identification of User Preferences

The initial contributor to the static contribution to relative importance is the user-specified preference. This is what is typically referred to in the literature when a decision method requires "weights" for evaluation of alternatives. A number of methods have been developed to help a user or group evaluate the relative importance of a pool of decision attributes. These range from basic ranking methods, pairwise comparison, individual rating, and many more. This document does not suggest any particular method but suggests the reader choose a method from the literature [Yoon and Hwang, 1995; Hwang and Yoon, 1981] suitable for the problem. However, the user is cautioned that in the absence of *strong* preference information, all attributes should be considered as equal. This allows the entropy and interdependence corrections, based on the nature of the decision space, to take their full intended effect.

6.4.2 Entropy Evaluation

The first major modification to the static importance contribution is the use of Zeleny's "entropy" formulation [Zeleny, 1982]. This adjusts relative importance based on the average contrast of a metric from its best value in the decision space. This "contrast intensity" is inversely related to the "entropy" of the metric with respect to the rest of the decision space. In this way, metrics with low contrast (most values very close to the best) are assigned lower

importance than those with high contrast (most values far from the best).

Some modifications of Zeleny's formulation are necessary. First, the normalization of the metrics is handled via the 2-norm as opposed to a ratio of the current value to the best value. This allows for negative values and changes the meaning of contrast to a Euclidean analogy. The second change involves measuring contrast from the *lesser* of the best or threshold values. As defined earlier, a threshold is a point beyond which further improvement in the metric is unimportant to the decision maker. The procedure for evaluating the threshold-modified entropy-based relative importance of a pool of metrics is given in Algorithm 1.

It is important to note that this algorithm relies on a representative random population of the decision space. This can be enforced by a relatively large random population sample of the design space mapped to the decision space via the integrated environment or polynomial surrogate models. The latter option is usually far faster, though the results will depend on the accuracy of the regressions. Also, this algorithm, and many others, depend on the knowledge of the best and worst values of each metric within the decision space, $\vec{R}^*$ and $\vec{R}^-$, respectively. These can be found via single-objective optimization of each metric with no constraints other than the side constraints limiting the design variables.

6.4.3 Interdependence Evaluation

The final contributor to the static relative importance follows from evaluation of the interdependence of the metrics. This procedure is possible only if polynomial surrogate models are created for each of the decision metrics, and these models are all of the exact same functional form. The overall procedure is a highly modified version inspired by Carlsson's interdependent decision making models [Carlsson and Fullér, 1996]. This procedure follows from determination of the vector angles of the response coefficients. The sums of the cosines of these vector angles provide a measure of interdependence for each metric. The method for evaluating the interdependent corrections is given in Algorithm 2.

This algorithm will only work if provided with a matrix of response surface coefficients, input row-wise per response. Also, the first entry for each response surface should be the intercept term. Otherwise, the algorithm will need slight modification. Note that this

Algorithm 1 Threshold-Modified Entropy-Based Relative Importance

Inputs: Random $m \times n$ population matrix $\mathbf{Rp}$ (m random population members, n decision metrics), best value vector $\vec{R}^*$, worst value vector $\vec{R}^-$, vector of thresholds $\vec{t}$
Output: Vector of entropy-based weights $\vec{\lambda}$

Find direction of improvement
$\vec{di} = \texttt{sign}(\vec{R}^* - \vec{R}^-)$

modify $\vec{R}^*$ for threshold values
for $j = 1 \ldots n$ **do**
  $R(j)_t^* = \texttt{min}[di(j) \cdot R(j)^*, di(j) \cdot t(j)]$
end for

Find normalized Euclidean distance
for $i = 1 \ldots m$ **do**
  for $j = 1 \ldots n$ **do**
    $R_{\text{temp}} = di(j) \cdot \texttt{min}[di(j) \cdot \mathbf{Rp}(i,j), di(j) \cdot t(j)]$
    $d(i,j) = 1 - \left[\frac{R_{\text{temp}} - R_t^*(j)}{R^-(j) - R_t^*(j)}\right]^2$
  end for
end for

Entropy evaluation
for $j = 1 \ldots n$ **do**
  $D(j) = \sum_{i=1}^{m} d(i,j)$
end for
$K = \frac{1}{\ln m}$
for $j = 1 \ldots n$ **do**
  $e(j) = -K \sum_{i=1}^{m} \frac{d(i,j)}{D(j)} \ln \sum_{i=1}^{m} \frac{d(i,j)}{D(j)}$
end for
$E = \sum_{j=1}^{n} e(j)$

Entropy-based relative importance
for $j = 1 \ldots n$ **do**
  $\lambda_j = \frac{1}{n-E}[1 - e(j)]$
end for

Algorithm 2 Interdependent Corrections to Static Relative Importance

Inputs: $n \times v$ coefficient matrix $\mathbf{B}$ (n decision metrics, v coefficients), best value vector $\vec{R}^*$, worst value vector $\vec{R}^-$
Output: Vector of interdependent corrections $\vec{\gamma}$

Find direction of improvement
$\vec{di} = \texttt{sign}(\vec{R}^* - \vec{R}^-)$

Modify $\mathbf{B}$ *for direction of improvement and eliminate intercept terms*
for $j = 1 \dots n$ **do**
  $\mathbf{B_v}(j,:) = di(j)\mathbf{B}(j, 2:v)$
end for

Find cosines of vector angles
for $i = 1 \dots n$ **do**
  $c\theta(i,i) = 1$
end for
for $i = 1 \dots n-1$ **do**
  for $j = (i+1) \dots m$ **do**
    $c\theta(i,j) = \frac{\mathbf{B_v}(i,:) \cdot \mathbf{B_v}(j,:)}{\|\mathbf{B_v}(i,:)\| \|\mathbf{B_v}(j,:)\|}$
    $c\theta(j,i) = c\theta(i,j)$
  end for
end for

Find grade of interdependency
for $i = 1 \dots n$ **do**
  $\Delta R(i) = -1 + \sum_{j=1}^{n} c\theta(i,j)$
  if $\Delta R(i) < 0$ **then**
    $\gamma(i) = |\Delta R(i)| + 1$
  else if $\Delta R(i) > 0$ **then**
    $\gamma(i) = \frac{1}{\Delta R(i)+1}$
  else
    $\gamma(i) = 1$
  end if
end for

method also requires direction of improvement information gathered from the best and worst values within the decision space.

6.4.4 Dynamic Model

The dynamic contribution of the two-part importance model modifies the relative importance of a metric locally to handle changes in perceived utility based on the value of the metric. The model allows for the total importance to equal the static importance plus one if the metric violates a constraint and equal to zero if the metric is beyond its threshold. Thus, the dynamic contribution should vary between a high of 1.0 and a low of $-w_j^s$ such that it negates the static relative importance beyond the threshold. This model is defined as

$$w_j^d(\vec{x}) = \begin{cases} \left[\frac{1}{2} - \frac{1}{\pi}\tan^{-1}\left[\alpha(\overline{y}_j(\vec{x}) - \overline{c})\right]\right] - w_j^s\left(1 - \frac{\overline{t} - \overline{y}_j(\vec{x})}{\overline{t} - \overline{c}}\right)^{\beta} & \overline{y}_j(\vec{x}) \leq \overline{t} \\ -w_j^s & \overline{y}_j(\vec{x}) > \overline{t} \end{cases} \tag{64}$$

where α is a scale factor for the smoothness of the constraint step function and β is an exponent describing the decay in utility between the constraint and threshold. The constraints and thresholds are as defined before, and are given from the requirements definition portion of the strategy. Some metrics may not have a constraint, threshold, or either. However, most should have such a value, though it may not be active in the decision domain. The basic procedure for evaluating the dynamic relative importance is given in Algorithm 3.

This algorithm depends on selection of an appropriate scale factor α and a power β. The scale factor used in the beam design problem was $\alpha = 200$ as this appeared to give a smooth enough step in the step function to not cause problems with the optimizer, yet sharp enough to adequately represent the constraint. The power $\beta = \frac{1}{4}$ was given in equations (43) and (44) in Chapter V and was used for the beam design problem. However, the user can tailor either of these factors as needed. Finally, it should be noted that this algorithm needs modification for metrics that do not have a constraint, threshold, or either.

6.4.5 Probabilistic Considerations

Execution of probabilistic decision making involves little change to this relative importance model. The entropy, interdependence, and dynamic contributions remain the same. The

Algorithm 3 Dynamic Relative Importance Contribution

Inputs: Vector of current value of responses $\vec{R}$, best value vector $\vec{R}^*$, worst value vector $\vec{R}^-$, vector of constraints $\vec{c}$, vector of thresholds $\vec{t}$, and vector of static relative importance $\vec{w}^s$

Outputs: Vector of dynamic weights $\vec{w}^d$

Normalize Responses, Constraints, and Thresholds
for j=1 ... n **do**
$R_n(j) = \frac{R(j)-0.5[R^*(j)+R^-(j)]}{0.5[R^*(j)-R^-(j)]}$
$c_n(j) = \frac{c(j)-0.5[R^*(j)+R^-(j)]}{0.5[R^*(j)-R^-(j)]}$
$t_n(j) = \frac{t(j)-0.5[R^*(j)+R^-(j)]}{0.5[R^*(j)-R^-(j)]}$
end for

Find constraint contribution
for $j = 1 \ldots n$ **do**
$cc_{\text{temp}} = -1\left[-0.5 + \frac{1}{\pi}\tan^{-1}\left[\alpha(R_n(j) - c_n(j))\right]\right]$
$cc(j) = \texttt{max}(cc_{\text{temp}}, 1)$
end for

Find threshold contribution
for $j = 1 \ldots n$ **do**
$R_n^{\textbf{low}}(j) = \texttt{max}(c_n(j), -1)$
if $R_n(j) \leq R_n^{\textbf{low}}(j)$ **then**
$tc_{\text{temp}} = 0$
else if $R_n(j) \geq t_n(j)$ **then**
$tc_{\text{temp}} = -w^s(j)$
else
$tc_{\text{temp}} = -w^s(j)\left(1 - \frac{t_n(j)-R_n(j)}{t_n(j)-c_n(j)}\right)^{\beta}$
end if
$tc(j) = \texttt{max}(tc_{\text{temp}}, -1)$
end for

Find total dynamic contribution
for $j = 1 \ldots n$ **do**
$w^d(j) = cc(j) + tc(j)$
end for

only change is to the user-specified relative importance, w_j^u in equation (63). Instead of a user-specified value, this now becomes a user-specified *distribution*. In this sense, the user specifies the type of distribution and its associated parameters. The beam design problem used a simple uniform distribution with a low limit of 1.0 and a high limit of 3.0 (relative variation of 50% from a mean of 2.0) to determine the sensitivity of the solution method to the relative importance. More appropriate distributions may include triangular or Gaussian distributions. One important consideration for distribution selection lies in the selection of negative values. Some distributions, such as Gaussian, are unbounded and therefore could potentially select a negative value. As such, steps must be taken by the user to ensure this does not happen, such as creating artificial bounds on the Gaussian distribution.

6.5 Decision Analysis

The most critical phase of design to multiple criteria is execution of the decision making algorithm. Compromise programming, modified for the use of the two-part relative importance model, gives promising results. This can be executed in a deterministic or probabilistic fashion with the only change being in how the user-specified relative importance $\vec{w}^u$ is handled.

The formal optimization statement for the final decision analysis follows as:

Minimize:

$$F(\vec{x}) = \left\{ \sum_{j=1}^{n} \left[\frac{w_j(w_j^u, \lambda_j, \gamma_j, \vec{x})(R_j(\vec{x}) - R_j^*)}{R_j^- - R_j^*} \right]^p \right\}^{\frac{1}{p}} \tag{65}$$

Subject to:

$$\vec{x}^{\,l} \leq \vec{x} \leq \vec{x}^{\,u} \tag{66}$$

where $w_j(w_j^u, \lambda_j, \gamma_j, \vec{x})$ is the two-part relative importance function given as the sum of the static importance given by equation (63) and the dynamic importance as in equation (64).

The execution of the probabilistic portion is handled via Monte Carlo simulation: thousands of analyses with distribution values taken from a random number generator coupled with a distribution function. This marks yet another advantage for polynomial surrogate

models as they have very fast execution times, whereas the original analysis routines may take far longer. Choice of the number of simulations to run is highly problem-dependent but usually is in the thousands to tens of thousands.

6.5.1 Computational Cost

The strategies outlined above come at a marginal computational cost when compared to current methods in decision making. The final increases in system execution time depend on which portions of the overall strategy are applicable to a given decision making problem. While specific costs depend on the algorithms used and the nature of the decision space, some guidance can be issued.

Changing from a constrained single objective formulation to multiple objectives adds little, if any, cost. The single objective constrained formulation requires evaluation of all of the system-level metrics to determine if constraints are active. The multiple objective formulation requires evaluation of the same number of metrics for each optimizer iteration, though they are instead assembled into a composite objective function. The only differences in computational cost will come if the number of optimizer iterations changes from a single objective to a multiple objective form. It is possible that the composite objective function is more difficult to solve and will therefore require more iterations; it is also quite possible that that the constrained single objective formulation is more difficult due to large infeasible regions in the decision space. In practice it seems that these differences are in a virtual dead heat with a slight edge in computational speed given to the single objective formulation.

The entropy assessment for the static relative importance imposes a one-time cost in terms of execution as it does not need to be repeated for every optimizer iteration. Its cost will depend on the number of random points used to evaluate the entropy of the decision space. In general this will be in the thousands, underscoring the need for faster executions such as those given by polynomial surrogate models. The entropy of the decision space should be reanalyzed only if the nature of the decision space has changed. This can occur through a change in the threshold of a metric, the addition or deletion of a metric, or if there are changes in the design space (such as the bounds for the design variables).

The dynamic relative importance model should come as little to no additional computational cost to the compromise programming algorithm. It simply needs the current values of the decision metrics, which are already required for each compromise programming iteration. The constraints and thresholds are set prior to decision making and do not change throughout the compromise algorithm.

The current formulation for the interdependent corrections simply relies on the coefficients of polynomial response surface approximations to the decision metrics. Thus, this comes as virtually no extra cost assuming the response surfaces have already been created and validated. However, creation of the response surfaces is not trivial and can require quite a bit of up-front computational time to generate. This depends greatly on the experimental design chosen and can range from tens to thousands of executions both for creation and again for validation. However, once created, these response surfaces greatly speed up other evaluation times, and as such can be used in the compromise algorithm and in entropy evaluation of the decision space. New response surfaces are only necessary if the bounds of the original design space change.

6.6 Multidimensional Visualization

The final step in large-scale decision making lies in visualization of the results. A number of different techniques exist, including scatterplots, bar charts, glyphs, and combinations thereof. A few of these visualization techniques are used throughout this document, though these are but a handful of multidimensional visualization techniques.

One of the simplest methods to compare multiple criteria performance is the examination of a scaled bar chart. This shows information for the metrics of a specified design (i.e. given $\vec{x}$) normalized with respect to the minimum and maximum ranges of the decision space. It is also best if normalized by direction of improvement, such that larger bars always signify better performance. For the beam example, this would mean that smaller-is-better requirements such as mass and deflection would be closer to their best values as the bars got larger. Figure 47 gives an example of a normalized bar chart from the beam design problem.

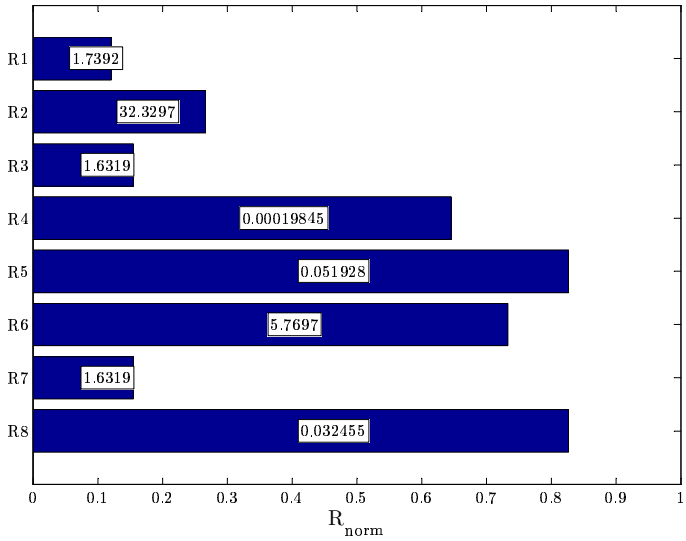

Figure 47: Normalized Bar Chart Visualization of Current Response Values

This particular chart also gives the current, non-normalized values of the decision metrics on the bar itself to provide a scale for each metric. Multiple concepts can be compared by viewing multiple bar charts side-by-side.

A good method for viewing Monte Carlo results or decision space limits is through the use of an n-dimensional scatterplot matrix. This is a collection of subplots that display pairwise scatterplots of each metric, usually with no subplots along the diagonal (because the plot of a metric versus itself is always a 45-degree straight line). Unfortunately, this type of chart loses its power as the number of decision metrics grow due to the growing number of pairwise scatterplots. Figure 25 in Chapter IV gives an example of a six-requirement scatterplot matrix, already at the limits of its display size.

Some remedies can make viewing scatterplot matrices more useful. The simplest solution is to simply view the data on a larger medium, such as a larger piece of paper or projection onto a large screen. Also, the scatterplot matrix can be set up to enable "zooming" on a particular pairwise plot; that is, the user moves a cursor over the plot of interest and selects it, causing a new, larger plot window to open with only the selected scatterplot. Unfortunately, both of these methods have limited utility due to the overwhelming amount of information available in high-dimensional scatterplot matrices. Brushing can be used

to emphasize certain regions or deemphasize others to limit information overload to some extent [Stump et al., 2002].

In some cases, it is possible to view a single, three-dimensional scatterplot with glyphs to represent other dimensions. This can be in the form of "arms" on a data point of different lengths, colored spheres, colors, and other methods to represent subsequent dimensions. The three spatial dimensions of the scatterplot are typically associated with spatial metrics, while the others may be performance or cost measures [Stump et al., 2002]. However, this form of multidimensional visualization generally becomes too crowded beyond seven or eight dimensions.

One of the contributions of this research is the identification of the *characteristic tradeoffs* of the decision space. This is an underlying linearly independent subset of the original requirements that can be arranged such that linear combinations of these characteristics can approximate the original requirements. This approach uses singular value decomposition of the coefficients of the polynomial surrogate models to determine the coefficients of the characteristic tradeoffs. These characteristic tradeoffs are ranked in importance by the singular values, and the lower values can usually be ignored with little loss in fidelity. This decomposition opens up compact multidimensional visualization techniques.

A variety of algorithms and built-in functions exist for singular value decomposition, so such an algorithm is not reproduced here. The reader is referred to Appendix B for a summary of SVD. In general, the process involves SVD of the matrix of response surface coefficients, input row-wise per response. This matrix, $\mathbf{B}$ from equation (50) in the previous chapter, should *not* include the intercept terms $\vec{b}_0$ as these do not vary with $\vec{x}$ and only serve as a translation term. The result of this decomposition should be three matrices: $\mathbf{U}$, $\mathbf{\Sigma}$, and $\mathbf{V}^{\mathrm{T}}$. Investigation of the diagonal of Σ provides the singular values in descending order.

Choice of the cutoff singular value will determine the number of characteristic tradeoffs used for the decomposition plots. Some guidance can be given by inspection of the recomposition matrix, given as the product of the $\mathbf{U}$ and $\mathbf{\Sigma}$ matrices. The columns of

this matrix indicate the contribution of each of the characteristic directions to the original requirements. Characteristics that contribute little to the recomposition of the original requirements can be ignored. Preliminary experiments indicate that singular values more than an order of magnitude below the largest singular value indicate characteristic tradeoffs that can be largely ignored for multidimensional visualization. The number of important characteristics is denoted by r, such that $r \leq n$.

These preliminaries ensure that decomposition-based visualization is possible for the system. From here, it is possible to create the datasets for the hybrid matrix scatterplots as seen previously in Figure 40. This involves finding two specific datasets: mapping the probabilistic response data from the n-dimensional decision space to the r-dimensional characteristic space, and finding the recomposition matrix $\mathbf{C}^{\oplus}$. This procedure is outlined in Algorithm 4.

This algorithm provides two matrices: $\mathbf{Vp}$ and $\mathbf{C}^{\oplus}$. The former is then compared row-wise via two-dimensional scatterplots on the off-diagonal matrix subplots. The latter is used for visualization of the relative contribution each characteristic makes to each requirement, and is displayed in the on-diagonal subplots. These contribution plots are very powerful and should be set up such that the requirements which vary the most for a given characteristic are placed at the top. Further, the *direction of improvement* information can be used in conjunction with these plots to determine if an increase in a given characteristic increases or decreases the desirability of a metric. This can be reproduced as a simple color code, such as blue for beneficial and red for detrimental. Examples of contribution plots were shown in Figure 39 in the previous chapter.

Algorithm 4 Datasets for Decomposition-Based Visualization

Inputs: $m \times q$ population matrix $\mathbf{Xp}$ (m random population members, q design variables), upper and lower bounds $\vec{x}^u$ and $\vec{x}^l$ of design variables, results from SVD of $\mathbf{B}$ matrix: $\mathbf{U}$, $\mathbf{\Sigma}$, and $\mathbf{V}^{\mathrm{T}}$, and number of characteristic requirements r

Outputs: $m \times r$ characteristic population matrix $\mathbf{Vp}$, $n \times r$ recomposition matrix $\mathbf{C}^{\oplus}$

Normalize population matrix

for $i = 1 \ldots m$ **do**
  for $j = 1 \ldots q$ **do**
    $\mathbf{Xp}_n(i,j) = -1 + 2\frac{\mathbf{Xp}(i,j) - x^l(j)}{x^u(j) - x^l(j)}$
  end for
end for

Create characteristic population matrix

for $i = 1 \ldots m$ **do**
  find $\widetilde{x}_{\text{temp}}$ for specific regression model from $\mathbf{Xp}_n(i,:)$ [see equation (49)]
  for $j = 1 \ldots r$ **do**
    $\mathbf{Vp}(i,j) = \mathbf{V}^{\mathrm{T}}(j,:) \times \widetilde{x}_{\text{temp}}$
  end for
end for

Create recomposition matrix

$\mathbf{\Sigma}^{\oplus} = \mathbf{\Sigma}(:, 1:r)$
$\mathbf{C}^{\oplus} = \mathbf{U} \times \mathbf{\Sigma}^{\oplus}$

CHAPTER VII

EXAMPLE APPLICATION: TRANSPORT DESIGN

The beam design problem provided an excellent example application for the development of the advanced decision making strategies outlined in the previous chapter. As informative as it was, it was a contrived example meant to illustrate the issues and new approaches towards probabilistic large-scale systems design. However, the motivation for this research came from the need for a new approach for decision making in aerospace systems design. As such, it is necessary to apply the strategy of Chapter VI to a problem of interest to the aerospace community.

NASA initiated a study in February of 2004 to assess a variety of development programs related to aerospace technology development. The team involved in this study was dubbed VISTA, for Vehicle Integration, Strategy, and Technology Assessment. The team was an offshoot of the Vehicle Systems Program (VSP) and composed of strategists from NASA Headquarters and four research centers. The goal was to assess new technologies, plan their development, create partnerships, and provide guidelines for the six vehicle sectors within the VSP [National Aeronautics and Space Administration, 2004].

The Subsonic Vehicle Sector of the VSP wished to evaluate a number of technologies related to large subsonic transports. These technologies represented advancements designed to reduce aircraft emissions and increase efficiency beyond the state of the art over the next 15 years. This program and its associated targets represents a challenging problem well-suited to the integration of a decision making framework as hypothesized in the previous chapters. This problem is especially attractive due to the availability of the models used by the Aerospace Systems Design Laboratory at Georgia Tech in collaborative studies with the VISTA subsonic sector team.

7.1 Requirements Definition

The Vehicle Systems Program created a number of notional vehicle concepts to test technology metrics [Wlezien, 2004]. The subsonic sector had several concepts, including the Quiet, Efficient Subsonic Transport (QuEST). Ten system-level metrics were used to evaluate the subsonic sector technologies on QuEST. This included an assessment of the state-of-the-art (SOA) to benchmark future goals against current capabilities [Collier, 2004]. The benchmark was a modern intercontinental commercial transport roughly indicative of a Boeing 777 [Boeing Commercial Airplanes, 2000]. The QuEST metrics are reproduced in Table 26.

Table 26: Notional Capabilities for a Quiet, Efficient Subsonic Transport [Collier, 2004]

Requirement	**SOA**	**5 Years**	**15 Years**
Takeoff gross weight, lbs	656,000	515,000	374,000
Community noise, EPNdB	Stage 3 - 8	Stage 3 - 18	Stage 3 - 28
NO_x emissions, kg/LTO	75.0	50.0	22.5
CO_2 emissions, kg/ASM	0.1438	0.1169	0.0719
Takeoff field length, ft	9,900	< SOA	< SOA
Approach speed, kts	138	< SOA	< SOA
Range, nmi	7,625	SOA	SOA
Payload, lbs	65,000	SOA	SOA
Cruise Mach number	0.84	0.87	0.90
Direct operating cost, cents/ASM	3.5	2.8	2.1
Utilization, hours/day	14	> SOA	> SOA

Another potential source of requirements are the regulations set by the Federal Aviation Administration (FAA) for transport category airplanes. The requirements for "community noise" from Table 26 reference "Stage 3," which is a series of noise regulations from Part 36 of Title 14 in the Code of Federal Regulations. These regulations specify three noise measurement metrics: *flyover* noise, taken from a location under the takeoff path of the airplane after the first power reduction (also known as *takeoff* or *cutback* noise); *lateral* noise, measured at a point parallel to the takeoff run (also known as *sideline* noise); and *approach* noise, measured at a point along the aircraft's approach path to landing [Federal Aviation Administration, 2003b]. The Stage 3 noise levels for the baseline aircraft of the QuEST study, based on the listed gross weight of 656,000 pounds, are:

- Flyover noise $\leq$ 99.5 EPNdB
- Lateral noise $\leq$ 105.0 EPNdB
- Approach noise $\leq$ 101.9 EPNdB

The noise levels are expressed in decibels (dB), and modified by a procedure to produce the Effective Perceived Noise Level (EPNL). Note that the baseline transport in the QuEST study is believed to have noise components eight decibels less than those given by the Stage 3 requirements above.

The QuEST study mentions a state-of-the-art capability for oxides of nitrogen (NO_x) emissions of 75 kilograms per landing-takeoff (LTO) cycle. These emissions are especially harmful at higher altitudes where they can cause ozone depletion in the upper atmosphere. As such, the FAA recently incorporated a regulation given by the Environmental Protection Agency designed to reduce NO_x emissions by newly manufactured aircraft [Environmental Protection Agency, 2005]. This rule is based on the overall pressure ratio and rated output of the engine, given as

$$NO_x \leq 7 + 2.0 \times OPR \times rO \text{ g/kN} \tag{67}$$

where OPR is the overall pressure ratio of the engine and rO is the total rated output of all operating engines in kN [Federal Aviation Administration, 2003a].

Other requirements have no associated regulations, so the constraints can generally be considered to keep a new solution from doing worse than the state-of-the-art. For example, there are no requirements currently in the FAA regulations regarding carbon dioxide emissions. The FAA advisory circular on aircraft emissions specifically states [Federal Aviation Administration, 2003a]:

> CO_2 is not considered a pollutant but its concentration is required for calculation and check purposes.

However, carbon dioxide emissions are becoming greater in importance due to being labeled a "greenhouse gas," hence, the aerospace community is charged with a reduction in

these emissions. This is an example of design to a requirement before a regulation exists, either in anticipation of its creation or of a general consciousness regarding the effect of these emissions.

The goals in Table 26 are particularly useful for this study because they provide a reference for definition of constraints and thresholds. Specifically, one can think of the constraints being the FAA requirements or current state-of-the art (whichever is more limiting), and the thresholds defined by the 15-year goals. One cannot fully enumerate these values at this moment, as these requirements must be calibrated to the baseline concept model.

7.2 Concept Identification

The QuEST program is designed to meet the needs for a 300-passenger long-range civil transport aircraft. As mentioned above, the state-of-the-art for this niche is filled by the Boeing 777, which represents a benchmark for future progress. While the 777 represents a standard wing-tail-tubular fuselage arrangement, NASA has identified a number of promising, more radical concepts to meet the needs of large subsonic transports [Collier, 2004]. These include the strut-braced wing, blended wing body, and C-wing configurations [Jones et al., 2000; McMasters et al., 1996].

Georgia Tech's involvement in the VISTA study specifically involved the effect of 29 technology programs mostly related to evolving engine technologies as applied to the 300-passenger commercial transport. The baseline for this technology application and evaluation was a conventional 777-like aircraft. The models created by the researchers at Georgia Tech used this baseline, so it will also be used as the concept for the studies in this document.

The effects of the 29 technologies were elucidated via the Technology Metrics Assessment and Tracking (TMAT) process [Kirby et al., 2001]. This technique enables a group of managers, systems engineers, and disciplinarians to identify the current and end-of-program impacts of individual technology programs, as well as quantify the uncertainty in their development. Equally important is the identification of the system-level effects of these technologies. The TMAT process enables identification of a vector of "k-factors" for each technology for further system-level analysis. These vectors, along with the top-level system

design variables, are extraordinarily important to the selection of the best suite of technology programs to meet specific program goals [Kirby, 2001].

The Georgia Tech / VISTA team identified 60 different system-level design variables and technology k-factors for the 300-passenger commercial transport technology selection problem [Mavris et al., 2004]. These 29 technologies resulted in a number of different combinations based on the input scenario. A total of 17 three-point deterministic technology selection scenarios were run for the 15-year program goals and 12 three-point assessments made for the 5-year goals. The three points represented optimistic, most likely, and pessimistic impacts for each technology.

These 87 deterministic selection scenarios would be cumbersome to implement as a full-scale example problem for the research in this document, so only one scenario was selected from the 5- and 15-year experiments. Also, a point was run at the state-of-the-art technology set (zero active technologies) to serve as a modified baseline for determination of the final constraint and threshold values. In all, this enabled selection of only seven system-level vehicle design variables, with the other 53 inputs as constants for each of the three cases. These seven variables and their ranges are listed in Table 27.

Table 27: Design Variables for 300-Passenger Transport Technology Impact and Requirements Analysis

Design Variable	**Symbol**	**Low Value**	**High Value**
Fan pressure ratio	FPR	1.46	1.56
Low pressure compressor pressure ratio	LPCPR	1.3	1.6
High pressure compressor pressure ratio	HPCPR	20	25
Wing quarter chord sweep, degrees	SWEEP	26	32
Airfoil shape factor	AITEK	2.0	2.2
Wing loading, lbs/ft^2	WSR	125	135
Thrust-to-weight ratio	TWR	0.25	0.29

The choice of some of these values as system-level design variables may seem curious at first; however, the choices were limited as this was primarily a study in engine technologies. Hence, some gross scaling of the aircraft is possible through the wing loading and thrust-to-weight ratio variables, and other airframe control is exerted through the wing sweep and

airfoil shape factor variables. The other three variables relate to engine design parameters. Turbine inlet temperature is absent because it was considered as a technology-limited variable in the Georgia Tech study.

7.3 Modeling and Simulation

The methods used to generate the models for the full technology impact study for the VISTA report were necessarily complex. A suite of numerical analysis tools were brought together, including NASA's Numerical Propulsion System Simulation (NPSS), Weight Analysis of Turbine Engines (WATE), Flight Optimization System (FLOPS), Aircraft Noise Prediction Program (ANOPP), and Aircraft Life Cycle Cost Analysis (ALCCA) [Mavris et al., 2004]. These detailed tools provided information on the cost, emissions, and performance of the vehicle with reasonable accuracy. However, the complexities and long execution times can make evaluation of technology impacts time-prohibitive; therefore, in keeping with the technology assessment method of Kirby, multiple response surfaces were created for each of the responses of interest. However, creating response surfaces for such a large and challenging problem, complete with 60 design and technology variables, is a daunting task.

One method for creating response surfaces for large environments involves a technique dubbed zooming, where multiple regressions are made at varying levels in the integrated environment. Instead of creating one response surface for a response encompassing all of the variables, only a portion are used in the top-level response along with the results of sub-regressions. This technique was employed with great success for the VISTA subsonic assessment, as well as others [Mavris and Kirby, 2003]. The net result of this process was a collection of interconnected response surfaces in a single integrated environment capable of handling all 60 system-level inputs for the calculation of 15 system-level metrics for technology assessment. This final collection was used as the base modeling and simulation environment for the implementation experiments of the decision-making strategy formulated in the previous chapter.

Three technology sets were selected from the VISTA study as the baselines for the SOA, 5-year, and 15-year analyses. The SOA case was the simplest, and represented the outputs

of the original analyses when all technologies were "off." The 5- and 15-year baselines were selected from the "Max Case 2" scenario resultant technology suites, representative of the "most likely" deterministic technology impacts. The reader is referred to the final report of the VISTA study for the validation and selection of these cases as that is beyond the scope of this document. The baseline inputs for all 60 variables are given in Appendix C.

Selection of the modeling and simulation environment and baseline SOA inputs finally allows for specification of the requirements for this series of decision making experiments, as well as the associated constraints and thresholds. The constraints were based off the more stringent of the SOA capabilities or current regulations, and followed from the QuEST goals. The thresholds were based on the same improvements for QuEST, though they too were adjusted based on the constraints. The final values are given in Table 28.

Table 28: Requirements and Associated Inflection Points for Decision Making Experiments

Requirement	**Symbol**	**Reg.**	**SOA**	**Constraint**	**Threshold**
Takeoff gross weight, lbs	TOGW	-	659,025	659,025	-
Flyover noise, EPNdB	TOn	99.53	91.97	91.97	71.97
Lateral noise, EPNdB	SLn	105.0	94.93	94.93	74.93
Approach noise, EPNdB	APPn	101.9	98.31	98.31	78.31
NO_x emissions, kg/LTO	NOx	63.10	53.79	53.79	22.5
CO_2 emissions, kg/ASM	CO2	-	0.1356	0.1356	0.0719
Takeoff field length, ft	TOFL	-	9,534	9,534	7200
Approach speed, kts	VAPP	-	123	123	-
Direct op. cost, cents/ASM	DOCi	-	4.348	4.348	2.1

The models from the VISTA study did not allow for varying cruise Mach number, so that requirement cannot be studied. Both payload and range were fixed for the study, so those too are dropped from the requirements specifications. Note that the community noise metric was replaced with the three FAA noise measurement points, and the threshold was adjusted down from the SOA value by 20 dB for each. The approach speed requirement appears much lower than that presented in Table 26; however, this value is a simple calculation based on the stall speed of the aircraft. It is likely that the VISTA target included the standard correction for gust and configuration changes of 15 knots [Flight Safety Foundation, 2000]. Finally, the takeoff field length threshold, though not specified by the VISTA 15-year targets,

represents a nominal value indicative of a smaller jet transport. The Boeing 737-300 can takeoff in approximately 7,200 feet [Boeing Commercial Airplanes, 2005] and serves a variety of regional markets. Hence, this value represents a good point of diminishing returns for the long-range transport model as it will likely never have to land at airports with runways too small for regional transports.

7.3.1 Creation of Surrogate Models

At first glance, it may seem foolish to create surrogate models of the original analyses as they too are a series of polynomial response surfaces. However, these response surfaces represent the effect of 60 variables on 15 responses. Further, these polynomials are not a direct mapping from the design space to the decision space; rather, the entire routine is an integrated system of equations based on the zooming principles described before. As such, creating new polynomial response surfaces to simply map the seven design variables to the nine responses for the decision-making experiments may be more efficient. This will further enable the evaluation of interdependence and decomposition-based visualization of this reduced set of responses. Attempting this on the original set of equations may give false results because of the many additional degrees of freedom posed by the intermediate variables.

A total of three sets of response surface equations are necessary: one for the baseline SOA evaluation, one for the 5-year technology set, and one for the 15-year technology set. These equations should be *similar* but they will not be the same. If the technologies have no interaction with the other aircraft design variables then the three sets of equations would indeed be the same save for different intercept terms, but this is highly unlikely. It is in the interactions that the true tradeoffs of design and technology selection are found.

Creation of response surfaces from other response surfaces may sound like an exercise in error propagation. However, the original surfaces for the 60 inputs were validated to reasonable degrees of precision over the ranges of the requirements. If the new reduced-order surfaces predict the original polynomials well, the overall solution should suffer from little additional regression error. A bonus of using the original surfaces is that execution time

is very fast, enabling rapid creation of data points for the new reduced-order polynomials.

With this in mind, response surfaces were made for the nine requirements listed in Table 28 from the seven inputs within the ranges listed in Table 27. A total of 2,000 cases were created within these ranges using Latin Hypercubes in an attempt to maintain a reasonably uniform search of the design space. However, Latin Hypercubes do not always capture the extremes of the design space [Barros et al., 2004], so an additional 143 cases were run using a central composite design. Finally, the baseline case was added to the dataset for a total of 2,144 datapoints per response.

The original response surfaces were contained in a large, macro-encoded spreadsheet that served as the basis of the analysis. The Latin Hypercube cases were created and run within Crystal Ball [Decisioneering, Inc., 2005], whereas the central composite design was created, executed, and collated in a very simple ModelCenter [Phoenix Integration, 2005] program. Figure 48 shows a simple schematic of this process.

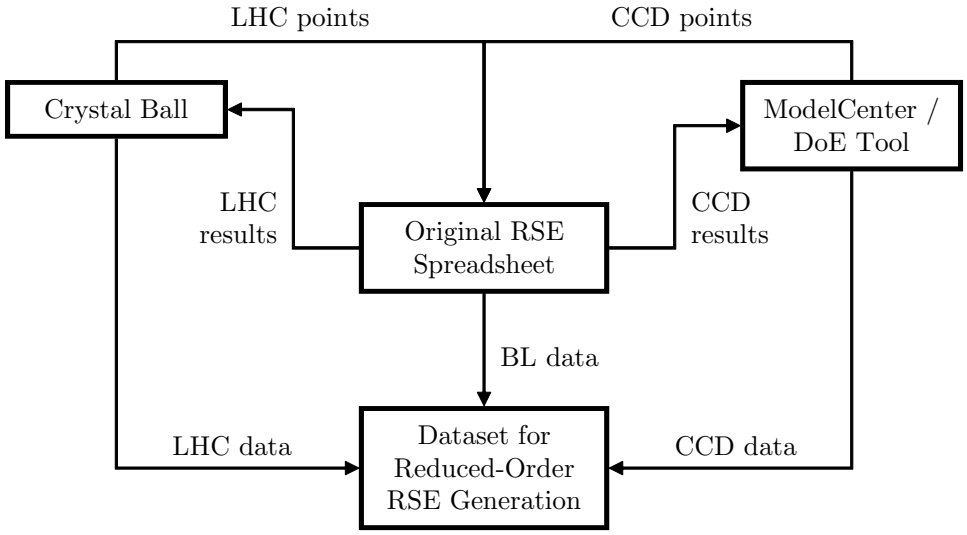

Figure 48: Creation of Datasets for Reduced-Order Surrogate Models

The datasets were collected into three large files; one for each series of equations. These were collected into a Matlab script to normalize each response. The inputs were first normalized from -1 to 1 by

$$\overline{x}_{ik} = -1 + 2\frac{x_{ik} - x_k^l}{x_k^u - x_k^l} \tag{68}$$

where $\overline{x}_{ik}$ is the k^{th} normalized design variable for the i^{th} point in the dataset, and the superscripts l and u refer to the lower and upper bounds of the design variable in its native units. A similar procedure was used to normalize the responses from -1 to 1, except an effort was made to center the responses on an approximate mean. The response data was normalized via

$$\overline{R}_{ij} = \frac{R_{ij} - 0.5(R_j^* + R_j^-)}{0.5(R_j^* - R_j^-)} \tag{69}$$

where $\overline{R}_{ij}$ is the j^{th} normalized response for the i^{th} point in the dataset, and the other notation is as before.

Validation of these reduced-order response surfaces was carried out by various whole-model tests to good effect. From here, 2,000 random cases were evaluated via Monte Carlo simulation to view the differences between actual results from the original nested polynomials versus the predictions of the reduced-order response surfaces. The fits were excellent, with only the sideline noise response showing some measurable error. The results of these validation cases are presented in Appendix D.

7.4 Relative Importance Model

The two-part relative importance model requires the determination of multiple contributors. Most of these values are for calculation of the static relative importance, given from equation (63). The dynamic model follows from the current value of the decision metrics. The creation of the reduced-order surrogate models, along with the final definition of the design and decision spaces with all pertinent inflection points, enables enumeration of the various contributors to relative importance.

7.4.1 User Preferences

No rigorous team-based technique was used to determine the user preference for relative importance of this application. Instead, all of the user preferences were assumed to be equal to be consistent with the approach used for the beam design example earlier. These values were probabilistically varied uniformly by 50% on either side much as in the earlier probabilistic examples. This was accomplished by allowing the user preference value to vary

uniformly between 1.0 and 3.0 for each of the metrics (noting that the total static relative importance will be normalized to sum to one). This variation was to determine sensitivity of the solution to user preferences.

7.4.2 Entropy Analysis

The entropy analysis was carried out by the process outlined earlier in Algorithm 1. A random population of 5,000 design space members were mapped to the decision space for determination of individual entropy for each of the three sets of responses. The resulting threshold-modified entropy-based relative importance is given in Table 29. As with all of the discrete entropy formulations, these are typical values and are generally accurate within a few percent.

Table 29: Entropy-Based Relative Importance for 300-Passenger Transport Model

Requirement	SOA	5 Year	15 Year
CO2	0.0354	0.0232	0.0135
DOCi	0.0349	0.0367	0.0274
NOx	0.0765	0.0768	0.0710
APPn	0.1079	0.1265	0.1436
SLn	0.1307	0.1224	0.1419
TOn	0.0822	0.0774	0.0815
TOFL	0.1010	0.0607	0.0603
TOGW	0.0323	0.0315	0.0232
VAPP	0.3991	0.4449	0.4376

Inspection of these values indicates that approach speed is by far the metric with the greatest normalized contrast intensity in the decision space. This is counterintuitive, as approach speed physically varies with the square root of wing loading, and the wing loading variation in the decision space is less than ten percent. This assertion can be verified by inspection of the ranges of requirements, given in Table 30. For brevity, this table only shows the worst values of the SOA configuration and the best values of the 15 year configuration. This displays the very largest possible ranges in all three decision spaces.

These ranges verify that the approach speed does not vary by much, totalling 3.7 knots across the entire three-configuration decision space. This represents less than a three percent improvement from the very worst value seen in this space. A pilot is not likely to notice

Table 30: Requirements Ranges

Requirement	Worst (SOA)	Best (15 Year)	Difference	% Difference
CO2	0.1495	0.1072	0.0423	28.3%
DOCi	4.736	3.633	1.103	23.3%
NOx	84.22	26.90	57.32	68.1%
APPn	100.0	93.87	6.15	6.2%
SLn	96.91	90.96	5.95	6.1%
TOn	94.04	88.36	5.67	6.0%
TOFL	10739	5607	5131	47.8%
TOGW	721623	535075	186548	25.9%
VAPP	124.3	120.7	3.7	2.9%

a three percent change in this metric, as it will have little effect on operations. Further, this value is only slightly larger than the numerical noise of the multiple regressions used to calculate it, so this metric can be completely omitted from the decision space.

Some may argue the same point for the noise constraints, all varying a little more than six percent across the three-configuration space. However, these values are measured in decibels, which is a logarithmic scale. Hence, a reduction by a few percent will actually have a noticeable impact. Furthermore, the distance between the constraints and thresholds is less than 30% of the worst values in the decision space, so even a small improvement will have a relatively large impact in the MCDM formulation.

With these points in mind, the final entropy-based relative importance values for all three configurations are given in Table 31. These values were found after omitting the contribution of the approach speed to the decision space variation, as its normalized impact adversely affected the other importance values.

Table 31: Final Entropy-Based Relative Importance for 300-Passenger Transport Model

Requirement	SOA	5 Year	15 Year
CO2	0.0653	0.0445	0.0244
DOCi	0.0639	0.0670	0.0499
NOx	0.1362	0.1350	0.1318
APPn	0.1932	0.2256	0.2550
SLn	0.2405	0.2251	0.2514
TOn	0.1507	0.1391	0.1426
TOFL	0.0910	0.1052	0.1028
TOGW	0.0591	0.0586	0.0420

These values seem consistent with the possible variation in the metrics. The noise constraints are all higher in relative importance due to their greater contrast intensity from the best values in the decision space. Takeoff field length is also relatively important; this comes as no surprise given the large variation seen in this metric.

7.4.3 Interdependence Analysis

Creation of the reduced-order surrogate models allowed for interdependence analysis by the procedure outlined in Algorithm 2. The resulting interdependence corrections are given in Table 32.

Table 32: Interdependence Corrections to Relative Importance

Requirement	SOA	5 Year	15 Year
CO2	0.4968	0.5352	0.5607
DOCi	0.7482	0.8447	0.9308
NOx	0.5353	0.9081	0.9023
APPn	0.4698	0.5343	0.5272
SLn	0.4742	0.5033	0.5877
TOn	0.4451	0.4538	0.4890
TOFL	3.5146	3.4282	2.9387
TOGW	0.6270	0.6780	0.7112

The most notable feature of the interdependent analysis is the modifier for takeoff field length. It is the only metric across all three configurations that has an interdependence correction greater than one, indicating that this requirement is opposed to most of the others in the decision space. All other metrics face a reduction in their static importance. It is interesting to note that the NOx and direct operating cost metrics appear to become more independent as the technology advances from the SOA configuration, indicated by these values approaching one. This also likely accounts for the reduction in the correction value for takeoff field length as the technology advances.

The enumeration of all user preferences, entropy values, and interdependence corrections allows for the calculation of the total static relative importance following from equation (63). The results for all of the configurations are given in Table 33. These values represent the total monotonic importance of each metric before the dynamic corrections.

Table 33: Final Static Relative Importance for 300-Passenger Transport Model

Requirement	SOA	5 Year	15 Year
CO2	0.0415	0.0264	0.0159
DOCi	0.0611	0.0628	0.0538
NOx	0.0932	0.1362	0.1378
APPn	0.1160	0.1339	0.1558
SLn	0.1458	0.1259	0.1712
TOn	0.0858	0.0701	0.0808
TOFL	0.4091	0.4005	0.3501
TOGW	0.0474	0.0442	0.0346

7.4.4 Dynamic Model

Implementation of the dynamic relative importance again revealed few surprises for the transport technology impact analysis. This model modifies the relative importance value based on two inflection points: the constraint, which if violated bumps up the relative importance like a step function; and the threshold, which represents the point of diminishing returns for a specific response.

The constraints and thresholds for this problem were identified earlier in Table 28. Only the takeoff gross weight does not have a threshold, indicating that in the absence of all other criteria, this requirement should be minimized. However, inspection of the requirement ranges from Table 30 shows that only the takeoff field length threshold is within the decision space. As such, the decision making algorithm will be counting contributions from most of the responses throughout the entire decision space span. This also seems to indicate that the decision making algorithm will behave somewhat like monotonic MCDM, though with penalty functions to ensure that constraints will not be violated.

The progression of the dynamic relative importance models throughout the three configurations helps to illustrate the impact of the technologies. The relative importance of each metric in the decision space for SOA, 5-year, and 15-year technology configurations are shown in Figures 49, 50, and 51, respectively. Note that these plots give the requirements variation according to the normalized response values in an effort to show the relative variation within the decision space.

The most striking comparison between these three charts is the amount of the decision

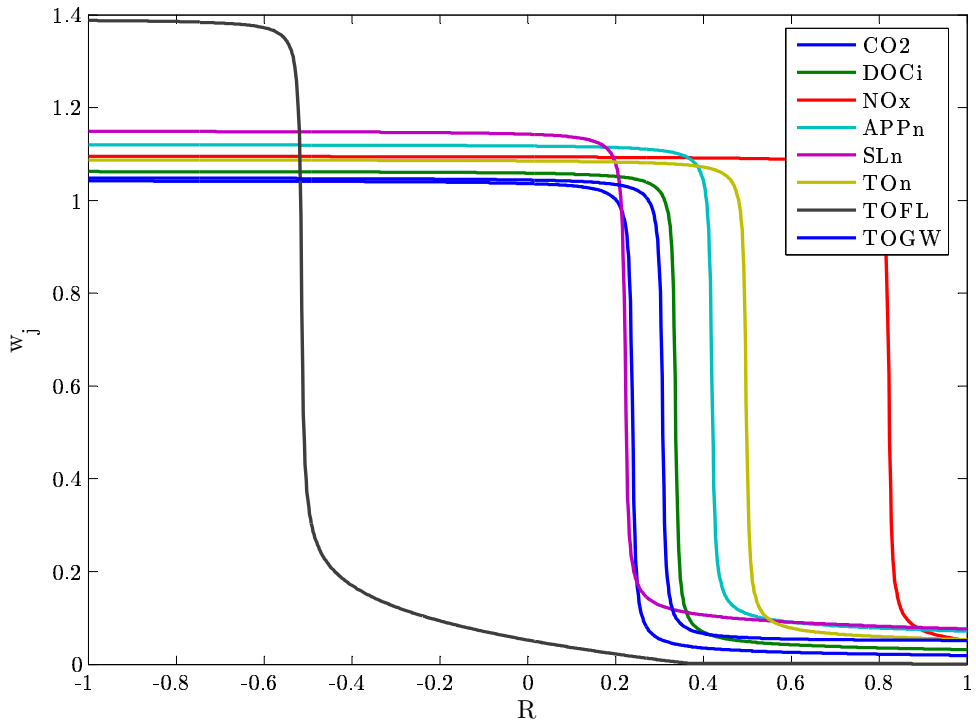

Figure 49: Total Relative Importance Variation for SOA Configuration

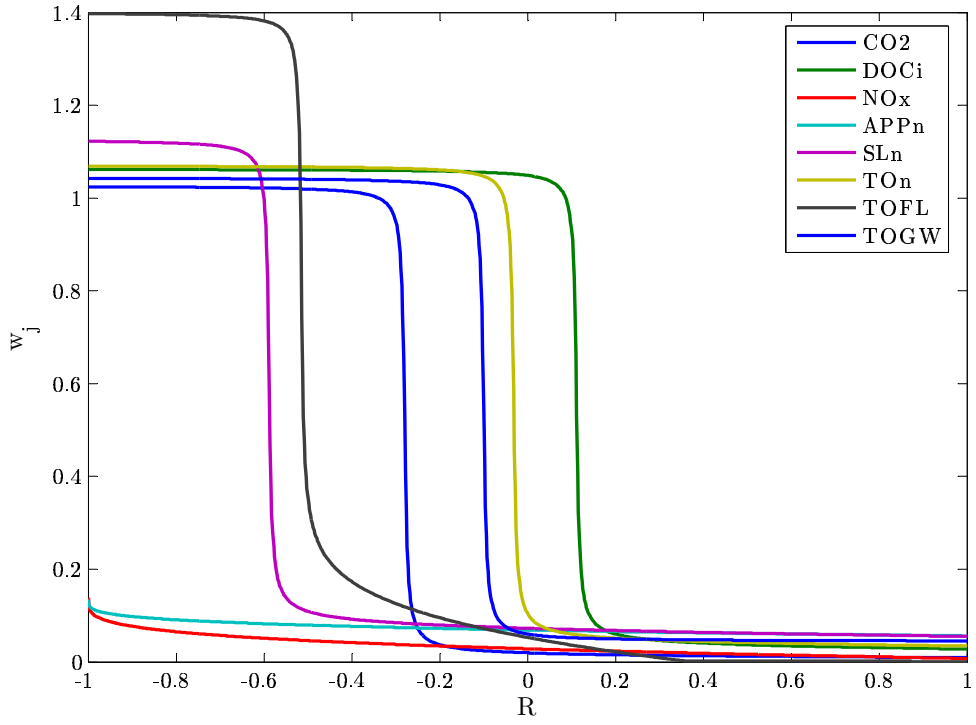

Figure 50: Total Relative Importance Variation for 5-Year Configuration

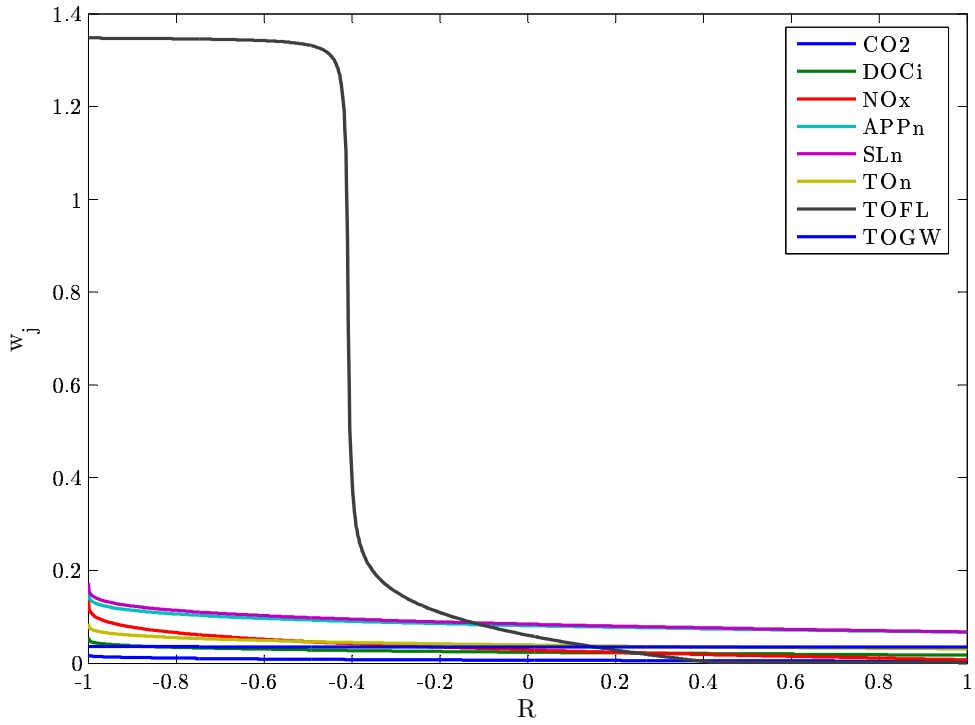

Figure 51: Total Relative Importance Variation for 15-Year Configuration

space that becomes unconstrained as the technology level increases. The SOA configuration is largely constrained, with the NOx constraint present throughout most of its associated dimension. The 5-year configuration still has the possibility of active constraints in the decision space, though more space is opened up for the decision making algorithm. Finally, the 15-year configuration only has one active constraint in takeoff field length. The takeoff field length response is interesting, notably because it is slightly more limiting for the 15-year technology set than for the others. This is likely because no technologies from the VISTA studies are designed to reduce field length (at least not in the subsonic transport studies; another VSP area is extreme short takeoff and landing, but those technologies are not covered here). In fact, the technologies that are used to reduce aircraft noise may have an adverse effect on field length. Further, the more desirable aircraft from a noise standpoint will have smaller engines, which will result in longer takeoff runs. This is also likely the reason why takeoff field length is found to be in opposition with the other requirements as seen in the interdependence analysis.

7.5 Decision Analysis

The models are now developed to the point for decision analysis. In an effort to determine the effect of this decision making strategy a total of six experiments were conducted per configuration. Four of these experiments used the deterministic formulation and the other two utilized probabilistic relative importance.

The deterministic experiments included two control groups: single-objective constrained optimization of takeoff gross weight and direct operating cost. These represent typical constrained optimization single-objective functions. Minimum takeoff gross weight is a zeroth-order estimate of an aggregate of minimum manufacturing cost (empty weight contribution) and minimum operating cost (fuel weight contribution), and is a classical objective for aircraft design [Simonds, 1956]. Minimum direct operating cost often is a goal that represents the zeroth-order interests of the airline (or other entity) operating the aircraft and has been a metric of interest in more recent years, especially for aircraft in environmental studies [Antoine and Kroo, 2004; Simos and Jenkinson, 1986]. This is likely because of the generally adverse effect emissions regulations have on operations.

The other two deterministic experiments involved MCDM algorithms, specifically compromise programming with $p = 2$. The first set of MCDM results followed from the user-specified relative importance only; hence, evenly-weighted CP. The second MCDM experiment used the full two-part relative importance model with threshold-modified entropy-based relative importance, interdependent corrections, and the dynamic importance model. All of this followed from the results of previous section.

The probabilistic experiments were conducted with the two MCDM formulations. The first simply varied the user-specified relative importance with a simple monotonic model with no corrections, while the other utilized the full dynamic model with all corrections. The resulting output distributions were then compared with Student's t-test to determine if the differences between the means of the distributions were significant.

The SOA configuration provided the first platform for the six experiments. The results for the four deterministic experiments are listed in Table 34. Note that this table, and those that follow, list the design variable settings first, followed by the values of the responses.

Table 34: Deterministic Results for SOA Configuration

Value	Min. TOGW	Min. DOCi	Even CP	Dynamic CP
AITEK	2.200	2.200	2.200	2.200
FPR	1.496	1.497	1.471	1.480
HPCPR	20.19	20.08	20.38	20.19
LPCPR	1.300	1.300	1.300	1.300
SWEEP	29.94	30.28	30.35	30.32
TWR	0.2561	0.2556	0.2698	0.2658
WSR	135.0	134.4	134.6	134.5
CO2	0.1303	0.1302	0.1333	0.1323
DOCi	4.267	4.267	4.369	4.336
NOx	53.79	53.64	52.62	52.79
APPn	98.16	98.16	97.87	97.97
SLn	94.78	94.79	94.54	94.66
TOn	91.97	91.97	91.82	91.89
TOFL	9534	9534	7954	8328
TOGW	641680	641810	656800	652000

The first noticeable feature of these experiments is the relative uniformity of the results. This comes as no surprise; as noted earlier the SOA dynamic relative importance model indicated that a large portion of the decision space was constrained (referring again to figure 49). As such, the CP results with the dynamic model should be very similar to the single-objective constrained solutions. Interestingly, both single-objective solutions are similar as well. The minimum TOGW solution has some differences from the minimum DOCi solution; however, these are relatively minor. This is likely because DOCi and TOGW are reasonably correlated. This is verified by inspecting the vector angle between the coefficients of the two responses, which is found to be a mere 7.3 degrees for the SOA models. It is unlikely that this will change much for the 5-year and 15-year models. As mentioned earlier, this study was primarily to determine the effects of various engine technologies, so the design and technology variables selected mostly affect the fuel consumption. Other variables, such as wing aspect ratio, were not modeled in the original study and therefore cannot be added here. The addition of this and other system-level design variables would likely lead to a greater difference between the minimum DOCi and TOGW solutions.

The results of the probabilistic study for the SOA models is given in Table 35 with the corresponding mean shift analysis in Table 36. The means are similar (though not

statistically so) but the standard deviation for the dynamic CP model is much lower than for the evenly weighted CP formulation. This indicates a much tighter distribution for the dynamic CP results. Some design variables, notably AITEK and LPCPR, have virtually no deviation for either formulation and do not exhibit a mean shift between the two forms.

Table 35: Probabilistic Results for SOA Configuration

	Standard CP			**Dynamic CP**		
Value	μ	σ	σ %	μ	σ	σ %
AITEK	2.200	1.73E-14	0.00%	2.200	1.73E-14	0.00%
FPR	1.474	0.01018	0.69%	1.480	0.0014886	0.10%
HPCPR	20.41	0.3963	1.94%	20.19	0.09474	0.47%
LPCPR	1.300	2.44E-14	0.00%	1.300	2.44E-14	0.00%
SWEEP	30.49	0.2600	0.85%	30.34	0.04655	0.15%
TWR	0.2681	0.006081	2.27%	0.2656	5.40E-04	0.20%
WSR	133.8	1.449	1.08%	134.5	0.5127	0.38%
CO2	0.1331	0.001133	0.85%	0.1323	4.28E-05	0.03%
DOCi	4.363	0.03879	0.89%	4.336	0.001497	0.03%
NOx	52.86	0.6286	1.19%	52.78	0.1727	0.33%
APPn	97.90	0.1418	0.14%	97.96	0.02584	0.03%
SLn	94.55	0.2520	0.27%	94.65	0.04708	0.05%
TOn	91.83	0.1529	0.17%	91.88	0.02560	0.03%
TOFL	8117	780.4	9.61%	8351	103.4	1.24%
TOGW	656040	5742	0.88%	652040	261.1	0.04%

Table 36: Mean Shift Analysis for SOA Configuration

Value	μ(sCP − dCP)	σ(sCP − dCP)	***t*-Statistic**	***p*-Value**
AITEK	0	0	-	-
FPR	-0.005945	0.01029	18.26	1.60E-64
HPCPR	0.2230	0.4095	17.22	2.19E-58
LPCPR	0	0	-	-
SWEEP	0.1449	0.2645	17.32	6.00E-59
TWR	0.002445	0.006115	12.64	4.33E-34
WSR	-0.6452	1.538	13.26	4.17E-37
CO2	7.82E-04	0.001133	21.84	9.66E-87
DOCi	0.02681	0.03879	21.86	6.88E-87
NOx	0.07993	0.6590	3.835	1.33E-04
APPn	-0.06175	0.1445	13.51	2.56E-38
SLn	-0.09674	0.2574	11.88	1.48E-30
TOn	-0.04678	0.1557	9.499	1.51E-20
TOFL	-234.3	789.3	9.388	3.99E-20
TOGW	4004	5744	22.04	4.60E-88

The same experiments were repeated for the five-year configuration. Recall that the relative importance variation for this vehicle showed that less of the decision space was constrained, opening up MCDM possibilities. The results of the deterministic studies are given in Table 37.

Table 37: Deterministic Results for 5-Year Configuration

Value	Min. TOGW	Min. DOCi	Even CP	Dynamic CP
AITEK	2.200	2.200	2.200	2.200
FPR	1.559	1.558	1.466	1.472
HPCPR	22.51	21.76	23.73	25.00
LPCPR	1.600	1.600	1.300	1.300
SWEEP	27.59	27.44	29.19	28.77
TWR	0.2531	0.2532	0.2710	0.2710
WSR	135.0	135.0	135.0	135.0
CO2	0.1214	0.1215	0.1267	0.1260
DOCi	4.098	4.097	4.325	4.308
NOx	40.75	39.30	31.33	33.09
APPn	96.24	96.20	94.99	95.10
SLn	94.31	94.31	93.49	93.49
TOn	91.97	91.97	90.92	91.01
TOFL	9534	9534	7789	7751
TOGW	610020	610130	639500	636600

These deterministic results are believed to be the global minimums. In most cases, one or two other local minima were also discovered. It is interesting to note that the CP results for the SOA configuration did not appear to have local minima during the execution of the experiments. This is likely because the decision space was mostly constrained, eliminating portions that would otherwise contain local minima.

Again, the single-objective solutions are very similar. The vector angle between the DOCi and TOGW responses was now calculated to be approximately nine degrees, again illustrating that these two objectives are very similar. The CP results start to differ more significantly from the control experiments. One change is to FPR, fan pressure ratio. The single-objective results appear to be pushing FPR to its upper limit, likely because of the positive effect this has on overall pressure ratio (OPR). An increase in OPR allows for more efficient combustion. Also, increasing FPR increases the thrust available from the bypass duct, which can increase propulsive efficiency. Both of these result in lowering the fuel

required and therefore TOGW and DOCi. However, the CP formulation pushes FPR near the lower limit of the design space. This is likely because a large source of noise in turbofan engines is the fan. A higher FPR indicates a more powerful fan, which is in turn noisier. The CP solutions also push the pressure ratio of the low pressure compressor (LPCPR) to the lower limit while the single-objective solutions keep this at its high value. Overall, the difference in OPR (the product of FPR, HPCPR, and LPCPR) between the single-objective and compromise solutions is approximately ten, a relatively large difference. This has the effect of increasing carbon dioxide emissions because more fuel is required; however, this further reduces turbomachinery noise and allows for reductions in NO_x emissions. In total, the CP solutions seem to be living up to their name - compromise. A better comparison between these two solutions can be seen by viewing the results of the probabilistic analyses, given in Table 38. The mean shift is analyzed in Table 39.

Table 38: Probabilistic Results for 5-Year Configuration

	Standard CP			**Dynamic CP**		
Value	μ	σ	σ %	μ	σ	σ %
AITEK	2.200	1.73E-14	0.00%	2.200	1.73E-14	0.00%
FPR	1.470	0.009553	0.65%	1.472	0.004094	0.28%
HPCPR	23.67	0.9961	4.21%	24.91	0.2038	0.82%
LPCPR	1.300	2.44E-14	0.00%	1.300	2.44E-14	0.00%
SWEEP	29.31	0.3568	1.22%	28.81	0.2170	0.75%
TWR	0.2692	0.006495	2.41%	0.2707	0.001236	0.46%
WSR	134.7	0.7178	0.53%	135.0	4.32E-04	0.00%
CO2	0.1265	9.40E-04	0.74%	0.1260	2.00E-04	0.16%
DOCi	4.314	0.03804	0.88%	4.307	0.008215	0.19%
NOx	31.42	1.110	3.53%	32.99	0.2464	0.75%
APPn	95.02	0.1170	0.12%	95.09	0.05614	0.06%
SLn	93.47	0.1927	0.21%	93.49	0.09459	0.10%
TOn	90.94	0.1505	0.17%	91.00	0.07361	0.08%
TOFL	8010	753.2	9.40%	7785	141.4	1.82%
TOGW	638250	4912	0.77%	636550	1073	0.17%

The probabilistic deviation values for the dynamic CP experiments for the 5-year configuration appear to increase slightly from those seen from the SOA configuration. This could be a problem of the optimizer selecting local minima in the probabilistic studies,

Table 39: Mean Shift Analysis for 5-Year Configuration

Value	μ(sCP − dCP)	σ(sCP − dCP)	***t*-Statistic**	***p*-Value**
AITEK	0	0	-	-
FPR	-0.002816	0.01024	8.692	1.44E-17
HPCPR	-1.247	1.012	38.95	1.34E-202
LPCPR	0	0	-	-
SWEEP	0.5021	0.4244	37.42	2.93E-192
TWR	-0.001512	0.006600	7.244	8.69E-13
WSR	-0.2866	0.7178	12.62	5.27E-34
CO2	4.81E-04	9.58E-04	15.86	1.06E-50
DOCi	0.007307	0.03872	5.968	3.33E-09
NOx	-1.567	1.139	43.49	1.11E-232
APPn	-0.07141	0.1282	17.62	1.08E-60
SLn	-0.01882	0.2103	2.829	0.004760
TOn	-0.06618	0.1652	12.67	3.19E-34
TOFL	225.0	764.9	9.301	8.51E-20
TOGW	1704	5004	10.77	1.16E-25

since these were largely automated and started from the deterministic compromise solution. Again, AITEK and LPCPR do not vary at all for both probabilistic formulations, though otherwise all variables and responses are different with statistical significance. The mean shift analysis shows that the gross weight, field length, CO_2 emissions, and operating cost are better for the dynamic CP case. This comes at the expense of the noise and NO_x requirements, though there is little impact on the noise. The field length and gross weight responses exhibit large changes, which begins to illustrate the strength of the interdependent corrections to the relative importance model.

The final set of experiments were conducted on the 15-year configuration. This represented the most advanced technology set and had the best chance of approaching the goals of the VISTA program. As was indicated in Figure 51 earlier, the decision space for this final configuration is virtually unconstrained. Table 40 gives the deterministic results of this configuration.

Now, the single-objective and multiple objective results appear to have diverged significantly. This is likely a result of the decision space being mostly free of constraints. The only exception is takeoff field length, and once again the single-objective solutions are riding that particular constraint. The biggest difference between the single- and multiple-objective

Table 40: Deterministic Results for 15-Year Configuration

Value	Min. TOGW	Min. DOCi	Even CP	Dynamic CP
AITEK	2.200	2.200	2.200	2.200
FPR	1.560	1.560	1.464	1.460
HPCPR	21.23	21.32	20.00	20.00
LPCPR	1.600	1.600	1.600	1.600
SWEEP	26.53	26.00	28.01	27.67
TWR	0.2532	0.2544	0.2755	0.2741
WSR	133.2	135.0	135.0	132.9
CO2	0.1079	0.1081	0.1117	0.1123
DOCi	3.642	3.640	3.799	3.814
NOx	38.14	38.31	31.80	31.63
APPn	95.20	95.21	94.13	94.08
SLn	92.48	92.51	91.44	91.32
TOn	90.09	90.11	88.86	88.79
TOFL	9534	9534	7561	7529
TOGW	535840	535940	557700	559700

solutions are the FPR values at the opposite ends of the design space limits. Also, the high pressure compressor ratio for all aircraft has actually decreased, now at the lower limit for the CP cases, though the low pressure compressor ratio is at its high limit. This is likely indicative of an increased emphasis to reduce turbomachinery and jet noise, at the cost of increased carbon dioxide emissions. One other effect this has is reducing the mean combustor temperature. All of these designs have a fixed turbine inlet temperature; however, by reducing the compressor outlet temperature (via lower OPR) the change in temperature must occur faster, possibly allowing for less dissociation of diatomic nitrogen. This would have the effect of reducing the NO_x emissions. However, this temperature jump relates directly to the amount of energy, and therefore fuel, added to the combustor. This, combined with the lower combustion efficiency due to the lower OPR, results in a greater fuel burn, which increases carbon dioxide emissions and operating costs. However, the one-for-one change between the single-objective and CP solutions between these metrics likely indicates why the compromise solutions elected for a lower OPR. The CP solutions do not appear to be very different from each other; this analysis is expanded in the probabilistic experiments. The results of these are given in Table 41, with the mean shift analyzed in Table 42.

The standard CP formulation appears to have a large spread once again, though now

Table 41: Probabilistic Results for 15-Year Configuration

	Standard CP			Dynamic CP		
Value	μ	σ	σ %	μ	σ	σ %
AITEK	2.200	1.73E-14	0.00%	2.200	1.73E-14	0.00%
FPR	1.467	0.007279	0.50%	1.460	5.39E-05	0.00%
HPCPR	20.09	0.2491	1.24%	20.02	0.1022	0.51%
LPCPR	1.589	0.02876	1.81%	1.600	8.88E-05	0.01%
SWEEP	28.08	0.4199	1.50%	27.61	0.6455	2.34%
TWR	0.2740	0.005573	2.03%	0.2738	0.001768	0.65%
WSR	134.6	0.8122	0.60%	132.8	1.699	1.28%
CO2	0.1117	5.48E-04	0.49%	0.1124	2.74E-04	0.24%
DOCi	3.794	0.02299	0.61%	3.814	0.007377	0.19%
NOx	31.85	0.7099	2.23%	31.65	0.1633	0.52%
APPn	94.16	0.07793	0.08%	94.08	0.009794	0.01%
SLn	91.48	0.1558	0.17%	91.32	0.02987	0.03%
TOn	88.89	0.1156	0.13%	88.79	0.02706	0.03%
TOFL	7713	607.7	7.88%	7561	122.8	1.62%
TOGW	557170	2962	0.53%	559850	984.7	0.18%

Table 42: Mean Shift Analysis for 15-Year Configuration

Value	$\mu(\text{sCP} - \text{dCP})$	$\sigma(\text{sCP} - \text{dCP})$	***t*-Statistic**	***p*-Value**
AITEK	0	0	-	-
FPR	0.006454	0.007281	28.03	4.84E-128
HPCPR	0.07111	0.2704	8.315	2.98E-16
LPCPR	-0.01058	0.02876	11.63	2.13E-29
SWEEP	0.4720	0.7699	19.39	2.62E-71
TWR	2.10E-04	0.005812	1.143	0.2532
WSR	1.824	1.894	30.47	1.07E-144
CO2	-7.40E-04	6.04E-04	38.77	2.22E-201
DOCi	-0.01982	0.02413	25.98	4.40E-114
NOx	0.2023	0.7331	8.727	1.08E-17
APPn	0.07625	0.07870	30.64	6.86E-146
SLn	0.1638	0.1590	32.57	3.89E-159
TOn	0.1011	0.1191	26.84	6.55E-120
TOFL	151.5	620.9	7.715	2.92E-14
TOGW	-2685	3108	27.32	3.59E-123

the dynamic formulation too exhibits a spread though to a smaller degree. At first, this may seem to be due to problems with local minima. However, this is unlikely, as the deterministic experiments found that the local minima were usually due to choice of starting point for LPCPR. However, the values for LPCPR are near the extreme with a very small standard deviation for both cases.

The mean shift analysis indicates few changes other than those experienced in the SOA and 5-year models. The only value that has a statistically insignificant mean shift is the TWR value with a p-value of 0.2532. However, all of the other distributions appear to have different means with large statistical significance, so it is most likely that the two methods produce significantly different results.

Overall, the results are promising for the two-part relative importance model. There are some issues with the modeling that could be remedied in subsequent iterations. Namely, there may be too many design variables related to pressure ratio that cause local minima or otherwise cause the optimizer to exit early. However, the contribution of all three components is important to noise characteristics, as well as other technology models such as highly loaded stages. A solution for this might be to have a design variable for controlling OPR, HPCPR, and LPCPR, with FPR calculated from the appropriate quotient. This would allow for modeling of the appropriate technology impact while giving the optimizer direct control over total pressure ratio. Also, it may be desirable to grant control of turbine inlet temperature to the optimizer so that it can reduce this value as needed. Certainly, turbine inlet temperature is a technology variable with an upper limit, but there are beneficial reasons for keeping it lower; namely, for NO_x emissions. This extra control may help the otherwise adverse relationship between NO_x and CO_2 (and DOCi). Finally, the AITEK variable seems to have no effect and is likely more of a technology parameter than a shape factor; hence, the next design iteration would likely eliminate this value from the design space.

7.6 Multidimensional Visualization

The design variable distributions for the probabilistic MCDM cases can be compared via simple n-D scatterplots. As before, it is difficult to view many dimensions, especially on the small format of the paper in this document. However, the design variables can still be viewed in their native form. Of the seven design variables, only six ever varied at all, so AITEK will be dropped from the visualization as its results will be uninformative. Figures 52 through 54 display these plots on the pages that follow. The unmodified CP results are given in blue, and the dynamic CP results are overlayed in red.

The progression viewed from these three figures is interesting. The results for the first two configurations show that the full dynamic relative importance model chooses from a much tighter cluster of inputs than the unmodified model. Further, the LPCPR choices appear to be invariant with changes in relative importance for both approaches in the first two configurations. The last configuration shows significant variation in choice of design variables, especially for TWR, SWEEP, and WSR. Indeed, the variation appears to actually be larger for the dynamic model with respect to WSR and SWEEP. This verifies the results from Table 41, which indicated the standard deviation of these variables was greater for the dynamic model.

The reasons for this variation can be manyfold. It does appear that there is a tradeoff occurring due to change in relative importance for WSR and SWEEP, (wing loading and wing sweep). This may be a manifestation of the algorithm attempting to maintain a balance of takeoff and cruise performance. Generally, lower wing loadings and wing sweep decreases takeoff field length but also decreases cruise efficiency, which will manifest as increases in DOCi and emissions. The negative correlation seen between SWEEP and WSR likely indicates that the algorithm is attempting to balance the aforementioned requirements by changing these design variables.

The overall increase in design variable spread is likely because the 15-year configuration represents a mostly unconstrained decision space that has yet to reach its threshold values. Once more thresholds are exceeded, the optimization starts to appear as a single-objective approach, whereas a mostly constrained space also limits the choices available. These

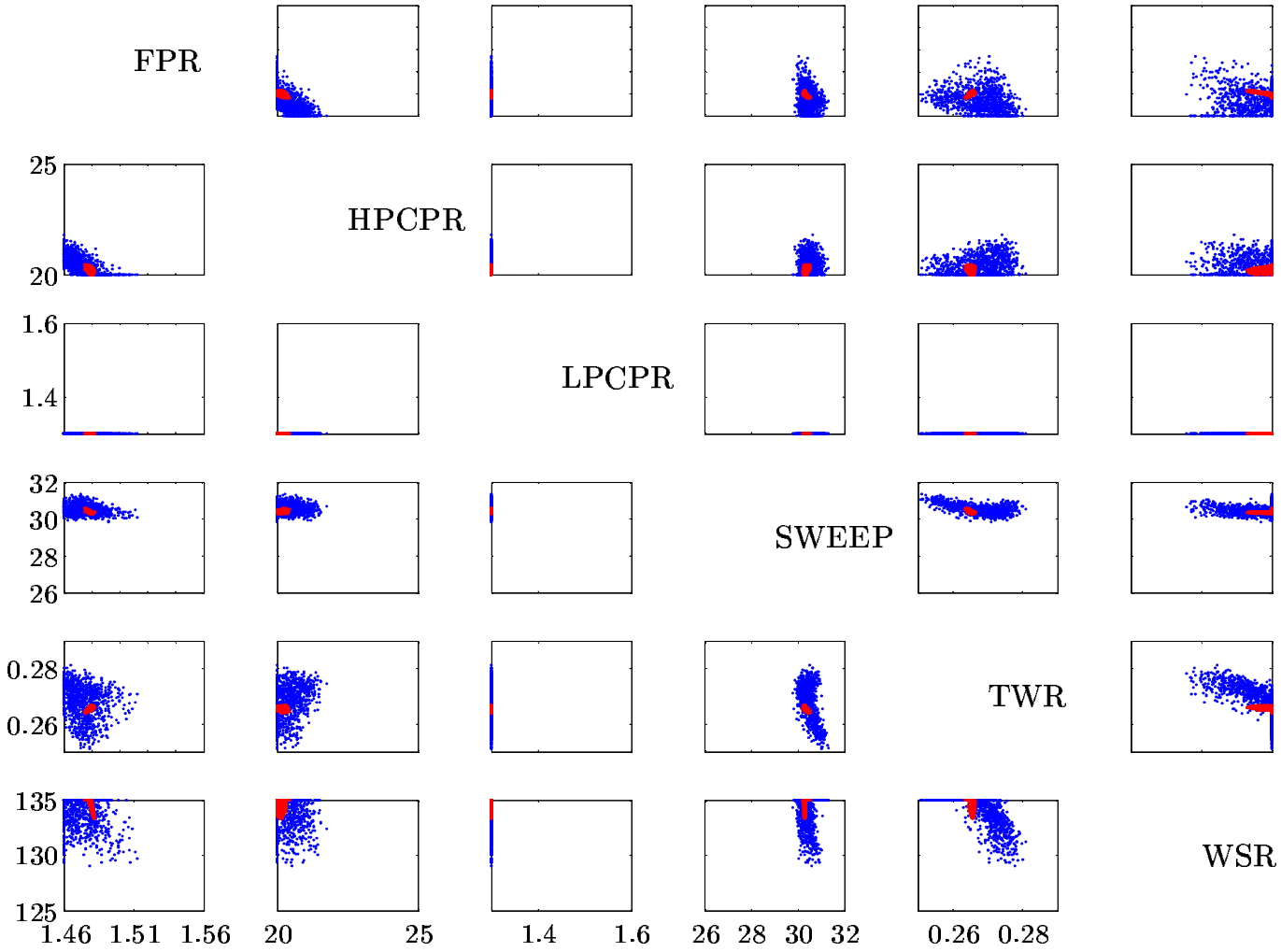

Figure 52: Design Variable Scatterplots for SOA Configuration (Dynamic Results in Red)

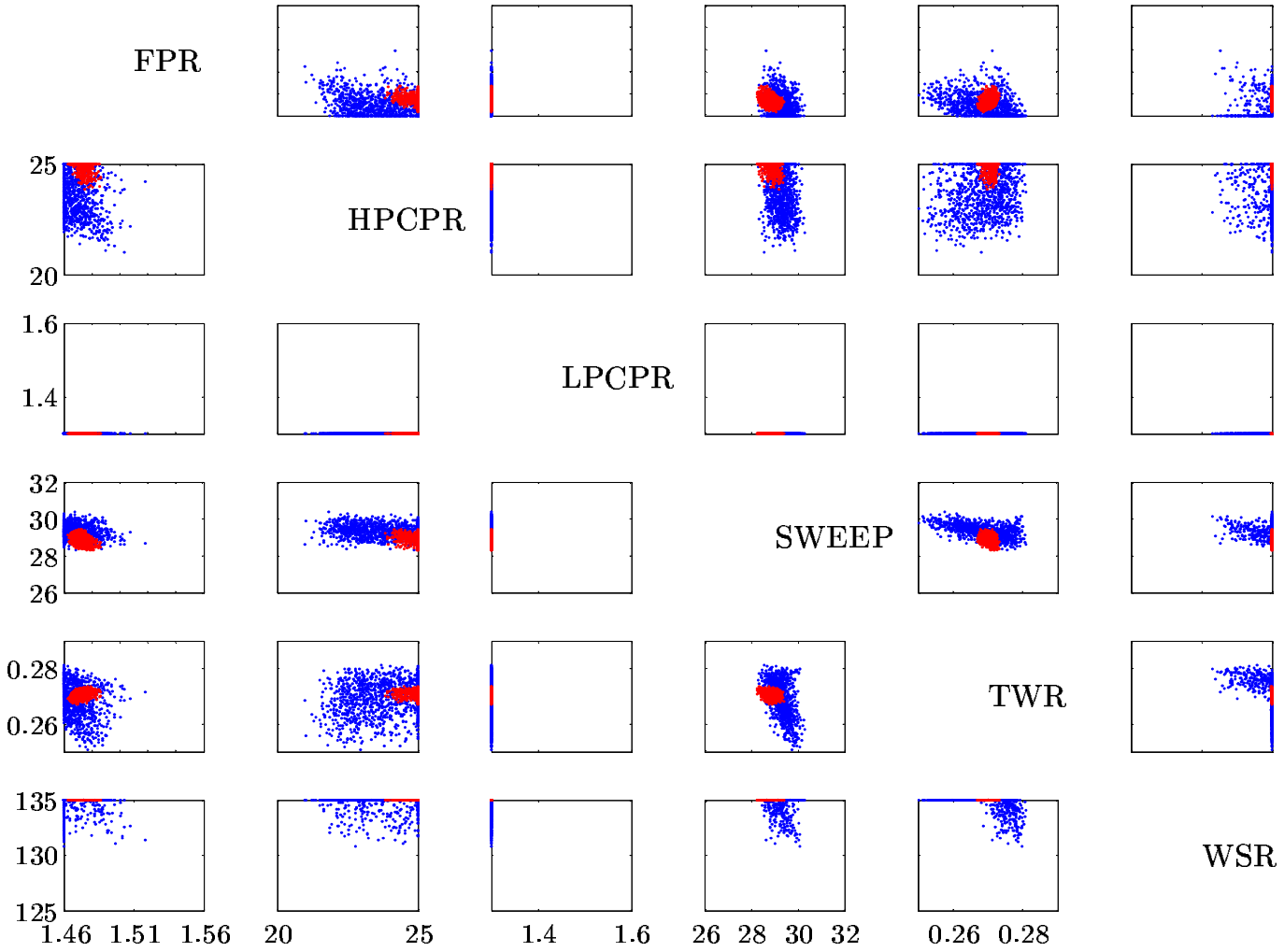

Figure 53: Design Variable Scatterplots for 5-Year Configuration (Dynamic Results in Red)

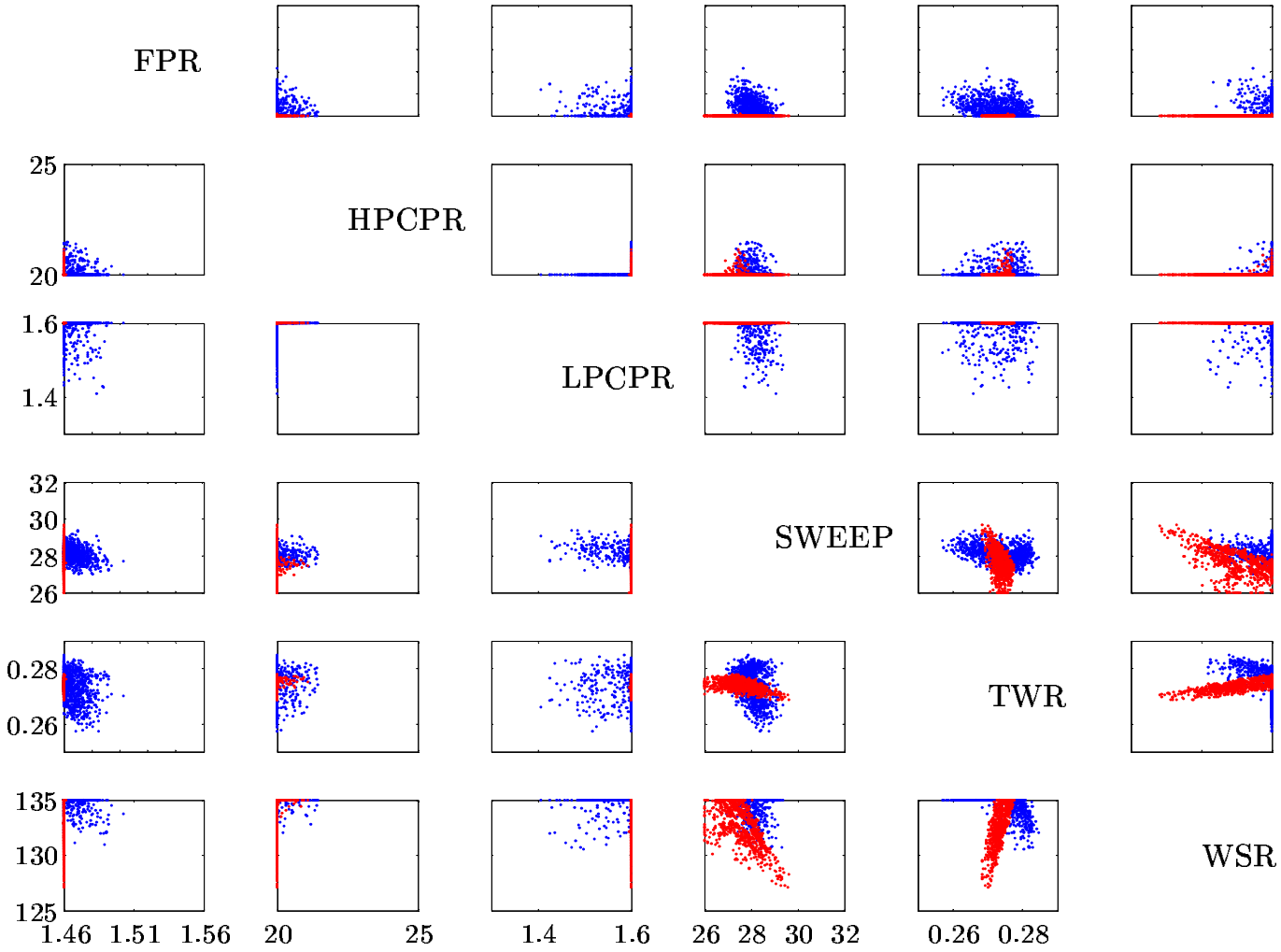

Figure 54: Design Variable Scatterplots for 15-Year Configuration (Dynamic Results in Red)

results indicate some of the strengths of the relative importance scheme proposed throughout this document: it appears as constrained optimization for constrained decision spaces and transitions to single-objective optimization as thresholds are met. During the transition, it simply appears as an interdependence-balanced set of MCDM tradeoffs.

7.6.1 Requirements Decomposition

More effective multidimensional visualization of the requirements is possible through singular value decomposition of the response surface coefficients. The procedure given in Algorithm 4 from the previous chapter was used to create the datasets necessary for decomposition-based visualization of the probabilistic experiments. One of the first steps of this procedure is to enumerate the singular values for the requirements and determine the cutoff point, generally given as where the singular value drops by about an order of magnitude from the highest singular value. Table 43 lists the singular values found by decomposition for each of the three configurations.

Table 43: Singular Values of RSE Coefficients for Three Transport Technology Configurations

SOA	5-Year	15-Year
1.206	1.165	1.214
0.9618	0.9441	0.8695
0.5455	0.5063	0.5221
0.4253	0.4717	0.5102
0.1300	0.1475	0.1848
0.08361	0.06610	0.09180
0.05047	0.05944	0.06251
0.02864	0.02382	0.02278

These singular values are similar across all three configurations. The breakpoint seems to be at the fifth singular value, though an argument could be made for only four characteristic tradeoffs. However, it does not hurt to allow for an additional singular value, so this study used $r = 5$ characteristics. This allowed for creation of the decomposed datasets for viewing the probabilistic response data. These are presented in Figures 55 through 57 on the pages that follow. The unmodified CP results are given with the blue points, with the dynamic results denoted by red points.

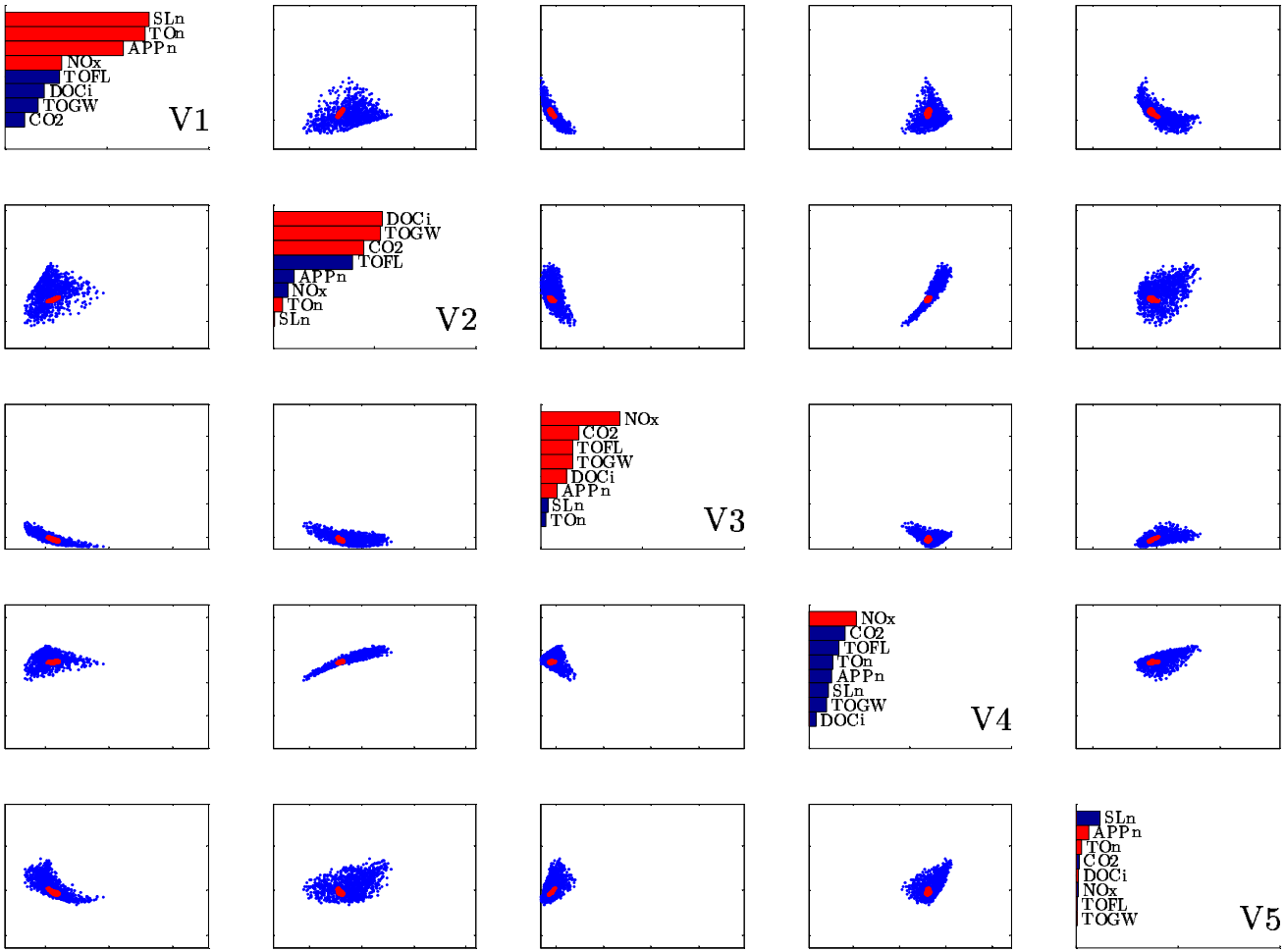

Figure 55: Characteristic Tradeoff Visualization for SOA Configuration (Dynamic Results in Red)

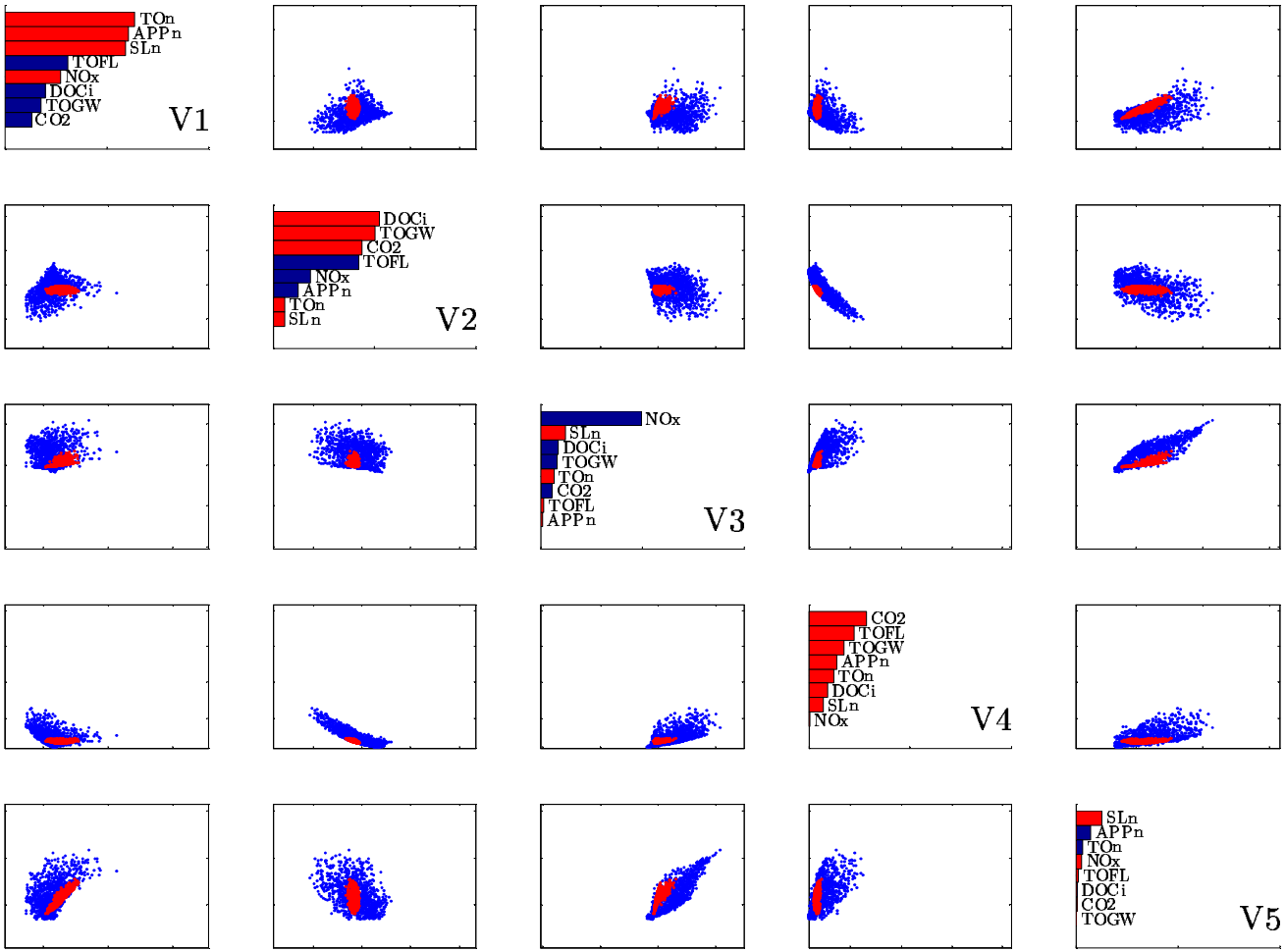

Figure 56: Characteristic Tradeoff Visualization for 5-Year Configuration (Dynamic Results in Red)

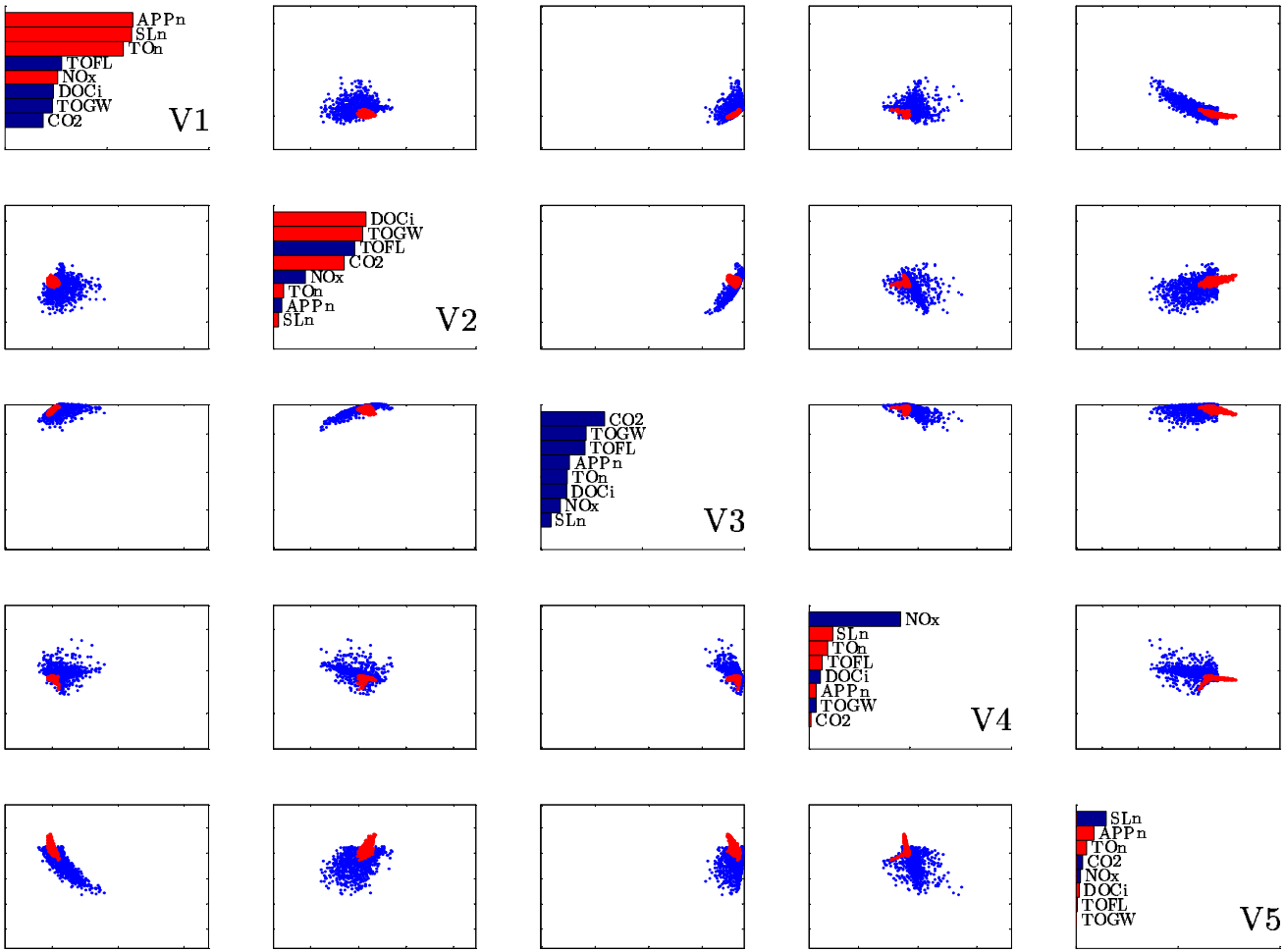

Figure 57: Characteristic Tradeoff Visualization for 15-Year Configuration (Dynamic Results in Red)

One of the most noticeable features of these plots is that all three indicate that the dynamic results (red points) are all more tightly clustered than the blue points. This is mostly in agreement with the distribution of the inputs seen earlier. However, as noted in the discussion regarding Figure 54, some of the inputs varied greatly. However, this appears to have been balanced enough, because the responses given in Figure 57 indicate that the resulting requirement distribution is far less variable, at least through the five most important characteristic tradeoffs.

Another notable feature is that the characteristics themselves do not line up across each configuration, as seen in the contribution plots along the diagonals. This is because the systems of equations representative of each configuration are different, and the algorithm used in the SVD execution depends on a litany of small factors. It is important to note that the characteristics may even switch sign by simply reordering the equations. However, the user can be sure that the characteristic requirements are linearly independent, and it appears as though the algorithm picks the first few characteristics to be similar regardless of the configuration. This is the power of such a visualization technique.

The differences in the characteristics are likely due to the slight differences in the response coefficients for each configuration. However, inspection of the contribution plots for the first two characteristics shows similarities across all three configurations. The first characteristic of all three negatively impacts the noise and NO_x requirements, while having a lessor but positive impact on the others. The subsequent scatterplot distributions show that this characteristic is consequently towards the lower portion of its range. The second characteristic also has the same basic contributions across all three configurations, this time as a strong negative impact on TOGW, DOCi, and CO_2 emissions, while having a strong positive impact on TOFL and a moderate positive impact on NO_x emissions. The optimizer seems to pick mid-lower values along this characteristic, likely because of its positive impact on field length. Note that the 15-year configuration results are more in the middle of the second characteristic, but that is likely due to a reduced negative impact of CO_2 along this dimension for this high-technology configuration.

Beyond the second characteristic the three configurations begin to vary. Perhaps some

of the most interesting results appear in the 15-year configuration plots. The third characteristic is entirely beneficial across the spread of requirements, and as such is near its maximum value in all the scatterplots. The fact that it is not at its maximum value indicates that there is a nonlinear interaction present with other dimensions; this is likely for all dimensions. As noted earlier, the characteristics are only *linearly* independent. The opposite behavior is exhibited by the SOA results along the third characteristic, as almost all metrics are in opposition to improvement in the $V3$ direction. Also, the fourth characteristic of the 15-year configuration has a strong positive impact on the NO_x emissions requirement while having little other impacts, positive or negative. This helps give some meaning to the fourth characteristic, and the choice of values selected by the optimizer.

In all, the decomposition of the transport requirements provides a compact multidimensional visualization tool while simultaneously giving some meaning to the tradeoffs taking place within the decision making routine. The results indicate that the dynamic model is working to keep the decision metrics within a relatively tight band despite large changes in the relative importance of the metrics. This points towards a solution that is robust with respect to changes in the individual importance of the requirements.

7.7 Goal Evaluation

The VISTA subsonic transport technology selection problem identified a number of metrics and associated goals for the evaluation of technology programs. Table 26 gave the original VISTA goals, which were presented in modified form in Table 28. The final evaluation of the VISTA goals and vehicles resulting from the dynamic CP deterministic experiments are given in Table 44 below.

In all, it appears that the projected technology programs will fall short of the program goals, though some of the goals are exceeded for the five-year model. The VISTA goals were created with alternative vehicle concepts in mind, not the simple wing-forward tail-aft tubular fuselage transport used in these studies. These results show that even advanced technologies will yield performance short of program goals for the design space and conventional design concept chosen. Either the goals must be compromised or the aircraft

Table 44: Comparison of Dynamic CP Results to QuEST Goals

Metric	SOA	5-Year	5-Year Goal	15-Year	15-Year Goal
CO2	0.1356	0.1260	0.1169	0.1123	0.0719
DOCi	4.348	4.308	2.800	3.814	2.100
NOx	53.79	33.09	50.00	31.63	22.50
APPn	98.31	95.10	88.31	94.08	78.31
SLn	94.93	93.49	84.93	91.32	74.93
TOn	91.97	91.01	81.97	88.79	71.97
TOFL	9534	7751	$<$ SOA	7529	$<$ SOA
TOGW	659025	636600	515000	559700	374000

configuration must be modified to meet the 5- and 15-year targets. Hence, these technologies must be developed concurrently with advanced aircraft concepts better capable of meeting future needs.

That said, these program goals are simply that: targets to be used in technology evaluation. Perhaps the decision-making strategy outlined by this research could be applied deterministically to more advanced aircraft concepts with forecast technology settings for better enumeration of the 15-year goals. This could help create a better balanced set of program targets, corrected to exploit the contrast and interdependence found amongst the metrics while targeting the key tradeoffs necessary to meet the needs of the future.

CHAPTER VIII

CONCLUSIONS AND RECOMMENDATIONS

Systems design is a necessarily complex and difficult undertaking, but a logical, scientific approach combined with expert knowledge can provide the means to solve all but the most difficult problems. This document has presented another piece of the systems engineering puzzle as it relates to perhaps the most difficult of problems: decision making for a large system in the presence of uncertainty. The techniques and strategies presented herein represent a systematic approach for large-scale problem solving that takes advantage of information already available to the systems designer. The only additional piece of information required by the knowledgeable expert is enumeration of threshold values – points for each metric beyond which further improvement is unimportant at the expense of the other requirements. It can also be important to quantify a range of user-specified relative importance as well, but the two-part relative importance scheme given by the research helps to reduce the overall variability of the solution due to changes in user preference.

8.1 Contributions to Aerospace Systems Design

This thesis identified a move from single-objective decision making toward a need for a multiple criteria formulation in aerospace systems design. This is exemplified in the modern focus on multi-mission systems and shifting paradigms for vehicle performance goals. The shift from single-objective optimization to multiple criteria decision making required a change in perspective for aerospace design. Throughout this thesis, a number of research questions and hypotheses identified the key areas necessary to enable this transition.

Question 1 asked *How do aerospace sizing and synthesis methods address multiple requirements?* A review of current approaches showed that most techniques focused on single-objective techniques and simply added the additional requirements as constraints to an optimization problem. This could quickly result in an infeasible or high-cost solution, as

no compromise is implied. Another alternative approach was to attempt to size the vehicle to a parametric requirements set, though this could be difficult for large expected changes in the requirements. This research proposed a *multipoint sizing scheme* for aerospace design, which treats the individual requirements as desired points or directions in a decision space. This required an internally unconstrained multiple criteria decision making framework capable of implicit tradeoffs as proposed in **Hypothesis 1**.

Question 2 asked *Can modern systems design methods adequately deal with changing requirements?* Most of the single-objective sizing techniques are ill-prepared to deal with changing requirements. The move towards a multiple criteria formulation allows for two ways to handle this as outlined by **Hypothesis 2**. First, the algorithm identifies the direction of improvement for each metric and conducts a series of implicit tradeoffs to push the solution towards a compromise solution within the decision space. The uncertainty can be mapped to probabilistic choices for the relative importance of each metric throughout this tradeoff process.

Question 3 asked *Is there a decision making formulation that is well-suited to systems design with uncertain requirements?* A review of modern decision making techniques found that various frameworks use different techniques in ranking solutions and evaluating compromise. **Hypothesis 3** proposed that aerospace decision making requires an adaptable formulation capable of handling non-convex compromise that would always choose a non-dominated solution. It also proposed that the compromise solution that was most invariant with respect to change in the relative importance of the metrics would be robust to changes in the requirements.

Question 4 asked *Is there a benefit to finding nondominated solutions in large-scale systems design?* Review of the literature lead to **Hypothesis 4**, stating that every solution in the decision becomes nondominated as the number of criteria increase. Furthermore, the effort required to resolve the nondominated solutions increases substantially in difficulty for a relatively small reduction in the decision space as more metrics are considered. This does require that the decision making algorithm always choose a nondominated solution, which happens to be one of the statements of the previous hypothesis.

The initial results of the proposed formulation were less than promising, resulting in some revision based on some follow-up observations of a few simple experiments. **Question 5** asked *Is there a simple utility approximation that can be easily implemented within classic MCDM techniques?* This was primarily due to the observation that the assumption of monotonically increasing utility appeared to be poor for large-scale systems design problems in the initial experiments. **Hypothesis 5** proposed a two-part relative importance model with a monotonic portion and a dynamic portion to update the utility based on local changes in the metric. The monotonic portion was found to be most effective when computations were made based on the diversity of the decision space and the interdependence of the metrics, along with user-specified importance. The dynamic value could be based on a simple utility model with two inflection points: the constraint, defined as the minimum acceptable performance; and the threshold, defined as a point of diminishing returns.

Question 6 related to the composition of the decision space, and asked *Is it beneficial to identify an independent subset of characteristic tradeoffs from the original requirements?* **Hypothesis 6** proposed that a linearly independent subset of the decision space could be created from the original requirements that would enable more compact visualization of tradeoffs. This resulted in *decomposition-based visualization* of the original requirements by viewing results in scatterplot matrix form along the *characteristic tradeoffs*. The contribution of each characteristic to the original requirements could be viewed in a *degree of conflict plot*.

These hypotheses were tested with a variety of experiments dubbed **Tasks**. These experiments were tested on two media: an simple example problem and a larger implementation problem. The results shaped the development of the decision-making strategy and helped to support the various hypotheses. Some of the lessons from these experiments are elaborated upon below.

8.2 Lessons from Implementation

Two example problems were used throughout the text, and both taught valuable lessons. The beam design problem provided a simple model with an easily understandable decision space that proved to be invaluable in the development of advanced decision making strategies. This problem was developed with the hope of identifying the weaknesses of current monotonic MCDM methods (both deterministic and probabilistic) and, if possible, to remedy these weaknesses with conceptually simple strategies. To this end, the beam design problem was very successful, leading to the development of the two-part relative importance model, consisting of a monotonic (static) value and a dynamic value. The static value was further based off of three contributors: user preference, entropy, and interdependence on other metrics. The dynamic value changed the overall relative importance locally by using a model based on two intuitive inflection points. Uncertainty in the requirements was mapped to uncertainty in the user-specified relative importance and propagated to the decision space via Monte Carlo simulation. Finally, the beam problem introduced decomposition methods, allowing for viewing of multidimensional data in a more compact form.

The formulation resulting from experiments on the beam design problem represented a vast improvement over current MCDM formulations. These experiments demonstrated a large reduction in compromise solution variation due to uncertainty in user preferences, namely due to the two-part relative importance model. Furthermore, they served as a prototype for development of the decomposition-based visualization interface.

However, the beam design problem was a contrived example created expressly to demonstrate the weaknesses of current MCDM methods, so it was necessary to apply the final strategy to a practical aerospace systems design problem. This problem was the long-range transport technology impact study. The decision-making strategy was not applied to the actual selection of technologies; rather, it was applied to three configurations representative of the state-of-the-art, a transport five years from now with a host of technologies, and a transport 15 years in the future with even greater technical development. This allowed for analysis of what are currently uncertain requirements within this technology selection problem. The end results of this analysis showed that a conventional aircraft concept cannot

meet the aggressive VISTA goals for large subsonic transports, even with a suite of new technologies. This points towards a need for advanced aircraft concepts with unconventional configurations to be developed concurrently with component-level technologies.

The probabilistic anlayses further solidified the strengths of the advanced decision making strategies identified by this thesis. The probabilistic results generally resulted in much tighter solution distributions than results generated with unmodified MCDM. The algorithms seemed much more proficient at logically exploiting the underlying features tradeoffs in the face of interdependence. It is interesting to note that the results from the unmodified MCDM form on the transport problem initially appeared adequate on their own. However, these results showed a marked disadvantage when compared with results from the advanced formulation in terms of repeatability in the face of uncertainty and exploitation of interdependence.

8.3 Improvements

The techniques presented in this document rely on a few basic algorithms and philosophies related to decision making. The new strategies were developed to be accurate and flexible without being too cumbersome to program and test. That said, there are a number of small improvements that could be made beyond the prototypes seen throughout this thesis.

The threshold-modified entropy algorithm is based on a discrete formulation given by Zeleny that was originally designed to be used with a predefined pool of concepts. This formulation is modified to normalize concepts to the Euclidean norm and to represent the continuous decision space with a random discrete population. It is likely possible to move this to a fully continuous formulation that integrates over the decision space. Such a large integral would be difficult to analytically evaluate, but could possibly be found through Monte Carlo integration [Press et al., 1997]. Also, the random population used for the decision space currently follows from a simple random number generator, prone to clustering and voids. One way to avoid this is to use quasirandom numbers, which are actually sequences designed to fill voids within a space while refraining from clustering. As such, these are often called low-discrepancy sequences. One sequence used to great effect

is the Sobol' sequence modified with Gray coding [Bratley and Fox, 1988; Joe and Kuo, 2003]. The use of such a sequence could also help in the quantification of the entropy-based importance. The combination of Monte Carlo integration of a continuous entropy function with a Sobol' sequence may yield much less error in the entropy-based importance than seen in the current formulation.

The implicit decision making routine used in this research was compromise programming, a technique that creates a composite objective function to minimize distance to the single-dimensional "best" solutions in the decision space. This method is attractive because it allows for tailoring to non-convex compromise solutions and is easily adaptable to the two-part relative importance model. However, the optimization routine used in this document, while sophisticated, was gradient-based and therefore capable of terminating at local minima. Larger problems will likely require the use of global optimization techniques such as genetic algorithms or simulated annealing to find the global minimum of the composite objective function. This can be especially important for a probabilistic study, as this requires thousands of optimization runs that would be difficult to individually monitor to ensure a global minimum was found.

The interdependence corrections to the static relative importance were based on the vector angles between the response surface coefficients. This *requires* that response surfaces be created for the problem, and further requires that they are of the exact same functional form. This is very limiting, as often a better fit can be obtained with variable transformation or by addition of one or two terms to a particular model. This retains the computational speed benefits of response surfaces but would create misleading vector angles for interdependence analysis. A more generalized formulation would allow for greater modeling flexibility. The interdependence model could be modified to find angles or other corrections based on statistical correlation coefficients or other global values of the decision space.

8.4 New Research Paths

Some of the concepts outlined in this document may open up exciting new research paths in decision making and visualization. The dynamic contribution from the two-part relative

importance model followed from a deliberately simplified utility model. The current form forces each requirement to have two inflection points and a specific functional mapping in between. This research deliberately avoided involving multiple attribute utility theory as quantification of individual utility functions for each metric is a cumbersome process. However, it may be possible to classify metrics into a taxonomy of utility approximations. This has the possibility of providing even more accurate and consistent tradeoffs with the two-part relative importance model.

The probabilistic analyses presented in this thesis stopped short of suggesting a robust solution with respect to changes in the requirements. Instead, it was used to show that the strategies developed herein are capable of reducing variation due to uncertain requirements. Combining the results of this analysis with a technique such as Joint Probabilistic Decision Making [Bandte, 2000] may allow for selection of the best design in the face of uncertainty. Sensitivity analysis could show which requirements have the greatest impact on the solution, and which appear to have little or no impact. The same could also show which design variables are critical to the decision making framework, as was alluded to during the analysis of the probabilistic results for the transport design problem.

Decomposition of the decision space was used to create compact visualization environments for large problems. However, the resulting "characteristic tradeoffs" may greatly simplify large-scale decision making by finding nominal values along the characteristics. The author briefly tried this path but ran into difficulty with consistently specifying any nominal values for a generalized decision space. Furthermore, it may be beneficial to attempt to label these characteristics such that a decision maker has a greater understanding of the tradeoffs. Some headway was made down this path using the degree of conflict plots, but this is likely just the surface of what could become *decomposition-based decision making*.

8.5 Caveat Cursor

There is a very powerful trajectory optimization code that was developed over the years called OTIS, for Optimal Trajectories by Implicit Simulation [Vlases et al., 1990]. This program is capable of incredibly detailed, accurate, and of course, optimal trajectories for

a wide variety of systems. The output of this program always starts with the phrase, "If it's OTIS, it's optimized!" followed immediately by "(Caveat Cursor)". The OTIS documentation elaborates on this:

> One of the first things an OTIS user sees when they run the program is the phrase "Caveat Cursor." This is Latin for "let the runner beware." This phrase was added to alert the user that OTIS is a complex program. Because of its complexity, the user has to assume a lot of responsibility.

Systems engineering is a developing science. It has an exceptional variety of tools and techniques that allow a design team to do all things related to the design process: requirements analysis, functional decomposition, creation of integrated tools and subsequent processing, multi-level optimization, decision making, ranking, probabilistic analysis . . . the list goes on and on. Systems engineering is generally about bringing together people and tools to share knowledge and use it effectively as it relates to complex systems. What could possibly go wrong?

This thesis begins with a statement written long ago by Arthur Mellen Wellington regarding the nature of engineering. It seems appropriate to end it with another maxim, this time by the late "Kelly" Johnson, two-time Collier trophy winner, founder of Lockheed-Martin's Skunk Works, and designer of such groundbreaking aircraft as the P-38, F-104, U-2, and of course the SR-71 [Johnson and Smith, 1990]:

> There is a tendency today, which I hate to see, toward design by committee–reviews and recommendations, conferences and consultations, by those not directly doing the job. Nothing very stupid will result, but nothing brilliant either. And it's in the brilliant concept that a major advance is achieved.

Caveat cursor.

APPENDIX A

RESPONSE SURFACE METHODOLOGY

Response Surface Methodology (RSM) is a special class of multiple linear regression utilizing a series of designed experiments. Usually, RSM is used to model main effects (linear), higher-order effects (nonlinear), and interaction effects (nonlinear) of a response or series of responses with respect to a number of design variables. If used properly, RSM provides a rapid and accurate evaluation of a series of responses valid within the design space of interest. What follows is by no means a comprehensive review of RSM, but rather an overview of some of the pertinent areas of this subject. For a more detailed review, the reader is referred to any of the large volumes of work related to this subject [Myers and Montgomery, 1995; Box and Draper, 1987; Neter et al., 1996].

A.1 Designed Experiments

Any form of multiple linear regression requires requires a dataset to regress. This dataset can be visualized in matrix form as a series of vectors of design parameters, where each individual vector represents a unique "experiment." If $\vec{x}$ represents a column vector of design parameter setting for a particular experiment, then the experiment dataset can be represented as

$$\mathbf{X} = \begin{bmatrix} \vec{x}_1^{\mathrm{T}} \\ \vec{x}_2^{\mathrm{T}} \\ \vdots \\ \vec{x}_m^{\mathrm{T}} \end{bmatrix} \tag{70}$$

where $\mathbf{X}$ is a generalized $m \times q$ experimental array with m experiments and q design variables. These experiments are comprised from observed levels of control variables, randomly selected levels of these control variables, or levels determined from *designed* experiments.

In design, the user has control over these variables and hence does not make simple observations; rather, they input various levels and record the outputs. Doing this randomly can result in poor and unrepeatable regressions due to correlation of the input variables. Designed experiments seek to *eliminate* potential correlation of design variables while *maximizing* the predictive power of each experiment. In doing so it is possible to create repeatable, high-fidelity regressions with lower computational or experimental effort.

Experimental designs are rooted in the development of fully orthogonal experimental arrays in an effort to reduce input correlations to zero. These orthogonal designs, sometimes referred to as a Design of Experiments (DoE), are often characterized by the number of *levels* at which the experiment is run and their associated *resolution*. The levels refer to the number of settings used for each design parameter; hence, a three-level design indicates that each design parameter will be investigated at a low, midpoint, and high value. In this case, the number of experiments of a *full factorial* design is P^q, where P refers to the number of levels and q is the number of design variables. A typical three-level full factorial design in three dimensions is depicted in Figure 58.

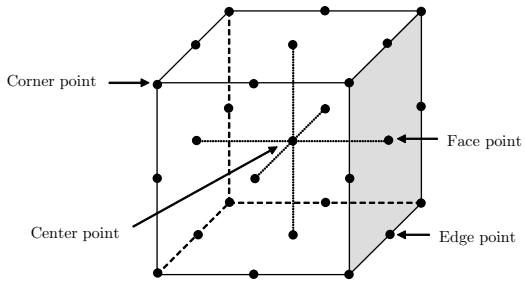

Figure 58: Notional Three-Level Full Factorial Design

The practicality of full factorial designs quickly diminishes as the number of design parameters increases, so a number of smaller designs exist at different resolutions, defined by their *confounding* structure. Simply put, confounding refers to the degree of linear dependence amongst effects within the design. If several experiments are eliminated from a full factorial design then some degree of confounding will always exist amongst effects. The goal of experimental design is to eliminate experiments (within a full factorial design) to minimize experimental or computational effort while building surrogate models, but to do

so in such a way as to minimize the confounding amongst the important effects contained within the model. Other effects that are neglected can be confounded with little loss in fidelity. Table 45 lists several levels of resolution of interest.

Table 45: Worst-Case Fractional Factorial Design Resolution [Neter et al., 1996]

Resolution	**Worst-Case Degree of Confounding**
III	Some main effects are confounded with two-factor interactions.
IV	Some main effects are confounded with three-factor interactions. Some two-factor interactions are confounded with other two-factor interactions.
V	Some main effects are confounded with four-factor interactions. Some two-factor interactions are confounded with three-factor interactions.

The resolutions defined in Table 45 indicate that a good design for a quadratic response surface model with all two-factor interactions would be resolution V or higher. Hence, for this situation one would search for a three-level, resolution V design. Several types of fractional-factorial design exist for this very purpose. One popular design for a somewhat small number of design variables ($q \leq 8$ or so) is a Central Composite Design (CCD) or Box-Behnken Design (BBD). CCD uses all of the design "corner points" along with the centers of each face of the design space known as "face points." Sometimes these face points are known as "star points" if an effort is made to place these points beyond the experimental "box" to equalize variance. The random error of the experiments is measured from several replications at the center point. BBD is similar to CCD except that fewer points are necessary; instead of using the corner points and face points this design utilizes the center points along each edge of the design space. Both of these designs are depicted in a notional three-dimensional design parameter space in Figure 59.

As the number of design variables increases, the experimental practicality of Central Composite and Box-Behnken designs diminishes. This is remedied by the availability of computer-designed fractional factorial experiments that maintain orthogonality and the desired resolution. Software packages such as JMP [SAS Institute, 2005] offer the user the ability to create custom fractional factorial designs for large numbers of design parameters.

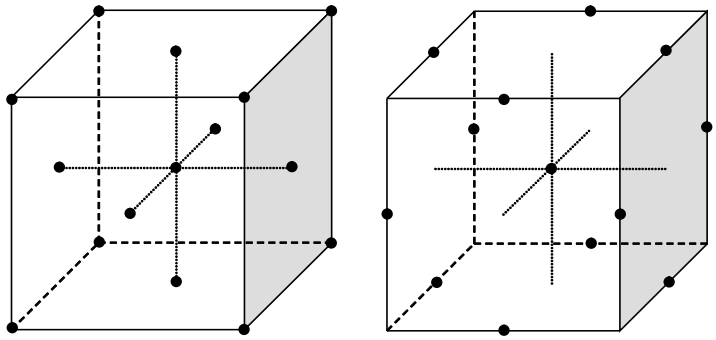

(a) Central Composite Design (b) Box-Behnken Design

Figure 59: Notional Central Composite and Box-Behnken Designs

For a comprehensive review of experimental designs, the reader is referred to the excellent work by Montgomery on the subject [Montgomery, 2001].

The computational effort to resolve very large fractional factorial experimental arrays can eventually become prohibitive. Many of these designs assume that three-factor interactions are unimportant and therefore do not attempt to resolve them. However, the probability that three-factor interactions are important increases as the number of design parameters are increased. Furthermore, three-level designs often neglect a large portion of the design space in order to properly model the extremes. A space-filling design may be more appropriate if the user is reasonably sure that the solution lies within the the design space and not at the extremes. These space-filling designs may require more experiments and may also have some correlation amongst the inputs but will generally have smaller Model Representation Error (this and other forms of error will be discussed in a subsequent section). Space-filling designs include Sphere Packing, Uniform, and Latin Hypercube methods. The advantages and disadvantages of these and other designs with respect to orthogonal arrays are discussed in greater detail by Barros [Barros et al., 2004].

A.2 Multiple Linear Regression

Linear regression refers to models that are linear in their parameters. This includes all polynomial models beyond truly "linear" models of order one. The process of multiple linear regression begins with the specification of the form of the regression equation with

respect to more than one predictor variable. In general, this equation may be given [Myers and Montgomery, 1995] as

$$y = \beta_0 + \beta_1 x_1 + \beta_2 x_2 + \cdots + \beta_q x_q + \epsilon \tag{71}$$

where y is the response being modeled, the β terms are the regression coefficients with respect to the $k = 1, 2, \ldots, q$ predictor (design) variables, and ϵ is the error between the predicted response and the actual response. The β_0 term is simply the intercept of the model. For second-order polynomial models with interaction effects, this regression equation is amended as

$$y = \beta_0 + \beta_1 x_1 + \beta_2 x_2 + \cdots + \beta_{11} x_1 x_1 + \beta_{12} x_1 x_2 + \cdots + \beta_{qq} x_q x_q + \epsilon \tag{72}$$

where the terms with two (or more) subscripts represent the regression coefficients for the higher-order terms. Note that $\beta_{ij} = \beta_{ji}$, so these symmetric terms are dropped from the model.

One of the most widely used methods to estimate the regression coefficients is through the *least-squares* approach. First, the user must make the assumption that the error is uniformly distributed with a mean of zero. Considering the predictor variable settings from the $\mathbf{X}$ matrix, the terms from equation (71) can be rewritten for each row (observation) within the $\mathbf{X}$ matrix such that

$$y_i = \beta_0 + \sum_{k=1}^{q} \beta_k x_{ik} + \epsilon_i \tag{73}$$

where y_i is the observation of the i^{th} experiment corresponding to the i^{th} row of $\mathbf{X}$ and ϵ_i is the error between the observation y_i and the value predicted solely by the regression coefficients. This can be reformulated easily for higher-order models such as that observed in equation (72).

The method of least squares chooses the β terms such that the sum of the squares of the errors ϵ_i are minimized. The least squares function is

$$L = \sum_{i=1}^{m} \epsilon_i^2 = \sum_{i=1}^{m} \left(y_i - \beta_0 - \sum_{k=1}^{q} \beta_k x_{ik} \right)^2 \tag{74}$$

where L is the least-squares estimator and all other nomenclature is as before for m observations. This minimization problem can be solved by first reformulating equation (71) into matrix form via

$$\vec{y} = \mathbf{X}\vec{\beta} + \vec{\epsilon} \tag{75}$$

where $\vec{y}$ is a vector of the m observations, $\vec{\beta}$ is a vector of the coefficients (this includes the intercept β_0, all "main effect" terms β_k, and any higher-order terms β_{jk}), and $\vec{\epsilon}$ is a vector of error terms. Note that including terms other than the main effects requires modification to the $\mathbf{X}$ matrix, such as

$$\mathbf{X} = \begin{bmatrix} 1 & x_{11} & x_{12} & \cdots & x_{11}x_{11} & x_{11}x_{12} & \cdots & x_{1q}x_{1q} \\ 1 & x_{21} & x_{22} & \cdots & x_{21}x_{21} & x_{21}x_{22} & \cdots & x_{2q}x_{2q} \\ \vdots & \vdots & \vdots & & \vdots & \vdots & & \vdots \\ 1 & x_{m1} & x_{m2} & \cdots & x_{m1}x_{m1} & x_{m1}x_{m2} & \cdots & x_{mq}x_{mq} \end{bmatrix} \tag{76}$$

where this particular matrix would be appropriate for a quadratic model with two-factor interactions. Now the least squares estimator can be rewritten in matrix form to solve for the minimum. Equation (74) is rewritten as

$$L = (\vec{y} - \mathbf{X}\vec{\beta})^{\mathrm{T}}(\vec{y} - \mathbf{X}\vec{\beta}) \tag{77}$$

where the superscript T denotes the transpose. The idea is to find the vector of least squares estimators $\vec{b}$ that minimizes equation (77). After finding the derivatives of L with respect to $\vec{\beta}$, the least squares estimators are found such that

$$\vec{b} = (\mathbf{X}^{\mathrm{T}}\mathbf{X})^{-1}\mathbf{X}^{\mathrm{T}}\vec{y} \tag{78}$$

where $\vec{b}$ represents the *least-squares estimators* for $\vec{\beta}$. The fitted regression model then becomes

$$\hat{\vec{y}} = \mathbf{X}\vec{b} \tag{79}$$

where $\hat{\vec{y}}$ is the vector of approximate observations with respect to the least-squares estimators. This process is repeated until there is a matrix of least-squares estimators $\mathbf{B} = [\vec{b}_1, \vec{b}_2, \ldots, \vec{b}_n]^T$ for all n decision metrics. This forms the matrix that is used throughout the requirements decomposition procedure and discussed at length in Chapter IV.

A.3 Validation of Response Surfaces

The response surfaces generated by least-squares regression generally exhibit three types of error. These are Model Fit Error (MFE), Model Representation Error (MRE), and other random error. Of these, MFE and MRE are the easiest to quantify, whereas random error is related to uncertainty due to noise in the observations. For computer-based experiments, error due to noise in the analysis is likely nonexistent unless there is a random or convergent process at work. Thus, the systems engineer is usually more concerned with MFE and MRE.

Model fit error refers to how well the regression coefficients fit the data within the experimental design **X**. This is relatively easy to quantify and therefore a variety of statistical techniques are available to test the suitability of the regression coefficients to predict the data points. Model representation error refers to the error of the regression model to all points within the design space, and can be quantified through comparison of actual versus predicted results for a random spread of points. The differences between MFE and MRE are depicted in Figure 60.

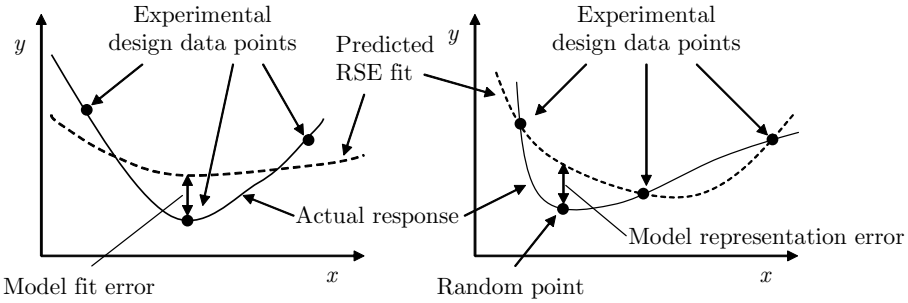

Figure 60: Comparison of Model Fit Error and Model Representation Error [Barros et al., 2004]

The basis of testing MFE is the ANalysis Of VAriance (ANOVA). This further breaks the total model error into error of the regression and residual error. The residual error is only present in designs where the number of experiments (rows of **X**) exceeds the number of regression coefficients (total number of β terms, denoted q'). It is important to note that some designs are setup especially to minimize the number of experiments and thus cannot have residual error, though one always needs at least as many experiments as there are

regression coefficients.

Basic ANOVA is very powerful for determining the MFE of a regression. It begins with determination of the error within the entire experiment through several measures. The sum of squares for each regression (SS_R) is found from

$$SS_R = \vec{b}^{\mathrm{T}}\mathbf{X}^{\mathrm{T}}\vec{y} - \frac{1}{m}\left(\sum_{i=1}^{m} y_i\right)^2 \tag{80}$$

and the sum of squares of the error (SS_E) becomes

$$SS_E = \vec{y}^{\mathrm{T}}\vec{y} - \vec{b}^{\mathrm{T}}\mathbf{X}^{\mathrm{T}}\vec{y} \tag{81}$$

where $\vec{y}$ is again the vector of observations. The total sum of squares (S_{yy}) is simply the sum of equations (80) and (81). The Mean Square of the regression and residual error, MS_R and MS_E respectively, are found by dividing the SS_R and SS_E terms by the number of degrees of freedom for the regression and the error.

These mean-squared error terms enable the first test of the regression: the hypothesis test for significance of the model. The null hypothesis for this test states that none of the regression coefficients contribute significantly to the model while the alternative hypothesis is that at least one of the coefficients is significant. The test statistic is the ratio of the mean square of the regression to the mean square of the error. If this is sufficiently high, then the first test of the model's validity has been established. Table 46 provides a summary of ANOVA and the associated statistical measures of MFE.

Table 46: Analysis of Variance for Significance of Regression

Source of Variation	**Sum of Squares**	**Degrees of Freedom**	**Mean Square**	$\mathbf{F_0}$
Regression	SS_R	q'	MS_R	$\frac{MS_R}{MS_E}$
Error or residual	SS_E	$m - q' - 1$	MS_E	-
Total	S_{yy}	$m - 1$	-	-

Another common measure for determining MFE is evaluation of the *coefficient of multiple determination*, known as R^2. This is defined as

$$R^2 = \frac{SS_R}{S_{yy}} = 1 - \frac{SS_E}{S_{yy}} \tag{82}$$

where R^2 is best described as a measure of the reduction in variability of y obtained by using the regressor variables $x_1, x_2, \ldots, x_q$ in the model. This value is always such that $0 \leq R^2 \leq 1$. However, a high value of R^2 does not necessarily imply the regression is acceptable, as this quantity will always increase as the number of predictor variables are increased. Furthermore, for repeatable experiments such as analytical computational solutions, the value of R^2 should be *very* high to be considered an adequate representation of the analysis.

A variety of other statistical tests exist for testing the whole model as well as the individual regressor variables and model coefficients, but this will not be detailed here. The reader is referred to any of the statistical modeling references given thus far for a more detailed discussion [Myers and Montgomery, 1995; Montgomery, 2001; Neter et al., 1996].

Quantification of MRE is slightly more difficult and involves more experiments. Lowering MFE is important as it ensures that the regression matches the "training" data points within the experimental design well. However, if the experimental design does not represent the richness of the overall design space well the regression may suffer from representation error. This can be quantified through additional, randomly generated points within the design space. The regressions are evaluated at these random points as are the original analyses. The results are plotted such that the "actual" results from the analyses are on one axis and the "predicted" results from the response surfaces are along the other. If the model is adequate, the plot will appear to be a tightly clustered collection of points about a line at a 45-degree angle to the origin. If the results are poor then the model likely suffers from representation error.

Often, designs that exhibit good MFE but poor MRE can be remedied with more data points in the original model or a different experimental design altogether. Switching from an orthogonal array to a space-filling design may bring about some correlation error but should help curb representation error. Other, simpler fixes include selection of smaller ranges to model within the design space or the addition of more levels into the experimental design.

APPENDIX B

SINGULAR VALUE DECOMPOSITION

Singular Value Decomposition (SVD) is a matrix factorization technique akin to Lower-Upper (LU) factorization and Gauss or Gram-Schmidt (QR) orthogonalization. It is an especially powerful matrix factorization with many uses, from determining the effective rank of a matrix to image processing and compression.

What follows is a brief overview of SVD and some of its salient characteristics. It is not meant to be a proof and the reader should have some understanding about linear algebra and matrix factorization. For a more comprehensive review of this subject the reader is directed to any number of linear algebra textbooks. What follows is taken from some of these texts [Strang, 1988; Nakos and Joyner, 1998].

B.1 SVD Basics

Singular Value Decomposition is closely related to the eigenvector-eigenvalue factorization seen for square matrices. In eigenanalysis, a square matrix $\mathbf{A}$ can be represented as the product of three matrices $\mathbf{Q}\mathbf{\Lambda}\mathbf{Q}^{\mathrm{T}}$. Here, $\mathbf{Q}$ is a matrix made up of the eigenvectors of $\mathbf{A}$ and $\mathbf{\Lambda}$ is a diagonal matrix of the associated eigenvalues. If $\mathbf{Q}$ on the left and $\mathbf{Q}^{\mathrm{T}}$ on the right are allowed to be *any two* orthogonal matrices (not necessarily transposes of each other) then factorization is possible for a non-square matrix $\mathbf{A}$. Furthermore, the diagonal (though rectangular) matrix in the middle can be made nonnegative. It will be denoted by $\mathbf{\Sigma}$, and its positive entries will be $\sigma_1, \ldots, \sigma_r$. These are the *singular values* of $\mathbf{A}$. They fill the first r places on the main diagonal of $\mathbf{\Sigma}$ and r is the rank of $\mathbf{A}$.

Formally, the Singular Value Decomposition of any $m \times n$ matrix $\mathbf{A}$ is

$$\mathbf{A} = \mathbf{Q}_1 \mathbf{\Sigma} \mathbf{Q}_2^{\mathrm{T}} \tag{83}$$

where the columns of $\mathbf{Q}_1$ are the eigenvectors of $\mathbf{A}\mathbf{A}^{\mathrm{T}}$ and the columns of $\mathbf{Q}_2$ are the

eigenvectors of $\mathbf{A}^{\mathrm{T}}\mathbf{A}$. The r singular values on the diagonal of $\mathbf{\Sigma}$ are the square roots of the nonzero eigenvalues of both $\mathbf{A}\mathbf{A}^{\mathrm{T}}$ and $\mathbf{A}^{\mathrm{T}}\mathbf{A}$. Note that $\mathbf{Q}_1$ is an $m \times m$ matrix, $\mathbf{Q}_2$ is $n \times n$, and $\mathbf{\Sigma}$ is $m \times n$.

B.2 Remarks

For positive definite matrices, this factorization is identical to eigenanalysis. For indefinite matrices, any negative eigenvalues in $\mathbf{\Lambda}$ become positive in $\mathbf{\Sigma}$ and $\mathbf{Q}_1$ is different then $\mathbf{Q}_2$. For complex matrices $\mathbf{\Sigma}$ remains real but $\mathbf{Q}_1$ and $\mathbf{Q}_2$ become unitary, and $\mathbf{A} = \mathbf{U}_1\mathbf{\Sigma}\mathbf{U}_2^{\mathrm{H}}$.

The columns of $\mathbf{Q}_1$ and $\mathbf{Q}_2$ form orthonormal bases for all four fundamental subspaces. Specifically, the bases are as follows:

- The first r columns of $\mathbf{Q}_1$: column space of $\mathbf{A}$
- The last $m - r$ columns of $\mathbf{Q}_1$: left nullspace of $\mathbf{A}$
- The first r columns of $\mathbf{Q}_2$: row space of $\mathbf{A}$
- The last $n - r$ columns of $\mathbf{Q}_2$: nullspace of $\mathbf{A}$

There are other characteristics of SVD that are remarkable but do not necessarily have a direct bearing on this research. Therefore, the reader is directed to further linear algebra texts for more details.

APPENDIX C

BASELINE INPUTS FOR LONG-RANGE TRANSPORT TECHNOLOGY STUDY

Table 47: Inputs for Transport Baseline Configurations

Variable Description	**Symbol**	**SOA**	**5-Year**	**15-year**
Fan polytropic efficiency	Fan_eff	0	0	0
Fan pressure ratio	FPR	1.5	1.5	1.5
LPC polytropic efficiency	LPC_eff	0	0	0
LPC pressure ratio	LPCPR	1.3	1.3	1.3
HPC polytropic efficiency	HPC_eff	0	0	-0.0116
HPC pressure ratio	HPCPR	20	25	25
HPC tip speed	HPC_TS	1.0629	1.0629	1.3225
HPC max FSPR	HPC_FSPR	1.6	1.6	2.02
HPC noise bleed flow	HPC_BL	0	0.004	0.004
NOx constant (UTEP)	Comb_NOx	0.305	0.72	0.72
Combustor cooling	Comb_cool	0.75	0.935	0.935
Combustor liner density	Comb_dens	0	-0.68585	-0.68585
Max T4	T4max	3285	3550	3550
HPT adiabatic efficiency	HPT_eff	0	0	0
HPT stage loading	HPT_Load	0	0	0.2
HPT 1st vane rel. temp	HPT_1VT	0	700	700
HPT 2nd vane rel. temp	HPT_2VT	0	200	278
HPT blade rel. temp	HPT_BT	0	200	278
HPT stator density	HPT_SD	0	0	-0.02244

Continued on next page

Table 47 – continued from previous page

Variable Description	Symbol	SOA	5-Year	15-year
HPT blade density	HPT_BD	0	0	-0.02244
Transition duct bleed flow	Duct_BL	0	0	0.005
LPT adiabatic efficiency	LPT_eff	0	0	0.02
LPT stage loading	LPT_Load	0	0	0.28
LPT vane rel. temp	LPT_VT	0	200	294
LPT blade rel. temp	LPT_BT	0	200	294
LPT stator density	LPT_SD	0	0	-0.02556
LPT blade density	LPT_BD	0	0	-0.02556
Total thrust loss	k_Fg	1	0.998	0.998
Wing quarter chord sweep	Sweep	31.64	31.64	31.64
Airfoil shape factor	AITEK	2	2	2
Subsonic drag factor	FCDSUB	1	0.98	0.98
Takeoff drag (CDTO array)	FTOCD	0	0	0
Landing CLmax (CLLDM)	k_CLLDM	0	-0.02	-0.02
Fuselage weight (FRFU)	FRFU	0	0	-0.24
Wing weight (FRWI)	FRWI	0	0	-0.18
Tail weight	FRHT, FRVT	0	0	-0.42
Wing surface controls (FRSC)	FRSC	0	0.0718	0.0718
Main landing weight (FRLGM)	FRLGM	0	0.01	0.01
Engine weight	EngWt	0	-0.00752	-0.0041
Wing loading	WSR	131.83	132.6	126.2
Thrust to weight ratio	TWR	0.253243	0.257	0.264
Aircraft price	AKPRICE	0	0.05102	-0.1145
Aircraft RDT&E	AKRDTE	0	0	0.03403
Aircraft utilization	Util	0	0	0
Engine cost	Eng$	0	0.0956	0.0956

Continued on next page

Table 47 – continued from previous page

Variable Description	Symbol	SOA	5-Year	15-year
Fan inlet noise at CB	Fan_In_CB	0	0	0
Fan inlet noise at AP	Fan_In_AP	0	0	0
Fan inlet noise at SL	Fan_In_SL	0	0	0
Fan inlet noise 4kHz - (AP)	Fan_In_f1	0	-2	-2.5
Fan inlet noise 4kHz - (CB, SL)	Fan_In_f2	0	0	-2.5
Fan exhaust noise at CB	Fan_Ex_CB	0	-1	-1
Fan exhaust noise at AP	Fan_Ex_AP	0	-3	-3
Fan exhaust noise at SL	Fan_Ex_SL	0	0	0
Fan exhaust noise 4kHz - (all)	Fan_Ex_f1	0	-0.25	-2.75
Total jet noise at CB	Jet_CB	0	0	0
Total jet noise at AP	Jet_AP	0	0	0
Total jet noise at SL	Jet_SL	0	-2.38	-2.38
Wing slat noise - approach	Slat_AP	0	-1	-1
Landing gear noise - approach	LG_AP	0	-3	-3
Total noise - AP	D_Noise_AP	0	-1	-1

APPENDIX D

VALIDATION OF REDUCED-ORDER RESPONSE SURFACES

D.1 Response Surface Coefficients

Table 48: SOA Response Surface Coefficients

	CO2	DOCi	NOx	APPn	SLn	TOn	TOFL	TOGW	VAPP
b_0	-0.3109	-0.2523	-0.1293	-0.1130	0.0665	-0.1690	-0.3347	-0.2663	0.0073
b_1	-0.3052	-0.1911	0.0002	-0.0533	-0.0386	-0.0109	0.0108	-0.2269	-0.0012
b_2	-0.2036	-0.2880	0.2547	0.6497	0.5646	0.5558	-0.1120	-0.2556	0.0001
b_3	0.0370	0.0593	0.3749	0.0696	0.0013	-0.0085	-0.0027	0.0410	0.0113
b_4	0.0134	0.0080	0.3430	0.0344	0.0078	0.0060	0.0048	0.0263	0.0056
b_5	-0.1407	-0.0716	0.0106	-0.0556	-0.0498	-0.0621	-0.0007	-0.0849	-0.0091
b_6	0.2241	0.2588	0.0060	0.0844	0.2430	0.2601	-0.7169	0.2400	0.0059
b_7	-0.0569	-0.0825	-0.0050	-0.0530	-0.0088	-0.0526	0.1497	-0.0987	0.9626
b_{11}	0.0732	0.0421	0.0011	0.0027	0.0127	0.0267	-0.0002	0.0477	0.0005
b_{12}	0.0262	0.0205	0.0017	-0.0042	0.0050	0.0087	-0.0020	0.0221	-0.0005
b_{13}	0.0061	0.0080	0.0001	0.0023	0.0019	0.0162	-0.0002	0.0083	0.0005
b_{14}	0.0052	-0.0029	-0.0003	0.0016	-0.0006	-0.0062	0.0000	0.0001	-0.0010
b_{15}	0.1091	0.0780	0.0016	0.0149	0.0269	0.0315	-0.0034	0.0886	0.0025
b_{16}	0.0262	0.0133	0.0000	0.0000	0.0029	-0.0002	-0.0051	0.0181	-0.0002
b_{17}	0.0032	0.0056	0.0004	0.0052	0.0114	0.0018	0.0025	0.0085	-0.0008
b_{22}	0.0885	0.0902	0.0088	0.0328	-0.1097	0.0157	-0.0003	0.0814	0.0001
b_{23}	0.0160	0.0161	0.0290	-0.0012	0.0115	0.0062	0.0024	0.0181	0.0019
b_{24}	0.0088	0.0001	0.0222	0.0100	-0.0124	-0.0076	0.0014	0.0005	0.0003
b_{25}	0.0317	0.0306	0.0009	-0.0018	-0.0174	-0.0101	-0.0017	0.0310	0.0012
b_{26}	0.1032	0.0441	0.0016	0.0231	0.0093	0.0370	0.0395	0.0612	-0.0004
b_{27}	0.0610	0.0432	-0.0011	0.0108	-0.0128	-0.0227	-0.0094	0.0427	-0.0019
b_{33}	0.0163	0.0181	0.0035	-0.0011	0.0184	0.0087	-0.0005	0.0183	-0.0005
b_{34}	0.0294	0.0196	0.0479	0.0125	0.0156	-0.0075	0.0038	0.0211	0.0000
b_{35}	0.0090	0.0065	0.0000	-0.0036	-0.0007	-0.0111	0.0010	0.0077	0.0013
b_{36}	0.0030	-0.0007	0.0024	0.0047	0.0023	0.0054	-0.0015	0.0018	0.0013
b_{37}	0.0049	-0.0005	-0.0001	0.0057	0.0139	-0.0003	-0.0007	0.0003	-0.0010
b_{44}	-0.0033	-0.0092	0.0087	-0.0078	0.0080	-0.0047	-0.0029	-0.0122	0.0003
b_{45}	0.0077	0.0068	0.0001	-0.0092	-0.0012	0.0082	-0.0001	0.0050	-0.0002
b_{46}	-0.0005	-0.0056	0.0019	-0.0083	-0.0174	0.0068	-0.0029	-0.0026	-0.0014
b_{47}	-0.0099	-0.0067	0.0001	0.0017	0.0072	-0.0027	0.0026	-0.0063	-0.0009
b_{55}	0.0475	0.0299	-0.0001	-0.0033	0.0029	0.0190	-0.0019	0.0387	0.0021
b_{56}	0.0428	0.0211	0.0010	-0.0072	0.0030	0.0008	-0.0027	0.0267	0.0002
b_{57}	0.0255	0.0114	0.0002	0.0060	-0.0045	0.0061	-0.0017	0.0181	0.0002
b_{66}	0.0694	0.0404	0.0012	0.0058	0.0024	0.0140	0.2276	0.0429	0.0005
b_{67}	0.0488	0.0247	0.0018	0.0023	0.0092	-0.0069	-0.0489	0.0270	-0.0006
b_{77}	0.0185	0.0094	0.0000	0.0157	-0.0022	0.0261	0.0036	0.0118	-0.0068

Table 49: 5-Year Response Surface Coefficients

	CO2	DOCi	NOx	APPn	SLn	TOn	TOFL	TOGW	VAPP
b_0	-0.4062	-0.2770	-0.1889	-0.1083	0.0793	-0.1736	-0.3242	-0.3053	0.0051
b_1	-0.2719	-0.1735	0.0012	-0.0543	-0.0715	-0.0725	0.0013	-0.2180	-0.0031
b_2	-0.2080	-0.3092	0.2462	0.6578	0.4890	0.5155	-0.1054	-0.2719	-0.0003
b_3	-0.0569	-0.0197	0.3823	0.0492	-0.0648	-0.0379	-0.0006	-0.0385	0.0098
b_4	-0.0176	-0.0191	0.3357	0.0049	-0.0396	-0.0088	0.0137	-0.0106	0.0043
b_5	-0.1288	-0.0553	0.0120	-0.0591	-0.0220	-0.0641	-0.0007	-0.0715	-0.0086
b_6	0.1707	0.2558	0.0025	0.1132	0.2589	0.2506	-0.7258	0.2171	0.0054
b_7	-0.0609	-0.0933	-0.0040	-0.0442	-0.0267	-0.0421	0.1415	-0.1023	0.9665
b_{11}	0.0703	0.0410	0.0018	0.0030	0.0077	0.0242	-0.0002	0.0494	0.0005
b_{12}	0.0252	0.0199	0.0029	-0.0047	0.0221	0.0079	-0.0019	0.0229	-0.0005
b_{13}	0.0058	0.0078	0.0003	0.0026	-0.0042	0.0147	0.0001	0.0086	0.0005
b_{14}	0.0050	-0.0028	-0.0004	0.0018	-0.0018	-0.0056	-0.0004	0.0001	-0.0010
b_{15}	0.1048	0.0760	0.0028	0.0166	0.0207	0.0286	-0.0034	0.0919	0.0025
b_{16}	0.0252	0.0130	0.0001	0.0000	0.0105	-0.0002	-0.0032	0.0188	-0.0002
b_{17}	0.0031	0.0055	0.0006	0.0058	0.0119	0.0016	0.0021	0.0088	-0.0008
b_{22}	0.0849	0.0879	0.0154	0.0364	-0.1313	0.0142	-0.0008	0.0844	0.0001
b_{23}	0.0153	0.0157	0.0379	-0.0014	0.0181	0.0056	0.0021	0.0188	0.0019
b_{24}	0.0085	0.0001	0.0299	0.0111	-0.0050	-0.0069	0.0009	0.0005	0.0003
b_{25}	0.0304	0.0298	0.0017	-0.0020	-0.0160	-0.0092	-0.0022	0.0322	0.0012
b_{26}	0.0991	0.0430	0.0025	0.0257	0.0317	0.0335	0.0376	0.0635	-0.0004
b_{27}	0.0586	0.0421	-0.0021	0.0121	0.0129	-0.0206	-0.0081	0.0442	-0.0019
b_{33}	0.0156	0.0177	0.0159	-0.0012	0.0069	0.0079	-0.0002	0.0189	-0.0005
b_{34}	0.0282	0.0191	0.0651	0.0139	0.0240	-0.0068	0.0031	0.0219	0.0000
b_{35}	0.0086	0.0063	0.0001	-0.0040	-0.0067	-0.0100	0.0004	0.0080	0.0013
b_{36}	0.0029	-0.0007	0.0040	0.0052	0.0024	0.0049	-0.0020	0.0018	0.0013
b_{37}	0.0047	-0.0005	-0.0001	0.0063	0.0022	-0.0003	-0.0009	0.0003	-0.0010
b_{44}	-0.0031	-0.0090	0.0152	-0.0086	0.0057	-0.0042	-0.0040	-0.0127	0.0003
b_{45}	0.0074	0.0066	0.0000	-0.0102	-0.0022	0.0074	-0.0002	0.0052	-0.0002
b_{46}	-0.0005	-0.0054	0.0032	-0.0092	-0.0105	0.0061	-0.0051	-0.0027	-0.0014
b_{47}	-0.0095	-0.0065	0.0004	0.0019	-0.0055	-0.0025	0.0025	-0.0065	-0.0009
b_{55}	0.0456	0.0291	-0.0002	-0.0037	0.0079	0.0172	-0.0019	0.0402	0.0021
b_{56}	0.0411	0.0206	0.0015	-0.0080	0.0057	0.0007	-0.0032	0.0277	0.0002
b_{57}	0.0244	0.0112	0.0005	0.0067	0.0081	0.0055	-0.0015	0.0188	0.0002
b_{66}	0.0666	0.0393	0.0020	0.0065	0.0120	0.0127	0.2299	0.0445	0.0005
b_{67}	0.0468	0.0241	0.0031	0.0026	0.0070	-0.0063	-0.0476	0.0280	-0.0006
b_{77}	0.0177	0.0091	0.0000	0.0174	0.0082	0.0237	0.0033	0.0122	-0.0068

Table 50: 15-Year Response Surface Coefficients

	CO2	DOCi	NOx	APPn	SLn	TOn	TOFL	TOGW	VAPP
b_0	-0.5544	-0.3549	-0.2059	-0.0837	0.1011	-0.1704	-0.3354	-0.3944	0.0073
b_1	-0.2744	-0.1800	-0.0046	-0.0564	-0.0530	-0.0652	0.0003	-0.2326	-0.0029
b_2	-0.1849	-0.2917	0.2428	0.6550	0.5583	0.5441	-0.1043	-0.2563	-0.0013
b_3	-0.0593	-0.0302	0.3880	0.0147	-0.0100	-0.0286	0.0085	-0.0317	0.0052
b_4	-0.0401	-0.0418	0.3396	0.0263	-0.0588	-0.0329	0.0099	-0.0475	0.0027
b_5	-0.1443	-0.0456	-0.0042	0.0061	-0.0269	-0.0701	0.0092	-0.0646	0.0039
b_6	0.0758	0.2032	0.0123	0.1647	0.2448	0.2078	-0.7197	0.1511	0.0051
b_7	-0.0294	-0.0778	0.0036	-0.0286	0.0001	-0.0449	0.1443	-0.0562	0.9784
b_{11}	0.0758	0.0566	0.0021	0.0034	0.0092	0.0238	-0.0002	0.0652	0.0005
b_{12}	0.0272	0.0275	0.0029	-0.0054	-0.0058	0.0077	-0.0019	0.0301	-0.0005
b_{13}	0.0063	0.0107	0.0005	0.0030	-0.0060	0.0144	0.0000	0.0114	0.0005
b_{14}	0.0054	-0.0039	-0.0005	0.0021	-0.0033	-0.0055	-0.0010	0.0001	-0.0010
b_{15}	0.1130	0.1049	0.0028	0.0190	0.0172	0.0281	-0.0028	0.1211	0.0025
b_{16}	0.0272	0.0179	0.0001	0.0000	0.0098	-0.0002	-0.0026	0.0247	-0.0002
b_{17}	0.0033	0.0075	0.0007	0.0067	0.0195	0.0016	0.0024	0.0116	-0.0008
b_{22}	0.0916	0.1214	0.0157	0.0418	-0.1849	0.0140	0.0003	0.1113	0.0001
b_{23}	0.0165	0.0217	0.0428	-0.0015	-0.0175	0.0055	0.0023	0.0248	0.0019
b_{24}	0.0091	0.0001	0.0300	0.0128	0.0012	-0.0067	0.0014	0.0007	0.0003
b_{25}	0.0328	0.0412	0.0017	-0.0023	0.0055	-0.0090	-0.0023	0.0424	0.0012
b_{26}	0.1069	0.0594	0.0029	0.0295	0.0261	0.0330	0.0373	0.0837	-0.0004
b_{27}	0.0632	0.0582	-0.0021	0.0138	0.0213	-0.0203	-0.0077	0.0583	-0.0019
b_{33}	0.0168	0.0244	0.0159	-0.0014	-0.0175	0.0078	-0.0007	0.0250	-0.0005
b_{34}	0.0304	0.0264	0.0719	0.0160	0.0204	-0.0067	0.0037	0.0288	0.0000
b_{35}	0.0093	0.0087	0.0000	-0.0045	-0.0005	-0.0099	0.0006	0.0105	0.0014
b_{36}	0.0031	-0.0010	0.0040	0.0060	-0.0044	0.0048	-0.0038	0.0024	0.0013
b_{37}	0.0050	-0.0007	-0.0003	0.0073	-0.0068	-0.0003	-0.0004	0.0004	-0.0010
b_{44}	-0.0034	-0.0124	0.0193	-0.0099	0.0105	-0.0042	-0.0037	-0.0167	0.0003
b_{45}	0.0079	0.0092	0.0000	-0.0117	0.0051	0.0073	0.0002	0.0069	-0.0002
b_{46}	-0.0005	-0.0075	0.0033	-0.0106	-0.0130	0.0060	-0.0048	-0.0035	-0.0015
b_{47}	-0.0102	-0.0090	0.0003	0.0022	0.0000	-0.0024	0.0024	-0.0086	-0.0010
b_{55}	0.0492	0.0402	-0.0004	-0.0042	0.0008	0.0169	-0.0022	0.0530	0.0021
b_{56}	0.0443	0.0284	0.0016	-0.0092	0.0005	0.0007	-0.0053	0.0365	0.0002
b_{57}	0.0264	0.0154	0.0004	0.0076	0.0026	0.0055	-0.0011	0.0248	0.0002
b_{66}	0.0718	0.0543	0.0019	0.0074	0.0056	0.0125	0.2268	0.0586	0.0005
b_{67}	0.0505	0.0332	0.0031	0.0030	0.0067	-0.0062	-0.0491	0.0370	-0.0006
b_{77}	0.0191	0.0126	0.0001	0.0200	0.0019	0.0233	0.0037	0.0161	-0.0069

D.2 Whole-Model ANOVA Tests

Refer to Appendix A for an explanation of these tests.

Table 51: SOA Response Tests

RSE	Source	SS	DoF	MS	F0	R^2
CO2	Regression	185.92	36	5.1644	7.98E+15	1
	Error	1.36E-12	2107	6.47E-16	-	-
	Total	185.92	2143	-	-	-
DOCi	Regression	167.92	36	4.6643	1.73E+17	1
	Error	5.68E-14	2107	2.70E-17	-	-
	Total	167.92	2143	-	-	-
NOx	Regression	264.91	36	7.3587	6.06E+06	0.99999
	Error	0.0025594	2107	1.21E-06	-	-
	Total	264.92	2143	-	-	-
APPn	Regression	356.66	36	9.9072	3.67E+17	1
	Error	5.68E-14	2107	2.70E-17	-	-
	Total	356.66	2143	-	-	-
SLn	Regression	308.39	36	8.5664	4521.9	0.9872
	Error	3.9915	2107	0.0018944	-	-
	Total	312.38	2143	-	-	-
TOn	Regression	309.1	36	8.5862	3.54E+16	1
	Error	5.12E-13	2107	2.43E-16	-	-
	Total	309.1	2143	-	-	-
TOFL	Regression	451.19	36	12.533	1.48E+05	0.9996
	Error	0.17864	2107	8.48E-05	-	-
	Total	451.37	2143	-	-	-
TOGW	Regression	163.4	36	4.5389	-1.68E+17	1
	Error	-5.68E-14	2107	-2.70E-17	-	-
	Total	163.4	2143	-	-	-
VAPP	Regression	738.93	36	20.526	-3.80E+17	1
	Error	-1.14E-13	2107	-5.40E-17	-	-
	Total	738.93	2143	-	-	-

Table 52: 5-Year Response Tests

RSE	Source	SS	DoF	MS	F0	R^2
CO2	Regression	153.98	36	4.2773	1.42E+15	1
	Error	6.37E-12	2107	3.02E-15	-	-
	Total	153.98	2143	-	-	-
DOCi	Regression	173.41	36	4.817	3.57E+16	1
	Error	2.84E-13	2107	1.35E-16	-	-
	Total	173.41	2143	-	-	-
NOx	Regression	255.14	36	7.0873	1.95E+06	0.99997
	Error	0.0076693	2107	3.64E-06	-	-
	Total	255.15	2143	-	-	-
APPn	Regression	360.28	36	10.008	2.38E+15	1
	Error	8.87E-12	2107	4.21E-15	-	-
	Total	360.28	2143	-	-	-
SLn	Regression	255	36	7.0834	6090	0.99048
	Error	2.4507	2107	0.0011631	-	-
	Total	257.45	2143	-	-	-
TOn	Regression	268.78	36	7.4662	7.91E+15	1
	Error	1.99E-12	2107	9.44E-16	-	-
	Total	268.78	2143	-	-	-
TOFL	Regression	452.92	36	12.581	1.45E+05	0.9996
	Error	0.18241	2107	8.66E-05	-	-
	Total	453.11	2143	-	-	-
TOGW	Regression	161.09	36	4.4746	1.66E+17	1
	Error	5.68E-14	2107	2.70E-17	-	-
	Total	161.09	2143	-	-	-
VAPP	Regression	744.31	36	20.675	4.53E+14	1
	Error	9.62E-11	2107	4.56E-14	-	-
	Total	744.31	2143	-	-	-

Table 53: 15-Year Response Tests

RSE	Source	SS	DoF	MS	F0	R^2
CO2	Regression	136.57	36	3.7935	4.39E+15	1
	Error	1.82E-12	2107	8.63E-16	-	-
	Total	136.57	2143	-	-	-
DOCi	Regression	153.5	36	4.2639	5.27E+16	1
	Error	1.71E-13	2107	8.09E-17	-	-
	Total	153.5	2143	-	-	-
NOx	Regression	258.85	36	7.1903	1.95E+06	0.99997
	Error	0.0077877	2107	3.70E-06	-	-
	Total	258.86	2143	-	-	-
APPn	Regression	371.08	36	10.308	3.82E+17	1
	Error	5.68E-14	2107	2.70E-17	-	-
	Total	371.08	2143	-	-	-
SLn	Regression	315.59	36	8.7664	6325.2	0.99083
	Error	2.9202	2107	0.0013859	-	-
	Total	318.51	2143	-	-	-
TOn	Regression	287.23	36	7.9786	1.76E+15	1
	Error	9.55E-12	2107	4.53E-15	-	-
	Total	287.23	2143	-	-	-
TOFL	Regression	460.1	36	12.781	1.60E+05	0.99963
	Error	0.16881	2107	8.01E-05	-	-
	Total	460.27	2143	-	-	-
TOGW	Regression	144.18	36	4.0049	-2.97E+16	1
	Error	-2.84E-13	2107	-1.35E-16	-	-
	Total	144.18	2143	-	-	-
VAPP	Regression	763.02	36	21.195	3.57E+15	1
	Error	1.25E-11	2107	5.94E-15	-	-
	Total	763.02	2143	-	-	-

D.3 Actual Versus Predicted Results for Random Cases

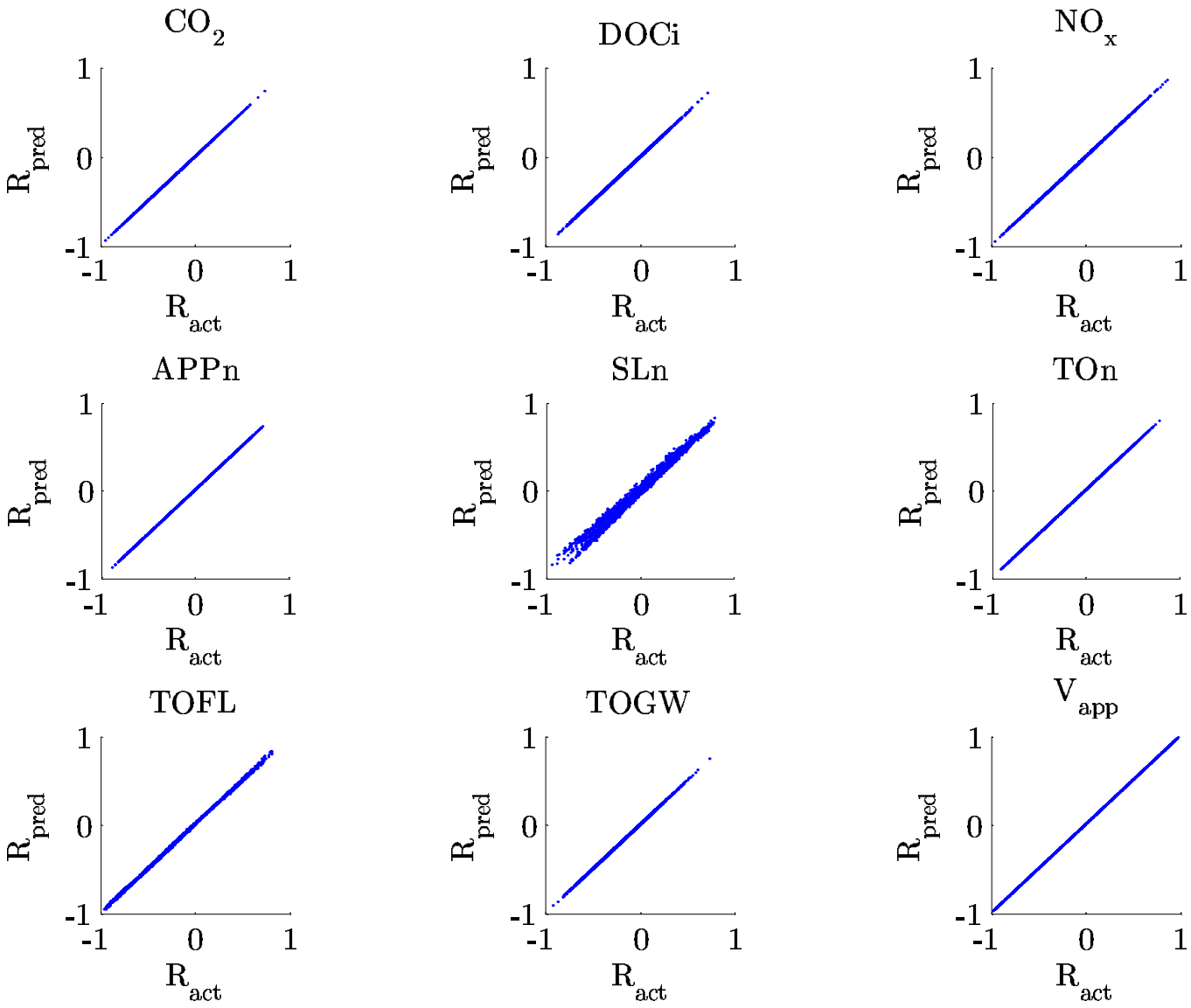

Figure 61: Actual Versus Predicted Results for SOA RSEs

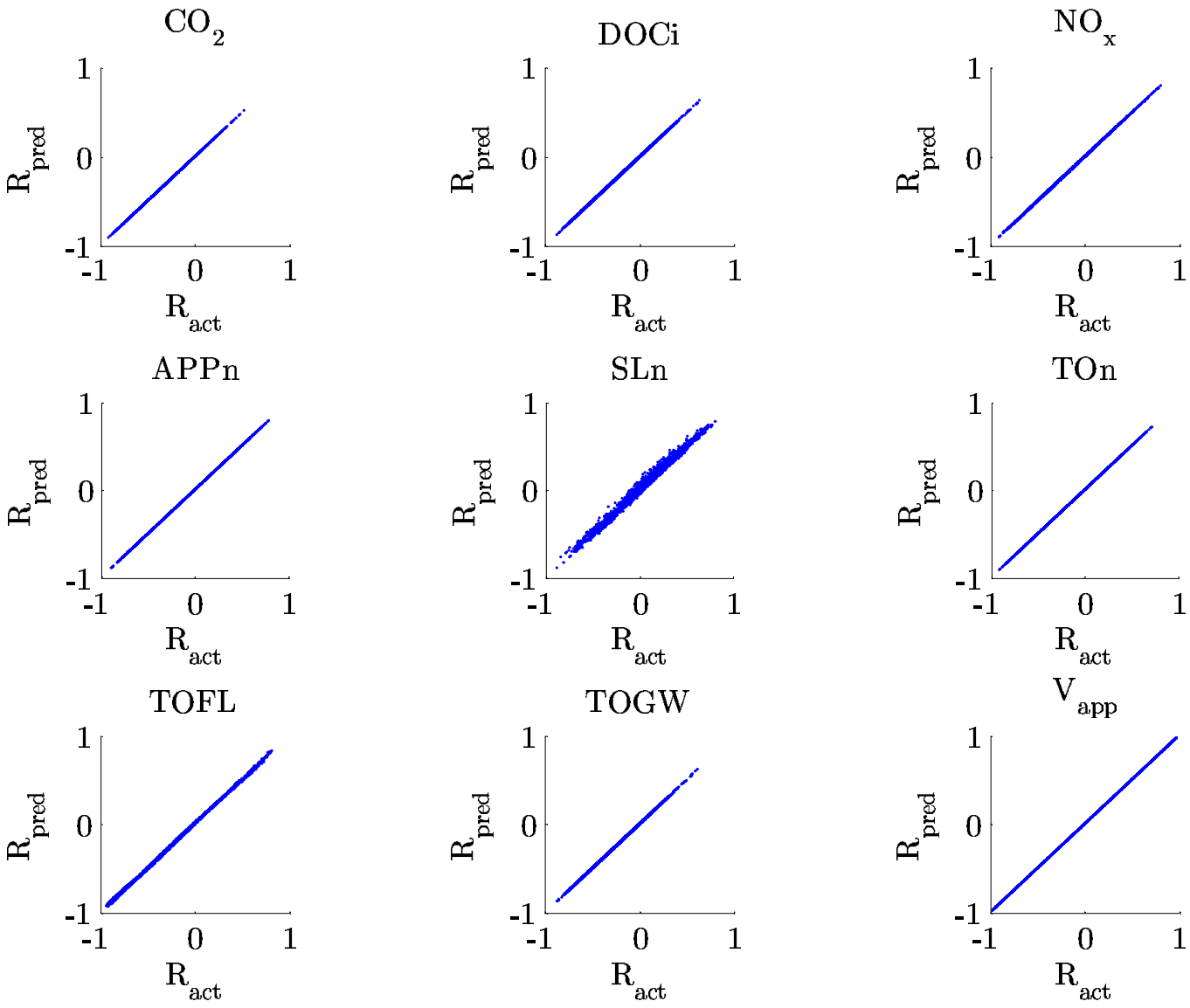

Figure 62: Actual Versus Predicted Results for 5-Year RSEs

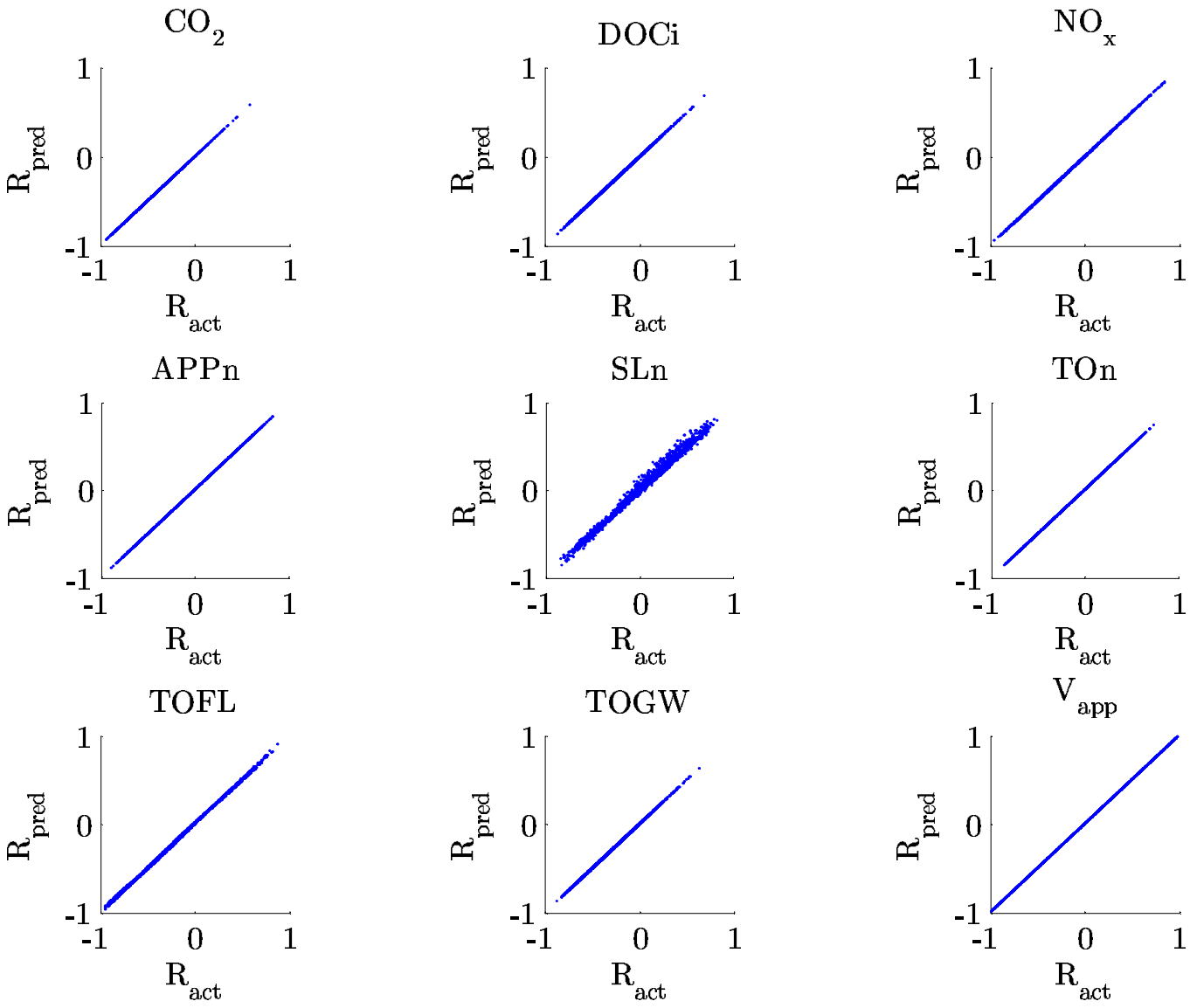

Figure 63: Actual Versus Predicted Results for 15-Year RSEs

Bibliography

AIAA Technical Activities Committee. Current state of the art on multidisciplinary design optimization (MDO). AIAA White Paper, 1991.

Anderson, Jr., John D. *Hypersonic and High Temperature Gas Dynamics*. McGraw-Hill, Inc., Boston, Massachusetts, 1989.

Antoine, Nicolas E. and Kroo, Ilan M. Aircraft optimization for minimal environmental impact. *Journal of Aircraft*, 41(4):790–797, 2004.

Asimow, Morris. *Introduction to Design*. Prentice-Hall, Englewood Cliffs, New Jersey, 1962.

Baker, Andrew P. *The Role of Mission Requirements, Vehicle Attributes, Technologies and Uncertainty in Rotorcraft System Design*. Ph.D. thesis, Georgia Institute of Technology, Atlanta, Georgia, 2002.

Baker, Andrew P. and Mavris, Dimitri N. Assessing the simultaneous impact of requirements, vehicle characteristics, and technologies during aircraft design. 2001-0533. 39th Aerospace Sciences Meeting and Exhibit, American Institute of Aeronautics and Astronautics, 2001.

Bandte, Oliver. *A Probabilistic Multi-Criteria Decision Making Technique for Conceptual and Preliminary Aerospace Systems Design*. Ph.D. thesis, Georgia Institute of Technology, Atlanta, Georgia, 2000.

Barros, Peter A., Kirby, Michelle R., and Mavris, Dimitri N. Impact of sampling technique selection on the creation of response surface models. 2004-01-3134. Aerospace Congress and Exhibition, Society of Automotive Engineers, 2004.

Baugher, Jay. USAAC / USAAF / USAF bomber aircraft. 2005. http://home.att.net/~jbaugher/usafbombers.html.

Boeing Commercial Airplanes. 777-200/300 airplane characteristics for airport planning. 2000. D6-58329.

Boeing Commercial Airplanes. 737 airplane characteristics for airport planning. 2005. D6-58325-6.

Borer, Nicholas K. and Mavris, Dimitri N. Requirements exploration for a notional multi-role fighter. 2003-6709. 3rd Aviation Technology, Integration, and Operations Technical Forum, American Institute of Aeronautics and Astronautics, 2003.

Borer, Nicholas K. and Mavris, Dimitri N. Formulation of a multi-mission sizing methodology for competing configurations. 2004-0535. 42nd Aerospace Sciences Meeting and Exhibit, American Institute of Aeronautics and Astronautics, 2004.

Box, George E. P. and Draper, Norman R. *Empirical Model-Building and Response Surfaces*. John Wiley and Sons, Inc., New York, New York, 1987.

Brassard, Michael and Ritter, Diane. *The Memory Jogger II*. GOAL / QPC, Salem, New Hampshire, 1994.

Bratley, Paul and Fox, Bennett L. Algorithm 659: Implementing Sobol's quasirandom sequence generator. *ACM Transactions on Mathematical Software*, 14(1):88–100, 1988.

Braun, Robert, Gage, Peter, and Kroo, Ilan. Implementation and performance issues in collaborative optimization. 96-4017. 6th Symposium on Multidisciplinary Analysis and Optimization, American Institute of Aeronautics and Astronautics, 1996.

Buonanno, Michael A. *A Method for Aircraft Concept Exploration Using Multicriteria Interactive Genetic Algorithms.* Ph.D. thesis, Georgia Institute of Technology, Atlanta, Georgia, 2005.

Carlsson, Christer, Fedrizzi, Mario, and Fullér, Robert. *Fuzzy Logic in Management.* Operations Research and Management Science. Kluwer, Norwell, Massachusetts, 2004.

Carlsson, Christer and Fullér, Robert. Multiple criteria decision making: The case for interdependence. *Computers & Operations Research*, 22:251–260, 1995.

Carlsson, Christer and Fullér, Robert. Fuzzy multiple criteria decision making: Recent developments. *Fuzzy Sets and Systems*, 78:139–153, 1996.

Carty, A. An approach to multidisciplinary design, analysis, and optimization for rapid conceptual design. 2002-5438. 9th Symposium on Multidisciplinary Analysis and Optimization, American Institute of Aeronautics and Astronautics, Atlanta, Georgia, 2002.

Chvátal, Vasek. *Linear Programming.* W. H. Freeman and Company, New York, New York, 1983.

Collier, Fay. Subsonic vehicle sector. Vehicle Systems Program 1st Annual Industry Meeting, National Aeronautics and Space Adminstration, 2004.

Czysz, P. A., Dighton, R. D., and W. P. Murden, Jr. Designing for air superiority. Technical Report 73-0800, McDonnell Aircraft Company, 1973.

Deb, Kalyanmoy. *Multi-Objective Optimization using Evolutionary Algorithms.* John Wiley and Sons, Chichester, England, 2001.

Decisioneering, Inc. Crystal Ball risk analysis software & consulting services. 2005. http://www.decisioneering.com/.

DeLaurentis, D., Mavris, D. N., and Schrage, D. P. System synthesis in preliminary aircraft design using statistical methods. 20th Congress of the International Council of the Aeronautical Sciences, International Council of the Aeronautical Sciences, Sorrento, Italy, 1996.

Department of the Navy. Navy historical center, naval aviation history branch. 2005. http://www.history.navy.mil/branches/nhcorg4.htm.

Dieter, George E. *Engineering Design: A Meterials and Processing Approach, Third Edition.* McGraw-Hill, Inc., Boston, Massachusetts, 2000.

Dunteman, George H. *Principal Components Analysis.* Quantitative Applications in the Social Sciences. Sage Publications, Newbury Park, California, 1989.

Eckels, W. E. Civil transport aircraft design methodology. 83-2463. Aircraft Design, Systems and Technology Meeting, American Institute of Aeronautics and Astronautics, Fort Worth, Texas, 1983.

Engineous Software. iSIGHT - integrate, automate, and optimize your manual design processes. 2005. http://www.engineous.com/product_iSIGHT.htm.

Environmental Protection Agency. Control of air pollution from aicraft and aircraft engines; emission standards and test procedures. *Federal Register*, 70(221):69664–69687, 2005.

Federal Aviation Administration. Fuel venting and exhaust emission requirements for turbine engine powered airplanes. Advisory Circular 34-1B, 2003a.

Federal Aviation Administration. Noise standards: Aircraft type and airworthiness certification. Advisory Circular 34-6C, 2003b.

Federal Aviation Administration. Airworthiness standards: Transport category airplanes. Code of Federal Regulations, Title 14, Part 25, 2005.

Federation of American Scientists. U.S. military aircraft. 2005. http://www.fas.org/man/dod-101/sys/ac/index.html.

Flight Safety Foundation. FSF ALAR briefing note 8.2 - the final approach speed. *Flight Safety Digest*, pages 163–166, 2000.

Fox, Eric P. The Pratt and Whitney probabilistic design system. 94-1442. 35th Structures, Structural Dynamics, and Materials Conference, American Institute of Aeronautics and Astronautics, 1994.

Gerhards, Roland, Meller, Frank, Dirks, Gregor A., and Szodruch, Joachim. Aircraft design optimizing operators, environmental system and manufacturers requirements. 2000-01-5546. 2000 World Aviation Congress, Society of Automotive Engineers, 2000.

Greenway, M. K. and Koob, S. J. Relating take-off-gross-weight and mission requirements to geometrically optimized aircraft. 78-0098. 16th Aerospace Sciences Meeting, American Institute of Aeronautics and Astronautics, 1978.

Guynn, M. D. and Olson, E. D. Evaluation of an aircraft concept with over-wing, hydrogen-fueled engines for reduced noise and emissions. Technical Report TM-2002-211926, National Aeronautics and Space Administration, Hampton, Virginia, 2002.

Hayter, Anthony J. *Probability and Statistics for Engineers and Scientists*. PWS, Boston, Massachusetts, 1996.

Hibbeler, R. C. *Mechanics of Materials, Third Edition*. Prentice Hall, Upper Saddle River, New Jersey, 1997.

Hwang, Ching-Lai and Masud, Abu Syed Md. *Multiple Objective Decision Making: Methods and Applications*. Lecture Notes in Economics and Mathematical Systems. Springer-Verlag, Berlin, Germany, 1979.

Hwang, Ching-Lai and Yoon, Kwangsun. *Multiple Attirbute Decision Making: Methods and Applications*. Lecture Notes in Economics and Mathematical Systems. Springer-Verlag, Berlin, Germany, 1981.

Ismail-Yahaya, Amir and Messac, Achille. Effective generation of the Pareto frontier: The normalized normal constraint method. 2002-1232. 43rd Structures, Structural Dynamics, and Materials Conference, American Institute of Aeronautics and Astronautics, 2002.

James, M. L., Smith, G. M., Wolford, J. C., and Whaley, P. W. *Vibration of Mechanical and Structural Systems: With Microcomputer Applications, Second Edition.* HarperCollins College Publishers, New York, New York, 1994.

Joe, Stephen and Kuo, Frances Y. Remark on algorithm 659: Implementing Sobol's quasirandom sequence generator. *ACM Transactions on Mathematical Software*, 29(1):49–57, 2003.

Johnson, Clarence L. and Smith, Maggie. *Kelly: More Than My Share of It All.* Smithsonian, 1990.

Jones, Gregory S., Bangert, Linda S., Garber, Donald P., Huebner, Lawrence D., McKinley, Robert E., Sutton, Kenneth, Swanson, Roy C., and Weinstein, Leonard. Research opportunities in advanced aerospace concepts. Technical Report TM-2000-210547, National Aeronautics and Space Administration, Hampton, Virginia, 2000.

Joy, D. P. and Simonds, R. M. The R_f graphical method of parametric analysis for the development of optimum preliminary design aircraft. Technical Report 107, Advanced Research Division of Hiller Helicopters, 1956.

Kam, J. Vander and Gage, P. The launch vehicle language (LVL) data model for evaluating reusable launch vehicle concepts. 2003-1330. 41st Aerospace Sciences Meeting and Exhibit, American Institute of Aeronautics and Astronautics, Reno, Nevada, 2003.

Kirby, M. R. and Mavris, D. N. Forecasting technology uncertainty in preliminary aircraft design. 1999-01-5631. 1999 World Aviation Conference, Society of Automotive Engineers, San Francisco, California, 1999.

Kirby, M. R. and Mavris, D. N. An approach for the intelligent assessment of future technology portfolios. 2002-0515. 40th Aerospace Sciences Meeting and Exhibit, American Institute of Aeronautics and Astronautics, Reno, Nevada, 2002.

Kirby, Michelle R. *A Methodology for Technology Identification, Evaluation, and Selection in Conceptual and Preliminary Aircraft Design.* Ph.D. thesis, Georgia Institute of Technology, Atlanta, Georgia, 2001.

Kirby, Michelle R., Mavris, Dimitri N., and Largent, Matthew C. A process for tracking and assessing emerging technology development programs for resource allocation. 2001-5280. 1st AIAA Aircraft Technology, Integration, and Operations Forum, American Institute of Aeronautics and Astronautics, Los Angeles, California, 2001.

Ledsinger, L. A. and Olds, J. R. Multidisciplinary design optimization techniques for branching trajectories. 98-4713. 7th Symposium on Multidisciplinary Analysis and Optimization, American Institute of Aeronautics and Astronautics, 1998.

Leonard, John. *Systems Engineering Fundamentals.* Defense Systems Management College, Fort Belvoir, Virginia, 1999.

Li, Wu and Padula, Sharon. Approximation methods for conceptual design of complex systems. In Neamtu, Schumaker, and Chui, editors, *Approximation Theory XI: Gatlinburg 2004*, pages 241–278. Nashboro Press, Brentwood, Tennessee, 2005.

Lin, R. and Afjeh, A. A. An extensible, interchangeable and sharable database model for improving multidisciplinary aircraft design. 2002-5613. 9th Symposium on Multidisciplinary Analysis and Optimization, American Institute of Aeronautics and Astronautics, Atlanta, Georgia, 2002.

Mattingly, Jack D., Heiser, William H., and Pratt, David T. *Aircraft Engine Design, Second Edition*. American Institute of Aeronautics and Astronautics, Reston, Virginia, 2002.

Mattson, Christopher A., Mullur, Anoop A., and Messac, Achille. Minimal representation of multiobjective design space using a smart Pareto filter. 2002-5458. 9th Symposium on Multidisciplinary Analysis and Optimization, American Institute of Aeronautics and Astronautics, 2002.

Mavris, D. N. and Kirby, M. R. Technology identification, evaluation, and selection for commercial transport aircraft. 2456. 58th Annual Conference of Society of Allied Weight Engineers, Society of Allied Weight Engineers, San Jose, California, 1999.

Mavris, D. N., Kirby, M. R., and Qiu, S. Technology impact forecasting for a high speed civil transport. 985547. 1998 World Aviation Conference, Society of Automotive Engineers, Anaheim, California, 1998.

Mavris, D. N., Mantis, G. C., and Kirby, M. R. Demonstration of a probabilistic technique for the determination of aircraft economic viability. 975585. 2nd World Aviation Congress and Exposition, Society of Automotive Engineers, Anaheim, California, 1997.

Mavris, Dimitri N. and Bandte, Oliver. Economic uncertainty assessment using a combined design of experiments / monte carlo simulation approach with application to an HSCT. 17th Annual Conference of the International Society of Parametric Analysts, International Society of Parametric Analysts, 1995.

Mavris, Dimitri N. and Bandte, Oliver. Comparison of two probabilistic techniques for the assessment of economic uncertainty. 19th Annual Conference of the International Society of Parametric Analysts, International Society of Parametric Analysts, 1997.

Mavris, Dimitri N. and Borer, Nicholas K. Development of a multi-mission sizing methodology applied to the common support aircraft. 2001-01-3014. World Aviation Congress and Exposition, Society of Automotive Engineers, 2001.

Mavris, Dimitri N. and DeLaurentis, Daniel. Methodology for examining the simultaneous impact of requirements, vehicle characteristics, and technologies on military aircraft design. 145.1. ICAS, 2000.

Mavris, Dimitri N. and Kirby, Michelle R. UEET program metrics assessment implementation for a supersonic business jet. Final report, NASA Contract Number NAS 3-00179, Task Order C-70354-T, 2003.

Mavris, Dimitri N., Kirby, Michelle R., and Tai, Jimmy. FY04 VISTA technology assessment. Final report, NASA Grant Number NNL04AD06T, Task Order NAS 3-00179, 2004.

McCullers, L. A. Aircraft configuration optimization including optimized flight profiles. In Sobieski, J., editor, *Proceedings of the Symposium on Recent Experiences in Multidisciplinary Analysis and Optimization*, CP-2327, pages 396–412. National Aeronautics and Space Administration, 1984.

McCullers, L. A. *Flight Optimization System Release 5.94 User's Guide*. National Aeronautics and Space Administration, 5.94 edition, 1998.

McDonnell-Douglas Corporation. *F/A-18C Substantiating Performance Data with F404-GE-402 Engines*. McDonnell-Douglas Corporation, MDC 91B0290 edition, 1996.

McMasters, J. H., Paisley, D. J., Hubert, R. J., Kroo, I., Bofah, K. K., Sullivan, J. P., and Drela, M. Advanced configurations for very large subsonic transport airplanes. Technical Report CR-198351, National Aeronautics and Space Administration, Hampton, Virginia, 1996.

Messac, Achille and Ismail-Yahaya, Amir. Required relationship between objective function and Pareto frontier orders: Practical implications. 2001-1495. 42nd Sturctures, Structural Dynamics and Materials Conference and Exhibit, American Institute of Aeronautics and Astronautics, 2001.

MIT Axiomatic Design Group. General axiomatic design concepts. 2005. http://web.mit.edu/axiom/www/introduction.shtml.

Montgomery, Douglas C. *Design and Analysis of Experiments*. John Wiley and Sons, Inc., New York, New York, fifth edition, 2001.

Moran, Michael J. and Shapiro, Howard N. *Fundamentals of Engineering Thermodynamics, Third Edition*. John Wiley and Sons, Inc., New York, New York, 1995.

Mullur, Anoop A., Mattson, Christopher A., and Messac, Achille. Pitfalls of the typical construction of decision matrices for concept selection. 2003-0466. 41st Aerospace Sciences Meeting and Exhibit, American Institute of Aeronautics and Astronautics, 2003.

Myers, Raymond H. and Montgomery, Douglas C. *Response Surface Methodology: Process and Product Optimization Using Design Experiments*. John Wiley and Sons, Inc., New York, New York, 1995.

Myklebust, Arvid and Gelhausen, Paul. Putting the ACSYNT on aircraft design. *Aerospace America*, pages 26–30, 1994.

Nakos, George and Joyner, David. *Linear Algebra with Applications*. Brooks/Cole, Pacific Grove, California, 1998.

National Aeronautics and Space Administration. VISTA team strategists guide course of aeronautics technology development. *NASA Aeronautics News*, 5(3), 2004.

Naval Air Systems Command. *Standard Aircraft Characteristics: F-14A Tomcat*. Naval Air Systems Command, NAVAIR 00-110AF14-1 edition, 1976.

Naval Air Systems Command. *Standard Aircraft Characteristics: Navy Model A-6E (TRAM) Aircraft*. Naval Air Systems Command, NAVAIR 00-110AA6-5 edition, 1984.

Naval Air Systems Command. *Standard Aircraft Characteristics: F/A-18C Hornet, (2) F404-GE-402 Engines.* Naval Air Systems Command, NAVAIR 00-110AF18-4 edition, 1996.

Nelson, J. M., Kawai, R. T., and Gregg, R. D. A study of the economic benefit potential of internodal transports. Technical Report CR-2001-210847, National Aeronautics and Space Administration, Hampton, Virginia, 2001.

Neter, John, Kutner, Michael H., Nactsheim, Chistopher J., and Wasserman, William. *Applied Linear Statistical Models, Fourth Edition.* McGraw-Hill, Boston, Massachusetts, 1996.

Olds, J. System sensitivity analysis applied to the conceptual design of a dual-fuel rocket SSTO. 94-4339. 5th Symposium on Multidisciplinary Analysis and Optimization, American Institute of Aeronautics and Astronautics, 1994.

Pareto, Vilredo. *Manual of Political Economy.* Augustus M. Kelley, New York, New York, 1971.

Parker, James L. Mission requirements and aircraft sizing. 86-2622. Aircraft Systems, Design, and Technology Meeting, American Institute of Aeronautics and Astronautics, 1986.

Phoenix Integration. Phoenix Integration Products: ModelCenter. 2005. http://www.phoenix-int.com/products/ModelCenter.php.

Piccirillo, Albert C. Origins of the F-22 raptor. 98-5566. Society of Automotive Engineers, 1998.

Press, William H., Teukolsky, Saul A., Vetterling, William T., and Flannery, Brian P. *Numerical Recipes in C: The Art of Scientific Computing, Second Edition.* Cambridge University Press, Cambridge, United Kingdom, 1997.

Pugliese, J. J. Design synthesis. The Aircraft Design Process Seminar, Society of Aeronautical Weight Engineers, Arlington, Texas, 1971.

Raymer, D. P. Vehicle scaling laws for multidisciplinary optimization: Use of net design volume to improve optimization realism. 2001-5246. 1st Aerospace Technology, Integration, and Operations Forum, American Institute of Aeronautics and Astronautics, Los Angeles, California, 2001.

Raymer, Daniel P. *Aircraft Design: A Conceptual Approach, Third Edition.* American Institute of Aeronautics and Astronautics, Reston, Virginia, 1999.

Rich, Ben R. and Janos, Leo. *Skunk Works.* Little, Brown and Company, Boston, Massachusetts, 1994.

Rogers, James L. Reducing design cycle time and cost through process resequencing. International Conferece on Engineering Design, 1997.

Roskam, Jan. *Airplane Design Part I: Preliminary Sizing of Airplanes.* Roskam Aviation and Engineering Corporation, Ottawa, Kansas, 1989.

SAS Institute. JMP Software - Data Analysis - Statistics - Six Sigma - DOE. 2005. http://www.jmp.com/.

Schrage, D. P. Technology for rotorcraft affordability through integrated product/process development (IPPD). American Helicopter Society 55th Annual Forum, American Helicopter Society, Montreal, Canada, 1999.

Shepard, Roger N. On subjectively optimum selection among multiattribute alternatives. In Shelly, Maynard W. and Bryan, Glenn L., editors, *Human Judgements and Optimality*, chapter 14. John Wiley and Sons, Inc., New York, New York, 1964.

Sherman, Robert and Hardiman, Matthew X. F-35 Joint Strike Fighter. 2003. http://www.fas.org/man/dod-101/sys/ac/f-35.htm.

Simonds, R. M. A generalized graphical method of minimum gross weight estimation. 135. The National Conference of the Society of Aeronautical Weight Engineers, Society of Aeronautical Weight Engineers, San Diego, California, 1956.

Simos, D. and Jenkinson, L.R. Optimisation of the conceptual design and mission profiles of short-haul aircraft. 86-2696. Aircraft Systems, Design, and Technology Meeting, American Institute of Aeronautics and Astronautics, Dayton, Ohio, 1986.

Sobieszczanski-Sobieski, Jaroslaw. Sensitivity analysis and multidisciplinary optimization for aircraft design: Recent advances and results. *Journal of Aircraft*, 27(12):993–1001, 1990.

Sobieszczanski-Sobieski, Jaroslaw, Agte, Jeremy S., and Sandusky, Robert R. Bi-level integrated system synthesis (BLISS). 98-4916. American Institute of Aeronautics and Astronautics, 1998.

Soofi, Ehsan S. Generalized entropy-based weights for mulitattribute value models. *Operations Research*, 38(2):362–363, 1990.

Soofi, Ehsan S. and Retzer, Joseph J. Adjustment of importance weights in multiattribute value models by minimum discrimination information. *European Journal of Operational Research*, 60:99–108, 1992.

Strang, Gilbert. *Linear Algebra and its Applications, Third Edition.* Brooks/Cole, Pacific Grove, California, 1988.

Stump, Gary, Simpson, Timothy W., Yukish, Mike, and Bennett, Lorri. Multidimensional visualization and its application to a design by shopping paradigm. 2002-5622. 9th Symposium on Multidisciplinary Analysis and Optimization, American Institute of Aeronautics and Astronautics, 2002.

Suh, Nam P. *The Principles of Design.* Oxford University Press, New York, New York, 1990.

The Mathworks, Inc. Matlab - the language of technical computing. 2005. http://www.mathworks.com/products/matlab/.

Toppan, Andrew. World navies today: U.S. Navy carrier air wings. 2003. http://www.hazegray.org/worldnav/usa/wings.htm.

Torenbeek, Egbert. *Synthesis of Subsonic Airplane Design*. Delft University Press, Delft, Holland, 1982.

Triantaphyllou, Evangelos. *Multi-Criteria Decision Making Methods: A Comparative Study*. Kluwer Academic Publishers, Dordrecht, The Netherlands, 2000.

Vanderplaats, Garret N. *Numerical Optimization Techniques for Engineering Design, Third Edition*. Vanderplaats Research and Development, Inc., Colorado Springs, Colorado, 1999.

Vincenti, Walter G. and Kruger, Jr., Charles H. *Introduction to Physical Gas Dynamics*. Krieger, Malabar, Florida, 1965.

Vlases, W. G., Paris, S. W., Lajoie, R. M., Martens, P. J., and Hargraves, C. R. Optimal trajectories by implicit simulation version 2.0 user's manual. Technical Report WRDC-TR-90-3056, Vol. II, Flight Dynamics Lab, WRDC, AFSC, 1990.

Weisstein, Eric W. Heaviside step function. 2005. http://mathworld.wolfram.com/ HeavisideStepFunction.html.

Wellington, Arthur Mellen. *The Economic Theory of the Location of Railways: An Analysis of the Conditions Controlling the Laying Out of Railways to Effect the Most Judicious Expenditure of Capital*. Wiley, New York, sixth edition, 1914.

Wlezien, Richard. The vehicle systems program. Vehicle Systems Program 1st Annual Industry Meeting, National Aeronautics and Space Adminstration, 2004.

Yoon, K. Paul and Hwang, Ching-Lai. *Multiple Attribute Decision Making: An Introduction*. Quantitative Applications in the Social Sciences. Sage Publications, Thousand Oaks, California, 1995.

Young, James A., Anderson, Ronald D., and Yurkovich, Rudolph N. A description of the F/A-18E/F design and design process. 98-4701. American Institute of Aeronautics and Astronautics, 1998.

Young, Warren C. and Budynas, Richard G. *Roark's Formulas for Stress and Strain*. McGraw-Hill, Boston, Massachusetts, 7th edition, 2001.

Zeleny, Milan. *Multiple Criteria Decision Making*. McGraw-Hill, New York, New York, 1982.

Zweber, J. V., Kabis, H., Follett, W. W., and Ramabadran, N. Towards an integrated modeling environment for hypersonic vehicle design and synthesis. 2002-5172. American Institute of Aeronautics and Astronautics, 2002.

VITA

Nick Borer was born in Anaheim, California, where he resided for his first 18 years. He went to Syracuse University in the fall of 1996 and received his Bachelor's Degree in Aerospace Engineering in May of 2000. He then enrolled at Georgia Tech for graduate school and was awarded a Master's Degree in Aerospace Engineering in December of 2001. He passed his Ph.D. qualifying exams in April of 2002 and will be awarded his Ph.D. in Aerospace Engineering in May of 2006.

Nick enjoys all things related to aviation and mechanical work. He holds a private pilot certificate which he received through the Georgia Tech flying club and is an active pilot, though less active then he'd like to be. He volunteers for restoration and maintenance duties on vintage aircraft with the Commemorative Air Force and has had an opportunity to ride in some of these priceless aircraft. He is also a member of the Experimental Aircraft Association and has ventured to Oshkosh and Sun-n-Fun every year since 2003, and plans to keep this as a regular occurrence.